DOCTOR OF PHILOSOPHY

Regulation of the Parkin E3 ligase by PINK1-dependent phosphorylation

Kazlauskaite, Agne

Award date:
2015

Regulation of the Parkin E3 ligase by PINK1-dependent phosphorylation

Agne Kazlauskaite

A thesis submitted for the degree of

Doctor of Philosophy

University of Dundee

September 2015

Nothing in life is to be feared, it is only to be understood. Now is the time to understand more, so that we may fear less.

Marie Curie

I. Acknowledgements

I would like to take this opportunity to express my gratitude towards people who provided me with technical and moral support throughout my project. First and foremost to my supervisors Dr. Miratul Muqit and Professor Dario R. Alessi for providing me with the opportunity to work at MRC PPU in addition to introducing me to the world of Parkinson's disease and providing excellent advice, conceptual inception as well as constant support and thorough advice. I would like to thank members of my thesis committee, Professor Anton Gartner and Professor John Rouse, for their support and advice. I would like to acknowledge Parkinson's UK and J. Macdonald Menzies Charitable Trust for funding my work.

My work would have never been possible without my collaborators contributions. I would like to express my deepest gratitude to all of them: Dr. Van Kelly, Dr. Patrick Pedrioli, Alba Gonzalez, Dr. Julien Peltier and Dr. Matthias Trost for mass-spectrometry experiments; Dr. Julio M. Torrez, Dr. Atul Kuman and Dr. Helen Walden for ITC and thermal shift assays; Dr. Kay Hoffman for alignments; Dr. Jinwey Zhang, Dr. Anthony Hope and Dr. Scott Wilkie for alphascreen assays; Dr. Alan Prescott for microscopy; Dr. Satpal Virdee and Professor Jason Chin for letting me contribute to their work.

In addition, I owe enormous thanks towards members of DSTT. Especially James Hastie and Hilary McLauchlan for running the facility so well; the entire cloning team with special thanks to Dr. Thomas Macartney, Dr. Mark Peggie and Dr. Nikki Wood for enormous amount of clones they generated for my work. I would also like to express my gratitude to the protein and antibody production, DNA sequencing facility along with everyone at Division of Signal Transduction Therapy.

I am forever grateful for the protein production and Assay Development team including Dr. Axel Knebel and Clare Johnson for the enormous amount of work they did to supply me with the proteins for the majority of my experiments. I could not have done it without you! Thanks to Robert Gourlay, David Campbell and Stella Ritorto for phosphopeptide mapping

and MALDI analysis, respectively. I would like to thank Kirsten McLeod and Janis Stark for their support in tissue culture. Thanks go to all the divisional support staff, particularly Alison Hart, Allison Bridges, Hannah Kendall, Judith Hare and Rachel Naismith.

The four years of my PhD would not have been the same without the people in the two labs I was a part of, I would therefore like to express my thanks to members of MM and DRA labs, past and present, for creating a lovely work environment. I would like to say a big thank you for my bay mates Eeva Sommer, Sourav Banerjee and Ayaz Najafov who have started me on this journey. It was epic! I am grateful to Chandana Kondapalli for being a wonderful friend without whom my work would not have been possible. Special thanks goes to Helen Woodroof for being a great friend and supporting me when the going got tough, Yu-Chiang and Kristin Balk for being a kind and a great colleagues, Esther Sammler for having someone to share my hobby with, to Helen Walden, Atul Kumar, Julio Martinez for advise and stimulating conversation, George Georghiou, Ruzica Bago, Max Fritsch and Ana Belen for help and advice as well as being great people to work with.

Outside of the lab, thanks go to Nadege, Priyanka, Diana, Romana, Riccardo, Orsolya and Anetta. You all made it worth it, thank you. Most of all, none of this would have been possible without my family, who have been a source of constant love and support and who believed in me when I have lost all faith. I thank my grandma for inspiring me and for not giving up hope even when it got too difficult to keep on going. This is for you.

II. Declarations

I hereby declare that the following thesis is based on the results of investigations conducted by myself, and that this thesis is of my own composition. Work other than my own is clearly indicated in the text by reference to the researchers or their publications. This thesis has not in whole or in part been previously presented for a higher degree.

Agne Kazlauskaite

We certify that Agne Kazlauskaite has spent the equivalent of at least nine terms in research work in the School of Life Sciences, University of Dundee and that she has fulfilled the conditions of the Ordinance General No. 14 of the University of Dundee and is qualified to submit the accompanying thesis in application for the degree of Doctor of Philosophy.

Dr. Miratul M. K. Muqit M.B. (Ch. B), PhD

Professor Dario Alessi, FRS, FRSE

III. List of Publications

The work described in this thesis has been published in the following articles:

Han C, Pao KC, Kazlauskaite A, Muqit MM, Virdee S (2015) A Versatile Strategy for the Semisynthetic Production of Ser65 Phosphorylated Ubiquitin and Its Biochemical and Structural Characterisation. *Chembiochem*

Kazlauskaite A, Kelly V, Johnson C, Baillie C, Hastie CJ, Peggie M, Macartney T, Woodroof HI, Alessi DR, Pedrioli PG, Muqit MM (2014a) Phosphorylation of Parkin at Serine65 is essential for activation: elaboration of a Miro1 substrate-based assay of Parkin E3 ligase activity. *Open Biol* **4:** 130213

Kazlauskaite A, Kondapalli C, Gourlay R, Campbell DG, Ritorto MS, Hofmann K, Alessi DR, Knebel A, Trost M, Muqit MM (2014b) Parkin is activated by PINK1-dependent phosphorylation of ubiquitin at Ser65. *The Biochemical journal* **460:** 127-139

Kazlauskaite A, Martinez-Torres RJ, Wilkie S, Kumar A, Peltier J, Gonzalez A, Johnson C, Zhang J, Hope AG, Peggie M, Trost M, van Aalten DM, Alessi DR, Prescott AR, Knebel A, Walden H, Muqit MM (2015) Binding to serine 65-phosphorylated ubiquitin primes Parkin for optimal PINK1-dependent phosphorylation and activation. *EMBO Rep*

Kondapalli C, Kazlauskaite A, Zhang N, Woodroof HI, Campbell DG, Gourlay R, Burchell L, Walden H, Macartney TJ, Deak M, Knebel A, Alessi DR, Muqit MM (2012) PINK1 is activated by mitochondrial membrane potential depolarization and stimulates Parkin E3 ligase activity by phosphorylating Serine 65. *Open Biol* **2:** 120080

Rogerson DT, Sachdeva A, Wang K, Haq T, Kazlauskaite A, Hancock SM, Huguenin-Dezot N, Muqit MM, Fry AM, Bayliss R, Chin JW (2015) Efficient genetic encoding of phosphoserine and its nonhydrolyzable analog. *Nat Chem Biol* **11:** 496-503

IV. Summary

Parkinson's disease (PD) is the second most common neurodegenerative disorder affecting around 1% of the population over the age of 65 worldwide. While the majority of cases are sporadic, groundbreaking genetic research over the last two decades has revealed a complicated network of genes underlying susceptibility and pathology of PD. Mutations in Parkin are the most common cause of early onset Parkinson's disease. Parkin encodes a RING-In Between RING-RING E3 ligase that normally resides in the cytoplasm and is regulated by autoinhibitory intramolecular interactions. PINK1 is a mitochondrial Ser/Thr kinase that is unique in possessing a N-terminal mitochondrial targeting sequence and three loop insertions within its kinase domain. At the outset of my PhD, PINK1 was discovered to phosphorylate Parkin at Serine 65 (Ser^{65}), however, little was known about how this phosphorylation affected Parkin function and E3 ligase activity. The work described in this thesis aims to address in detail the molecular interactions between these proteins.

In Chapter 3, I describe the development of novel tools and assays to study the PINK1-Parkin interaction. I demonstrate that PINK1 robustly phosphorylates Parkin at Ser^{65} *in vitro* as well as in cells. I further show that Parkin is activated via PINK1 mediated phosphorylation of Ser^{65}. I validate the mitochondrial GTPase Miro1 as a direct substrate of Parkin and employ this novel substrate-based assay to demonstrate a multitude of effects conferred by Parkin disease mutations on its phosphorylation and E3 ligase activity.

In Chapter 4, I describe work that revealed a novel PINK1 substrate – ubiquitin. I demonstrate that Ubiquitin gets phosphorylated at a homologous Ser^{65} residue and this is critical for PINK1-mediated Parkin activation. I provide further evidence that both phosphorylation events are necessary for optimal Parkin E3 ligase activity.

Following up on this work, in Chapter 5, I investigate the mechanism by which phosphorylated ubiquitin contributes to Parkin activation. I demonstrate that binding of phosphorylated ubiquitin to Parkin significantly enhances its phosphorylation by PINK1 and

thereby its activation. I further identify Histidine 302 and Lysine 151 as Parkin residues critically involved in binding phosphorylated ubiquitin and confirm their importance for Parkin phosphorylation and activation *in vitro* as well as in cells.

Overall, the work described in this thesis elaborates the mechanism by which Parkin is regulated by PINK1-dependent phosphorylation. In parallel this work provides the PINK1/Parkin field with a set of valuable tools to evaluate this mechanism. My work not only reveals PINK1-dependent Parkin activation via direct phosphorylation of the Parkin Ser^{65} residue, but goes on to identify a new key player in this pathway – Ser^{65} phosphorylated ubiquitin. Finally my studies provide novel and original insights into the interplay of these three proteins towards driving Parkin activation.

V. Amino acid codes

Amino acid	Three letter code	One letter code
Alanine	Ala	A
Arginine	Arg	R
Asparagine	Asn	N
Aspartic acid	Asp	D
Cysteine	Cys	C
Glutamine	Gln	Q
Glutamic acid	Glu	E
Glycine	Gly	G
Histidine	His	H
Isoleucine	Ile	I
Leucine	Leu	L
Lysine	Lys	K
Methionine	Met	M
Phenylalanine	Phe	F
Proline	Pro	P
Serine	Ser	S
Threonine	Thr	T
Tryptophan	Trp	W
Tyrosine	Tyr	Y
Valine	Val	V

VI. List of abbreviations

A_{280}	Absorbance at 280 nm
ADP	Adenosine 5'-diphosphate
Amp	Ampicillin
aPK	atypical protein kinase
ATP	Adenosine 5'-triphosphate
A.U.	Arbitrary units
BLAST	Basic Local Alignment Search Tool
BSA	Bovine serum albumin
°C	Degrees Celsius
CaMKI/II	Calcium/calmodulin-dependent kinase I/II
cAMP	cyclic adenosine monophosphate
CCCP	Carbonyl cyanide *m*-chlorophenyl hydrazone
Cdc	Cell division cycle
CDK	Cyclin-dependent kinase
CK1/2	Casein kinase 1/2
CLK	Cdc-like kinase
CNS	Central nervous system
cpm	counts per minute
Da	Daltons
DMPK	Myotonic dystrophy protein kinase
DMSO	Dimethyl sulfoxide
DNA	Deoxyribonucleic acid
DTT	Dithiothreitol
DUB	Deubiquitinating enzyme
ECL	Enhanced chemiluminescence
EDTA	Ethylenediaminetetraacetic acid
EGTA	Ethylene glycol tetraacetic acid
ePK	eukaryotic protein kinase
ERK	Extracellular signal regulated kinase
g	Gram or gravity
GSK3	Glycogen synthase kinase 3
GST	Glutathione-S-transferase
h	Hour
HECT	Homologous to the 6-AP Carboxyl Terminus
HEK293	Human embryonic kidney 293 cell line
HEPES	4-(2-hydroxyethyl)-1-piperazineethanesulfonic acid
HOM	Homozygous
HRP	Horseradish peroxidase
HtrA2/Omi	High temperature requirement protein A2
IBR	In-Between Ring
IGFR	Insulin-like growth factor receptor
IMM	Inner mitochondrial membrane
IMS	Intermembrane space
IPTG	Isopropyl-β-D-1-thiogalactoside
JNK1/2	c-Jun N-terminal kinase
kDa	kilo Dalton
KI	Kinase inactive
l	Litre

LB	Luria-Bertani media
LC-MS	Liquid chromatography-mass spectrometry
LRRK2	Leucine-rich repeat kinase 2
MALDI	Matrix-assisted laser desorption ionisation
MAPK	Mitogen-activated protein kinase
M	milli
M	Molar
µ	micro
MBP	Maltose binding protein
MEK1	Mitogen-activated ERK-activating kinase 1
min	Minute
mol	Mole
MPP	Mitochondrial processing peptidase
MPTP	1-methyl-4-phenyl-1,2,3,6-tetrahydropyridine
MTS	Mitochondrial targeting sequence
MW	Molecular weight
MWCO	Molecular weight cut-off
n	nano
NEK4	Never in mitosis A-related kinase 4
Ni-NTA	Nickel-nitrilotriacetic acid resin
OD_{600}	Optical density at 600 nm
OMM	Outer mitochondrial membrane
PAGE	Polyacrylamide gel electrophoresis
PARL	Presenilin-associated rhomboid-like protein
PD	Parkinson's disease
PDB	Protein Dat Bank
PDK1	Phosphoinositide-dependent kinase-1
PH	Pleckstrin homology domain
PhcPINK1	*Pediculus humanus corporis* PINK1
PINK1	PTEN-induced kinase 1
PIP_3	Phosphatidylinositol (3,4,5)-trisphosphate
PKA	cAMP-dependent protein kinase
PKB	Protein kinase B
PKC	Protein kinase C
PKG	cGMP-dependent protein kinase
PKR	Protein kinase RNA-activated
PMSF	Phenylmethanesulphonyl fluoride
PTEN	Phosphatase and tensin homologue
PTM	Post-translational modification
PVDF	Polyvinylidene difluoride
RBR	Ring-Between-Ring
REM	Rapid eye movement
REP	Regulatory element of Parkin
RF-1	Release factor-1
RING	Really Interesting New Gene
RNA	Ribonucleic acid
rpm	revolutions per minute
RT	Room temperature
ROS	Reactive oxygen species
SD	Standard deviation
SDS	Sodium dodecyl sulphate
sec	seconds

SENP1	Sentrin-specific protease 1
SILAC	Stable isotope labelling with amino acids in culture
SNCA	α-synuclein
SRPK	Serine/arginine-rich-protein kinase
STRADα	STE20-related kinase adapter protein
SUMO	Small ubiquitin-like modifier
TB	Terrific Broth
TCEP	Tris(2-carboxyethyl)phosphine
TcPINK1	*Tribolium castaneum* PINK1
TEMED	*N*,*N*,*N*′,*N*′-Tetramethylethane-1,2-diamine
TIMM	Translocate of the inner mitochondrial membrane
TOM	Translocase of the outer membrane
TRAP1	Tumor necrosis factor type 1 receptor-associated protein
Ubl	Ubiquitin-like
UV	Ultraviolet
V	Volts
VDAC	Voltage-dependent anion channel
v/v	Volume per volume
WT	Wild type
w/v	Weight per volume

VII. Table of Contents

VIII. List of Figures

IX. List of Tables

1 Chapter 1 Introduction

1.1 Parkinson's Disease

1.1.1 Historical overview

The first mentions of an akinetic movement disorder date back to 5000 BC in Indian practice of medicine, known as Ayurveda. However, it was not until 1817 when the first formal description and classification of the clinical features was reported in the famous essay by physician James Parkinson, entitled 'An essay on the shaking palsy' wherein he describes 6 cases bearing a syndrome that now bears his name Parkinson's disease (Pearce, 1989, Parkinson, 1817):

'SHAKING PALSY (Paralysis Agitans)

Involuntary tremulous motion, with lessened muscular power, in parts not in action and even when supported; with a propensity to bend the trunk forwards, and to pass from a walking to a running pace: the senses and intellects being uninjured.'

The initial description of the illness was greatly expanded by French physician Trousseau who recognised muscle rigidity, displacement of the centre of gravity, bradykinesia as well as eventual damage to the patient's intellect as symptoms associated with PD in his 15th Lecture on Clinical Medicine (Trousseau, 1868). While James Parkinson had wrongly suggested that the cause of the disease might lie in the ' medulla spinalis' (spinal cord), it was not until the early 20th century that the substantia nigra located in the midbrain was firmly established as the major site of pathology. The very first mention of substantia nigra as the potential 'anatomical basis of Parkinson's disease' is attributed to Brissaud (Brissaud, 1895), however it was admittedly speculative and further validation was needed. It was the doctoral work of Russian student Tretiakoff, who examined the substantia nigra in post mortem brains of 9

individuals with paralysis agitans and 3 with postencephalitic Parkinsonism and observed lesions, loss of pigmented nigral neurons and the appearance of Lewy bodies in the surviving neurones, that indicated that the substantia nigra was the primary anatomical place of origin for PD (Trétiakoff, 1919, Lewy, 1912).

In the 1950s and 1960s seminal discoveries set the stage for the current understanding of dopamine involvement in PD as well as its modern treatment with L-3,4-dihydroxyphenylalanine (L-dopa)– a natural dopamine precursor (Riederer et al., 2006). First, dopamine as a neurotransmitter was discovered to have a biological function distinct from noradrenaline and other known catecholamines (Blaschko, 1957), followed by the finding of its involvement in regulation of movement control as well as central motoric function (Bertler and Rosengren, 1959, Sano et al., 1959). Clear demonstration of the reduction in dopamine levels in PD brains (Ehringer and Hornykiewicz, 1960) combined with the knowledge that L-dopa is a natural precursor to dopamine, encouraged Hornykiewicz to start the first clinical trials of L-dopa as a treatment for PD, leading to the 'dopamine miracle' and later its adaptation as common medical treatment for PD:

'Bed-ridden patients who were unable to sit up, patients who could not stand up when seated, and patients who when standing could not start walking performed all these activities with ease after L-dopa [levodopa]. They walked around with normal associated movements and they could even run and jump. The voiceless, aphonic speech, blurred by palilalia and unclear articulation, became forceful and clear as in a normal person' (Birkmayer and Hornykiewicz, 1961).

1.1.2 Clinical symptoms and pathology of Parkinson's Disease

Parkinson's disease is the second most common neurodegenerative disorder, characterised by progressive loss of neurons from substantia nigra pars compacta, dopamine loss in striatum and accumulation of pathogenic cytoplasmic inclusion bodies known as Lewy bodies. Lewy bodies are rich in ubiquitin, α-synuclein, neurofilaments and molecular chaperones (Spillantini

et al., 1998, Forno, 1996). The main risk factor associated with PD is age and positive family history. As the average life expectancy continues to increase in developed countries, so does the incidence and prevalence of Parkinson's - the current life-time risk of developing the disease being 1.5% (Bower et al., 1999) – and this is expected to rise exponentially therefore increasing socioeconomical burden (Dorsey et al., 2007)

PD is characterised by two classes of symptoms – motor and non-motor. Motor symptoms encompass resting tremor, bradykinesia (slowness of movement), rigidity and postural imbalance – also known as the PD quartet. The onset of the symptoms is typically unilateral and continues to progress and persist asymmetrically. It was estimated that the manifestation of motor symptoms occurs only after 50-60 % of dopaminergic neurons have been lost (Riederer and Wuketich, 1976) and therefore marks a relatively late stage of disease progression. While the non-motor symptoms are less well known, they can be equally, if not more so, debilitating - these include loss of sense of smell, constipation, alterations in REM behaviour, mood disorders, orthostatic hypotension as well as a range of neurobehavioral disturbances - and can appear well before the motor symptoms (Beitz, 2014).

1.1.3 Genetics of Parkinson's disease

While the aetiology of Parkinson's at large remains a mystery, the majority of cases are believed to be caused by a combination of environmental and genetic factors. Over 90 % of the cases are believed to be sporadic, however, a long-acknowledged high prevalence of positive family history in PD patients has led to exploration of possible genetic causes. It was not until 1997 that the first gene causing the illness was identified (Polymeropoulos et al., 1997). Since then at least 10 other monogenic forms of PD with both autosomal dominant and recessive forms of inheritance have been discovered and have opened a path for exploration of the molecular pathways underlying the illness (Bras et al., 2015). The genes were denoted with PARK to mark their putative association with PD and numbered in a chronological order of discovery. Table 1.1 summarises the genes known to cause monogenic PD.

Table 1.1 PD Mendelian genes

Gene	Gene locus	Disorder	Inheritance	Protein
SNCA	4q21-22	EOPD	AD	α-synuclein
Parkin	6q25.2-q27	EOPD	AR	Parkin
PINK1	1p35-36	EOPD	AR	PINK1
DJ1	1p36	EOPD	AR	DJ1
LRRK2	12q12	Classical PD	AD	LRRK2
ATP13A2	1p36	juvenile parkinsonism	AR	ATP13A2
PLA2G6	22q13.1	juvenile parkinsonism	AR	PLA2G6
FBXO7	22q12-q13	juvenile parkinsonism	AR	FBOX7
VPS35	16q11.2	Classical PD	AD	VPS35
DNAJC6	1p31.3	juvenile parkinsonism	AR	DNAJC6
SYNJ1	21q22.2	juvenile parkinsonism	AR	SYNJ1

EOPD-early onset PD; AD-autosomal dominant; AR-autosomal recessive

1.1.4 Autosomal dominant Parkinson's Disease

Three genes are confirmed to cause autosomal dominant Parkinson's disease – α-synuclein, leucine rich repeat kinase 2 (LRRK2) and vacoular protein sorting-associated protein 35 (VPS35).

SNCA (PARK1/4) gene, encoding α-synuclein, was the first gene to be identified causally linked to Parkinson's disease (Polymeropoulos et al., 1997). Originally, the investigators identified a point mutation – A53T – however, gene duplications (Ibanez et al., 2004) and triplications (Singleton et al., 2003) are much more common. Since then, several other single point mutations have been identified including A30P (Narhi et al., 1999), E46K (Zarranz et al., 2004), H50Q (Proukakis et al., 2013), and G51D (Lesage et al., 2013). The function of α-synuclein remains unknown although it has been implicated in hippocampal neurogenesis

(Winner et al., 2012). Nevertheless, the pathogenicity of mutant α-synuclein forms is attributed to their increased propensity to aggregate into toxic oligomers, leading to formation of β–sheets (Bertoncini et al., 2005). Patients with SNCA multiplications suffer from earlier-onset, and more rapidly progressive PD with strong correlation to gene-dosage effects (Fuchs et al., 2007).

Mutations in LRRK2 (PARK8) gene are the most common cause of autosomal dominant PD and are commonly found in idiopathic cases; they were first identified in 2004 in multiple studies carried out in different parts of the world (Cookson, 2015, Zimprich et al., 2004, Paisan-Ruiz et al., 2004). LRRK2 encodes a large (›250 kDa) protein and contains both a kinase and GTPase domain; in addition, several other domains involved in protein-protein interaction have been identified, however, the physiological function of the protein is still unknown. Multiple mutations linked to PD have been reported with the most prevalent being G2019S, demonstrated to significantly increase kinase activity by 2-3 fold (Jaleel et al., 2007, West et al., 2005). While being common, the G2019S mutation does not demonstrate full-penetrance, suggesting that additional factors might be important for manifestation of symptoms (Cookson, 2015).

VPS35 has been identified relatively recently (Vilarino-Guell et al., 2011) and suggest that vesicle and endosomal trafficking may be implicated in PD but further work is needed to understand how mutations in this gene confer pathogenicity.

1.1.5 Autosomal recessive Parkinson's Disease

While multiple genes with autosomal recessive mode of inheritance have been linked to PD (Table 1.1), only three have been extensively studied and will be discussed here: Parkin, PINK1 and DJ1.

Mutations in Parkin (PARK2) gene, first identified in 1998 (Kitada et al., 1998), are the leading cause of autosomal recessive Parkinson's disease. Over 100 missense mutations and a

multitude of gene rearrangements have been identified leading to early onset PD (EOPD) (age of onset <40) and juvenile parkinsonism (age of onset <21) (Klein and Westenberger, 2012). Parkin encodes an E3 ligase that has been implicated in monitoring mitochondrial quality control, further discussed below.

The PINK1 (PARK6) gene has also been linked to EOPD (Valente et al., 2004). The PINK1 gene encodes a mitochondrial serine/threonine kinase PINK1 (PTEN (phosphatase and tensin homologue)-induced kinase 1), mutations in which have been found to disrupt the kinase activity (Woodroof et al., 2011) and confer the second most common cause of early-onset PD.

The link between mutations in DJ-1 (PARK7) and EOPD was first established in 2003 (Bonifati et al., 2003). Mutations in DJ-1 amount to only 1-2 % of the cases (Pankratz et al., 2006) with a phenotype that resembles other EOPD syndromes linked to PINK1 and Parkin (Hardy et al., 2006). DJ-1 is thought to encode an oxidative chaperone that is ubiquitously expressed, mutation of which (L166P) renders the protein unstable and leads to its rapid degradation by the 20S proteasome (Anderson and Daggett, 2008).

1.2 Post-translational modifications

Post-translational modifications (PTMs) are amongst the most universal regulatory mechanisms across all living species. They are defined as (mostly) enzyme-catalysed covalent modifications of polypeptide chains and roughly fall into one of three classes: linkage, breakage or cross-linking (Farriol-Mathis et al., 2004). PTMs are highly diverse, dynamic and reversible with over 400 identified to date (Khoury et al., 2011). While some of the PTMs are stable (e.g. glycosylation, lipidation, etc.) and serve a function in protein folding, stability and localisation, others, such as phosphorylation, methylation, acetylation and

ubiquitylation, are far more transient and serve an important function in cellular signalling via regulation of protein activity, degradation and localisation.

Post-translational modifications encompass the second level of governance in the cell after the gene regulation resulting in exponential increase in the cellular proteome complexity and creating a multi-layered fine-tuned organisational system. Despite what the name suggests, PTMs can occur before (deamidation), during (cleavage of signalling peptides) and after (phosphorylation) an amino acid has been incorporated to a polypeptide chain. They can be induced by extracellular or intracellular signalling events and can affect multiple different proteins or be directed at a highly specific pool of proteins. More than one PTM can be found on a protein at any one time and indeed it has been found that several different PTMs can serve in concert or in opposition of each other.

1.2.1 Ubiquitylation

1.2.1.1 Ubiquitin

Ubiquitin is a small, 76 amino acid, modifier protein first discovered in 1975 that is ubiquitously expressed in eukaryotes and is highly conserved from yeast to humans (Schlesinger and Goldstein, 1975, Goldstein et al., 1975). It is encoded by four separate genes in mammals 2 of which encode a polyubiquitin precursor while the other 2 encode a monoubiquitin moiety fused to an essential ribosomal subunit; after expression, the polypeptides are cleaved by deubiquitylating enzymes (DUBs) and a monoubiquitin is released (Kimura and Tanaka, 2010). Ubiquitin is a part of a family of ubiquitin-like modifiers (UBLs) that share a structural homology – the β-grasp fold - and include autophagy related protein-8 (ATG8) and -12 (ATG12), human leukocyte antigen F associated transcript 10 (FAT10), Fau ubiquitin-like protein (FUB1), neural precursor cell expressed developmentally down-regulated protein 8 (NEDD8), small ubiquitin-like modifier (SUMO), interferon-α-stimulated gene-15 (ISG15), ubiquitin-like protein-5 (UBL5), ubiquitin fold-modifier-1 (UFM1) and ubiquitin-related modifier-1 (URM1) (Hochstrasser, 2009). Ubiquitin is an

essential constituent of ubiquitylation – a master regulatory reversible PTM that has been demonstrated to play a key role in regulating protein degradation, signal transduction, protein trafficking and others (Kimura and Tanaka, 2010). The reversal of ubiquitylation is called deubiquitylation and is mediated by DUBs.

1.2.1.2 Ubiquitylation cascade

The ubiquitylation cascade facilitates covalent ubiquitin attachment to the ε-amino group of a substrate lysine. It involves 3 relay steps, each of which is catalysed by a different class of enzymes. The cascade is initiated when ubiquitin is activated by E1 ubiquitin activating enzyme in an ATP-dependent manner, followed by ubiquitin transfer to the catalytic cysteine on the E2 ubiquitin conjugating enzyme and finally its ligation to the target protein carried out by an E3 ubiquitin ligase (Figure 1.1). During the cascade a single ubiquitin moiety can be attached to a single target lysine (monoubiquitylation), or to several lysines on the substrate protein (multi-monoubiquitylation). Alternatively, further ubiquitin moieties can be conjugated onto the first ubiquitin in a head to tail manner via the N-terminal methionine (called linear or M1 chain formation) or one of the seven native ubiquitin lysines (Lys6, Lys11, Lys27, Lys29, Lys33, Lys48 and Lys63) – this process is called polyubiquitylation.

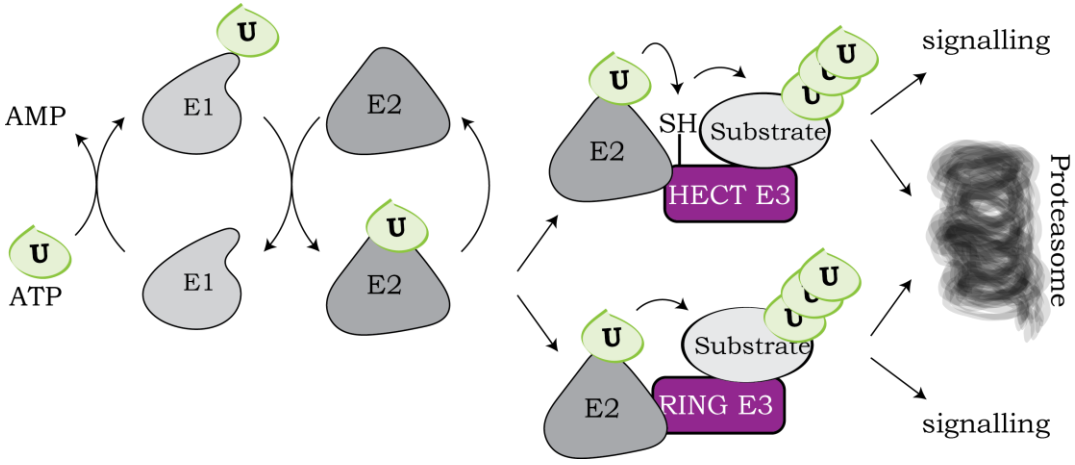

Figure 1.1 Ubiquitylation cascade.

Ubiquitin activating enzyme E1 activates the C-terminus of ubiquitin in an ATP-dependent manner. Ubiquitin is next transferred to the catalytic cysteine of ubiquitin conjugating enzyme E2 ensuing interaction with an E3 ubiquitin ligating enzyme. RING E3s bind and coordinate the E2-ub and substrate pair to facilitate a direct transfer of ubiquitin while HECTs have a catalytic cysteine that forms a thioester intermediate with the ubiquitin moiety before its transfer to the target protein. The ubiquitylated proteins are subjected to various fates including degradation and cell signalling.

Polyubiquitin chains can be of varying lengths and constructed in a variety of different ways. The consecutive ubiquitins can be added on the same lysine repeatedly, leading to formation of homotypic ubiquitin chains or incorporate several different linkage types leading to heterotypic and/or branched chain formation (Figure 1.2). It is the chain topology, length and linkage type that define the interaction with ubiquitin-binding domains on a variety of proteins (Hicke et al., 2005) and determine the end outcome of the ubiquitin signalling event.

Protein degradation was the first physiological outcome of ubiquitylation to be described (Ciehanover et al., 1978), it was only later that ubiquitin' s role in the regulation of cell cycle, transcription and DNA repair were discovered. Indeed, even now ubiquitylation carries a strong connotation towards degradative cellular pathways, although a vast variety of signalling outcomes have been discovered (reviewed in (Kulathu and Komander, 2012)).

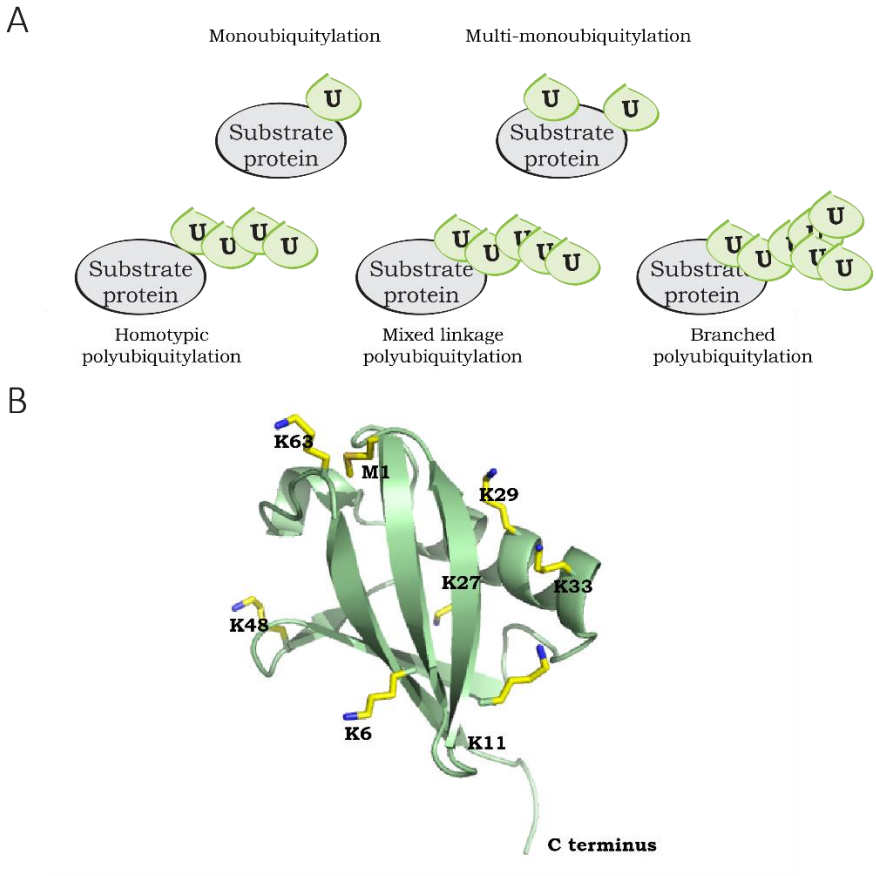

Figure 1.2 Ubiquitin chain topologies

A Summary of different ways ubiquitin can be attached to a target protein. Mono ubiquitylation ensues when a single ubiquitin moiety is attached to the substrate protein. Multi-mono ubiquitylation is attachment of more than one ubiquitin that do not form a chain. Polyubiquitin chains can be homotypic meaning the same linkage type is formed between all ubiquitin molecules or heterotypic – different linkage types can be found in the same ubiquitin. If two or more ubiquitin moieties are attached to a preceding ubiquitin, branched chain formation is observed. **B** Ubiquitin structure showing N-terminal methionine and lysine residues all of which can act as linkage points for the formation of polyubiquitin chains. PDB ID: 1UB

1.2.1.3 Catalytic triad of ubiquitin system

The first step of the ubiquitylation cascade is catalysed by E1 activating enzymes. As its name suggests, E1 activates ubiquitin. It achieves this in a two-step manner, wherein it first acyl-adenylates the carboxy terminus of the ubiquitin sacrificing an ATP molecule. The E1 catalytic cysteine then attacks the adenylated ubiquitin, forming an E1-ubiquitin thioester

bond that is accessible to E2 enzymes (Schulman and Harper, 2009). Two E1 genes have been identified in human genome, UBE1 (Haas et al., 1982) and UBE1L2 (Jin et al., 2007).

The next step in the signal relay is catalysed by one of over 40 E2 conjugating enzymes. It is achieved by a nucleophilic attack on the E1-ubiquitin bond by the E2 catalytic cysteine and formation of another high-energy thioester bond between the E2 and ubiquitin. E2 enzymes are heterogeneous in their preference for E1 enzyme and usually interact with more than one E3 ligase (Ye and Rape, 2009). The pairing of the E2 and E3 is extremely important for determining ubiquitin chain topology – it has been demonstrated that pairing of E3 ligases CHIP and MuRF1 with E2 UbcH5 results in a branched, heterotypic chain formation, while the same E2 pairing with E6AP E3 ligase resulted in homotypic K48 chain formation, and in addition, when dimeric E2 UbcH13/Uev1a was tested, CHIP and MuRF1 produced homotypic K63 chains (Kim et al., 2007).

Ubiquitin transfer onto the substrate protein is catalysed by an E3 ubiquitin ligating enzyme. It is estimated that the human genome encodes over 600 E3 ligases, the majority of which belong to the RING (really interesting new gene) superfamily (Li et al., 2008). RING E3s act as scaffold proteins, bringing the ubiquitin-bound E2 (E2-ub) and substrate together and orienting them in a manner that allows a direct ubiquitin transfer to occur. RING E3s are characterised by the presence of a RING domain that typically contains 8 cysteine or histidine residues (with some exceptions) that coordinate zinc ions in a cross-brace conformation and help maintain the globular domain folding (Deshaies and Joazeiro, 2009). The canonical RING domains recruit and bind an E2 ligase as well as a hydrophobic patch on the donor ubiquitin; some also directly interact with substrate proteins (Deshaies and Joazeiro, 2009). Lacking a bona-fide catalytic cysteine, RING E3s catalyse the transfer of ubiquitin to substrate via activation of the E2-ub conjugate by conformational rearrangement (Metzger et al., 2013), the mechanistic insights of which have been revealed in recent studies (Plechanovova et al., 2012, Branigan et al., 2015). Recent structural analysis of the RING E3 ligase, RNF4, in complex with the E2, UbcH5A linked to ubiquitin via an isopeptide bond has shed light on the mechanism and reveals alteration of the E2 active site that primes it

for catalysis to enable deprotonation of the incoming substrate lysine residue (Plechanovova et al., 2012). The majority of RING E3s exist in multimeric complexes and are found as homo- or hetero-dimers, e.g. cIAP (Mace et al., 2008) and BRCA1-BARD1 (Hashizume et al., 2001), others can oligomerise and be a part of supramolecular complexes (Kentsis et al., 2002) although some monomeric E3s can also be found. Substrate recognition of RING E3s is commonly facilitated by interacting proteins that contain F-box, SOCS box, VHL box or BTB domains (Metzger et al., 2013).

The other catalytic class of E3 ligases are HECT (Homologous to E6-AP C-Terminus) E3s. Unlike RING E3s, HECT ligases have a catalytic cysteine and catalyse the ubiquitylation reaction in a two-step mechanism, wherein the ubiquitin from E2-ub first forms a thioester bond with the E3 forming an unstable intermediate and leading to the subsequent ubiquitin transfer to the target protein (Kamadurai et al., 2013). HECT E3s contain a C-terminal HECT domain that carries the evolutionary-conserved catalytic cysteine, while their N-termini are diverse and usually involved in substrate recognition (Berndsen and Wolberger, 2014, Scheffner and Kumar, 2014). HECT E3s display a preference for their cognate E2, specifically UbcH7 and members of UbcH5 family have been shown to be preferentially recruited by these E3s (Schwarz et al., 1998).

RING – In Between RING – RING (RBR) could be called the ‘ misfits’ of the E3 ligases since they do not fit exclusively in either of the above described categories. Traditionally believed to belong to RING E3 superfamily, due to presence of two RING domains, RBR ligases carry a catalytic cysteine that forms a thioester intermediate with ubiquitin (Wenzel et al., 2011) therefore displaying HECT-like properties. Indeed, RBRs have been reclassified as RING/HECT hybrids (Spratt et al., 2014, Smit and Sixma, 2014) and were found to have several unusual properties. First, they are able to overcome the requirement for E2 and are able to interact with E1-ub thioester directly (Smit et al., 2012, Stieglitz et al., 2012a, Chew et al., 2011). In addition, their ubiquitin thioester intermediate is difficult to trap/detect, suggesting that it might be highly unstable. Finally, all the RBRs studied so far display a tight regulation and auto-inhibition (Smit et al., 2012, Stieglitz et al., 2012a, Chew et al.,

2011, Chaugule et al., 2011, Burchell et al., 2012). Parkin, the main topic of my thesis, is an RBR E3 ligase and will be discussed further in section 1.3.

1.2.1.4 Ubiquitin system and human disease

Given the diversity of ubiquitylation functions, some of which have likely not yet been discovered, it is no wonder that misregulation of this system at any level leads to a variety of human diseases, e.g. two missense mutations in E1 UBA1 enzyme have been linked to X-linked infantile spinal muscular atrophy (Ramser et al., 2008), while mutations in Ube2H have been implicated in X-linked mental retardation syndrome (Nascimento et al., 2006).

Mutations in E3 ligases and their interacting proteins have been linked to a variety of disease, including cancers and neurological disorders (Petroski, 2008). Mutations in E3 ligase BRCA1 (breast cancer type 1) have been strongly linked to predisposition to breast and ovarian cancer (Futreal et al., 1994, Hall et al., 1990). Three different ubiquitin-related proteins are linked to Parkinson's disease. Mutations in RBR E3 ligase Parkin – topic of this thesis - are the most common cause of early onset Parkinson's Disease (Kitada et al., 1998). Mutations in Fbxo7 – F-box protein that is part of SKP1-Cullin E3 ligase complex – are linked to juvenile Parkinsonism (Shojaee et al., 2008). UCHL1 – a carboxy terminal ubiquitin hydrolase – has also been linked to PD (Wintermeyer et al., 2000). Angelman's syndrome – a complex neurodevelopmental disorder – has been shown to be caused by mutations in HECT E3 ligase E6-AP (Kishino et al., 1997) while another E3 HUWE1 has been implicated in a mental retardation syndrome (Froyen et al., 2008). This is by all means not a complete list of disorders and illnesses caused by mutations in the ubiquitin system, but it serves to show how important it is and opens new avenues for discovery and progress – in particular the ubiquitin proteasome system has been scrutinised recently as a potential target for drug discovery. It is therefore paramount to gain as much information about molecular, cellular and physiological mechanisms governing its correct regulation and thereby ways to manipulate them.

1.2.2 Phosphorylation

1.2.2.1 Phosphorylation – general overview

Protein phosphorylation is a reversible formation of a phosphoester bond between a phosphoryl group of the donor ATP and hydroxyl group of one of three amino acids - serine, threonine or tyrosine (Figure 1.3). It was first discovered in 1954 when G. Burnett and E. Kennedy have radioactively labelled casein by incubating it with mitochondrial fractions from rat livers (Burnett and Kennedy, 1954). Phosphorylation plays an important role in a number of cellular events, including metabolism, transcription, cytoskeletal rearrangements, cell cycle progression and others with up to 30% of the human proteome estimated to be subject to phosphorylation (Kreegipuu et al., 1999). Addition of a double negative charge of the phosphate group on to a substrate protein, commonly on more than one residue, induces a large change in the local chemical environment of the protein that might lead to formation of new hydrophobic and/or electrostatic interactions (Johnson and Lewis, 2001). Such alterations can cause conformational and/or activity shifts in the substrate protein (Figure 1.3). In fact, kinase self-activation via auto-phosphorylation is a commonly employed mechanism. In addition, phosphorylation might lead to changes in protein-protein interactions resulting in altered protein function, localisation or stability (Figure 1.3).

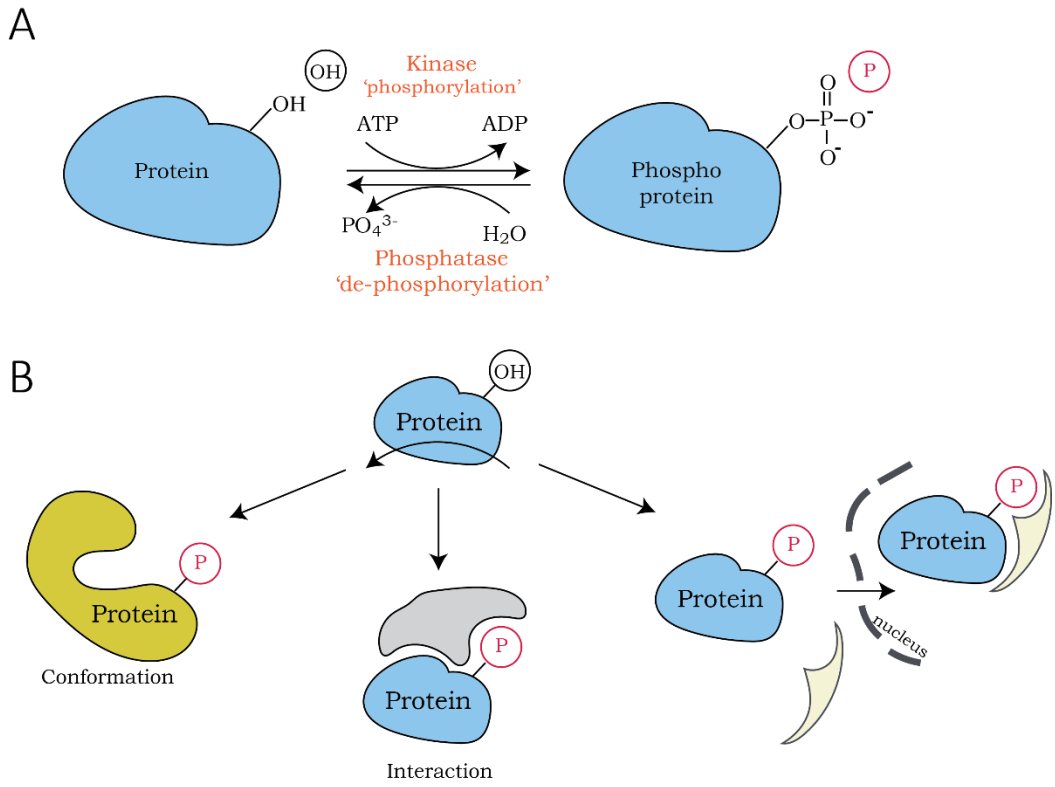

Figure 1.3 Protein phosphorylation

A Proteins can be phosphorylated by kinases in an ATP-dependent manner. The process can be reversed by a class of proteins named phosphatases. **B** Protein phosphorylation can lead to a variety of changes, including shifts in protein structure and/or activity, interaction with other proteins and target protein localisation.

Protein phosphorylation is catalysed by a family of 518 enzymes, termed kinases, while its reversal is achieved via hydrolysis facilitated by the phosphatase family members. Protein kinases (PKs) can be classified by amino acid they phosphorylate or by sequence homology of their kinase domain. The first method gives rise to serine/threonine kinases and tyrosine kinases (TKs), which are further subdivided into receptor and non-receptor TKs. The second method was used in a landmark bioinformatic study that has classified all known and newly identified human kinases according to their sequence similarities and giving rise to the human kinome (Manning et al., 2002). Kinases in the eukaryotic protein kinase (ePK) superfamily were divided into TK; TKL (tyrosine kinase-like); STE (containing the homologues of yeast Sterile 7, Sterile 11 and Sterile 20 kinases); CK1 (casein kinase 1); AGC (containing PKA, PKG and PKC families); CAMK (calcium/calmodulin-dependent protein kinases); and

CMGC (containing the CDK, MAPK, GSK3 and CLK families) subfamilies (Manning et al., 2002). A smaller kinase superfamily with an atypical protein kinase (aPK) domain comprised of 13 families was also reported (Manning et al., 2002).

Protein phosphatases catalyse the removal of the phosphate group(s) from a phosphoprotein via hydrolysis leading to the release of a phosphate ion. Unlike PKs, phosphatases have evolved in separate families that have distinct structural and functional differences (Tonks, 2006). They are therefore classified into 3 distinct families depending on their catalytic activity as well as sequence and structure into protein Serine-Threonine phosphatases, Tyrosine phosphatases, and dual (S/T-Y) phosphatases (Cohen, 2011). Representing a far smaller group of proteins, protein phosphatases are more promiscuous than their kinase counterparts, however, their activity is very finely controlled. This is achieved through a dynamic association and dissociation of the catalytic and regulatory subunits that is spatially and temporally controlled (Tonks, 2006, Shi, 2009).

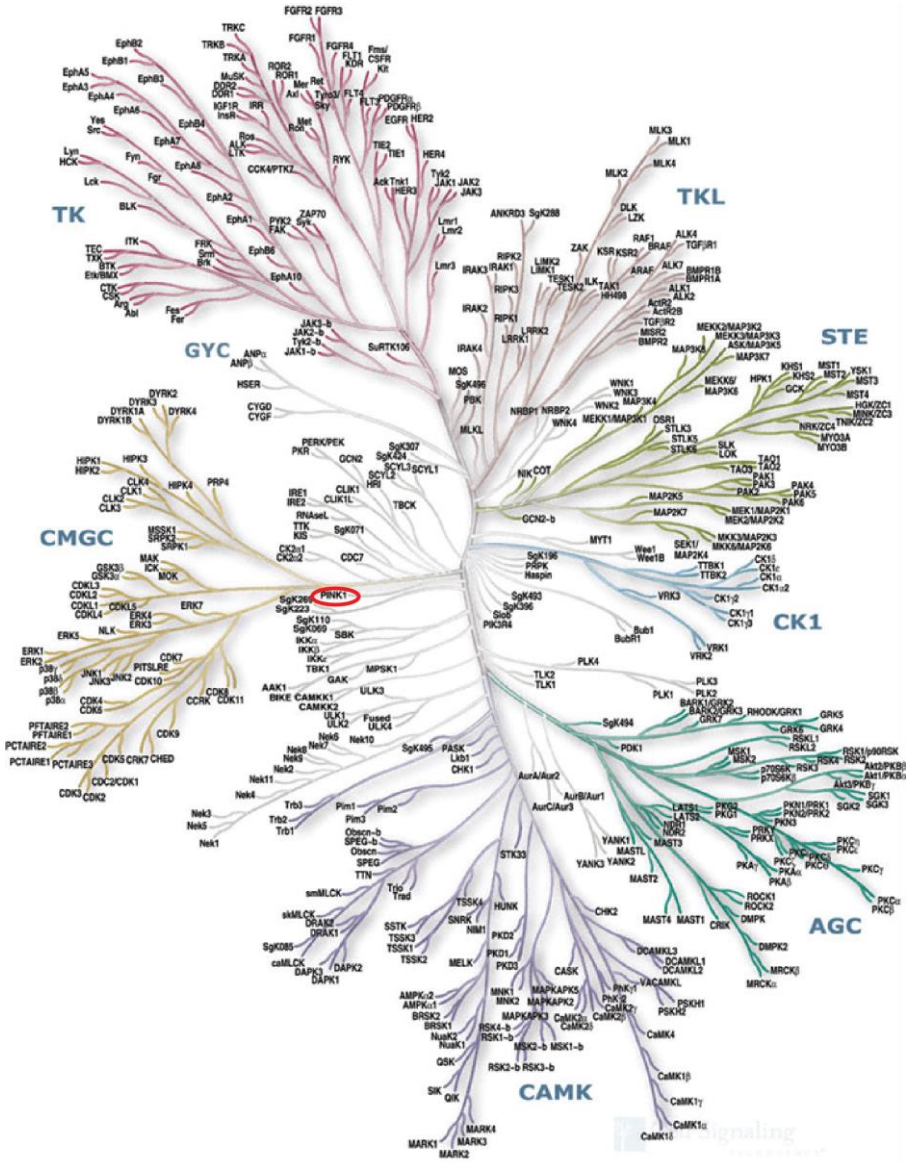

Figure 1.4 The human kinome

Classification ePKs by Manning et al, 2002: TK (tyrosine kinase); TKL (tyrosine kinase-like); STE (containing the homologues of yeast Sterile 7, Sterile 11 and Sterile 20 kinases); CK1 (casein kinase 1); AGC (containing PKA, PKG and PKC families); CAMK (calcium/calmodulin-dependent protein kinases); and CMGC (containing the CDK, MAPK, GSK3 and CLK families). PINK1, a kinase mutated in PD, is highlighted in a red oval.

1.2.2.2 Protein kinases and human disease

Protein phosphorylation is a ubiquitous regulatory mechanism evolutionary conserved in all living organisms, including bacteria, archaea and eukaryotes. It therefore comes as no surprise that upon failure to preserve normal kinase functions, whether due to genetic inheritance or sporadic mutations, diseases can arise. Mutations in kinases have been associated with neurological disorders, cancers and autoimmune diseases summarised in (Lahiry et al., 2010) and http://www.cellsignal.com/common/content/content.jsp?id=science-tables-kinase-disease. The ever-increasing number of kinase mutations associated with human disease has led to research into molecular pathways underlying pathologies and human kinases have become a popular drug target (Cohen and Alessi, 2013). The proof of concept was achieved with Imatinib (Gleevec) that was designed to inhibit a constitutively active TK Bcr-Abl that causes the development of chronic myeloid leukaemia (Capdeville et al., 2002). To date, 28 small molecule kinase inhibitors have been approved by Food and Drug Administration (FDA), two of which were approved earlier this year (Wu et al., 2015).

1.3 Parkin

Autosomal-recessive mutations in Parkin were first identified in an Asian cohort of PD patients in 1998 (Kitada et al, 1998) and have since been established as the most common cause of early onset (‹40 yr) PD (˜20% worldwide, ˜50% of familial forms, ˜80% in cases when onset ‹20yr) (Hedrich et al., 2004, Periquet et al., 2003, Lucking et al., 2000). The PARK2 gene is the second largest in the human genome, spanning over 1.3 MB; it contains 12 exons and encodes a 465 amino acid (52 kDa) protein that functions as an E3 ligase (Zhang et al., 2000, Shimura et al., 2000).

Parkin is a complex multi-domain protein that belongs to the RBR family of E3 ligases (Figure 1.5). It has an N-terminal regulatory Ubl domain that shares 31% identity and 61% similarity with ubiquitin (Tanaka et al., 2001). The C-terminal portion of the protein harbours a RING1 domain separated by an IBR domain from the catalytic IBR-like RING2

domain forming a catalytic core of the enzyme. The two ends of the protein are connected via unique Parkin domain (UPD) (Figure 1.5). Parkin was first identified as a candidate E3 ligase due to sequence homology with other RING domains and upon testing it was shown to have E2-dependent ubiquitylation activity (Zhang et al., 2000, Shimura et al., 2000). While mutation-induced failure to regulate canonical proteasome-dependent degradative pathways was the first leading hypothesis as per mode of pathology, it was soon challenged by the discovery of non-degradative functions of Parkin – formation of Parkin-dependent K48 and K63 polyubiquitin chains was demonstrated on synphilin1 (Lim et al., 2005). In addition, Parkin was shown to possess auto-ubiquitylation, mono and multi-mono ubiquitylation activities (Hampe et al., 2006). In recent years the understanding of Parkin-dependent ubiquitylation function has become even more complicated due to reports demonstrating Parkin's apparent lack of preference for a single ubiquitin type topology both *in vitro* and in cells (Kazlauskaite et al., 2014a, Ordureau et al., 2014).

In addition to a large functional variety, Parkin displays a great range of neuroprotective effects. In different model systems Parkin has been shown to mediate neuroprotection against mitochondrial-dependent apoptosis, dopamine-mediated toxicity, kainate-induced excitotoxicity, the toxicity associated with overexpression of parkin substrates or other proteins (Pael-R, p38/JTV-1, mutant α-synuclein, CDCrel-1, mutant tau and an expanded polyglutamine ataxin-3 fragment), proteasomal inhibition, mitochondrial toxins (MPP^+ and rotenone) and manganese toxicity among others (Moore, 2006). *Vice versa*, parkin-deficient cells are characterized by an increased vulnerability to stress-induced cell death (Exner et al., 2012). It is therefore paramount to understand the molecular details underlying Parkin regulation and function to gain a better understanding of neuronal vulnerability.

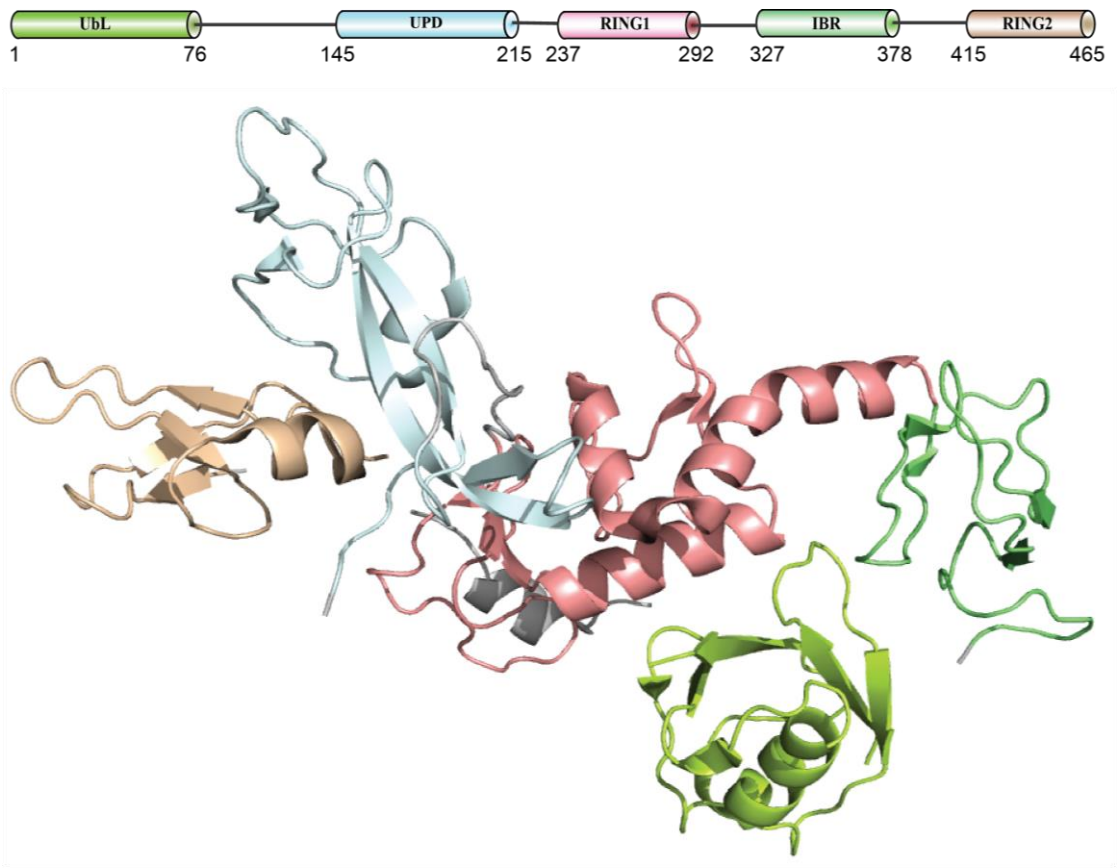

Figure 1.5 Domain architecture and structure of Parkin

Top. Representative view of Parkin domain architecture. Ubl – ubiquitin like domain, UPD, RING1 and RING2 – really interesting new gene domains 0, 1 and 2, IBR – in between RING domain. **Bottom.** Crystal structure of full-length Parkin, colouring the same as above. PDB ID: 4k95

Parkin normally resides in the cytoplasm, but upon mitochondrial stress it translocates to the mitochondria via mechanisms discussed later in this chapter. Historically, Parkin was believed to be a constitutively active RING E3 ligase. It was work by Wenzel and colleagues that had revealed for the first time that Parkin contains a catalytic cysteine in the RING2 domain, Cys431, thereby suggesting it may have RING-HECT hybrid properties (Wenzel et al., 2011). Further analysis revealed that Parkin exists in an auto-inhibited conformation mediated by its Ubl domain (Chaugule et al., 2011) and that addition of N-terminal tags displaces this mechanism and leads to constitutive enzyme activation (Burchell et al., 2012). The panoply of auto-inhibitory intramolecular interactions was greatly expanded once Parkin structures were solved: Ubl domain and repressor element (REP) of Parkin were shown to bind RING1 where the putative E2 binding site is located (Riley et al., 2013, Wauer and Komander, 2013, Trempe et al., 2013) (Figure 1.5). Furthermore, the interaction between the UPD and RING2 domains was revealed to partially occlude the catalytic site, suggesting that several molecular rearrangements need to occur for Parkin activation. The key upstream signal leading to initiation of these conformational changes – phosphorylation by PINK1 – is the main subject of this thesis.

1.4 PINK1

PINK1 gene was first described in 2001 when it was found to be up-regulated upon introduction of exogenous PTEN in endometrial cancer cells (Unoki and Nakamura, 2001), the same year that the PARK6 locus was identified in a consanguineous Sicilian family with EOPD (Valente et al., 2001). However, it was not until 2004 with the identification of two other consanguineous families (one from Italy and one from Spain) that homozygous autosomal recessive mutations were mapped onto PINK1 (Valente et al., 2004).

PINK1 gene is ubiquitously expressed in humans with higher abundance detected in heart, skeletal muscle and testis (Unoki and Nakamura, 2001). PINK1 encodes a 581 amino acid Ser/Thr protein kinase that is unique amongst all other PKs. It has an N-terminal mitochondrial targeting sequence (MTS) and a transmembrane domain. The catalytic kinase

domain resides in the C-terminal portion of the protein and contains three insertions that are not conserved with other human kinases (Cardona et al., 2011).

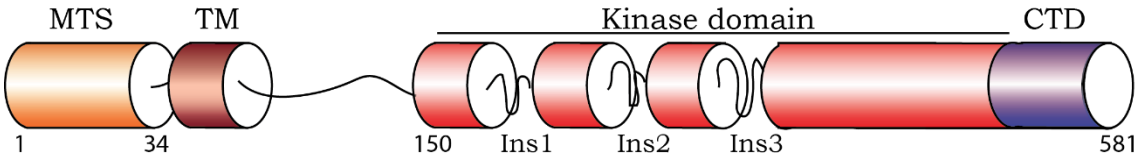

Figure 1.6 Domain architecture of PINK1.

MTS- mitochondrial targeting sequence, TM –transmembrane helix, Ins1, Ins2, Ins3 – insertions 1,2 and 3 respectively, CTD – C-terminal domain.

The presence of the N-terminal MTS dictates that in cells PINK1 gets imported to mitochondria (Figure 1.7). Translocase of the outer membrane (TOM) is a multi-subunit complex on the outer mitochondrial membrane that selectively recognises and successively imports PINK1 across the inner mitochondrial membrane via TIM40 and TIM23 (Figure 1.7) (Model et al., 2002, Lazarou et al., 2012). Upon mitochondrial import, PINK1 undergoes sequential cleavage by mitochondrial proteases MPP (mitochondrial processing peptidase) and PARL (presenilin-associated rhomboid-like protein) (Figure 1.7) (Deas et al., 2011, Jin et al., 2010, Whitworth et al., 2008, Greene et al., 2012); the C-terminal fragment of PINK1 lacking the first 103 amino acids is then released to the cytoplasm where its N-terminal residue, Phe, signals it for rapid degradation via the N-end rule pathway (Yamano and Youle, 2013) (Figure 1.7). Consequently, very low levels of PINK1 are detectable in healthy cells.

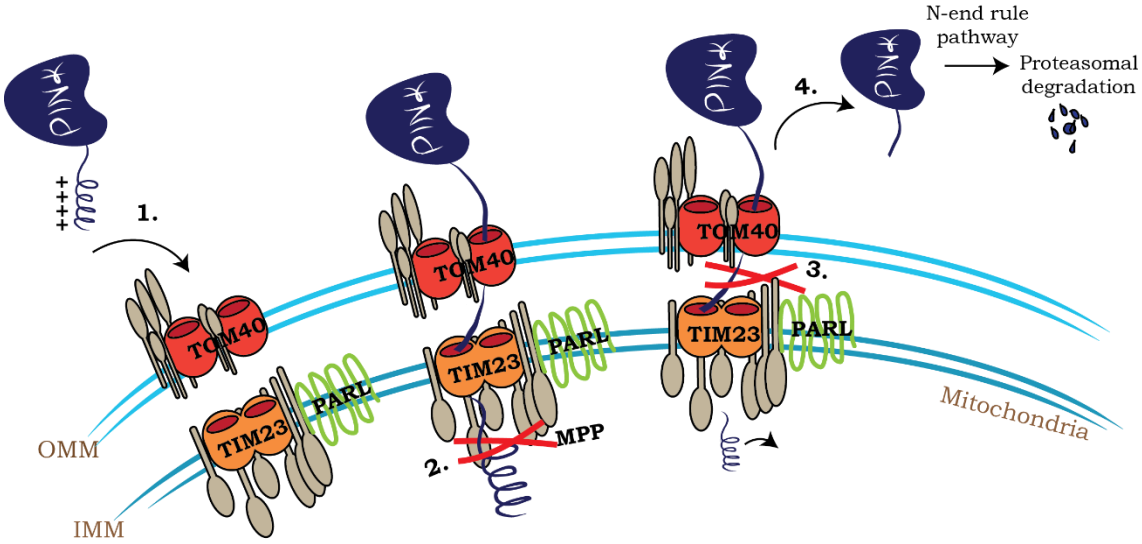

Figure 1.7 PINK1 import and processing.

PINK1 gets imported to mitochondria via its N-terminal positively charged MTS through TOM/TIM machinery as depicted above. It then gets sequentially cleaved by MPP and PARL. Releasing a C-terminal fragment lacking first 103 amino acids. This is then recognized by N-end rule pathway and degraded by proteasome.

PINK1 stability was first found to be regulated by mitochondrial membrane potential in a seminal study wherein cellular treatment with valinomycin was found to inhibit PINK1 cleavage and hence degradation (Lin and Kang, 2008). This in turn led to its accumulation on the outer mitochondrial membrane (OMM) (Lin and Kang, 2008) where its kinase domain is exposed to cytosol and available for substrates (Zhou et al., 2008). Further studies have demonstrated that a mitochondrial ionophore, carbonyl cyanide m-chlorophenyl hydrazone (CCCP), also leads to PINK1 accumulation on the mitochondria (Meissner et al., 2011, Matsuda et al., 2010, Narendra et al., 2010) due to inhibition of PARL protease that is dependent on mitochondrial potential (Jin et al., 2010).

1.5 PINK1, Parkin and mitochondrial integrity

1.5.1 Mitochondria in Parkinson's disease

It was a batch of illicitly produced heroin and a group of Californian drug addicts that provided the first compelling link between mitochondrial dysfunction and PD (Langston et

al., 1983). The botched heroin contained a neurotoxic byproduct MPTP (1-methyl-4-phenyl-1,2,3,6-tetrahydropyridine) that readily crosses brain-blood barrier and is rapidly incorporated into the acidic organelles of astrocytes where it is oxidised to MPP^+ (1-methyl-4-phenylpyridinium) (Brady et al., 2005). Upon release to the extracellular matrix, MPP^+ is taken up by dopaminergic nerve terminals via dopamine transporters, where it exercises its effects via complex I (NADH ubiquinone oxidoreductase) inhibition leading to a severe dopaminergic loss and Parkinsonism (Nicklas et al., 1985).

Mitochondrial dysfunction in PD is further supported by increased incidence of atypical Parkinsonism syndromes in Guadeloupe, where consumption of teas containing complex I inhibitor annonacin is common (Exner et al., 2012). Reduction in complex I activity levels has also been reported in substantia nigra pars compacta neurons and frontal cortex of post-mortem PD brains (Parker et al., 2008, Schapira et al., 1989). In addition, complex I subunits isolated from the frontal cortex samples from PD patients displayed oxidative damage and reduction in levels attributed to decreased stability caused by oxidative damage (Keeney et al., 2006). Altogether, this evidence has strongly implicated mitochondrial damage in PD, but it was not until the discovery of PINK1 that first direct link has been established.

1.5.2 PINK1 and Parkin - sensors of mitochondrial damage

The very first suggestion of a mechanistic link between PINK1 and Parkin came from phenotypic studies of PD patients harbouring mutations in either one of these genes and their striking clinical resemblance (Khan et al., 2002). The decisive evidence of epistatic interaction between the two genes followed from studies of PINK1 $^{-/-}$ and Parkin $^{-/-}$ mutant *Drosophila melanogaster* flies. *Drosophila* PINK1 null flies were shown to exhibit reduced life span, mitochondrial abnormalities, neuronal loss, motor and morphological changes including altered wing posture and flight muscle degeneration – a phenotype remarkably alike Parkin null flies (Clark et al., 2006, Park et al., 2006, Greene et al., 2003). Furthermore, PINK1 $^{-/-}$ phenotype could be rescued by Parkin overexpression, but not vice versa, placing PINK1

upstream of Parkin in a putative mitochondrial pathway (Clark et al., 2006, Park et al., 2006).

Parkin normally resides in mitochondria, however, ground breaking work revealed that upon mitochondrial damage Parkin could be selectively recruited to damaged mitochondria and stimulate their autophagic removal termed mitophagy (Narendra et al., 2008). Given the epistatic regulation of PINK1 and Parkin and knowledge that upon mitochondrial damage PINK1 accumulates on the OMM with its catalytic core exposed to the cytosol, it was plausible that the two proteins interact directly. Indeed, it was later shown that Parkin recruitment was PINK1 dependent and could be induced in healthy cells by exogenous introduction of non-cleavable forms of PINK1 (Geisler et al., 2010, Matsuda et al., 2010, Narendra et al., 2010, Vives-Bauza et al., 2010).

The mechanisms underpinning Parkin recruitment to mitochondria remained elusive for a long time. In the last several years it has been discovered that PINK1 stabilisation was associated with an increase in its catalytic kinase activity and autophosphorylation at Ser228, Thr257 and Ser402 providing the first direct evidence that mammalian PINK1 was an active kinase (Kondapalli et al., 2012, Okatsu et al., 2012). Parkin recruitment was also shown to be directly dependent on PINK1 activity (Geisler et al., 2010, Matsuda et al., 2010, Narendra et al., 2010, Vives-Bauza et al., 2010). The first evidence of direct regulation of Parkin by PINK1 came from studies from our lab. Utilizing catalytically active PINK1 insect orthologues (Woodroof et al., 2011) Dr Chandana Kondapalli demonstrated that Parkin is directly phosphorylated by PINK1 at Serine 65 (Ser^{65}) (Kondapalli et al., 2012) which was confirmed by another group (Shiba-Fukushima et al., 2012) and provided the framework for my project and subsequent analysis of PINK1 phosphorylation-dependent activation of Parkin.

It was initially postulated that PINK1-dependent phosphorylation might serve to alter Parkin localisation and lead to its recruitment to OMM, however, Ser65Ala (S65A) mutant lacking phosphorylation site displayed only a partial defect in mitochondrial translocation, suggesting that additional factors or PINK1 substrates were required (Shiba-Fukushima et al., 2012).

Very recently work in our lab and two others have identified the missing molecular player – PINK1 phosphorylated ubiquitin (Kazlauskaite et al., 2014c, Kane et al., 2014, Koyano et al., 2014), which was later shown to be the missing link for Parkin translocation (Okatsu et al., 2015). It is perhaps ironic that having come to do my PhD at MRC Protein Phosphorylation and Ubiquitylation Unit, I have been part of a team of scientists that have observed and defined the interaction of the two in its most acute form.

1.5.3 PINK1, Parkin and mitophagy

Mitochondria serve key functions in eukaryotic cells including generation of ATP, calcium signalling and pre-programmed cell death as well as participation in generation and removal of reactive oxygen species (ROS) (Suliman and Piantadosi, 2016), it is therefore no wonder that health and integrity of mitochondria are closely monitored and well maintained. Mitochondria are formed by an expansive network of organelles undergoing constant dimensional and structural changes aimed at meeting the energy requirements of the cell (Suliman and Piantadosi, 2016). The mass, shape and function of mitochondria is largely regulated by its biogenesis opposed by selective degradation of damaged or senescent mitochondria via mitochondria-specific autophagy termed mitophagy. Interruption of these processes results in failure to maintain healthy mitochondria has been linked to a large number of pathologies (Wallace et al., 2010). Upon induction of mitophagy, the proteins on the OMM get ubiquitylated (further discussed below) leading to recruitment of LC3-interacting region (LIR)-containing autophagy receptors (mitophagy receptors) that in turn interact with phagophore which enlarges to fully engulf the damaged organelle and form an autophagosome (Hamacher-Brady and Brady, 2015). The autophagosome then fuse with an endolysosome leading to formation of a mature autolysosome wherein the lysosomal hydrolases degrade its contents (Hamacher-Brady and Brady, 2015).

There is accumulating evidence that implicates PINK1-Parkin signalling in the selective removal of damaged mitochondria via mitophagy (Pickrell and Youle, 2015). PINK1 levels in healthy cells are tightly regulated due to its mitochondrial processing and continued

degradation via the N-end rule pathway. However, upon dissipation of mitochondrial membrane potential PINK1 gets stabilised and activated making it a perfect sensor for mitochondrial damage. The subsequent recruitment of Parkin leads to generation of mitochondrial phospho-ubiquitin signal (Matsuda et al., 2010, Geisler et al., 2010). NDP52 and optineurin have recently been proposed to be the key adaptor proteins responsible for coupling mitochondrial ubiquitin and recruitment of autophagic machinery (Lazarou et al., 2015, Heo et al., 2015).

Mitochondria are highly dynamic organelles known to undergo changes in their size, shape and localisation. Mitochondrial size and shape are predominantly regulated by fusion and fission, forming highly interconnected tubular network when fusion predominates or fragmented spherical structures caused by high levels of fission (Exner et al., 2012). Their subcellular localisation is regulated by transport on cytoskeletal tracts. Several of these regulatory components have been found to be ubiquitylated and/or degraded by the PINK1/Parkin pathway including Mitofusins 1 and 2 (Mfn1 & Mfn2) – key regulators of fusion of OMM, and Miro 1 and 2 – Rho-like GTPases that facilitates anterograde and retrograde mitochondrial transport (Sarraf et al., 2013, Liu et al., 2012, Wang et al., 2011, Poole et al., 2010). It is therefore possible to conceive that PINK1/Parkin pathway plays a key role in regulating mitochondrial remodelling. Degradation of Mfn 1&2 prevents mitochondrial fusion, promoting sequestering of damaged mitochondrial units, while removal of Miro 1 & 2 stops its transport and boosts clustering (Tanaka et al., 2010, Wang et al., 2011, Liu et al., 2012). What role, if any, this plays in the subsequent mitophagy remains to be seen since studies from Mfn1 and 2 knockout fibroblasts revealed that Parkin-dependent mitophagy was not affected (Narendra et al., 2008).

1.6 Project aims

Whilst a genetic interaction between PINK1 and Parkin was discovered in 2006 (Park et al., 2006, Clark et al., 2006) defining a linear pathway with PINK1 upstream of Parkin, little was known about its molecular details. Progress was greatly hampered by lack of functional kinase

assays due to low PINK1 activity *in vitro* as well as low levels of PINK1 in cells. This was overcome by the discovery of active insect PINK1 orthologues (Woodroof et al., 2011) which were used to demonstrate that Parkin is a direct substrate of PINK1 and gets phosphorylated at Ser^{65} (Kondapalli et al., 2012). At the time I started the project in 2011, the first reports suggesting that Parkin is an autoinhibited E3 ligase that has a catalytic cysteine were being published (Burchell et al., 2012, Chaugule et al., 2011, Wenzel et al., 2011). These groundbreaking insights provided a platform upon which I could rigorously explore the PINK1/Parkin interaction and the role of phosphorylation on Parkin activation. The work presented in this thesis therefore addresses the following questions that were unsolved at the time my work commenced:

- ✓ *What is the functional relationship between PINK1 and Parkin?*
- ✓ *What is the consequence of Ser^{65} phosphorylation on the Parkin Ubl domain and Parkin E3 ligase activity?*
- ✓ *Based on PINK1 activation of Parkin, is it possible to elaborate a specific substrate based assay of Parkin E3 ligase activity in vitro and assess the impact of disease mutations?*
- ✓ *Are there any additional factors involved in Parkin regulation by PINK1?*
- ✓ *How does ubiquitin phosphorylation influence Parkin's activity in vitro?*
- ✓ *What is the mechanism of activation of Parkin by phosphorylated ubiquitin and where does phosphorylated ubiquitin bind Parkin?*
- ✓ *How does phosphorylated ubiquitin binding to Parkin confer activation in cells?*

2 Chapter 2 Materials and Methods

2.1 Materials

2.1.1 Reagents

Acetone, ethanol, formic acid, glycerol, glycine, 4-(2-Hydroxyethyl)piperazine-1-ethanesulfonic acid (Hepes), isopropanol, methanol, 2-mercaptoethanol, orthophosphoric acid, potassium chloride, sodium chloride, sodium ethylenediaminetetraacetic acid (EDTA), magnesium acetate, sodium ethylene glycol tetraacetic acid (EGTA), sodium fluoride, sodium β-glycerophosphate, sodium orthovanadate, pentobarbital, puromycin, adenosine 5'-triphosphate sodium salt (ATP), anti-HA-agarose, ammonium bicarbonate, ammonium persulphate (APS), ampicillin, benzamidine, bovine serum albumin (BSA), bromophenol blue (BPB), dexamethasone, doxorubicin, dimethyl pimelimidate (DMP), dimethyl sulphoxide (DMSO), hydrogen peroxide, iodoacetamide, phenylmethanesulphonylfluoride (PMSF), Ponceau S, sodium dodecyl sulphate (SDS), sodium tetraborate, N, N, N', N'-Tetramethylethylenediamine (TEMED), triethylammonium bicarbonate, Nonidet P40, Triton-X-100 and Tween-20 were from Sigma-Aldrich (Poole, UK). Sucrose and Tris(hydroxymethyl)methylamine (Tris) were from BDH (Lutterworth, UK). Cellophane films and Precision Plus protein markers were from BioRad (Herts, UK). 3-[(3-Cholamidopropyl)dimethylammonio]-1-propanesulfonate (CHAPS) was from Calbiochem (Merck Biosciences, Nottingham, UK). Polybrene was from SantaCruz Biotechnology (Heidelberg, Germany). Cell culture dishes and flasks, cryovials and Spin-X columns were from Corning (NY, USA). Cell scrapers were from Costar (Cambridge, USA). 40% (w/v) 29:1 Acrylamide:Bis-Acrylamide solution was from Flowgen Bioscience (Nottingham, UK). Protein A-agarose, Protein G-sepharose, Glutathione-sepharose, Enhanced chemiluminescence (ECL) kit, Hyperfilm MP, Protran nitrocellulose membrane, P81 paper, 3mm chromatography paper were from GE Healthcare (Piscataway, USA). [γ-^{32}P] ATP was from Perkin Elmer (USA). Cell dissociation buffer, Dulbecco's modified eagle medium

(DMEM), RPMI-1640 medium, Phosphate buffered saline (PBS), Trypsin/EDTA, L-glutamine, non-essential amino acids, sodium pyruvate, antibiotic/antimycotic, NuPAGE Novex SDS Bis-Tris gels, NuPAGE MOPS running buffer, NuPAGE reducing agent, NuPAGE LDS sample buffer and primers were from Invitrogen (Paisley, UK). Photographic developer (LX24) and liquid fixer (FX40) were from Kodak (Liverpool, UK). X-ray films were from Konica (Japan). Polyethylenimine (PEI) was from Polysciences (Warrington, PA). Skimmed milk (Marvel) was from Premier Beverages (Stafford, UK). Plasmid Maxiprep kits were from Qiagen Ltd (Crawley, UK). Acetonitrile (HPLC grade) was from Rathburn Chemicals (Walkerburn, UK). Protease inhibitor cocktail was from Roche (Lewes, UK). Horseradish peroxidase (HRP)- and Alexafluor-conjugated secondary antibodies, Bradford reagent and Fetal Bovine Serum (FBS) were from Thermo-scientific (Essex, UK). Trypsin (mass spectrometry grade) were from Promega (Southampton, UK). InstantBlue protein staining solution was from Expedeon (Harston, UK).

2.1.2 Instruments

The Procise 494C Sequenator was from Applied Biosystems (Foster City, USA). Centrifuge tubes, rotors and centrifuges were from Beckmann (Palo Alto, USA). Trans-Blot Cells, automatic western blot processors and gel dryer apparatus were from BioRad (Herts, UK). SpeedVacs were from CHRIST (Osterode, Germany). HPLC system components were obtained from Dionex (Camberley, UK). Thermomixer IP shakers were purchased from Eppendorf (Cambridge, UK). The Biofuge microcentrifuge was from Heraeus Instruments (Osterode, Germany). pH meters and electrodes were from Horiba (Kyoto, Japan). X-Cell SureLock Mini-cell electrophoresis systems and X-Cell II Blot modules were from Invitrogen (Paisley, UK). X-omat autoradiography cassettes, with intensifying screens, were from Kodak (Liverpool, UK). The Konica automatic film processor was from Konica Corporation (Japan). The LiCOR odyssey infrared imaging system was from LiCOR biosciences (Cambridge, UK). CO_2 incubators were from Mackay and Lynn (Dundee, UK). Tissue culture class II safety cabinets were from Medical Air Technology (Oldham, UK). The PCR thermocycler (PTC-200) was from MJ Research. The 96-well Versamax plate reader was from Molecular Devices

(Wokingham, UK). The Vydac 218TP54 C18 reverse phase HPLC column was from Separations group. The LTQ-Orbitrap mass spectrometer and Nanodrop was from Thermo Scientific. Scintillation counter (Tri-Carb 2800 TR) was from Perkin-Elmer. Vibrax-VR platform shaker was from IKA. Vydac 218TP54 C18 reverse phase HPLC column was from Separations Group. Dionex HPLC system components were from Dionex GINA50 autosampler, Dionex P580 pump, DionexUVD1705 detector, EG&G Berthold Radioflow Detector LB509 and Gilson FC204 fraction collector.

2.1.3 In-house reagents

Primers were synthesised by the University of Dundee oligonucleotide synthesis service. Bacterial culture medium Luria Bertani (LB) broth and LB agar plates were provided by the University of Dundee media kitchen facility. The Protein Production Team at Division of Signal Transduction and Therapy (DSTT) expressed and purified His-SUMO-Miro1 as well as kinases used in the ubiquitin kinase screen. His-SUMO-Protein purification of recombinant Parkin was carried out by the Protein Production and Assay Development (PPAD) team led by Dr Axel Knebel.

2.1.4 Antibodies

In-house antibodies (Table 2.1) were raised in sheep and affinity purified on the appropriate antigen by the DSTT. In-house antibodies were used at 1 μg/mL in 5% (w/v) skimmed milk in 0.1% Tween/TBS (TBST) and the in-house phospho-specific antibodies were used at 1 μg/mL in 5% (w/v) BSA-0.1%TBST supplemented with 10 μg/mL non-phospho peptide to increase specificity. Table 2.2 summarizes commercial antibodies used. The anti-SUMO-1 antibody was a kind gift from Professor Ron Hay (Dundee). Epitomics raised anti-Parkin^{PhosphoSer65} rabbit monoclonal antibody in collaboration with the Michael J Fox Foundation for Research.

Table 2.1 In house antibodies used in this study

Antibody	Immunogen	Sheep Number	Bleed Number
Parkin human	GST-Parkin full length	S966C	3rd
Parkin human	GST-Parkin 1-108	S229D	3rd
Parkin phospho Ser 65	RDLDQQS*IVHIVQR [residues 60 - 72 of human PARKIN]	S210D	2nd

Table 2.2 Commercial antibodies used in this study

Antibody	Catalogue number	Company	Host
Parkin human	Sc-32282	SantaCruz	Mouse
PINK1 human	BC-100-494	Novus	Rabbit
GAPDH	2118	Cell Signaling	Rabbit
Actin	A2066	Sigma	Rabbit
CISD1	16006-1-AP	Proteintech Europe	Rabbit
TOMM70A	14528-1-AP	Proteintech Europe	Rabbit
MBP-HRP	E8038S	New England Biolabs	Mouse
FLAG-HRP	A8592	SIGMA	Mouse

2.1.5 DNA constructs

Dr M. Peggie, Dr R. Toth, Dr N. Wood, Mrs M. Wightman and Mr T. Macartney performed the cloning, subcloning and mutagenesis of the constructs described in this thesis. Constructs used are shown in Table 2.3 & Table 2.4. All constructs encoded the human version of the gene unless otherwise indicated.

Table 2.3 Parkin constructs used

Expressed	Plasmid	Vector Type	DU Number
6His SUMO Parkin	pET156P	Bacterial	DU40847
6His SUMO Parkin 1-76	pET156P	Bacterial	DU39607
6His SUMO Parkin 80-465	pET156P	Bacterial	DU39813
6His SUMO Parkin 80-465 K151A	pET156P	Bacterial	DU46032
6His SUMO Parkin 80-465 H302A	pET156P	Bacterial	DU46034
6His SUMO Parkin K27N	pET156P	Bacterial	DU39837

6HIs SUMO Parkin R33Q	pET156P	Bacterial	DU39824
6HIS SUMO Parkin R42P	pET156P	Bacterial	DU39784
6His SUMO Parkin A46P	pET156P	Bacterial	DU44510
6His SUMO Parkin S65A	pET156P	Bacterial	DU23314
6His SUMO Parkin K151A	pET156P	Bacterial	DU46082
6His SUMO Parkin K161A	pET156P	Bacterial	DU43800
6His SUMO Parkin K161N	pET156P	Bacterial	DU44321
6His SUMO Parkin R163A	pET156P	Bacterial	DU43801
6His SUMO Parkin K211A	pET156P	Bacterial	DU43818
6His SUMO Parkin K211N	pET156P	Bacterial	DU23325
6His SUMO Parkin R275W	pET156P	Bacterial	DU43127
6His SUMO Parkin H302A	pET156P	Bacterial	DU46033
6His SUMO Parkin R305A	pET156P	Bacterial	DU46035
6His SUMO Parkin Q316A	pET156P	Bacterial	DU46037
6His SUMO Parkin G328E	pET156P	Bacterial	DU44322
6HIS SUMO Parkin T415N	pET156P	Bacterial	DU39786
6His SUMO Parkin G430D	pET156P	Bacterial	DU43129
6His SUMO Parkin C431F	pET156P	Bacterial	DU46232
6His SUMO Parkin R455A	pET156P	Bacterial	DU46030
6His SUMO parkin 80-465 biotin affinity peptide (BAP)	pET156P	Bacterial	DU39836
6His SUMO parkin 80-465 BAP H302A	pET156P	Bacterial	DU46812
GST-Parkin 1-76	pGEX6P	Bacterial	DU37369
GST-Parkin 1-108	pGEX6P	Bacterial	DU37370
Parkin	pcDNA5-FRT/TO	Mammalian	DU23307
Parkin S65A	pcDNA5-FRT/TO	Mammalian	DU23315
Parkin H302A	pcDNA5-FRT/TO	Mammalian	DU48502
Parkin C431F	pcDNA5-FRT/TO	Mammalian	DU23340

Table 2.4 PINK1 constructs used

Expressed	**Plasmid**	**Vector Type**	**DU Number**
PINK1 - FLAG	pcDNA5-FRT/TO	Mammalian	DU17461
PINK1 - FLAG D384A	pcDNA5-FRT/TO	Mammalian	DU17462
FLAG-empty	pcDNA5 FRT/TO	Mammalian	DU 41457
MBP-PINK1 (Tribolium castaneum)	pMal4c	Bacterial	DU34701
MBP-PINK1 (Tribolium castaneum) D359A	pMal4c	Bacterial	DU34832
GST-Pediculus humanus corporis PINK1	pGEX6P1	Bacterial	DU26052

2.1.6 Buffers and solutions

Lysis buffer inhibits proteases, kinases, phosphatases and other divalent cation-dependent enzymes ensuring that the phosphorylation and expression levels of proteins are fixed at the levels in which they are found *in vivo*. Benzamidine and PMSF or complete protease inhibitor tablets prevent the action of metallo, aspartic, cysteine and serine proteases. EDTA chelates Mg^{2+} and EGTA chelates Ca^{2+}. Sodium fluoride, sodium-ß-glycerophosphate and sodium pyrophosphate are Ser/Thr phosphatase inhibitors. Sodium orthovanadate is a Tyr phosphatase inhibitor. Sodium orhovanadate was prepared, as recommended by the manufacturer, by repeated rounds of boiling and cooling until the solution was colourless at pH10 at room temperature to ensure that it is in the monomeric state that favours Tyr phosphatase inhibition. Buffers used in this thesis are summarised in Table 2.5.

Table 2.5 Commonly used buffers

Buffer	Composition
Mammalian cell lysis buffer	25 mM Tris (pH 7.5), 1 mM EDTA, 1 mM EGTA, 1% Triton X-100, 50 mM NaF, 5 mM sodiumpyrophosphate, 1 mM sodium orthovanadate, 10 mM sodium b-glycerophosphate, 1 mM benzamidine, 0.2 mM PMSF, 0.1% 2-mercaptoethanol, 0.27 M sucrose and one mini Complete™protease inhibitor cocktail tablet per 10ml of lysis buffer.
TBS-Tween buffer	50 mM Tris-HCl (pH 7.5), 0.15 M NaCl and 0.1% (v/v) Tween-20.
5X sodium dodecyl sulphate (SDS) sample buffer	250 mM Tris-HCl (pH 6.8), 5% SDS, 5% (v/v) 2 - mercaptoethanol, 32.5% (v/v) glycerol, 0.05% bromophenol blue.
Tris-Glycine SDS running buffer	25 mM Tris-HCl (pH 8.3), 192 mM glycine, 0.1% (w/v) SDS.
Tris-Glycine transfer buffer	48 mM Tris-HCl (pH 8.3), 39 mM glycine, 20% (v/v) methanol.
Kinase assay reaction buffer	50mM Tris-HCl (pH 7.5), 0.1 mM EGTA, 10 mM MgCl2, 2 mM DTT and 0.1 mM [γ-32P] ATP (approx. 500 cpm/pmol).
Enhanced chemiluminescence Reagent (ECL)	ECL1: 100 mM Tris-HCl pH 8, 2.5 mM Luminol, 0.4 mM p-Coumaric Acid. ECL2: 100 mM Tris-HCl pH 8, 5.6 mM H2O2. Stored in the dark at 4ºC. Equal volumes ECL1 and ECL2 are mixed immediately before the use.

2.1.7 Inhibitors/treatments

Carbonyl cyanide 3-chlorophenylhydrazone (CCCP) was purchased from SIGMA, dissolved in DMSO and stored at -20 °C.

2.2 Methods

2.2.1 Transformation of chemically competent *Escherichia coli* (*E.coli*)

Calcium competent *E.coli* DH5α (Inoue et al., 1990) cells were provided by the DSTT. Approximately 10-50 ng DNA was added to 50 µl of competent cells and incubated on ice for 5 min. Bacterial cells were then subjected to heat shock at 42 °C in a water bath for 90 seconds to induce the uptake of DNA and briefly placed back on ice. Cells were streaked onto LB agar plates containing 200 µg/mL ampicillin and plates incubated at 37 °C overnight.

2.2.2 Purification of plasmids from E.coli

Transformed DH5α *E.coli* were cultured in 250 mL LB containing 200 µg/mL ampicillin at 37 °C while shaking at 180 rpm overnight. Cells were pelleted by centrifugation at 5000 *x g* for 15 min at 4 °C. Plasmid DNA was purified using the Qiagen plasmid Maxiprep kit according to the manufacturer's instructions.

2.2.3 Measurement of DNA and RNA concentration

DNA and RNA concentrations were measured using NanoDrop as per manufacturer's instructions based on RNA and DNA absorption at 260 nM. Absorbance was also measured at 280 nM to enable calculation of 260/280 ratio for estimation of purity. Ratios greater than 1.8 were indicative of high purity. Lower ratios were suggestive of the presence of phenol, protein or other contaminants.

2.2.4 DNA mutagenesis

Site-directed mutagenesis was performed using the QuikChange kit (Stratagene) and KOD polymerase (Novagen). Mutation incorporation was verified by DNA sequencing.

2.2.5 DNA sequencing

Plasmid sequencing was performed by the DNA Sequencing service (School of Life Sciences, University of Dundee, www.dnaseq.co.uk) using Applied Biosystems Big-Dye v. 3.1 chemistry on an Applied Biosystems model 3730 automated capillary DNA sequencer.

2.2.6 Cell culture

All procedures were carried out in aseptic conditions meeting biological safety category 2 regulations. Cells were maintained at 37 °C in a 5 % CO_2 water saturated incubator. The passaging of cells was performed by washing the cells with PBS followed by incubation with Trypsin/EDTA to detach the cells. Detached cells were resuspended in cell culture medium and split at a 1:2 – 1:20 ratios for continued culture. Human embryonic kidney 293 (HEK293) and HeLa cells were cultured in Dulbecco's modified eagle medium (DMEM); neuroblastoma SH-SY-5Y cells were cultured in 50:50 mixture of DMEM and Ham's F12 media. All cell lines were grown in the presence of 10 % (v/v) foetal bovine serum (FBS), 2 mM L-glutamine, 100 U/mL penicillin and 0.1 mg/mL streptomycin. HeLa PINK1 CAS9 knock-out cells (Narendra et al., 2013b) and HeLa T-REX flp-in culture medium was additionally supplemented with 1x non-essential amino acids.

2.2.7 Freezing / thawing cells

Confluent cells grown in T-75 flasks were trypsinized and collected in culture media by centrifuging at 500 *x g* for 5 min. Culture media was aspirated and cells were resuspended in 3 ml of freezing media (50:50 mixture of DMEM and FBS supplemented with 10% DMSO). 1 mL aliquots were placed in cryovials in Nalgene Mr Frosty Freezing Containers at -80 °C

for 24 hrs prior to long-term storage in liquid nitrogen. Cells were thawed in a 37 °C water bath, resuspended in 20 ml of growth medium and allowed to adhere overnight prior to medium change.

2.2.8 Transfection of cells using polyethylenimine (PEI)

Cells were transiently transfected using the polyethylenimine (PEI) method (Fortier et al., 2013). PEI stock (1 mg/mL) was prepared by dissolving PEI powder in 20 mM Hepes (pH 7). Aliquots were filter sterilized (0.22 μm) and stored at -80 °C.

Cells were grown to 30-40 % confluency on 15 cm dishes; 9 μg of DNA was mixed with 60 μL 1mg/mL PEI and 2 mL serum-free DMEM, vortexed for 10 sec and incubated for 20 - 40 min at room temperature before being added to cells. Cells were harvested 24-72 hrs post transfection.

2.2.9 Generation of stable cell lines

To ensure low-level uniform expression of recombinant proteins, manufacturer's instructions (Invitrogen) were followed to generate stable cell lines that express proteins of interest (cDNA subcloned into pcDNA5-FRT-TO plasmid) in a doxycycline-inducible manner. Flp-In T-Rex-293 host cells containing integrated FRT recombination site sequences and Tet repressor, were co-transfected with 9 μg of pOG44 plasmid (which constitutively expresses the Flp recombinase), and 1 μg of pcDNA5/FRT/TO vector containing a hygromycin resistance gene for selection of the gene of interest under the control of a tetracycline-regulated promoter. Cells were selected for hygromycin and blasticidin resistance three days after transfection by adding new medium containing hygromycin (100 μg/ml) and blasticidin (7.5 μg/ml). After 3 – 4 weeks of selection, remaining colonies were trypsinized and expanded. Expression of the recombinant protein was induced with 0.1 μg/ml of doxycycline for 24 - 72 hours.

2.2.10 Treatment of cells with mitochondrial depolarising agents

Cells were treated with 10 μM CCCP (Sigma) dissolved in DMSO; it was added to the cell culture medium and incubated at 37 °C and 5% CO_2 for the times indicated in the figure legends. The equivalent volume of DMSO was added to another dish as a vehicle control.

2.2.11 Cell lysis and mitochondrial fractionation

Cells were lysed using mammalian cell lysis buffer as listed in Table 2.6; 0.5 ml of lysis buffer per 15 cm dish was used. Lysates were clarified by centrifugation at 14,000 *x g* for 15 min at 4 °C and the supernatant was collected. For mitochondrial fractionation, cells were harvested in ice-cold PBS and later swelled in hypotonic mitochondrial fractionation buffer (Table 2.6) at 4 °C. Cells were disrupted using a glass hand held homogeniser (40 passes) and lysates were clarified by sequential centrifugation: first, 10 min at 1200 *x g* at 4°C after which the supernatant was collected and further centrifuged at 14,000 *x g* for 10 min at 4°C. The resultant supernatant was retained as the cytosolic fraction. The pellet containing the mitochondrial fraction was resuspended in the lysis buffer and centrifuged at 14,000 *x g* for 10 min. This final supernatant contained solubilized mitochondrial proteins. All lysates were snap-frozen at -80 °C until use.

EDTA and EGTA was used to chelate divalent cations, which serve as co-factors for proteolytic activity. Sodium fluoride, sodium pyrophosphate, sodium β-glycerophosphate inhibit serine/threonine protein phosphatases; and sodium orthovanadate (Na3VO4) inhibits protein tyrosine phosphatases. Benzamidine and PMSF were added to inhibit serine proteases and metallo, aspartyl, cysteinyl, and seryl proteinases.

Table 2.6 Buffers used for cell lysis

Buffer	Composition
Cell lysis buffer	25 mM Tris (pH 7.5), 1 mM EDTA, 1 mM EGTA, 1 % Triton X-100, 50 mM NaF, 5 mM sodiumpyrophosphate, 1 mM sodium orthovanadate, 10 mM sodium β-glycerophosphate, 1 mM benzamidine, 0.2 mM PMSF, 0.1% 2-mercaptoethanol, 0.27 M sucrose and one mini Complete™protease inhibitor cocktail tablet per 10ml of lysis buffer.
Mitochondrial frantionation buffer	20 mM HEPES, 3 mM EDTA, 1 % (w/v) 1 mM sodium orthovanadate,10 mM sodium β-glycerophosphate, 250 mM sucrose, 50 mM NaF, 5 mM sodium pyrophosphate, pH 7.5 and one mini Complete™protease inhibitor cocktail tablet per 10ml of buffer.

2.2.12 Quantification of protein concentration with Bradford assay

The protein concentration of lysates was estimated using the Bradford assay in a 96 well plate in triplicates (Bradford, 1976). 200 µl of Bradford reagent, containing Coomassie Brilliant Blue G250, was added to 10 µl of sample, diluted 5-20 times in water. The assay utilizes the shift of maximum absorbance of Coomassie reagent from 465 nm to 595 nm upon binding protein in acidic medium; it is therefore possible to generate a standard curve by plotting absorbance at 595 nm against BSA standards and use it to back-calculate the sample concentrations.

2.2.13 Quantification of protein concentration with bicinchoninic acid (BCA) assay

The protein concentration of lysates containing detergent was estimated using the BCA assay. The samples were prepared the same as for Bradford assay, then 200 µl of working reagent was added to each well. The samples were incubated in the dark at 37 °C for 30 min before reading at a plate reader. The absorbance measurements at 562 nm was made. Standard curve was generated and concentrations were calculated as before. The assay uses a

colorimetric shift that is proportional to copper(II) reduction to copper(I) by peptide bonds present in the sample followed by binding of copper(I) to bicinchoninic which produces purple colour that absorbs light at 562nm.

2.2.14 Covalent coupling of antibodies

Antibodies were coupled to protein G-sepharose using a dimethyl pimelimidate (DMP) cross-linker, a homo-bifunctional imidoester that reacts with primary amine groups in the pH range 7.0 – 10.0. Protein G, isolated from Group G *Streptococci*, binds to the F_c region of IgG-class antibodies with a high affinity for antibodies generated in various species. Protein G-beads were washed in PBS 4 times followed by coating with antibody - 1 µg of antibody per 1 µl of resin was incubated for 1 hr at 4 °C. The unbound antibody was washed off with PBS followed by three washes with 10 times the bead volume of 0.1 M sodium tetraborate pH 9.3. Beads were then incubated with 20 mM DMP in 0.1 M sodium tetraborate (prepared fresh) twice for 30 min at room temperature followed by four washes with 50 mM glycine pH 2.5 to remove any non-covalently coupled antibody and further two washes with 0.2 M Tris-HCl pH 8 to neutralise the pH. Finally, the beads were incubated for 2 hrs in 0.2 M Tris-HCl pH 8 at room temperature to quench any residual DMP, before storing in PBS at 4 °C.

2.2.15 Immunoprecipitation of proteins

5 µL of covalently coupled antibody was mixed with 1 mg of lysate for 2 hrs at 4 °C on a rotating wheel. Beads were then washed twice with lysis buffer containing 0.5 M NaCl and twice with lysis buffer containing 0.15 M NaCl. Reducing agent was omitted from the washes. The immunoprecipitates were eluted by resuspending the beads in 1x LDS sample buffer lacking reducing agent for 10 min with gentle shaking followed filtering through Spin-X columns to remove the beads. Reducing agent was added to the eluted samples and the samples were heated on the heat block at 92 °C for 5 min.

2.2.16 Ubiquitin enrichment in membrane fractions

His-Halo-Ubiquilin1 UBA-domain tetramer (UBA^{UBQLN1}) was expressed in *E.coli* BL21 cells, affinity purified on Ni-NTA-agarose and dialysed into 50 mM Hepes pH 7.5, 10 % glycerol, 150 mM NaCl, 1 mM DTT. UBA^{UBQLN1} was coupled to HaloLink Resin as described previously (Kristariyanto et al., 2015a). 1 mg of mitochondria-enriched fractions were then subjected to pull downs as described previously (Kristariyanto et al., 2015a).

2.2.17 Resolution of protein samples via SDS-PAGE

Polyacrylamide gel electrophoresis (PAGE) is commonly used to separate proteins according to their electrophoretic mobility. Anionic reagents, such as sodium dodecyl sulphate (SDS) or lithium dodecyl sulphate (LDS), bind proteins linearizing them and giving them a net negative charge that is proportional to the molecular mass of the protein. Consequently, the protein migration through a PAGE matrix represents a linear function of the logarithm of their molecular weight.

Home-made isogradient and commercial 4-12% gels were used to resolve different protein species. The home-made gel constituents included a resolving gel (375 mM Tris-HCl (pH 8.6), 0.1 % SDS and 8/10/12 % acrylamide) and a stacking gel (125 mM Tris HCl pH 6.8, 0.1 % SDS, 4 % acrylamide). TEMED and ammonium persulphate (APS) were used to initiate polymerisation.

Samples for pre-cast NuPAGE 4-12% Bis-Tris gels were prepared in 1x LDS sample buffer with or without reducing agent as specified; the electrophoresis was carried out at 180 V for 50 min. Samples for home-made gels were made in 1x SDS buffer and heated at 92 °C for 2 min. The electrophoresis was initiated at 80V until the dye front entered the resolving gel; the voltage was then increased to $160 - 180$ V until the dye front reached the end of the resolving gel. 5-30 µg of lysate or 10-30 µL of immunoprecipitate were loaded per lane alongside protein standards

2.2.18 Coomassie staining of polyacrylamide gels

Polyacrylamide gels were stained in Instant Blue staining solution for 1 hr and destained with MilliQ water overnight. Gels were scanned on a Li-Cor Odyssey infrared system for imaging and quantification. For mass spectrometry, gels were stained with Colloidal Coomassie (Invitrogen) according to the manufacturer's instructions.

2.2.19 Dessication of polyacrylamide gels and autoradiography

Gels, carrying samples incorporating ^{32}P were dried to enhance signal. They were incubated in 5 % glycerol for 10 min and sandwiched between two sheets of pre-wet cellophane. The gel was then dried in a GelAir Dryer for 40-100 min. Dried gels were exposed to Hyperfilm MP for 1-72 hrs in an X-Omat autoradiography cassette. Films were developed using a Konica auto-developer.

2.2.20 Transfer of proteins onto nitrocellulose membranes

Gels were sandwiched between nylon sponges, Whatman 3 mm filter papers and nitrocellulose or PVDF membrane (pre activated in 100 % methanol) all soaked in transfer buffer. The transfer cell was submerged in transfer buffer in Biorad Trans-Blot Cell and transfer was carried out at 90 V for 2 hrs.

2.2.21 Immunoblotting

After transfer, membranes were blocked with 5% (w/v) skimmed milk or BSA in TBST for 1 hour at room temperature. Membranes were then incubated with primary antibodies diluted in either 5% (w/v) skimmed milk or BSA in TBST at 4 °C for 16 hrs. Unbound antibody was then collected and membranes were washed four times for 15 minutes with TBST at room-temperature. Horseradish peroxidase (HRP)-conjugated secondary antibodies diluted at 1:2500 in 5% (w/v) skimmed milk in TBST were incubated with the membranes for 1 hr at room temperature and the membranes were washed four more times with TBST.

Membranes were incubated with the enhanced chemiluminescence (ECL) substrate and exposed to X-ray films for various lengths of time. Films were developed using a Konica automatic developer.

2.2.22 Immunofluorescence

HeLa cells stably expressing untagged Parkin WT, S65A or H302A were plated on glass coverslips and treated as described. Immunofluorescence was performed as previously described in (Allen et al., 2013). Briefly, coverslips were washed twice with phosphate-buffered saline (PBS), fixed with 3.7 % formaldehyde, 50 mM Hepes pH 7.0 for 10 min, washed twice with and then incubated for 10 min with DMEM, 10 mM HEPES pH7.4. Cells were permeabilized by incubation with 0.2% Triton X-100 in PBS followed by two washes and blocking for 15 min at RT with PBS supplemented with 1 % BSA (PBS/1 % BSA). Cells were stained with the primary antibodies as follows: Parkin$^{\text{Phospho-Ser65}}$ (1:500) antibody for 16 h at 4 °C; total Parkin antibody (1:1000) for 1 h at 37 °C; followed by anti–mouse or anti–rabbit Alexa Fluor 405– or Alexa Fluor 488–conjugated secondary antibodies (Life Technologies). Mitochondria were stained using MITO-ID Red detection kit (Enzo Life Sciences) for 30 min at 37 °C.

Immunofluorescently labelled cells were imaged using a Zeiss LSM 700 laser scanning confocal microscope with the Alpha Plan-Apochromat x100/NA 1.46 objective (optical section thickness 0.7 μm). Parkin-Alexa 405 was excited with the 405 laser, P-Parkin-Alexa 488 was excited with the 488 laser and Mitochondria MITO-IDff Red was excited with the 555 laser. All labels were excited independently to prevent cross-channel bleed through.

2.2.23 Gel filtration chromatography analysis of complexes – performed by Dr. Axel Knebel

A Superdex 200 Increase 10/300 GL column (GE-Healthcare Life Sciences) was equilibrated with 50 mM Tris pH 7.5, 150 mM NaCl. The proteins: 100 µg of Dac-Ubiquitin, Dac-Ubiquitin^{PhosSer65}, Parkin (1-465) or Parkin 1-465 H302A or mixtures thereof, were made and subjected to chromatography on the column at a flowrate of 0.3 ml/min. Mixtures were incubated for 30 minutes prior to chromatography. The elution of the proteins was monitored by UV-absorption at 280 nm.

2.2.24 Alphascreen binding assay – performed by Dr. Scott Wilkie

Serial three fold, 10-point dilution curves of inhibitor proteins ubiquitin^{PhosSer65} and ubiquitin were prepared in PBS + 0.1 % BSA + 0.1 % Triton X-100 with a maximum concentration of 400 nM. Similar three fold 10-point dilution curves of Ubl^{PhosSer65} and Ubl were produced with a maximum concentration of 24.7 mM. Biotinylated wild-type or H302A mutant Parkin protein and GST-Ubl were diluted to 40 nM in PBS + 0.1 % BSA +0.1 % Triton X-100. 5 µl of inhibitor, 5 µl of GST-Ubl and 5 µl of Parkin protein were added to a white-walled 384 well plate (Griener Bio-one). Plates were centrifuged at 500 x g for 3 min and mixed on an orbital shaker at 450 rpm for 3 min prior to incubation at RT for 20 min. 5 µl of a 20 µg/ml mixture of Streptavidin donor and Glutathione acceptor beads in PBS + 0.1 % BSA +0.1 % Triton X-100 were added to all wells. Plates were briefly centrifuged and incubated at RT in the dark for 1 h prior to reading on PHERAstar (BMG LABTECH) using an AlphaLISA optical module (excitation wavelength = 680 nm and emission wavelength = 615 nm).

2.2.25 Isothermal calorimetric Assay – performed by Dr. Julio R. Martinez

ITC measurements were carried out on an ITC_{200} Microcalorimeter (GE Healthcare). Wild-type, H302A, and K151A mutant Parkin and ubiquitin^{PhosSer65} were dialyzed in buffer containing 50 mM HEPES (pH 8.0), 150 mM NaCl and 500 µM of TCEP. The sample cell

contained 50 µM of wild-type or mutant Parkin and sufficient amount of ubiquitin^{PhosSer65} was titrated in the injection syringe to achieve a complete binding isotherm. All binding experiments were undertaken in duplicate at constant temperature of 20 °C. A total of 20 injections of 2.0 µl were dispensed with a 5 second addition time and spacing of 120 seconds. Data was analysed and titration curves fitted using MicroCal Origin software assuming a single binding site mode.

2.2.26 Thermal shift assay - performed by Dr. Julio R. Martinez

Thermal denaturation experiments were performed using *Differential Scanning Fluorimetry* (DSF). 5 µg of wild-type, His302Ala or Lys151Ala mutant Parkin protein was added to 45 µl reaction buffer (50 mM Hepes pH 8.0, 150 mM NaCl, 500 µM TCEP), and 2.5 µl of 100 × Sypro Orange (Invitrogen) fluorescent dye to yield a final reaction volume of 50 µl. Each experiment was repeated three times in a 96-well plate in a Bio-Rad iQ5 thermal cycler, with a temperature gradient set from 10 °C to 95 °C at steps of 0.5 °C per minute.

2.2.27 Mass spectrometry

2.2.27.1 Processing protein bands for analysis by mass spectrometry

To minimise contamination with proteins such as keratin, samples were handled in a laminar flow hood. Protein bands were excised from the gel and washed sequentially with 0.5 ml of water, 50 % acetonitrile (v/v), 0.1 M NH_4HCO_3 and 50 % acetonitrile (v/v)/ 50 mM NH_4HCO_3 until the gel pieces were colourless. All washes were performed for 10 min on a Vibrax shaking platform. Proteins were then reduced with 10 mM DTT/ 0.1 M NH_4HCO_3 at 65 °C for 45 min and alkylated with 50 mM Chloroacetamide/0.1 M NH_4HCO_3 for 20 min at room temperature. They were then washed with 0.5 ml 50 mM NH_4HCO_3 and 50 mM NH_4HCO_3 / 50 % acetonitrile (as before). Gel pieces were shrunk with 0.3 ml acetonitrile for 15 min. Acetonitrile was aspirated and trace amounts removed by drying sample in a Speed-

Vac at 45 °C. Gel pieces were then rehydrated and proteins were digested in 25 mM triethylammonium bicarbonate containing 5 µg/ml trypsin at 30 °C for 16 hrs on a shaker. An equivalent volume of acetonitrile (same as trypsin) was added to each sample and further incubated on a shaking platform for 15 min. The supernatants were dried by Speed-Vac. Another extraction was performed by adding 100 µl 50 % (v/v) acetonitrile/2.5 % (v/v) formic acid for 15 min. This supernatant was combined with the first extract and dried by Speed-Vac at 45 °C. Peptides were purified on C18 MicroSpin Columns (The Nest Group) and stored at -20 °C before MS analysis as described below.

2.2.27.2 In-solution protein digestion for Miro1 ubiquitylation site identification

In-vitro ubiquitylation assays were terminated with 1 % Rapigest™ and reduced in 5 mM TCEP (Tris-(2-carboxyethyl)phosphine) at 50 °C for 30 min. Additional Tris-HCl was added to 10 mM to ensure buffering at pH 7.5 followed by cysteine alkylation in 10 mM chloroacetamide at 20 °C in the dark for 30 min. Samples were diluted to 0.1% Rapigest™ and digested with 1:50 (w/w) trypsin overnight at 37 °C. Peptides were acidified with 1 % TFA (trifluoroacetic acid) and incubated at 37 °C for 1 hr before precipitating acid-cleaved Rapigest™ by centrifugation at 17,000 x *g* for 10 min. Peptides were purified on C18 MicroSpin Columns (The Nest Group) before MS analysis.

2.2.27.3 Mass Spectrometry

Approximately 30 ng of peptide was analysed by C18 LC–MS/MS over a 60 min gradient from 1-37 % acetonitrile/0.1 % formic acid. Mass spectrometric analysis was conducted by data-dependent acquisition with spectra acquired by collision-induced dissociation on an LTQ Orbitrap Velos (Thermo Fisher Scientific). Data were analysed using Mascot

(www.matrixscience.com) and ion signals were extracted using Skyline (MacLean et al., 2010).

2.2.28 Mapping the site on ubiquitin phosphorylated by TcPINK1 - performed by Robert Gourlay

Flag-ubiquitin (10 μg) (Boston Biochem) was incubated with 10 μg of either wild-type MBP-TcPINK1 (1–570) or kinase-inactive MBP TcPINK1 (D359A) for 80 min at 30 °C in 50 mM Tris-HCl (pH 7.5), 0.1 mM EGTA, 10 mM MgCl2, 0.15 β-Mercaptoethanol and 0.1 mM [γ-^{32}P] ATP (approx. 20 000 cpm/pmol) in a total reaction volume of 50 μl. The reaction was terminated by addition of LDS sample buffer with 10 mM DTT, boiled and subsequently alkylated with 50 mM iodoacetamide before samples were subjected to electrophoresis on a Bis–Tris 4 – 12 % polyacrylamide gel, which was then stained with Colloidal Coomassie blue (Invitrogen). Phosphorylated ubiquitin was digested with trypsin and 78 % of the ^{32}P radioactivity incorporated into ubiquitin was recovered from the gel bands. Peptides were chromatographed on a reverse phase HPLC Vydac C18 column (Cat no. 218TP5215, Separations Group, Hesperia, CA) equilibrated in 0.1 % (v/v) trifluoroacetic acid and the column developed with a linear acetonitrile gradient at a flow rate of 0.2 ml/min and fractions (0.1 ml each) were collected and analysed for ^{32}P radioactivity by Cerenkov counting. Isolated phosphopeptides were analysed by LC-MS/MS on a Thermo U3000 RSLC nano liquid chromatography system coupled to a Thermo LTQ-Orbitrap Velos mass spectrometer. The resultant data files were searched using Mascot (www.matrixscience.com) run on an in-house system against a database containing the ubiquitin sequence, with a 10 ppm mass accuracy for precursor ions, a 0.6 Da tolerance for fragment ions, and allowing for Phospho (ST), Phospho (Y), Oxidation (M) and Dioxidation (M) as variable modifications. Individual MS/MS spectra were inspected using Xcalibur v. 2.2 software (Thermo, Bremen, Germany). The site of phosphorylation of these ^{32}P-labelled peptides was determined by solid-phase Edman degradation on a Shimadzu PPSQ33A sequencer (Hyoto, Japan) of the peptide

coupled to Sequelon-AA membrane (Applied Biosystems) as described previously (Campbell and Morrice, 2002).

2.2.29 MALDI analysis - - performed by Dr. Maria S. Ritorto and Alba Gonzalez

MALDI-TOF was used to confirm and establish the ratios of phosphorylated versus non-phosphorylated protein species. An aliquot of the reaction (2 µl, 400-600 fmols) was added to 2 µl of the matrix (2,5-dihydroxyacetophenone, 15 mg/ml in 80% ethanol, 20 % of 12 mg/ml ammonium citrate bibasic) and 2 µl of 2 % (v/v) trifluoroacetic acid was added before spotting 0.5 µl of the sample on to an AnchorChip target (Bruker Daltonics). The analysis was performed manually in linear positive mode using an UltrafleXtreme (Bruker Daltonics) MALDI–TOF mass spectrometer. For external calibration, six average masses were used: insulin $[M+H]^{+}$avg (m/z 5734.520), cytochrome c $[M+2H]^{2+}$avg (m/z 6181.050), myoglobin $[M+2H]^{2+}$avg (m/z 8476.660), ubiquitin I $[M+H]^{+}$avg (m/z 8565.760) and cytochrome C [M+H]+avg (m/z 12360.970).

2.2.30 Analysis of Ser65 phosphorylation of Parkin by aquapeptides and mass spectrometry - performed by Dr. Julien Peltier

In order to quantify phosphorylation stoichiometry, 2 ng of Parkin or Phospho-Parkin were digested with trypsin and analysed by absolute quantitation selected reaction monitoring (SRM) LC mass spectrometry (Surinova et al., 2013). Samples were separated by a 60 min gradient on a 50 cm Acclaim PepMap 100 analytical column (75 µm ID, 3 µm C18) in conjunction with a PepMap trapping column (100 µm x 2 cm, 5 µm C18) (Thermo-Fisher Scientific) in a Dionex Ultimate 3000 Nano LC system (Dionex/Thermo Fisher) coupled to a QTRAP 5500 (ABSCIEX) mass spectrometer. Synthetic peptides were used to define retention time and the optimal 10 transitions per peptide, based on optimal intensity of precursor charge state and fragment ions. One pmol of heavy labelled peptides of Parkin

NDWTVQN[C(CAM)]DLDQQSIVHIVQRPW[**R**(13C6; 15N4)], R.NDWTVQN[C(CAM)]DLDQQ[S(PO3H2)]IVHIVQRPW**R**(13C6; 15N4)] (AQUA QuantPro, Thermo Scientific) was mixed with the trypsin digest of phosphoParkin and the ratio of peak intensities of ten distinct transitions for light (endogenous) and heavy peptides was used to calculate the amount of endogenous proteins. Data were analysed with Skyline software (MacLean et al., 2010).

2.2.31 *In-vitro* assays

2.2.31.1 Kinase assays

Reactions were set up in a volume of 25 µl, using 1 µg of the indicated kinase (or as stated in figure legend) and varied amounts of substrate protein in 50 mM Tris-HCl (pH 7.5), 0.1 mM EGTA, 10 mM $MgCl_2$, 2 mM DTT and 0.1 mM [γ-^{32}P] ATP (approx. 500 cpm/pmol). Assays were incubated at 30 °C with shaking at 1050 r.p.m. and terminated after 60 min or times indicated in figure legends by addition of LDS sample loading buffer. The reaction mixtures were then resolved by SDS-PAGE. Proteins were detected by Coomassie staining and gels were imaged using an Epson scanner and dried completely using a gel dryer (Bio-Rad). Incorporation of [γ-^{32}P] ATP into substrates was analysed by autoradiography using Amersham Hyper-Film.

2.2.31.2 *In-vitro* ubiquitylation assays

Wild-type or indicated mutant Parkin (2 µg) was initially incubated with 1µg (or indicated amounts) of *E. coli*-expressed wild-type or kinase-inactive (D359A) MBP-TcPINK1 in a reaction volume of 25 µl (50 mM Tris-HCl (pH 7.5), 0.1 mM EGTA, 10 mM Magnesium acetate, 1 % β-mercaptoethanol and 0.1 mM ATP. Kinase assays were incubated at 30 °C for 60 min followed by addition of ubiquitylation assay components and Mastermix to a final volume of 50 µl (50 mM Tris-HCl (pH 7.5), 0.05 mM EGTA, 10 mM $MgCl_2$, 0.5% β-

mercaptoethanol, 0.12 µM human recombinant E1 purified from Sf21 insect cell line, 1 µM human recombinant UbcH7 and 2µg 6xHis-Sumo-Miro1 (WT or point mutants) both purified from *E. coli*, 0.05 mM Flag-Ubiquitin (Boston Biochem) and 2 mM ATP). Ubiquitylation reactions were incubated at 30 °C for 60 min and terminated by addition of LDS sample buffer. For all assays, reaction mixtures were resolved by SDS-PAGE. Ubiquitylation reactions were subjected to analysis by immunoblotting.

During experiments investigating the effect of ubiquitin$^{Phospho\text{-}Ser65}$ and Ubl$^{Phospho\text{-}Ser65}$ on Parkin activity, ubiquitylation reactions were performed in the absence of PINK1 in a final volume of 50 µl (50 mM Tris-HCl (pH 7.5), 5 mM $MgCl_2$, 0.12 µM UbE1, 1 µM UbcH7 and 2 µg 6xHis-Sumo-Miro, 2 mM ATP). When effects of ubiquitin$^{Phospho\text{-}Ser65}$ were investigated, the total amount of ubiquitin used per assay was 25 µg: increasing concentrations of ubiquitin$^{Phospho\text{-}Ser65}$ or non-phosphorylated ubiquitin were added as indicated and the final amount of ubiquitin was reached by addition of Flag-ubiquitin (Boston Biochem). When effects of Ubl$^{Phospho\text{-}Ser65}$ were investigated, 0.05 mM Flag-Ubiquitin was used and the Ubl$^{Phospho\text{-}Ser65}$ or non-phosphorylated-Ubl were added as indicated. Ubiquitylation reactions were incubated at 30 °C for 60 min; terminated by addition of LDS sample buffer and subjected to immunoblotting as described.

For the E2 scan, a version of the E2^{scanTM} kit was obtained from Ubiquigent and 1 µg of each E2 enzyme was used per reaction.

2.2.31.3 *In-vitro* E2 discharge assays

Wild-type or indicated mutant Parkin (2 µg) was incubated with 1 µg of *E. coli* expressed wild-type or kinase-inactive (D359A) MBP-TcPINK1 in a reaction volume of 15 µl (50 mM HEPES (pH 7.5), 0.1 mM EGTA, 10 mM Magnesium acetate and 0.1 mM ATP). Kinase assays were incubated at 30 °C for 60 min. E2-charging reaction was assembled in parallel in 5 µl containing Ube1 (0.5 µg), an E2 (2µg), 50 mM HEPES pH 7.5 and 10 µM ubiquitin in

the presence of 2 mM magnesium acetate and 0.2 mM ATP. After initial incubation of 60 min at 30 °C, the reactions were combined and allowed to continue for a further 15 min or indicated times at 30 °C. Reactions were terminated by the addition of 5 µl of LDS loading buffer and subjected to SDS-PAGE analysis in the absence of any reducing agent. Gels were stained using InstantBlue.

During experiments investigating the effect of ubiquitin$^{\text{Phospho-Ser65}}$ and Ubl$^{\text{Phospho-Ser65}}$ on the Parkin mediated E2 discharge, 1 µg of the indicated ubiquitin and Ubl species were combined with the E2 discharge reaction.

2.2.32 Protein purification

2.2.32.1 MBP-tagged protein purification from *E. coli*

Full-length wild-type and kinase-inactive TcPINK1 was expressed in *E. coli* as maltose binding protein (MBP) fusion protein and purified as described. BL21 Codon+ transformed cells were grown at 37 °C to an OD_{600} of 0.3, then shifted to 16 °C and induced with 250 µM IPTG (isopropyl β-D-thiogalactoside) at OD_{600} of 0.5. Cells were induced with 250 µM IPTG at OD 0.6 and were further grown at 16 °C for 16 h. Cells were pelleted at 4000 r.p.m., and then lysed by sonication in lysis buffer (Table 2.7). Lysates were clarified by centrifugation at 30 000*g* for 30 min at 4 °C followed by incubation with 1 ml per litre of culture of amylose resin for 1.5 h at 4 °C. The resin was washed thoroughly in wash buffer (Table 2.7), then equilibration buffer (Table 2.7), and proteins were then eluted. Proteins were dialysed overnight at 4 °C into storage buffer (Table 2.7), snap-frozen and stored at −80 °C until use.

Table 2.7 Buffers used in MBP-tagged protein purification

Buffer	Composition
Lysis buffer	50 mM Tris-HCl (pH 7.5), 150 mM NaCl, 1 mM EDTA, 1 mM EGTA, 5 % (v/v) glycerol, 1 % (v/v) Triton X-100, 0.1 % (v/v) 2-mercaptoethanol, 1 mM benzamidine and 0.1 mM PMSF
Wash buffer	50 mM Tris-HCl (pH 7.5), 500 mM NaCl, 0.1 mM EGTA, 5 % (v/v) glycerol, 0.03 % (v/v) Brij-35, 0.1% (v/v) 2-mercaptoethanol, 1 mM benzamidine and 0.1 mM PMSF
Equilibration buffer	50 mM Tris-HCl (pH 7.5), 150 mM NaCl, 0.1 mM EGTA, 5 % (v/v) glycerol, 0.03 % (v/v) Brij-35, 0.1 % (v/v) 2-mercaptoethanol, 1 mM benzamidine and 0.1 mM PMSF
Elution buffer	Same as equilibration buffer with the addition of 12 mM maltose.
Storage buffer	Same as equilibration buffer with the addition of 0.27 M sucrose and glycerol—PMSF and benzamidine were omitted.

2.2.32.2 Purification of Parkin constructs – performed by Clare Johnson

Wild-type and indicated mutant untagged Parkin (His-SUMO cleaved) was expressed and purified using a modified protocol (Chaugule et al., 2011). No significant difference in solubility or expression between the mutants and wild-type Parkin protein was observed. BL21 cells were transformed with His-SUMO-tagged Parkin constructs, overnight cultures were prepared and used to inoculate 12 × 1 l LB medium, 50 μg/ml carbenicillin, 0.25 mM $ZnCl_2$. The cells were grown at 37 °C until the $OD_{600}$was 0.4 and the temperature was dropped to 16 °C. At OD_{600} = 0.8 expression was induced with 25 μM IPTG. After overnight incubation the cells were collected and lysed in lysis buffer (Table 2.8). After sonication and removal of insoluble material, His-SUMO-Parkin was purified via Ni^{2+}-NTA-Sepharose chromatography. The protein was collected in elution buffer (Table 2.8). This was dialysed twice against cleavage buffer (Table 2.8) in the presence of His-SENP1 415–643 at a ratio of 1 mg His-SENP1 per 5 mg His-SUMO-Parkin. The protease, the His-SUMO tag and any uncleaved protein was removed by two subsequent incubations with Ni^{2+}–NTA–Sepharose.

The cleaved Parkin was further purified in wash buffer (Table 2.8) over a Superdex 200 column.

Table 2.8 Buffers used for Parkin purification

Buffer	Composition
Lysis buffer	75 mM Tris pH 7.5, 500 mM NaCl, 0.2 % Triton X-100, 25 mM imidazole, 0.5 mM Tris(2-carboxyethyl)phosphine (TCEP), 1 mM Pefablok, 10 μg ml^{-1} Leupeptin
Equilibration buffer	50 mM Tris, pH 8.2, 200 mM NaCl, 10 % glycerol, 0.03 % Brij-35, 0.5 mM TCEP
Elution buffer	Same as equilibration buffer with the addition of 400 mM imidazole.
Cleavage buffer	50 mM Tris pH 8.2, 200 mM NaCl, 10 % glycerol, 0.5 mM TCEP
Wash buffer	50 mM Tris, pH 8.2, 200 mM NaCl, 20 % glycerol, 0.03 % (v/v) Brij-35, 0.5 mM TCEP

2.2.32.3 Purification of His-SUMO-Miro1 – performed by DSTT

Wild-type 6xHis-Sumo-Miro1 (1 – 592) and K572R and K567R mutants were expressed in *E. coli*. Briefly, BL21 CodonPlus (DES)-RIL transformed cells were grown at 37 °C to an OD600 of 0.4, then induced at 15 °C with 10 μM IPTG at an OD600 of 0.6. Cells were then grown at 15 °C for a further 20 hours. Cells were pelleted at 4200 x g and then lysed by sonication in lysis buffer (Table 2.9). Lysates were clarified by centrifugation at 30 000 g for 30 min at 4 °C followed by incubation with Cobalt resin at 4 °C for 45 min. The resin was washed thoroughly in high salt buffer (Table 2.9), then equilibrated in low salt buffer, and the proteins were then eluted (Table 2.9). The eluted Miro1 proteins were further purified by anion exchange chromatography. Proteins were applied to a Mono-Q HR 5/5 column and chromatographed with a linear gradient of NaCl from 0 M to 0.5 M. Fractions containing the purified Miro1 protein were then dialysed (Table 2.9), snap frozen in liquid nitrogen and stored at -80 °C.

Table 2.9 Buffers used for Miro1 purification - performed by DSTT

Buffer	Composition
Lysis buffer	50 mM Tris-HCl pH 7.5, 150 mM NaCl, 0.1 % Triton, 1 mM Pefabloc, 20 ug/ml Leupeptin, 1 mM Benzamidine and 0.5 mM TCEP
High salt buffer	50 mM Tris-HCl pH 7.5, 500 mM NaCl, 20 mM imidazole 1 mM Pefabloc, 20 ug/ml Leupeptin, 1 mM Benzamidine and 0.5 mM TCEP
Low salt buffer	50 mM Tris-HCl pH 7.5, 150 mM NaCl, 10 mM imidazole 1 mM Pefabloc, 20 ug/ml Leupeptin, 1 mM Benzamidine and 0.5 mM TCEP
Elution buffer	50 mM Tris-HCl pH 7.5, 150 mM NaCl, 300 mM imidazole 1 mM Pefabloc, 20 ug/ml Leupeptin, 1 mM Benzamidine and 0.5 mM TCEP
Dialysis buffer	50 mM Tris-HCl, 150 mM NaCl, 0.1 mM EGTA, 270 mM Sucrose, 0.1 % B-mercaptethanol

2.2.33 Purification of phospho-proteins – performed by Dr. Axel Knebel

2.2.33.1 Purification of Ser65-phosphorylated ubiquitin and Ser65-phosphorylated Parkin Ubl domain (residues 1-76)

23 µM bovine ubiquitin (SIGMA) was phosphorylated for 24 h with 3.7 µM MBP-PINK1 at 22 °C in the presence of 100 µM ATP and 10 mM $MgCl_2$. To replace ADP with ATP, the reaction was dialysed against Mg-ATP solution. Ubiquitin was filtered through a 30 kDa Vivaspin filter to remove MBP-PINK1, concentrated in a 3 kDa MWCO filter device, washed extensively with water and loaded onto a Mono Q-column, which bound phospho-ubiquitin but not bind ubiquitin, . The former was recovered by washing the column with 50 mM Tris pH 7.5, which was sufficient to elute stoichiometrically phosphorylated ubiquitin. Similarly, Parkin Ubl domain (residues 1-76) was expressed as previously described (Kondapalli et al., 2012) and was phosphorylated with MBP-TcPINK1, recovered by filtration and applied to a Mono-Q column. Phospho Parkin Ubl bound to the column and eluted with about 100 mM NaCl. At least 60 % purity was achieved.

2.2.33.2 Purification of Ser65-phosphorylated Parkin

Ser^{65}-phosphorylated Parkin was produced by expression of His-SUMO-tagged Parkin then captured by Ni^{2+}-NTA-Sepharose as described above. After extensive washes, captured His-SUMO-Parkin was incubated with MBP-PINK (Parkin : PINK1 ratio of 2:1) twice consecutively for 3 h in the presence of 0.5 mM ATP and 10 mM Mg-acetate at 27 °C. PINK1 was removed and Parkin was eluted with 0.4 M imidazole and further incubated for 16 h with MBP-PINK1 in solution. The proteins were concentrated using VivaSpin filters and then diluted again to reduce the imidazole concentration to 20 mM to recapture His-SUMO-Parkin on Ni-agarose. Residual MBP-PINK1 was removed by extensive washes, before His-SUMO-Parkin was eluted with 0.4 M imidazole and further purified as described above.

2.2.33.3 Purification of Dac-ubiquitin and Ser^{65}-phosphorylated Dac-ubiquitin

The Dac-tag is a fragment of *E.coli* Penicillin Binding Protein 5, comprising residues 37-297, where the N-terminus was modified to MSAIPG to allow efficient mRNA translation (Lee et al., 2012b). pET28-Dac-Ubiquitin was transformed into BL21 cells. Protein expression was induced with 250 µM IPTG for 16 h at 26 °C. Cells were sedimented and lysed in 50 mM Tris pH 7.5, 0.5 % Triton X-100, 0.1 mM EDTA, 0.1 mM EGTA, 1 mM Pefablocff, 10 µg/ml Leupeptin. After sonication insoluble material was removed by centrifugation. Dac-ubiquitin fusion protein was captured by incubation for 45 min at 22 °C with ampicillin-Sepharose. The ampicillin-Sepharose was thoroughly washed and the protein was eluted with 50 mM Tris pH 7.5, 150 mM NaCl, 5 % glycerol, 10 mM ampicillin, 0.03 % Brij35. The protein was dialysed into 40 mM HEPES, pH 7.5, 100 mM NaCl, 1 mM DTT.

Ser^{65}-phosphorylated Dac-ubiquitin (Dac-$Ubiquitin^{PhosSer65}$) was prepared by phosphorylation of Dac-Ubiquitin with GST-*Pediculus humanus* PINK1 126-end (ratio Dac-Ub: GST PhPINK of 6.25:1) for 3 h in the presence of 20 mM Mg-acetate and 2 mM ATP. Dac-Ubiquitin was

repurified over Ampicillin Sepharose and concentrated to match the concentration of Dac-ubiquitin.

3 Chapter 3: PINK1 and Parkin - a molecular interaction

3.1 Introduction

Whilst familial Parkinson's disease (PD) patients with mutations in the ubiquitin E3 ligase Parkin and the serine/threonine protein kinase PINK1 (PTEN (phosphatase and tensin homologue)-induced kinase 1) exhibit a similar phenotype (Khan et al., 2002), it was initially difficult to reconcile a molecular link between these two proteins since Parkin is localised to the cytosol, whereas PINK1 is localised to the mitochondria.

A decisive functional genetic link between Parkin and PINK1 was first established in 2006, when it was shown in a *Drosophila melanogaster* model that Parkin null flies have a mitochondrial phenotype that is near-identical to that of PINK1 null flies – namely defects in mitochondrial morphology, flight muscle degeneration and motor deficits (Clark et al., 2006, Park et al., 2006, Yang et al., 2006). Moreover, epistatic analysis revealed that over-expression of Parkin rescued the PINK1 null phenotype but that the effect was not reciprocal, suggesting that PINK1 acts upstream of Parkin (Clark et al., 2006, Park et al., 2006, Yang et al., 2006).

In mammalian cell studies, a major breakthrough came from the discovery that Parkin is recruited to damaged mitochondria upon induction of mitochondrial depolarisation, and furthermore that Parkin promotes autophagic degradation of mitochondria via a process termed mitophagy (Narendra et al., 2008). Subsequent studies described the requirement of mammalian PINK1 for Parkin recruitment to mitochondria following depolarisation (Geisler et al., 2010, Matsuda et al., 2010, Narendra et al., 2010, Vives-Bauza et al., 2010) and provided a second line of evidence for linear regulation within the signalling pathway, placing Parkin firmly downstream of PINK1. However, the mechanism by which Parkin is recruited and activated by PINK1 remains a major point of enquiry.

Elucidation of the molecular basis of the pathway was largely hindered by difficulties in detecting mammalian PINK1 activity *in vitro*. This was overcome by the discovery in our

laboratory of active insect orthologues of PINK1, specifically *Tribolium castaneum* (TcPINK1) and *Pediculus humanus corporis* (PhcPINK1), which could be purified from *E. coli* (Woodroof et al., 2011). These insect orthologues of PINK1 are active against generic substrates including myelin basic protein, and enabled elaboration of a peptide substrate termed PINKtide (Woodroof et al., 2011). Furthermore, this discovery facilitated direct assessment of the effects of ~20 PINK1 human pathogenic mutations that were conserved in the insect PINK1 orthologues, which revealed that the majority of PINK1 mutations lead to a disruption of catalytic activity (Woodroof et al., 2011). Following this finding, a member of our laboratory, Dr. Chandana Kondapalli, deployed TcPINK1 to screen a panel of proteins linked to forms of PD with Mendelian inheritance in order to identify potential PINK1 substrates, and found Parkin to be phosphorylated (Kondapalli et al., 2012). She subsequently mapped the site of phosphorylation to a single residue at serine 65 (Ser^{65}) (Kondapalli et al., 2012), later validated by other groups (Shiba-Fukushima et al., 2012, Iguchi et al., 2013, Koyano et al., 2013), providing the first evidence of a direct regulatory link between these enzymes.

Ser^{65} lies within the N-terminal Ubl domain of Parkin. Historically, Parkin was thought to be a constitutively active RING E3 ligase, but in 2011, ground-breaking work revealed that Parkin exhibits HECT-like properties (Wenzel et al., 2011) and furthermore that it exists in an auto-inhibited conformation, mediated by the interactions of the N-terminal ubiquitin-like domain (Ubl) domain with the rest of the protein (Burchell et al., 2012, Chaugule et al., 2011). Since then, multiple high resolution structures of Parkin lacking the Ubl domain (Riley et al., 2013, Trempe et al., 2013, Wauer and Komander, 2013) and one low resolution structure of the full-length protein (Trempe et al., 2013) have been determined, revealing a complex auto-inhibited state mediated by multiple intramolecular interactions. However, the molecular mechanism of inhibition mediated via the N-terminal Ubl domain, within which Ser^{65} is found, remained obscure.

I have set out to establish the importance of PINK1-mediated Ser^{65} phosphorylation and to determine the impact of PINK1 phosphorylation on Parkin function and activity. In order to

address this goal, I have sought to investigate and confirm the phosphorylation of Parkin in mammalian cells, as well as to establish a robust E3 ligase assay *in vitro*. To date, the majority of Parkin assays had been based on measuring Parkin autoubiquitylation activity *in vitro* and in cells and there were no robust substrate-based assays of Parkin E3 ligase activity available. To address this, I have tested whether Miro1, an atypical mitochondrial GTPase, which has emerged as a candidate Parkin substrate (Sarraf et al., 2013, Liu et al., 2012, Wang et al., 2011), could be deployed as a substrate to enable *in vitro* measurement of Parkin activity.

3.2 Tool development and validation

3.2.1 Generation and characterisation of novel Parkin antibodies

In order to establish effective tools to detect Parkin in cells, I designed and raised two antibodies against different human Parkin epitopes in conjunction with the Division of Signal Transduction Therapy (DSTT) and compared these to two commercially available antibodies raised against the full length protein (Figure 3.1). In addition, a phospho-Ser^{65} specific antibody was raised using a peptide epitope (Figure 3.1). The antibodies were compared by assessing their ability to immunoblot and immunoprecipitate overexpressed Parkin in cell extracts.

Lysates of HEK293 cells, both those transiently overexpressing full-length untagged Parkin, and untransfected controls, were analysed. Both in-house antibodies were able to selectively recognise Parkin in whole cell lysates as judged by the detection of two bands, representing the full-length and an N-terminally truncated version of the E3 ligase (Henn et al., 2005) (Figure 3.2 A, B). The antibodies were also able to successfully immunoprecipitate overexpressed Parkin (Figure 3.2 E).

A

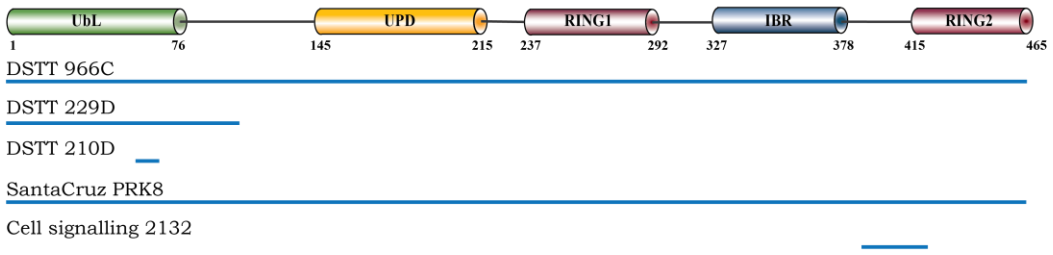

B

Antibody	Source	Species	Immunizing agent
966C	DSTT	Sheep	GST-Parkin (full length)
229D	DSTT	Sheep	GST-Parkin (1-108)
210D	DSTT	Sheep	peptide equivalent to residues 60-72 (RDLDQQS*IVHIVQR)
PRK8	Santa Cruz	Mouse	Parkin (full length)
2132	Cell signalling	Rabbit	peptide equivalent of amino acids around Q400

Figure 3.1 Schematic representation of Parkin antibody epitopes generated.

(A) Schematic representation of Parkin protein domains and epitope regions against which in-house (DSTT) and commercial antibodies were raised. **(B)** Table summarizing antibodies tested.

Two commercial antibodies were tested – the Santa Cruz biotechnologies PRK8 was previously successfully used in biochemical studies (Berger et al., 2009, Yamauchi et al., 2008) and could immunoblot and immunoprecipitate Parkin (Figure 3.2 C, F top panel); the Cell signalling 2132 antibody, which has also been used in previous studies (Cesari et al., 2003), was able to immunoblot Parkin in lysates (Figure 3.2 D) but failed to immunoprecipitate Parkin (Figure 3.2 F bottom panel) and was therefore not used in future experiments in HEK293 cells. The DSTT 210D antibody was raised against a peptide encompassing Parkin phospho-Ser^{65} ($Parkin^{Phospho\text{-}Ser65}$) (Figure 3.1 B) and was tested on 200 µg immunoprecipitates from Flp-in T-Rex PINK1 HEK293 cell lines transiently overexpressing either wild-type (WT)

or a non-phosphorylatable Ser65Ala (S65A) mutant Parkin and stimulated with 10 μM CCCP (a mitochondrial depolarising agent) or DMSO for 3 h. Both the first and second bleeds detected Parkin$^{\text{Phospho-Ser65}}$ following CCCP treatment (Figure 3.2 G). Only the second bleed did not detect any phosphorylation under unstimulated conditions, and was therefore used for subsequent experiments.

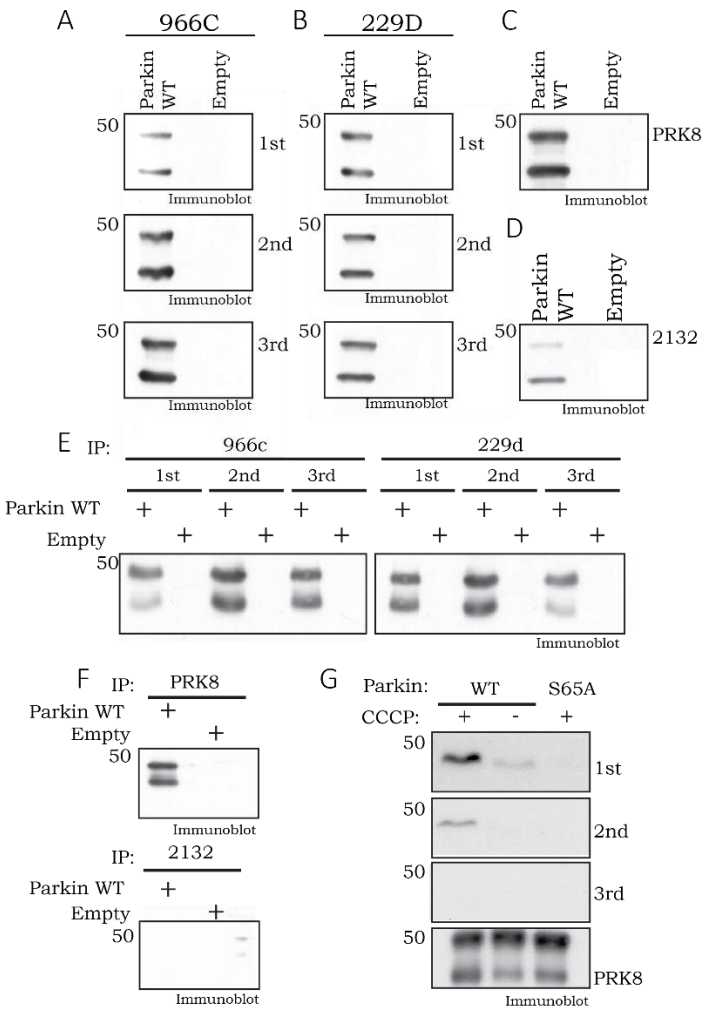

Figure 3.2 Characterisation of Parkin antibodies in overexpressed system

(A) HEK293 transfected with untagged Parkin and untransfected cells were lysed and 30µg of lysates were analysed by immunoblotting with indicated bleeds of DSTT 966C antibody. **(B)** As in (A) except DSTT 229D antibody was used. **(C)** As in (A) except PRK8 antibody was used. **(D)** As in (A) except 2132 antibody was used. **(E, F)** as in (A) except 0.5mg of lysates were immunoprecipitated (IP) with the indicated antibodies and the IPs were analysed by immunoblotting with PRK8antibody. **(G)** as in E except the IP was done from Flp-in T-Rex wild-type PINK1-FLAG HEK293 cells overexpressing indicated Parkin constructs using the 2nd bleed of DSTT 966C antibody and analysis was done by immunoblotting using the indicated bleeds of DSTT 210D antibody.

3.2.2 Evidence that PINK1 phosphorylates Parkin in cells

To examine whether Parkin becomes phosphorylated following the activation of PINK1, Flp-In T-Rex HEK293 cells stably expressing wild-type PINK1-FLAG were transiently transfected with WT or S65A Parkin and stimulated with 10 μM CCCP or DMSO for the indicated amount of time (Figure 3.3). Parkin was immunoprecipitated from 250 μg of lysate followed by immunoblotting with the anti-Parkin Ser^{65} ($Parkin^{Phospho\text{-}Ser65}$) antibody. Parkin phosphorylation could be first observed 5 minutes after the addition of CCCP (Figure 3.3) and reached maximum levels at 40 minutes. The peak in Parkin phosphorylation coincided with the appearance of a PINK1 bandshift, suggesting that the bandshift is related to, but does not correlate as well with PINK1 activity as Parkin phosphorylation (Figure 3.3). When Parkin S65A was overexpressed, no Ser^{65} phosphorylation was detected 3 hours after addition of CCCP, confirming the specificity of the antibody (Figure 3.3).

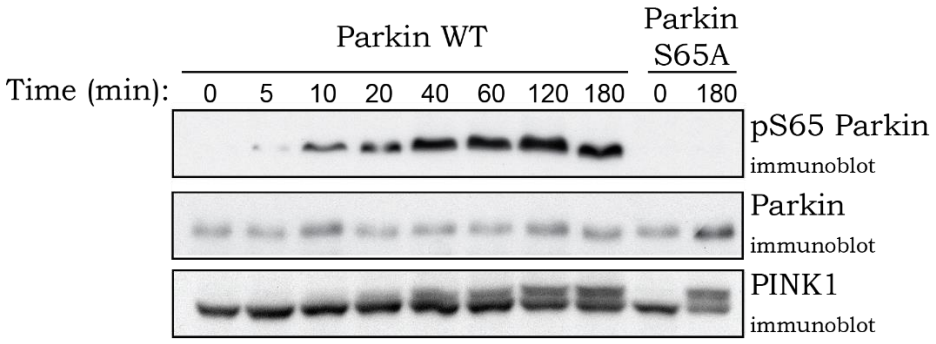

Figure 3.3 Time course analysis of Parkin phosphorylation in cells

Flp-In T-Rex PINK1 HEK293 cells were transfected with untagged wild-type (WT) or Ser65Ala (S65A) Parkin mutant, induced with doxycycline and stimulated with CCCP for the indicated amount of time. 0.25 mg of the whole-cell lysate was immunoprecipitated using the 2nd bleed of DSTT 966C antibody and analysed by immunoblotting with the 2nd bleed of DSTT 210D antibody in the presence of dephosphorylated peptide. 1% of the immunoprecipitate was blotted with PRK8 antibody to determine the total Parkin levels. 1.5 mg of the lysates were immunoprecipitated using anti-FLAG agarose beads and immunoblotted with total PINK1 antibody.

3.2.3 Parkin is phosphorylated by TcPINK1 *in vitro*

Previous work in our lab has identified active insect orthologues of PINK1 (Woodroof et al., 2011), including *Tribolium castaneum* (TcPINK1), that are capable of phosphorylating human Parkin at Ser^{65} *in vitro* (Kondapalli et al., 2012). To determine the stoichiometry of Parkin phosphorylation by TcPINK1, a kinase assay using three different amounts of the kinase was carried out (Figure 3.4). The stoichiometry of phosphorylation at Ser^{65} was determined to be approximately 0.07 moles of phosphate incorporated per mole of Parkin after 60 min reaction irrespective of the quantity of TcPINK1 present in the reaction. Since this low stoichiometry of phosphorylation precluded facile production of phosphorylated Parkin, I chose to study the effects of Parkin phosphorylation via a 2-step assay combining an initial kinase assay followed by a ubiquitylation assay.

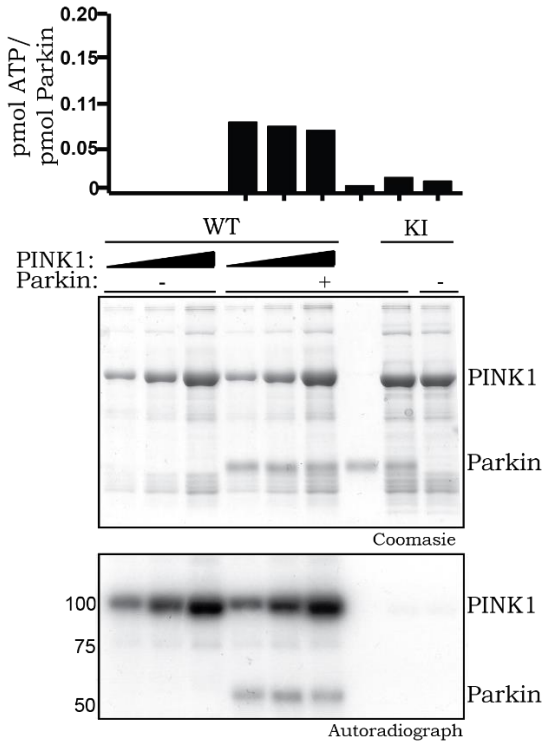

Figure 3.4 Stoichiometry of Parkin phosphorylation by PINK1.

0.5, 1 and 2 µg of wild-type (WT) or kinase-inactive (KI) PINK1 were incubated in the presence or absence of 1 µg of Parkin in a kinase assay as described in Section 2.2.28.1. Reactions were then analysed by SDS-PAGE. Proteins were detected by Coomassie staining. Incorporation of [γ-^{32}P] ATP into substrates was analysed by autoradiography. Stoichiometry of incorporation was determined by scintillation counting. The bar chart displays mol of ATP incorporated per mol of Parkin.

3.2.4 Phosphorylation of Parkin at Ser^{65} stimulates its E3 ligase activity

Ser^{65} is a highly conserved residue that lies in the core of the N-terminal Parkin Ubiquitin-like (Ubl) domain, which has been previously shown to be required for the regulation and auto-inhibition of Parkin E3 ligase activity (Burchell et al., 2012, Chaugule et al., 2011). I therefore hypothesised that PINK1 phosphorylation of Ser^{65} might act to relieve this Ubl-mediated autoinhibition by causing electrostatic repulsion at the interface of the inhibitory intramolecular interaction, thus leading to structural rearrangements and activation.

To test this, I established a Parkin auto-ubiquitylation E3 ligase assay. In order to generate highly pure full-length recombinant Parkin purified from *E.coli* with no epitope tags that might interfere with Ubl-mediated Parkin autoinhibition (Burchell et al., 2012), I adapted a purification protocol first reported by Helen Walden's laboratory (Chaugule et al, 2011). As an initial step, Parkin was phosphorylated by TcPINK1. Reactions were initiated by incubating wild-type or Ser65Ala Parkin with the indicated amounts of kinase (Figure 3.5) in the presence of [γ-^{32}P] ATP; after 60 min, half of the reaction volume was used to determine Parkin phosphorylation levels (Figure 3.5 middle panel). The autoubiquitylation activity of phosphorylated Parkin was then tested by adding the E3 ligase assay components (E1 ubiquitin-activating ligase, UbcH7 ubiquitin conjugating ligase, Flag-ubiquitin and Mg-ATP) to the kinase assays and incubating the reaction for a further 60 min at 30 °C. The reactions were terminated using SDS sample buffer containing β-mercaptoethanol (β-Me) and E3 ligase activity was assessed by blotting for ubiquitin, Parkin and TcPINK1 using anti-Flag, anti-Parkin and anti-MBP antibodies respectively.

In agreement with previous reports (Burchell et al., 2012, Chaugule et al., 2011), Parkin displayed no significant E3 ligase activity in the absence of PINK1 (Figure 3.5 A, lane 1). Upon addition of increasing levels of TcPINK1 and the resultant increased levels of Parkin phosphorylation (Figure 3.5 A, middle panel), I excitingly observed appearance of non-reducible polyubiquitin species migrating between 30 kDa and 50 kDa that increased corresponding to PINK1 concentration (Figure 3.5, top panel). Consistent with this effect being Ser^{65} phosphorylation dependent, the appearance of polyubiquitin chains was inhibited by introducing an Asp359Ala (D359A) point mutation in PINK1 that ablates catalytic activity (Figure 3.5 B) or by mutating Ser^{65} in Parkin to a non-phosphorylatable Ala residue (S65A) (Figure 3.5 C).

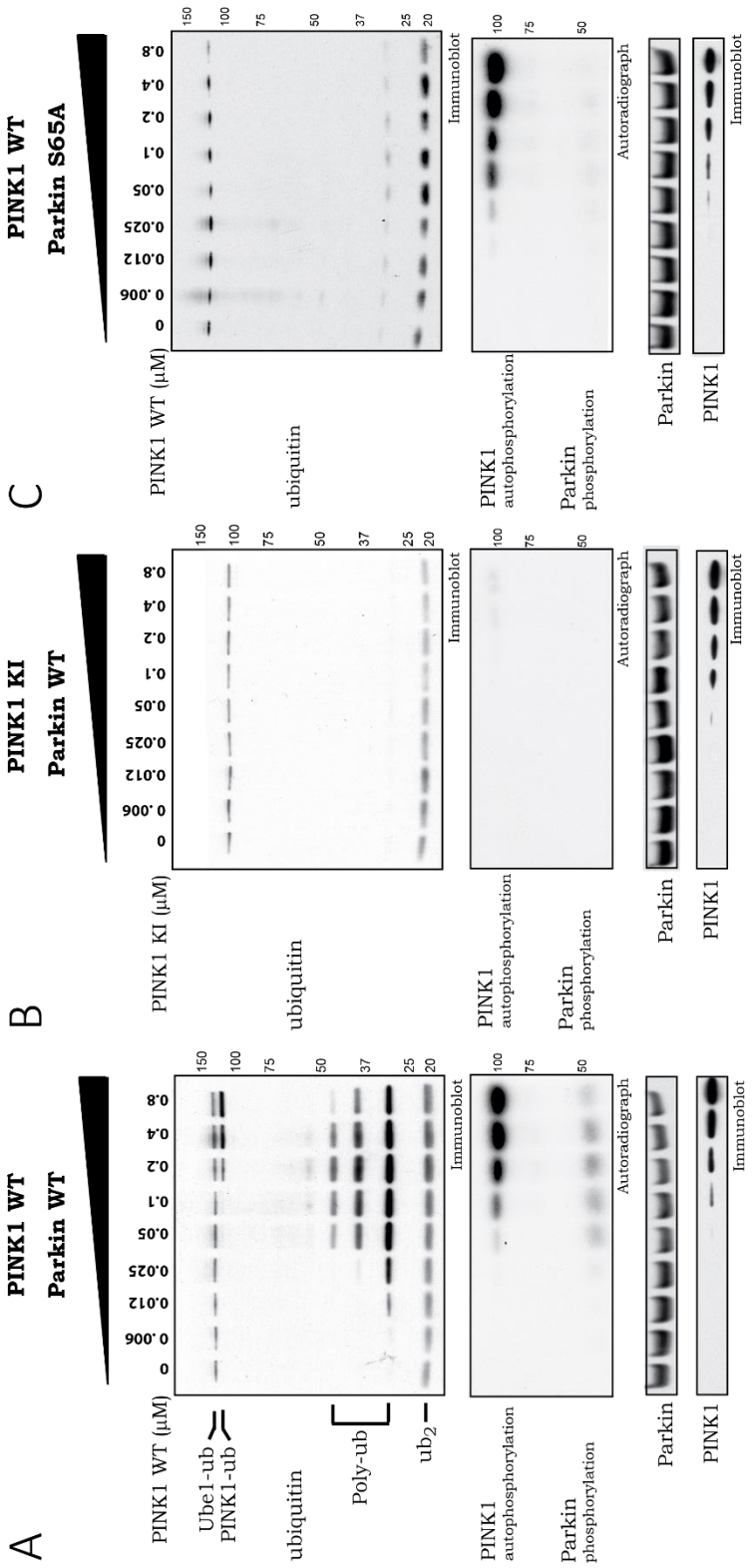
A
PINK1 WT
Parkin WT
PINK1 WT (µM)
0
0.006
0.012
0.025
0.05
0.1
0.2
0.4
0.8
Ube1-ub
PINK1-ub
ubiquitin
Poly-ub
ub2
Immunoblot
PINK1 autophosphorylation
Parkin phosphorylation
Autoradiograph
Parkin
PINK1
Immunoblot
B
PINK1 KI
Parkin WT
PINK1 KI (µM)
ubiquitin
C
PINK1 WT
Parkin S65A
PINK1 WT (µM)
ubiquitin

Figure 3.5 PINK1 phosphorylation of Parkin at Ser65 mediates activation of Parkin E3 ligase activity.

Wild-type (WT) **(A)** but not kinase-inactive (KI) (D359A) **(B)** TcPINK1 activates wild-type (WT) Parkin, but does not alter the activity of Ser65Ala (S65A) mutant Parkin **(C).** Two micrograms of WT or S65A Parkin were incubated with indicated amounts of WT or KI TcPINK in a kinase reaction for 60 min. Half of reaction was terminated and incorporation of [γ-^{32}P] ATP was detected by autoradiography (middle panel). The ubiquitylation reaction was then initiated and allowed to run for a further 60 min, then terminated by addition of loading buffer and resolved by SDS-PAGE. Ubiquitin (anti-Flag), Parkin (anti-Parkin) and PINK1 (anti-MBP) were detected by immunoblotting. E1-ubiquitin (Ub-Ube1) and ubiquitin dimer (Ub_2) formation occurred in all conditions (A-C). Ubiquitylation of PINK1 (Ub-PINK1) is indicated (A). Formation of polyubiquitin chains (poly-Ub) upon Parkin activation (A) is indicated. Representative of five independent experiments.

3.2.5 Analysis of the effects of Parkin phosphorylation via elaboration of a substrate-based Parkin E3 ligase assay

To validate the discovery that phosphorylation by PINK1 activates Parkin, I chose to develop an *in vitro* substrate-based Parkin activity assay. Miro1 was chosen as a candidate substrate since it had been previously reported to be targeted by Parkin in multiple cellular and genetic studies (Sarraf et al., 2013, Liu et al., 2012, Wang et al., 2011). Since full-length recombinant His-SUMO-Miro1 (residues 1- 618) expressed in *E.coli* was insoluble (data not shown), a C-terminal truncation removing the transmembrane domain (residues 1-592) (subsequently referred to as Miro1) was expressed and purified to homogeneity and used in subsequent assays.

Reactions were carried out as described in Section 3.2.4 with the addition of 0.5 μM Miro1. Consistent with previous findings, in the absence of phosphorylation, Parkin was inactive (Figure 3.6 A, lane 1). However, when wild-type TcPINK1 was added, free polyubiquitin chain formation was observed, together with Miro1 multi-monoubiquitylation (a major mono- and minor multi-ubiquitylated species) (Figure 3.6) providing the first evidence that Miro1 is a direct substrate of Parkin. No significant Miro1 ubiquitylation or polyubiquitin chain formation was observed in the presence of the kinase-inactive TcPINK1 (Figure 3.6 B) or using the Ser65Ala (S65A) Parkin point mutant (Figure 3.6 C) indicating that Parkin activity as judged by Miro1 ubiquitylation is critically dependent on Ser^{65} phosphorylation.

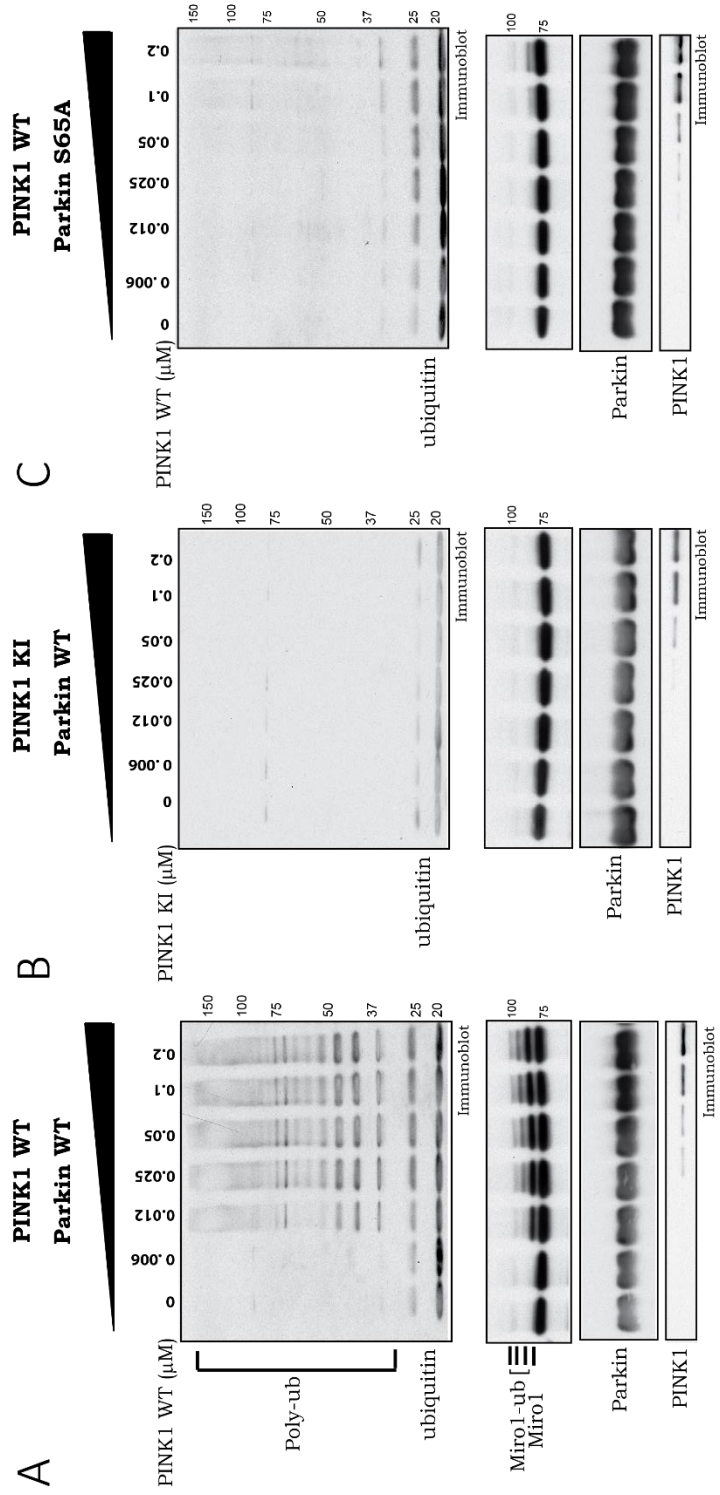
A
PINK1 WT
Parkin WT
PINK1 WT (µM)
0
0.006
0.012
0.025
0.05
0.1
0.2
150
100
75
50
37
25
20
Poly-ub
ubiquitin
Immunoblot
Miro1-ub
Miro1
100
75
Parkin
PINK1
Immunoblot
B
PINK1 KI
Parkin WT
PINK1 KI (µM)
ubiquitin
Immunoblot
Parkin
PINK1
Immunoblot
C
PINK1 WT
Parkin S65A
PINK1 WT (µM)
ubiquitin
Immunoblot
Parkin
PINK1
Immunoblot

Figure 3.6 PINK1-dependent phosphorylation of Parkin Ser^{65} leads to activation of Parkin E3 ligase activity and multi-monoubiquitylation of Miro1.

(A) Wild-type (WT), but not kinase-inactive (KI) (D359A) **(B)** TcPINK1 activates wild-type (WT) Parkin leading to Miro1 ubiquitylation; activation is blocked by Parkin Ser65Ala (S65A) mutation **(C)**. Two micrograms of wild-type or Ser65Ala Parkin were incubated with indicated amounts of WT or KI TcPINK in a kinase reaction for 60 min. The ubiquitylation reaction was initiated as described in Section 2.2.28.2 in the presence of 0.5 μM His-Sumo-Miro1. Reactions were terminated after 60 min by addition of loading buffer and resolved by SDS-PAGE. Miro1, Ubiquitin, Parkin and PINK1 were detected using anti-SUMO, anti-FLAG, anti-Parkin and anti-MBP antibodies, respectively. Representative of 3 independent experiments.

3.2.6 Phosphorylation of Parkin at Ser^{65} promotes discharge of ubiquitin from loaded UbcH7 E2 ligase

To obtain further evidence that PINK1-dependent phosphorylation of Parkin leads to Parkin activation, I assessed whether phosphorylation might influence other readouts of Parkin activity, including binding of ubiquitin-loaded E2 to the RING1 domain and/or E2-mediated ubiquitin transfer. In order to address these questions, I set up an E2 discharge assay. Several E2s were initially tested (data not shown), however UbcH7 was chosen for future experiments due to its consistent loading and discharge. UbcH7 was loaded with ubiquitin by incubation with the E1 (Ube1) and ubiquitin in the presence of Mg-ATP for 60 min at 30 °C. Various Parkin species were then added to the reaction mixture and incubated for a further 15 min. In all experiments, a control reaction without E3 ligase was included to enable assessment of the efficiency of UbcH7 loading. Reactions were terminated using LDS loading buffer without any reducing agent and immediately analysed by SDS-PAGE, followed by Coomassie staining. The electrophoretic separation of the proteins enabled the facile discrimination of ubiquitin conjugated UbcH7 (UbcH7-ub) from free UbcH7.

To determine the effect of phosphorylation of Ser^{65} on Parkin's ability to discharge ubiquitin, Parkin pre-phosphorylated by wild-type TcPINK1, and non-phosphorylated Parkin (either incubated in the presence of kinase-inactive TcPINK1 or in the absence of TcPINK1) was added to the loaded UbcH7. Non-phosphorylated Parkin species failed to induce a significant discharge of ubiquitin from UbcH7, however, Parkin$^{\text{Phospho-Ser65}}$ mediated robust ubiquitin

discharge, as demonstrated by a reduction of the UbcH7-ub thioester band (Figure 3.7 A). A Parkin-ubiquitin thioester was not observed in this experiment, consistent with a previous analysis of full length Parkin (Sarraf et al., 2013, Spratt et al., 2013, Wenzel et al., 2011).

I next undertook a time course analysis to gain further insights into Parkin phosphorylation-dependent stimulation of UbcH7 discharge. Parkin pre-phosphorylated by TcPINK1 was added to the loaded UbcH7 and reactions were allowed to continue for the indicated times (Figure 3.7 B) before being stopped with LDS loading buffer. Under the conditions used, maximal ubiquitin discharge induced by Parkin$^{\text{Phospho-Ser65}}$ occurred within 4-5 min (Figure 3.7 B). To ensure that the discharge is indeed mediated by phosphorylation at Ser^{65}, the Parkin Ser65Ala mutant was included in this analysis, and I observed that the mutation prevented ubiquitin discharge from UbcH7 even in the presence of wild-type TcPINK1 (Figure 3.7 C).

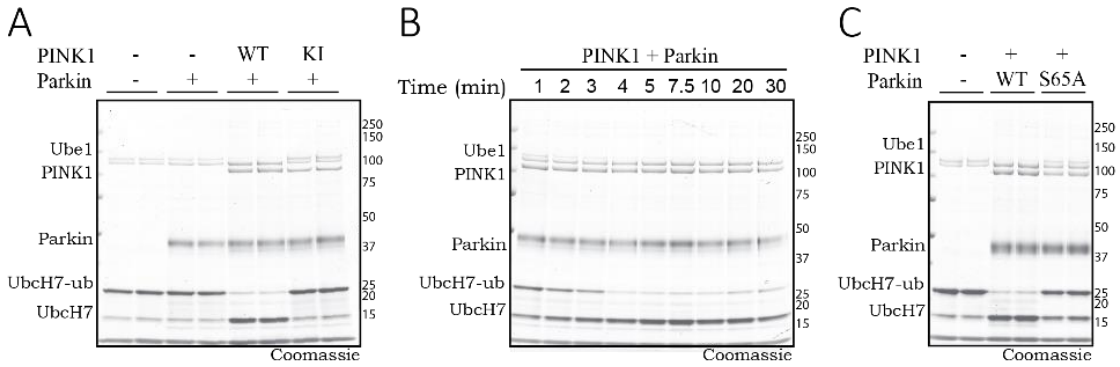

Figure 3.7 PINK1-dependent phosphorylation of Parkin Ser^{65} stimulates discharge of ubiquitin from loaded E2, UbcH7.

(A) Parkin alone or pre-phosphorylated with wild-type (WT) or kinase-inactive (KI) TcPINK1 was incubated with two micrograms of UbcH7 loaded with ubiquitin (UbcH7-ub). Reactions were allowed to continue for 15 min, stopped using LDS loading buffer in absence of reducing agent. Samples were resolved by SDS-PAGE; proteins were detected by Coomassie staining. Ubiquitin discharge was monitored by qualitatively assessing reduction in UbcH7-ub band. **(B)** As in (A), but only Parkin with WT TcPINK1 was used. Reactions were allowed to continue for indicated times. **(C)** Parkin Ser65Ala (S65A) was compared with wild-type Parkin for its ability to discharge UbcH7-ub.

3.3 Parkin phosphorylated at Ser^{65} catalyses multi-monoubiquitylation of Miro1

3.3.1 Parkin Ubl domain is required for efficient Miro1 ubiquitylation

Full-length Parkin is maintained in an auto-inhibited conformation and is catalytically inactive, however multiple reports have revealed that deletion of the Ubl domain is sufficient to activate Parkin (Chaugule et al., 2011, Wenzel et al., 2011). To probe the potential role of the Ubl domain in substrate ubiquitylation, I chose to investigate the effect of deletion of the said domain on Miro 1 ubiquitylation. A Parkin fragment lacking this domain (ΔUbl-Parkin, residues 80-465) was expressed and tested (Figure 3.8). ΔUbl-Parkin alone was assayed in parallel with full-length Parkin pre-incubated with 0.8 μM of either wild-type or kinase-inactive TcPINK1. This optimal concentration, equivalent to 1 μg of TcPINK1 in the final assay, was chosen based on the results displayed in Figure 3.5.

Whilst ΔUbl-Parkin exhibited autoubiquitylation activity comparable to phosphorylated full-length Parkin, it could not efficiently catalyse Miro1 ubiquitylation or stimulate the formation of low molecular weight polyubiquitin chains (Figure 3.8). These data suggest that the Ubl domain is required for the full spectrum of Parkin activity and that the Ubl domain phosphorylated at Ser^{65} might have additional roles in enabling substrate ubiquitylation beyond potentially mediating relief of Parkin autoinhibition.

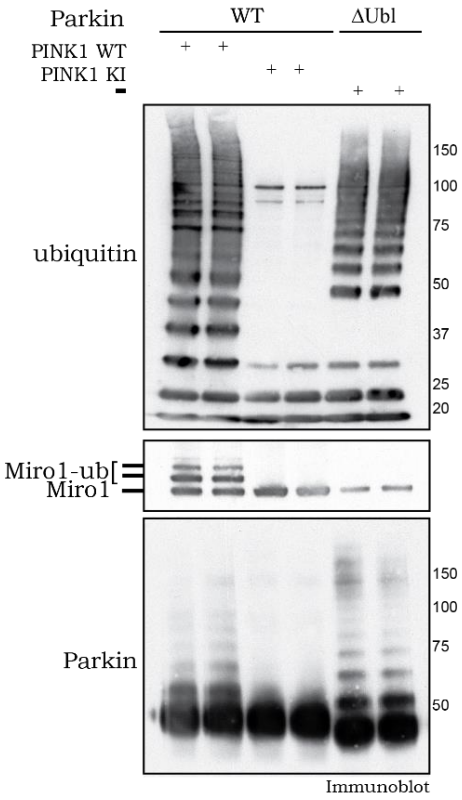

Figure 3.8 Ubl domain of Parkin is required for optimal substrate ubiquitylation.

Full length (lanes 1, 2), but not ΔUbl-Parkin (lanes 5, 6) ubiquitylates Miro1. ΔUbl-Parkin alone was tested in parallel with full-length (WT) Parkin pre-phosphorylated by wild-type (WT) or kinase-inactive (KI) TcPINK1 in an *in vitro* ubiquitylation assay. Reactions were analysed by SDS-PAGE; Miro1, Ubiquitin and Parkin were detected using anti-SUMO, anti-FLAG and anti-Parkin antibodies, respectively.

3.3.2 Identification of Parkin-mediated Miro1 ubiquitylation sites

Post-translational protein modification with ubiquitin constitutes a major cell regulatory system (Finley et al., 2004). One of the key outstanding questions in the field remains identification of ubiquitylation sites. Commonly, a mass spectrometry approach utilizing a tryptic Gly-Gly (GG) remnant of ubiquitin on the substrate lysine (Goldknopf and Busch, 1977) is used to determine sites of ubiquitylation. I have utilized this approach to determine the major site(s) of Miro1 ubiquitylation by TcPINK1-activated Parkin. To achieve this, an

in vitro Miro1 ubiquitylation assay using Parkin pre-incubated with wild-type or kinase-inactive TcPINK1 was performed; the reaction was then subjected to SDS-PAGE followed by staining and in-gel tryptic digestion (Figure 3.9). Mass spectrometric analysis was conducted by Dr. Van Kelly (laboratory of Dr. Patrick Pedrioli).

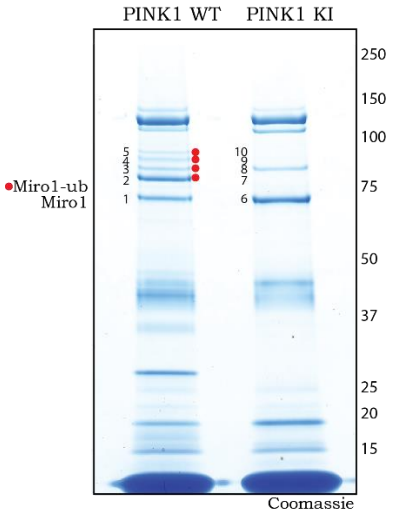

Figure 3.9 Sample preparation for Mass spectrometry analysis

In vitro ubiquitylation assay using wild-type (WT) or kinase-inactive (KI) PINK1 was carried out as described in Section 3.2.5. 80% of the sample was subjected to analysis by SDS-PAGE. Miro1 and ubiquitylated Miro1 (Miro1-ub) gel bands were excised and analysed by LTQ-Orbitrap mass spectrometry.

Five unique peptides carrying a K-GG tryptic remnant were identified in samples incubated with Parkin and wild-type TcPINK1, but were absent in the presence of Parkin and kinase-inactive TcPINK1 (Figure 3.10 B). Lysine 153 (Lys^{153}) was found in a tryptic peptide located within the first GTPase domain; lysine 230 (Lys^{230}) and lysine 235 (Lys^{235}) were found carrying K-GG remnants in two independent peptides found within the central linker region and Lys^{330} was identified in fourth peptide located within the second EF-hand domain of Miro1 (Figure 3.10 A,B). A fifth peptide containing a K-GG remnant at Lys^{572} was located within the C-terminal non-catalytic region of Miro1, between the second GTPase domain and the transmembrane domain (Figure 3.10 A, B).

In parallel, an in-solution tryptic digest was set up and yielded a miscleaved peptide, MPPPQAFTCNTADAPSKDIFVK(GG)LTTMAMYPHVTQADLK, spanning lysine 572 (Lys^{572}) and another highly conserved lysine residue, lysine 567 (Lys^{567}) (data not shown). Peptide fragmentation pattern analysis supported the modification occurring at Lys^{572}. To validate the finding, two point mutants – Lys567Arg (K567R) and Lys572Arg (K572R) – of Miro1 were generated and ubiquitylation assays were undertaken. Lys572Arg Miro1 displayed a significant reduction in monoubiquitylated as well as multi-monoubiquitylated species (Figure 3.11), whereas the Lys567Arg mutant behaved like the wild-type Miro1 under the assay conditions used (Figure 3.11). This mutagenesis analysis is consistent with the mass spectrometry data and indicates that Lys^{572} is a major site of Miro1 ubiquitylation.

These analyses indicate that Miro1 undergoes multi-monoubiquitylation and that Lys^{153}, Lys^{230}, Lys^{235}, Lys^{330}, and Lys^{572} are the major sites of Miro1 ubiquitylation targeted by activated Parkin. All the sites identified are highly conserved (Figure 3.10 C), and several of these residues in Miro1 (Lys^{153}, Lys^{235}, and Lys^{572}) have also recently been reported to be ubiquitylated in cells over-expressing tagged Parkin (Sarraf et al., 2013).

A

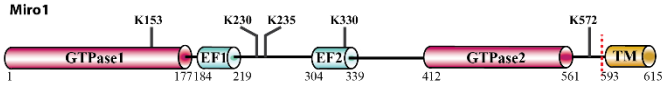

B

Site	Peptide sequence	Theoretical m/z	Observed m/z	Ppm error	Charge state	Mascot score
K153	NLKNISELFYYAQK	615.6562	615.6586	3.84	3	35
K230	ICFNTPLAPQALEDVKNVVR	800.0898	800.4228	417*	3	22
K235	KHISDGVADSGLTLK	827.9416	827.9421	0.61	2	29
K330	DCALSPDELKDLFK	588.9539	588.9533	-1.07	3	28
K572	DIFVKLTTMAMYPHVTQADLK	846.1028	846.102	-0.95	3	38

C

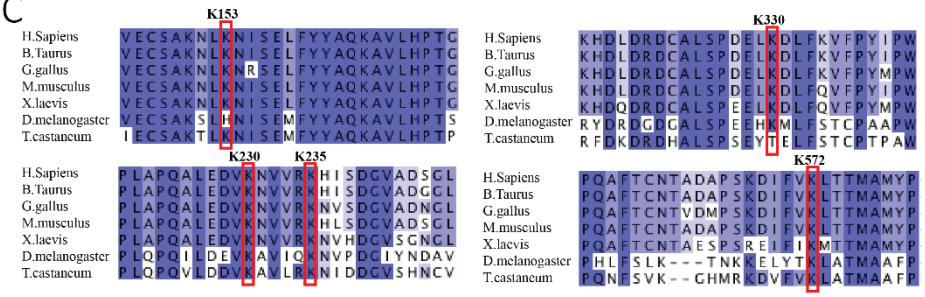

Figure 3.10 Miro1 ubiquitylation sites

(**A**) Schematic representation of Miro1 domain architecture showing the identified ubiquitylation sites and truncation site (red dotted line). (**B**) Table summarizing peptide sequences used to identify Lys^{153}, Lys^{230}, Lys^{235}, Lys^{330} and Lys^{572} as ubiquitylation sites on Miro1. Ubiquitin isopeptides were identified by Mascot (www.matrixscience.com) and spectra were manually validated to ensure peptide fragmentation gave good sequence coverage (* 417 ppm error equates to a -1.81 ppm error around the C13 isotope). (**C**) Sequence alignment showing high degree of conservation of residues surrounding Lys^{153}, Lys^{230} and Lys^{235} (left), Lys^{330} and Lys^{572} (right) in human Miro1 and a variety of lower organisms.

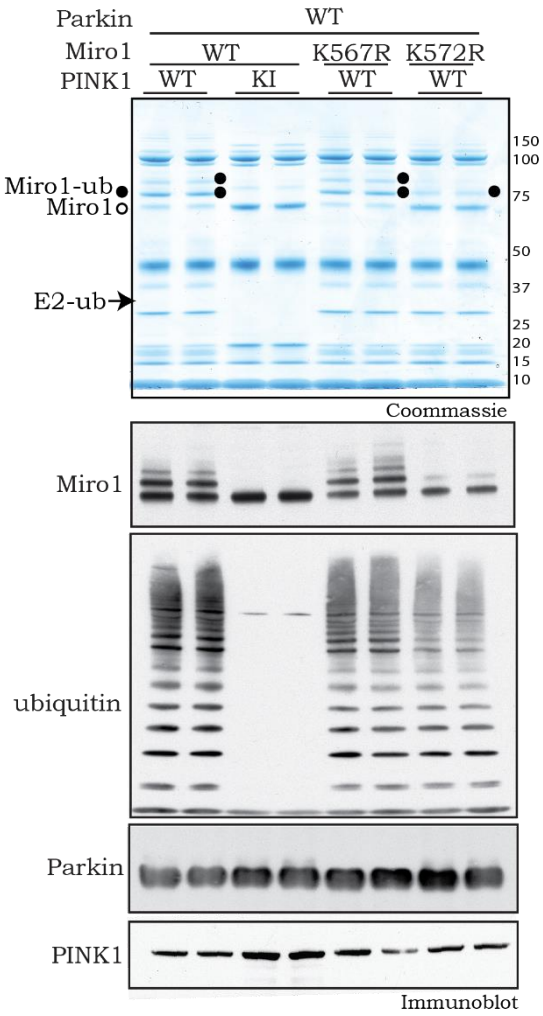

Figure 3.11 Miro1 Lys572 is a major site of ubiquitylation catalysed by activated Parkin.

Mutation of Lys572Arg (K572R) but not Lys567Arg (K567R) substantially reduces ubiquitylation by activated Parkin. Wild-type Miro1 (WT) and two point mutants (K567R, K572R) were used in a ubiquitylation assay with WT Parkin pre-incubated with WT or KI TcPINK1 as described in Section 2.2.28.2. Proteins were detected by Coomassie blue staining or immunoblotting using anti-Sumo, anti-FLAG, anti-Parkin and anti-MBP antibodies to detect Miro1, ubiquitin, Parkin and TcPINK1 respectively. Multi-monoubiquitylated Miro1 (Miro1-ub) is denoted by black dots.

3.3.3 Analysis of Parkin-generated ubiquitin isopeptide linkages

Ubiquitin signalling cascade outcomes rely heavily on the topology of the polyubiquitin chain(s) synthesised (Komander and Rape, 2012). I next attempted to determine the chain topology or topologies present following Parkin ubiquitylation in my assay. A similar mass spectrometry approach, as described in the previous section, identifying K-GG remnants on ubiquitin backbone was utilised. In order to rigorously determine the critical role of Parkin activation by PINK1 phosphorylation at Ser^{65} a number of different conditions, summarised in Table 3.1, were analysed.

Table 3.1 Summary outline of experimental conditions for identification of Parkin-generated ubiquitin chain topologies

PINK1	WT	KI	-	WT	WT	WT	WT
Parkin	WT	WT	WT	T415N	S65A	-	WT
UbcH7	+	+	+	+	+	+	-
Expected phosphorylation at Ser65	✓	×	×	✓	×	×	✓
Expected Parkin activity	✓	×	×	×	×	×	×

Wild-type (WT) Parkin was phosphorylated by wild-type (WT) TcPINK1 and ubiquitylation assays with and without UbcH7 were carried out. Samples lacking the E2 ubiquitin conjugating ligase were used in order to identify any ubiquitin bonds that might be present in the Flag-ubiquitin source. WT TcPINK1 with Ser65Ala (S65A) Parkin as well as kinase-inactive (KI) PINK1 with WT Parkin were used as controls to validate the critical role of Parkin phosphorylation at Ser^{65} for chain formation. A sample lacking TcPINK1 was included as a control for potential peptide carry-over from the TcPINK1 samples. Two conditions reflecting lack of Parkin activity – one omitting the E3 ligase and one with a Parkin Thr415Asn (T415N) catalytically inactive point mutant - were included to ensure that ubiquitin chains generated were dependent on Parkin E3 ligase activity.

The ubiquitylation assays were carried out as previously described and subjected to in-solution digestion followed by LTQ-Orbitrap mass spectrometry performed by Dr. Van Kelly

(laboratory of Patrick Pedrioli). The methods used to determine the relative quantities of peptides carrying K-GG remnants in different conditions enabled determination of Parkin-catalysed formation of polyubiquitin linkage types. The formation of both canonical (K48 and K63) and non-canonical (K6, K11, K33) ubiquitin chain linkages in a Parkin$^{\text{Phospho-Ser65}}$-dependent manner was detected (Figure 3.12). K27 isopeptides were also detected, but were independent of Parkin (Figure 3.12).

Unfortunately, due to limitations of the mass spectrometry methodology employed, it was not possible to determine if Parkin was responsible for the formation of branched ubiquitin chain topologies or if distinct homogenous chains of each linkage type were being formed. Consistent with my analysis, a recent study has confirmed the Parkin-dependent formation of most of these chain types on the mitochondria of cells stimulated with CCCP (Ordureau et al., 2014).

Site	Peptide sequence	Theoretical m/z	Observed m/z	Ppm error	Charge state	Mascot score
K6	GGMQIFVKTLTGK	498.6097	498.6129	6.46	3	24
K11	TLTGKTITLEVEPSDTIENVK	801.4269	801.4301	4.05	3	42
K27	TITLEVEPSDTIENVKAK	701.039	701.0391	0.26	3	25
K33	IQDKEGIPPDQQR	819.4157	819.4151	-0.75	2	18
K48	LIFAGKQLEDGR	730.8964	730.8994	4.01	2	63
K63	TLSDYNIQKESTLHLVLR	748.7376	748.7445	9.24	3	32

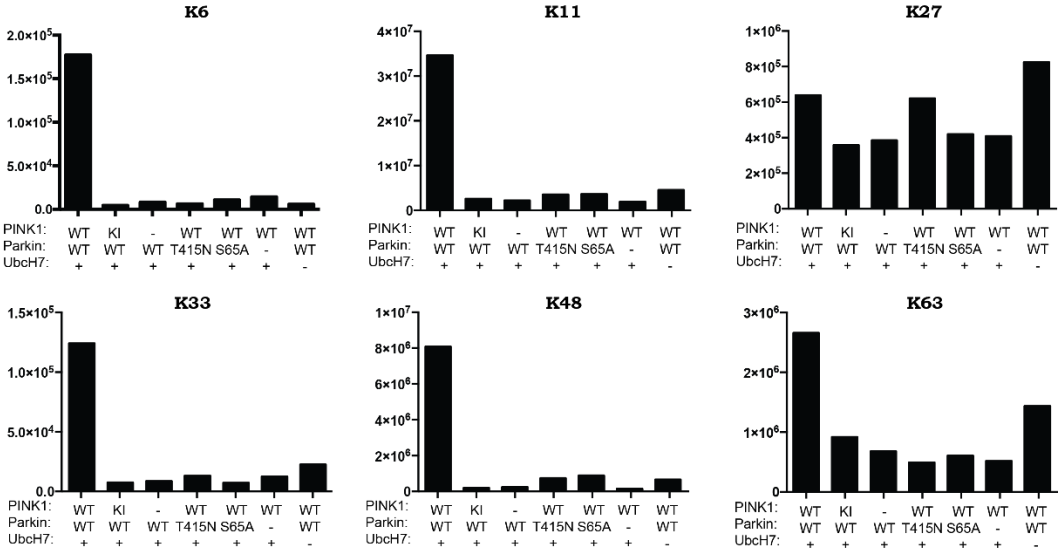

Figure 3.12 Identification and relative quantification of ubiquitin-ubiquitin chain linkage isopeptides generated by Parkin.

Ubiquitylation assays were carried out as described in Section 2.2.28.2, followed by in-solution tryptic digestion and analysis by LTQ-Orbitrap mass spectrometry. Ubiquitin isopeptides were identified by Mascot (www.matrixscience.com) on six lysines in the wild-type PINK1/wild-type Parkin/+UbcH7 sample (top). Note that the FLAG-tag on ubiquitin prohibited analysis of linear M1 conjugation and additional amino acids (arising from the FLAG tag) were observed on the K6 peptide. The most abundant charge state identified was selected for relative quantification of each ubiquitin isopeptides across all samples (bottom). Chromatographic peak areas were extracted for the theoretical m/z of MS1 precursor ion signals and two isotopes using Skyline (MacLean et al., 2010). With the exception of K27, all observed linkages were depended on wild-type parkin and PINK1. K29 was not detected. Chain composition differences between free and substrate bound ubiquitin chains could not be determined in the present analysis without prior fractionation of substrates.

3.3.4 Analysis of the influence of Parkin Ser^{65} phosphorylation on Parkin-E2 interactions

Parkin was first designated as an E3 ligase due to its similarity to another E3 ligase HHARI and the subsequent demonstration of its E2-dependent autoubiquitylation activity (Zhang et al., 2000). Multiple studies have since identified UbcH7 (UBE2L3), UbcH8 (UBE2L6), UBC6 (UBE2J1), UBC7 (UBE2G1, UBE2G2), and the Ubc13/Uev1a heterodimer (UBE2N/UBE2V1) (Lazarou et al., 2013, Walden and Martinez-Torres, 2012, Wenzel and Klevit, 2012, Dawson and Dawson, 2010) as partnering E2s for tagged Parkin in autoubiuqitylation assays. Furthermore, Parkin was unexpectedly found to be capable of E2-independent monoubiquitylation *in vitro* (Chew et al., 2011). However, evidence to support the identity of the physiological E2(s) that Parkin interacts with has remained elusive. Since Parkin was historically thought to behave as a RING E3 ligase, determining the partnering E2(s) was regarded as crucial since the RING E3 - E2 interaction plays an important role in specifying the diversity and specificity of ubiquitin conjugates (Metzger et al., 2013, Deshaies and Joazeiro, 2009).

I therefore set out to test how a panel of 25 E2 ligases influenced the ability of Parkin to catalyse free chain formation and monoubiquitylation of Miro1 by assessing Parkin free chain formation and Miro1 ubiquitylation in the presence of each of these E2s, using E2 Ube2L3 (UbcH7) as a control to provide a reference level for Parkin activity. This experiment was repeated three times in duplicate and each E2 was tested under three conditions: firstly, without any PINK1 or Parkin to enable visualisation of E3-independent activity; or in the presence of Parkin with wild-type; or kinase-inactive, TcPINK1. Results were analysed by immunoblotting for ubiquitin, Miro1 and PINK1.

Strikingly, activated Parkin exhibited a similar pattern of free chain formation and Miro1 ubiquitylation in the presence of 18 out of 25 E2s, UBE2L3 included (Figure 3.13) with varying levels of free chain formation and Miro1 ubiquitylation observed when pre-phosphorylated Parkin was added (Figure 3.13). The other 7 E2s tested, e.g. Ube2T, did not permit activated Parkin to catalyse the formation of free ubiquitin chains but still enabled

Miro1 to become ubiquitylated by Parkin in the presence of wild-type TcPINK1 in all cases (Figure 3.13).

Since the ubiquitin signal strength as well as the band pattern differed slightly depending on the E2 ligase used, this suggests that free chain formation, in addition to the resultant chain topology, may be critically dependent on the E2-E3 interaction, akin to canonical RING E3 ligases. At the time that these experiments were conducted, the first evidence of Parkin acting as a RING-HECT hybrid was revealed (Wenzel et al., 2011). In contrast to RING E3 ligases, the specification of substrate/ubiquitin chain topology by HECT E3 ligases is largely independent of the identity of the E2, and instead the topology and pattern of ubiquitin conjugates is conferred primarily by the E3 - substrate interaction. The results from this E2 scanning experiment are consistent with the observation that Parkin exhibits mainly HECT-like properties, wherein ubiquitylation of Miro1 is governed principally by its interaction with Parkin itself.

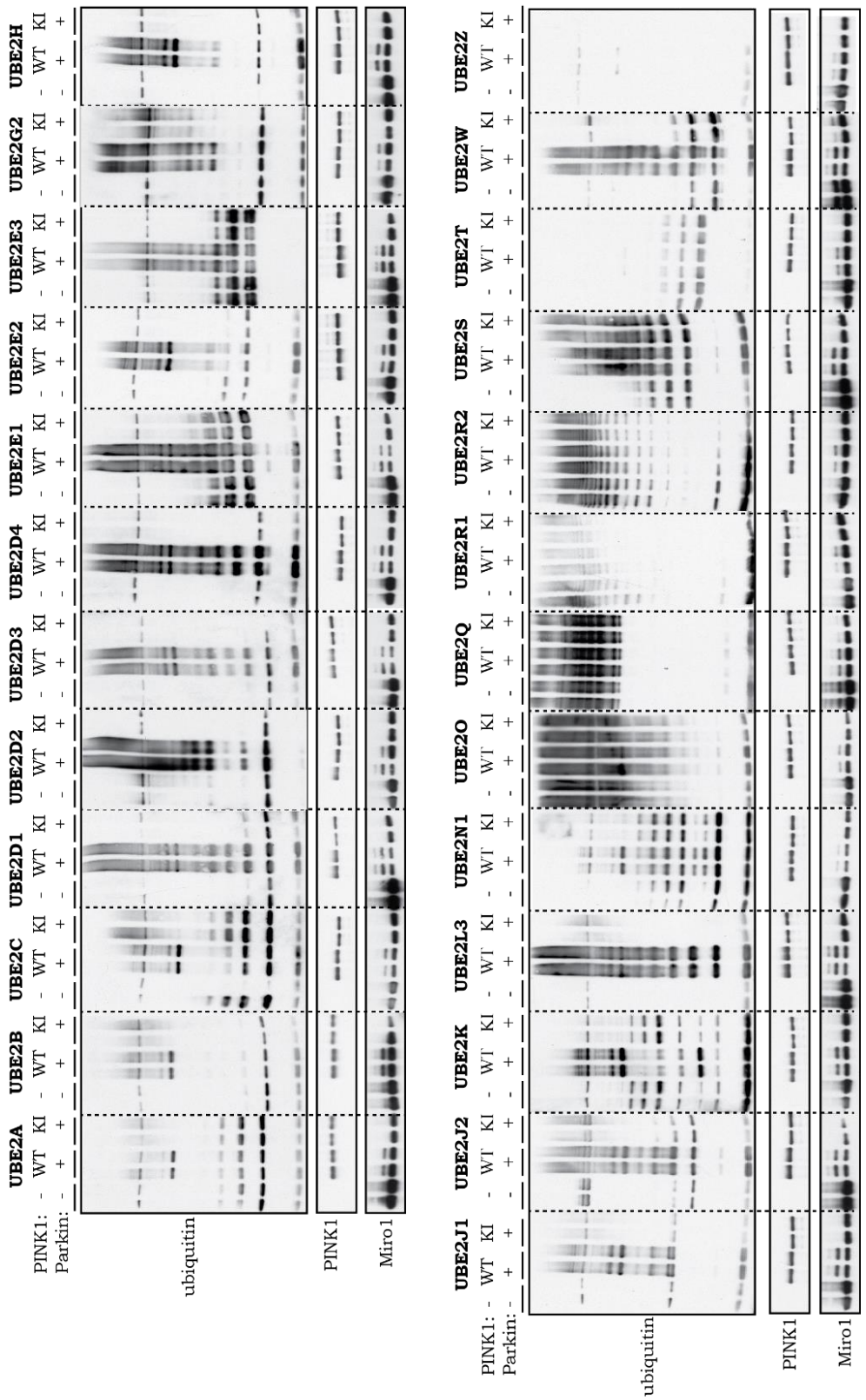
UBE2A UBE2B UBE2C UBE2D1 UBE2D2 UBE2D3 UBE2D4 UBE2E1 UBE2E2 UBE2E3 UBE2G2 UBE2H
PINK1: - WT KI - WT KI - WT KI - WT KI - WT KI - WT KI - WT KI - WT KI - WT KI - WT KI - WT KI - WT KI
Parkin: - + + - + + - + + - + + - + + - + + - + + - + + - + + - + +
ubiquitin
PINK1
Miro1
UBE2J1 UBE2J2 UBE2K UBE2L3 UBE2N1 UBE2O UBE2Q UBE2R1 UBE2R2 UBE2S UBE2T UBE2W UBE2Z
PINK1: - WT KI - WT KI - WT KI - WT KI - WT KI - WT KI - WT KI - WT KI - WT KI - WT KI - WT KI - WT KI
Parkin: - + + - + + - + + - + + - + + - + + - + + - + + - + + - + +
ubiquitin
PINK1
Miro1

Figure 3.13 Parkin can interact with multiple different E2 conjugating enzymes to catalyse Miro1 ubiquitylation with or without free ubiquitin chain formation.

An E2 scan of 25 different E2 conjugating enzymes was undertaken. Two micrograms of wild-type Parkin were incubated with one microgram of wild-type (WT) or kinase-inactive (KI) (D359A) TcPINK in a kinase reaction for 60 min, as described in Section 2.2.282. Activated Parkin was then added into pre-assembled ubiquitylation reactions containing one microgram of the E2 ubiquitin conjugating enzyme, as indicated. Reactions were terminated after 60 min by addition of SDS loading buffer and resolved by SDS-PAGE. Miro1, Ubiquitin and PINK1 were detected by immunoblotting using anti-SUMO, anti-FLAG and anti-MBP antibodies, respectively.

3.4 Analysis of Parkin disease mutants on Parkin E3 ligase activity

Mutations in Parkin were first associated with autosomal recessive juvenile Parkinsonism in a Japanese patient cohort in 1998 (Kitada et al., 1998). They have since been linked with familial cases of early-onset Parkinson's disease (PD) in a wide range of studies (Lucking et al., 2000, Abbas et al., 1999). To date, over 200 mutations in the PARK2 gene have been mapped (http://www.molgen.vib-ua.be/). Whilst the impact of mutations on Parkin function has been previously reported, the majority of studies have used either N-terminally tagged or N-terminally truncated versions of Parkin (Trempe et al., 2013, Wauer and Komander, 2013, Hampe et al., 2006, Matsuda et al., 2006, Sriram et al., 2005, Ren et al., 2003, Shimura et al., 2001, Shimura et al., 2000). Consequently, several conflicting lines of evidence regarding the changes in activity mediated by disease mutations exist. Shimura and colleagues reported the Arg42Pro (R42P) mutant to be ligase-inactive (Shimura et al., 2001, Shimura et al., 2000) whereas others have reported no effect on activity (Matsuda et al., 2006, Hampe et al., 2006); the Lys161Asn (K161N) mutation was reported to be ligase-inactive (Trempe et al., 2013, Ren et al., 2003), whilst other groups reported no effect on ligase activity (Wauer and Komander, 2013, Matsuda et al., 2006, Hampe et al., 2006).

In order to shed light on this controversial issue, I chose to utilise my novel substrate-based assay for Parkin activity to assess the effect of disease-assocated Parkin mutations on Miro 1 ubiquitylation. In order to avoid any artefactual effects on Ubl-mediated inhibition that might be caused by tagging the N-terminus of Parkin, a range of disease-associated mutations were introduced into full-length untagged Parkin. The selected variants of Parkin encompassed

mutations affecting every functional domain of Parkin and are as follows: Lys27Asn (K27N), Arg33Gln (R33Q), R42P, and Ala46Pro (A46P) (Ubl domain); K161N, Lys211Asn (K211N) (UPD domain); Arg275Trp (R275W) (RING1 domain); Gly328Glu (G328E) (IBR domain); Thr415Asn (T415N); Gly430Asp (G430D); and Cys431Phe (C431F) (RING2 domain). These mutations were chosen since they have been reported as homozygous or compound heterozygous mutations that co-segregate with the disease in early-onset PD cases (Figure 3.14).

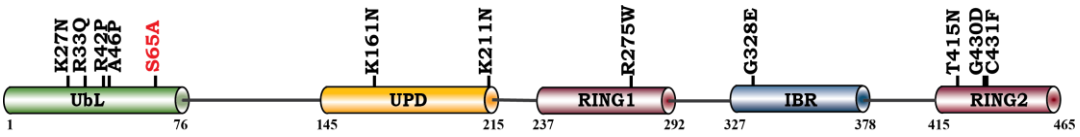

Figure 3.14 Location of Parkinson's disease-associated mutations in Parkin

A schematic representation of Parkin domain architecture showing the location of disease-associated Parkin mutants.

3.4.1 Parkin disease-associated mutants exhibit differential effects on Parkin-mediated ubiquitylation following Ser^{65} phosphorylation

The above mentioned Parkin mutants, together with wild-type and Ser65Ala controls, were tested for their ability to catalyse Miro1 ubiquitylation and/or formation of free ubiquitin chains after activation by TcPINK1 (Figure 3.15 top). To determine if their phosphorylation by TcPINK1 is affected, a kinase assay with [γ-^{32}P] ATP was set up in parallel (Figure 3.15 bottom). Diverse effects on Parkin E3 ligase activity were observed, enabling mutations to be classified into several distinct groups. In Group 1, two mutations, C431F, which disrupts the catalytic cysteine, and the RING1 mutant R275W, completely abolished Parkin activity (Figure 3.15). In Group 2, three mutations caused a marked reduction in both free ubiquitin chain formation and Miro1 ubiquitylation; the G430D mutation that lies adjacent to the catalytic cysteine, the UPD mutant K161N and the RING2 mutant T415N (Figure 3.15). In Group 4, two mutations abolished free ubiquitin chain formation while promoting Miro1 monoubiquitylation rather than multi-monoubiquitylation (Figure 3.15), these were the Ubl

mutant A46P and the UPD mutant K211N. Furthermore, in Group 5, two mutants exhibited a differential increase in Parkin E3 ligase activity: both the Ubl mutant R33Q and the IBR mutant G328E led to increased Miro1 ubiquitylation, while increased free chain formation was only observed with R33Q. This effect might be explained by the observation that the phosphorylation of the R33Q and G328E mutants was significantly higher than that of wild-type Parkin (Figure 3.15 bottom panel). Finally, mutations in Group 6, which comprise the Ubl domain mutations K27N and R42P, had no effect on Parkin mediated ubiquitylation. No mutations led to a decrease/abolition of Miro1 ubiquitylation with free ubiquitin chain formation remaining unaffected.

Following activation of Parkin, TcPINK1 undergoes monoubiquitylation observed in a bandshift detectable by ubiquitin immunoblotting that is absent when kinase-inactive TcPINK1 or Ser65Ala Parkin is used (Figure 3.5). During the mass-spectrometry analysis, the site of ubiquitylation was mapped to a lysine residue located within the N-terminal MBP tag (Lys306 lying in the SYEEELVKDPR sequence motif; data not shown). MBP-TcPINK1 ubiquitylation was lost in mutants associated with a decrease in either Miro1 ubiquitylation or free chain formation (A46P, K211N) or both (S65A, R275W, C431F, G430D, K161N, T415N) (Groups 1-3) (Figure 3.15), and was unaltered in mutants that had no effect or increased Parkin activity (WT, K27N, R33Q, R42P, G328E) (Groups 4-6) (Figure 3.15).

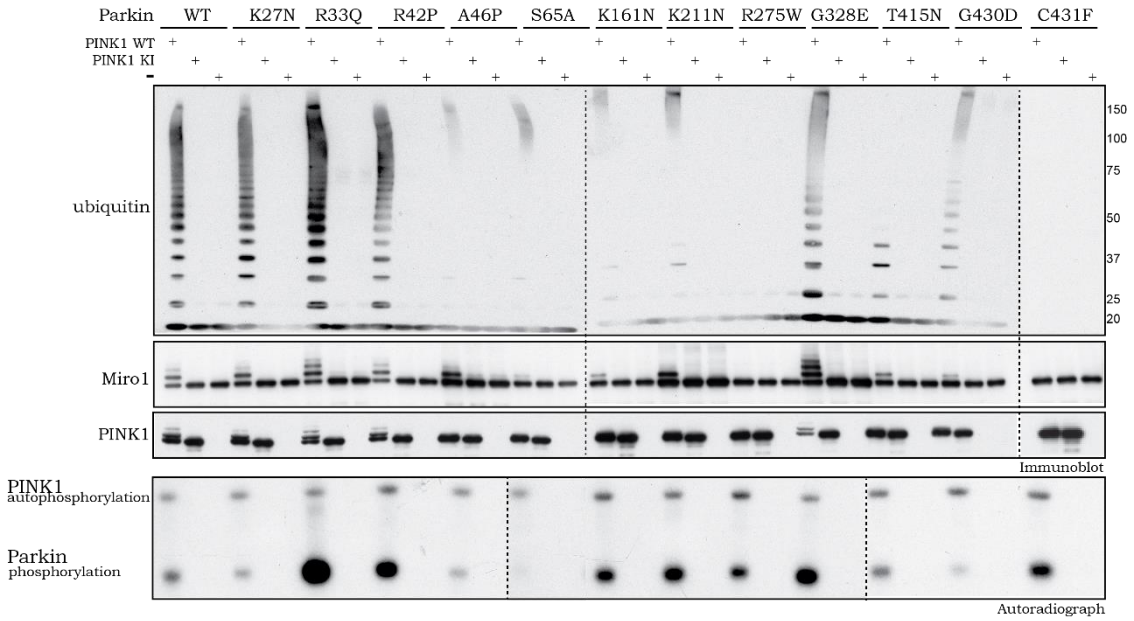

Figure 3.15 Heterogeneity of the impact of Parkinson's disease associated point mutations on Parkin E3 ligase activity.

Parkin mutations exhibit diverse effects on E3 ligase activity. Assays using wild-type (WT) and kinase inactive (KI) PINK1 (D359A) in combination with WT and indicated mutants of Parkin and the substrate Miro1 were undertaken as described in Section 2.2.28.2. A kinase reaction including 0.1 mM [γ-32P] ATP (approx. 500 cpm/pmol) was carried out in parallel for 60 min to confirm the phosphorylation as described in Section 2.2.28.1. Reactions were terminated after 60 min by addition of SDS loading buffer and resolved by SDS-PAGE. Miro1, Ubiquitin, Parkin and PINK1 were detected using anti-SUMO, anti-FLAG, anti-Parkin and anti-MBP antibodies, respectively. Representative of 3 independent experiments.

3.4.2 Impact of disease-associated point mutations on ubiquitin discharge from loaded UbcH7 following Ser^{65} phosphorylation

Subsequently, I sought to further my investigation into the effect of disease-associated mutations on Parkin activity by analysing their impact on ubiquitin discharge from UbcH7. E2 discharge reactions were set up as previously described (Section 2.2.28.3). Each of the disease mutants, as well as the wild-type and Ser65Ala Parkin, was incubated with charged UbcH7, both without kinase as well as with wild-type and kinase-inactive TcPINK1 (Figure 3.16). Reactions were subjected to SDS-PAGE, followed by Coomassie staining and LICOR quantification of the stained bands. Since ubiquitin discharge generates free E2, the ratio of UbcH7:UbcH7-ub was used as a measure of ubiquitin discharge (Figure 3.16, upper panel). All active mutants displayed maximal unloading of ubiquitin from the E2 when incubated with wild-type TcPINK1. Samples containing kinase-inactive TcPINK1 or no kinase showed none to minimal discharge, comparable to the Parkin empty control.

Parkin mutants that exhibited normal or increased ubiquitylation of Miro1, namely K27N, R33Q, R42P, and G328E, showed no significant changes in their ability to stimulate ubiquitin discharge (Figure 3.16). However, a possible Parkin-ubiquitin thioester was observed for the R33Q mutant, suggesting that this point mutation may lead to conformational changes that increase the stability of the thioester bond (Figure 3.16). Further experiments examining the nature of the bond will be necessary to clarify this.

The Parkin mutants A46P, R275W and T415N displayed a considerably reduced level of E2-ubiquitin discharge, similar to that of the S65A mutant and the active site mutant C431F, suggesting that these residues might impact E2 binding or ubiquitin discharge upon Parkin Ser^{65} phosphorylation. The remaining mutants, comprising the UPD mutants K161N, K211N and the RING2 mutant G430D, exhibited intact or modestly reduced (K211N) Ser^{65} phosphorylation-dependent E2 discharge.

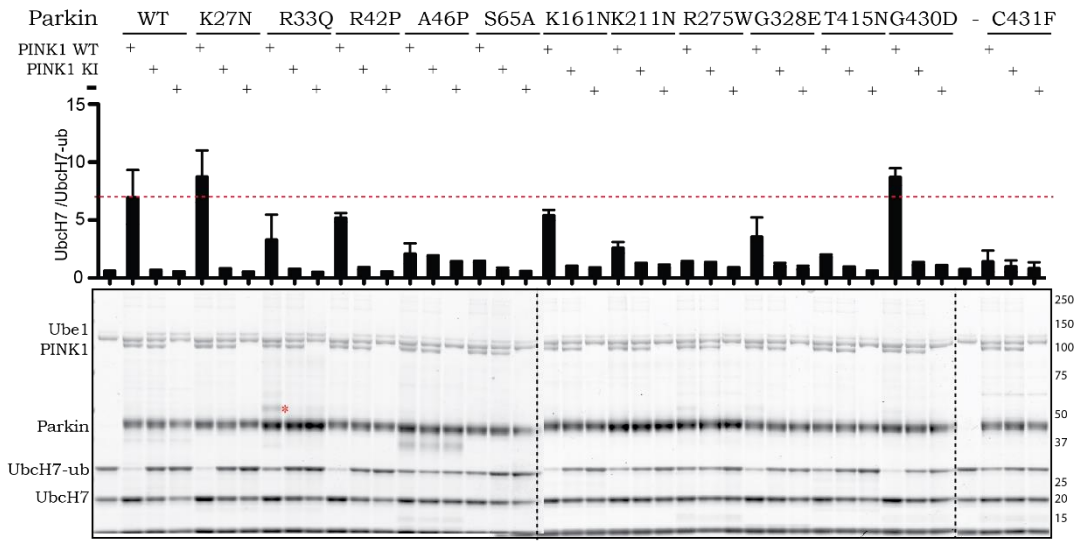

Figure 3.16 Analysis of the effect of Parkin disease-associated mutations on ubiquitin discharge from UbcH7 following Ser^{65} Parkin phosphorylation.

Parkinson's disease associated mutants of Parkin were phosphorylated by wild-type (WT) or kinase-inactive (KI) TcPINK1 alongside a control reaction lacking kinase carried out in parallel. E2 discharge reactions were performed by incubation of Parkin after the kinase assay with ubiquitin loaded UbcH7 (UbcH7-ub) for 15 min at 30 °C. Discharge was estimated by quantifying UbcH7-ub and UbcH7 bands by LICOR and calculating the ratio of UbcH7:UbcH7-ub. Mean values ± standard deviation of 3 independent experiments are presented. Red dotted line indicates the WT activity. * indicates the R33Q Parkin–ubiquitin thioester.

3.5 Discussion

3.5.1 Phosphorylation of Parkin at Ser^{65} by PINK1 stimulates its E3 ligase activity

Whilst genetic studies (Clark et al., 2006, Park et al., 2006, Yang et al., 2006) and cell biological studies (Geisler et al., 2010, Matsuda et al., 2010, Narendra et al., 2010, Vives-Bauza et al., 2010) have linked PINK1 and Parkin in a linear signalling pathway, the molecular details of how these proteins interact have remained obscure. The discovery that PINK1 phosphorylates Parkin at Ser^{65} and the demonstration that phosphorylation stimulates the activation of Parkin E3 ligase activity represents a fundamental advance in our understanding of how these proteins interact although a further regulatory mechanism will be revealed in Chapter 4. Furthermore, the elaboration of both a novel E3 ligase assay (monitoring free-poly-ubiquitin chain formation as well as substrate ubiquitylation) (Figure 3.5 & Figure 3.6 respectively) and UbcH7 ubiquitin discharge assay (Figure 3.7) has enabled demonstration of the dependence of Parkin activity on Ser^{65} phosphorylation, and provides powerful new tools for the field to probe Parkin biology and activity.

3.5.2 Miro1 is a direct Parkin substrate

Miro1 plays a crucial role in mitochondrial trafficking by tethering mitochondria to KIF5 motor proteins, enabling mitochondria to be transported along microtubules (Macaskill et al., 2009). Its levels were shown to be regulated by PINK1 and Parkin in two previous studies (Wang et al., 2011, Liu et al., 2012). Wang and colleagues reported that over-expression of PINK1 and/or Parkin resulted in decreased Miro1 levels in HEK 293T cells, mediated by PINK1-dependent phosphorylation of Miro1 at Ser^{156} (Wang et al., 2011). In contrast, Liu and colleagues found no evidence of Miro1 phosphorylation at Ser^{156} and reported a decrease in Miro1 levels upon PINK1 knockdown by siRNA in HeLa cells, as well as in PINK1 knock-out MEFs when compared to levels in wild type MEFs (Liu et al., 2012). A global Parkin ubiquitylome analysis reported Miro1 Lys^{153}, Lys^{194}, Lys^{235} and Lys^{572} sites in cells over-expressing tagged Parkin stimulated with CCCP (Sarraf et al., 2013). Unfortunately, due to

the limitations of global mass spectrometry analysis, this study failed to address if Miro1, amongst other ubiquitin-modified proteins, was ubiquitylated directly by Parkin. The *in vitro* results presented in this chapter are the first to demonstrate that Miro1 is a direct substrate of Parkin.

Furthermore, I have demonstrated that the Miro1 Lys572Arg mutation causes a drastic reduction of ubiquitylation (Figure 3.11), suggesting that Lys^{572} is a major Parkin-targeted site. I also identified Lys^{230}, and Lys^{330} as direct sites of Parkin ubiquitylation, neither of which have previously been reported (Figure 3.10). Whilst I did not identify a K-GG remnant on Miro1 Lys^{194}, as has been previously reported from a mass spectrometry analysis (Sarraf et al., 2013), I cannot rule it out as a direct Parkin-mediated ubiquitylation site, since it may be of lower stoichiometry and therefore undetectable in the present analysis (Figure 3.10). Alternatively, the inherent lack of selectivity in global mass-spectrometry approaches raises the possibility of this site being modified by an alternative E3 ligase which in itself is regulated by the PINK1 pathway.

Several of the identified sites lie within or near functional domains of Miro1, including Lys^{153}, which is located within the N-terminal GTPase domain, Lys^{330}, which lies within the second EF hand domain, and Lys^{572}, which lies in a C-terminal linker region, near the transmembrane domain that localises Miro1 to the outer mitochondrial membrane. In a recently solved structure of *D. melanogaster* orthologue of Miro1, Glu^{354} was shown to be involved in Ca^{2+} coordination (Klosowiak et al., 2013). This residue lies one amino acid away from Lys^{356}, which is homologous to Lys^{330} in human Miro1 and which we identified as a Parkin ubiquitylation site. Given that Parkin induces multi-monoubiquitylation of Miro1, as opposed to attachment of a polyubiquitin chain, it is tempting to speculate that ubiquitylation of Lys^{330} could impact Ca^{2+} binding of Miro1. In addition, Miro1 was shown to be rapidly ubiquitylated after activation of the PINK1-Parkin pathway with CCCP, however its degradation by the proteasome was delayed (Birsa et al., 2014), suggesting a dual regulation by ubiquitin. It is possible that an initial ubiquitylation event acts to change the function of Miro1, leading perhaps to segregation of damaged mitochondria. Recruitment of additional

adaptor proteins via this ubiquitylation event might be required before its subsequent degradation by the proteasome. In future studies it would therefore be exciting to test whether Parkin-mediated ubiquitylation of Miro1 leads to direct alteration of its function, for example its GTPase activity, localisation, calcium binding, or role in mitochondrial transport.

Previous studies employing N-terminally tagged Parkin have also observed monoubiquitylation activity. The Tanaka laboratory first reported that MBP-Parkin could catalyse *in vitro* MBP monoubiquitylation in *cis* (Matsuda et al., 2006), and multimonoubiquitylation activity has also been reported in an autoubiquitylation assay employing GST-Parkin (Hampe et al., 2006). Monoubiquitylation and multimonoubiquitylation have been shown to play a role in a range of cellular functions including histone regulation, DNA repair, viral budding and endocytosis (Sadowski et al., 2012, Hicke, 2001). The consequences of mono/multimonoubiquitylation of outer mitochondrial membrane proteins such as Miro1 are as yet unknown. This modification could be critical for intermolecular signalling at the mitochondria - in endocytosis, many proteins, such as Eps15, contain ubiquitin interaction motifs (UIMs) that bind monoubiquitin (Husnjak and Dikic, 2012). Alternatively, monoubiquitylated Miro1 and other Parkin substrates may be targeted by other E3 ligases. This has been demonstrated for the ubiquitylation of proliferating cell nuclear antigen (PCNA), which binds DNA during DNA replication (Bergink and Jentsch, 2009). However, the possibility that Parkin itself can catalyse the formation of polyubiquitylated Miro1 under specific cellular conditions or in the presence of a regulatory protein missing from our assay cannot be excluded. The E4 CHIP has previously been shown to enhance Parkin-mediated polyubiquitylation of the substrate Pael-R (Imai et al., 2002), providing prior evidence for this phenomena.

3.5.3 Parkin-E2 interactions

Given that Parkin possesses both RING and HECT-like properties it was not obvious how the nature of the ubiquitin conjugates might be influenced by the partnering E2. I therefore tested the activity of Parkin in conjunction with a panel of 25 different E2s, and observed

that the ubiquitylation of the substrate Miro1 by Parkin was not influenced by the vast majority of the E2s tested when compared to the control E2 Ube2L3 (UbcH7) (Figure 3.13).

This observation suggests that Parkin exhibits mainly HECT-like properties, such that the interaction between Parkin and Miro1 is the critical feature governing the ubiquitylation of Miro 1. Differential effects in the ability of the tested E2s to enable Parkin to catalyse the formation of free ubiquitin chains were nevertheless observed. For example, UBE2L3 enabled both Miro1 ubiquitylation and free chain formation, whereas UBE2T restricted Parkin to Miro1 ubiquitylation. This does suggest that the formation of free chains may be dependent on the E2-E3 interaction. The molecular mechanisms underpinning E2-mediated ubiquitin chain formation remain poorly understood, with a few exceptions. In yeast, the Anaphase promoting complex/cyclosome (APC) has been shown to promote multi-monoubiquitylation of cyclin B in the presence of Ubc4 *in vitro,* whereas Ubc1 enabled it to catalyse polyubiquitin chain formation (Rodrigo-Brenni and Morgan, 2007). Moreover, APC has been shown to exploit the differential selectivity of both E2s in targeting substrates for ubiquitylation *in vivo* (Rodrigo-Brenni and Morgan, 2007). It would be interesting to uncouple substrate ubiquitylation and polyubiquitin chain formation by Parkin and repeat the E2 screen to better understand how the E2-RING1 interaction influences the outcome. Unfortunately, the data presented in this chapter suggests that *in vitro* analysis is unlikely to be helpful in pinpointing the E2 ligases that act with Parkin under physiological conditions. To address this question in future, *in vivo* approaches could be utilised, such as selective ablation of E2s using CRISPR/Cas9 technologies and monitoring of downstream effects on substrate ubiquitylation, mitochondrial segregation and mitophagy initiation.

3.5.4 Differential effects of Parkin disease mutants

A major breakthrough in understanding Parkin molecular biology came in 2013, when several high-resolution structures of Parkin were solved and published (Trempe et al., 2013, Riley et al., 2013, Wauer and Komander, 2013). Inspection and analysis of these structures can potentially shed light on the structural effects of Parkin disease-associated mutations and

suggest an explanation for the molecular mechanisms by which these mutations exert their myriad effects on Parkin activity summarised in Table 3.2.

Table 3.2 Summary of Parkinson's disease mutation effects on Parkin activity

Parkin mutation	Location	E3 activity		E2 discharge
		Miro1-ub	Free-chains	
WT	N/A	↔	↔	↔
K27N	Ubl	↔	↔	↔
R33Q	Ubl	↑	↑	↔
R42P	Ubl	↔	↔	↔
A46P	Ubl	↔	No	↓
S65A	Ubl	No	No	↓
K161N	UPD	↓	↓	↔
K211N	UPD	↔	No	↔
R275W	RING1	No	No	↓
G328E	IBR	↑	↔	↔
T415N	RING2	↓	↓	↓
G430D	RING2	↓	↓	↔
C431F	RING2	No	No	↓

Residue Cys^{431} lies within the RING2 domain and acts as the active site cysteine of Parkin. The Parkin crystal structures reveal that this residue is obscured by an autoinhibitory interface between the RING2 and UPD domains, suggesting that this is a major mechanism through which Parkin autoinhibition is maintained.

The finding that the C431F disease mutation abolishes human Parkin E3 ligase activity in an *in vitro* substrate assay (Figure 3.15) lends further support to the essential catalytic role of Cys^{431} and is consistent with previous analyses (Matsuda et al., 2006, Sriram et al., 2005, Ren et al., 2003). In addition, the demonstration of C431F mutation abrogating ubiquitin discharge from UbcH7 (Figure 3.16) correlates well with reports showing that mutation of the catalytic cysteine to alanine in other RBR family enzymes, such as Cys357Ala mutation in HHARI and the Cys885Ala mutation in HOIP prevents E2-ubiquitin discharge (Duda et al., 2013, Stieglitz et al., 2012b).

The R275W mutation is located in RING1 and leads to complete abolition of Parkin E3 ligase activity (Figure 3.15). Furthermore, the R275W mutant displayed significantly reduced ubiquitin discharge from the E2 (Figure 3.16). This mutation has been the subject of intense investigation since it was identified as a compound heterozygote mutation in a family with evidence of Lewy body pathology at post-mortem (Farrer et al., 2001). The nature of its pathogenicity was unknown, since all prior studies of the R275W mutant had found no effect on E3 ligase activity (Hampe et al., 2006, Matsuda et al., 2006, Sriram et al., 2005). As mentioned, Arg^{275} lies within the core of the RING1 helical domain, therefore, its mutation might disrupt the proper fold of the protein, altering or disrupting E2 binding to the RING1 domain and/or transfer of ubiquitin from the loaded E2 onto the ubiquitin acceptor Cys^{431} in the RING2 domain.

Lys^{161} lies within the UPD domain, and structural analysis suggests that it forms a salt bridge with the RING2 domain as well as a putative phospho-peptide binding pocket that may be important for Parkin activation (Wauer and Komander, 2013). The K161N mutation leads to a significant decrease in the E3 ligase activity of Parkin; both Miro1 ubiquitylation and free chain formation are reduced (Figure 3.15). Previous reports on the K161N mutation have

been conflicting - most studies employing autoubiquitylation assays have found no effect on Parkin activity (Wauer and Komander, 2013, Hampe et al., 2006, Matsuda et al., 2006, Gu et al., 2003), whilst a few studies found that the mutation dampened it down (Trempe et al., 2013, Ren et al., 2003). This mutation did not affect E2-ubquitin discharge, suggesting an alternative mechanism for ubiquitylation disruption. Structural analysis of Parkin has revealed a sulphate-binding pocket, which Lys^{161} contributes to (Wauer and Komander 2013). In future work, it will be important to determine whether Lys^{161} indeed forms part of a phospho-peptide binding pocket and whether the Ser^{65} phosphorylated Ubl might dock there.

The K211N and A46P mutations are located in RING1 and Ubl domains respectively and displayed differential effect on Parkin E3 ligase activity; while Miro1 ubiquitylation ability was preserved, free chain formation was reduced (Figure 3.15). Such differential effects imparted by disease-associated mutations or artificial mutations have not been previously reported for either Parkin or other members of the RBR E3 ligase family of enzymes. As mentioned, Lys^{211} lies within the UPD domain and has also been suggested to form part of the previously mentioned putative phospho-peptide binding pocket (Wauer and Komander, 2013), whilst Ala^{46} lies within the Ubl domain. Previous autoubiquitylation assays have failed to show any changes in K211N mutant activity compared to wild-type Parkin (Hampe et al., 2006, Matsuda et al., 2006), whereas the A46P mutant was reported to be hyperactive in an autoubiquitylation assay (Chaugule et al., 2011). Interestingly, both the A46P and K211N mutants led to a decrease in E2-ubiquitin discharge (Figure 3.16), suggesting that E2 binding and ubiquitin discharge may be essential for the formation of free ubiquitin chains but dispensable for the catalytic activity of Parkin directed towards Miro1 ubiquitylation.

Two mutants, R33Q and G328E, found within the Ubl domain and IBR respectively, exhibited increased Parkin E3 ligase activity upon phosphorylation by PINK1. A previous report has demonstrated the Ubl domain mutants R33Q, K27N and R42P to be constitutively hyperactive (Chaugule et al., 2011). In contrast with this finding, I have observed low basal autoubiquitylation activity for R33Q when compared to wild-type Parkin in the absence of PINK1 (data not shown). Furthermore, upon phosphorylation by PINK1, the activity of the

R33Q mutant increased (Figure 3.15). This was associated with a striking increase in the phosphorylation of R33Q when compared to that of wild-type Parkin (Figure 3.15). Residue Arg^{33} is located within the α1 helix of the Ubl domain, which forms extensive interactions with a beta-sheet comprising strands 2, 1 and 5 and contributes to the integrity of the Ubl domain (Sakata et al., 2003, Tashiro et al., 2003, Tomoo et al., 2008). Mutation of Arg^{33} to glutamine might disrupt a stabilising hydrogen bond between Arg^{33} and the adjacent residue, glutamine 34 (Figure 3.17). Molecular dynamics simulations of the R33Q mutation in the murine Ubl domain (Tomoo et al., 2008) predicted that loss of this hydrogen bond would lead to decreased stability of the α1 helix, and as a result, increased structural fluctuations in the β2, 1, 5 sheet. Ser^{65} is located at the N-terminus of β5 and in all structures of the Ubl domain is partially buried, however it is plausible that fluctuations in the structure of this strand induced by the R33Q mutation might lead to greater surface exposure of Ser^{65}. This would then lead to increased accessibility and phosphorylation of this residue by TcPINK1, potentially explaining the increase in E3 ligase activity observed in this mutant (Figure 3.17 & Figure 3.15). However, enhanced phosphorylation of the R33Q mutant was not associated with an increase in UbcH7 ubiquitin discharge (Figure 3.16) suggesting that an alternative mechanism might be responsible for the increased activity of this mutant.

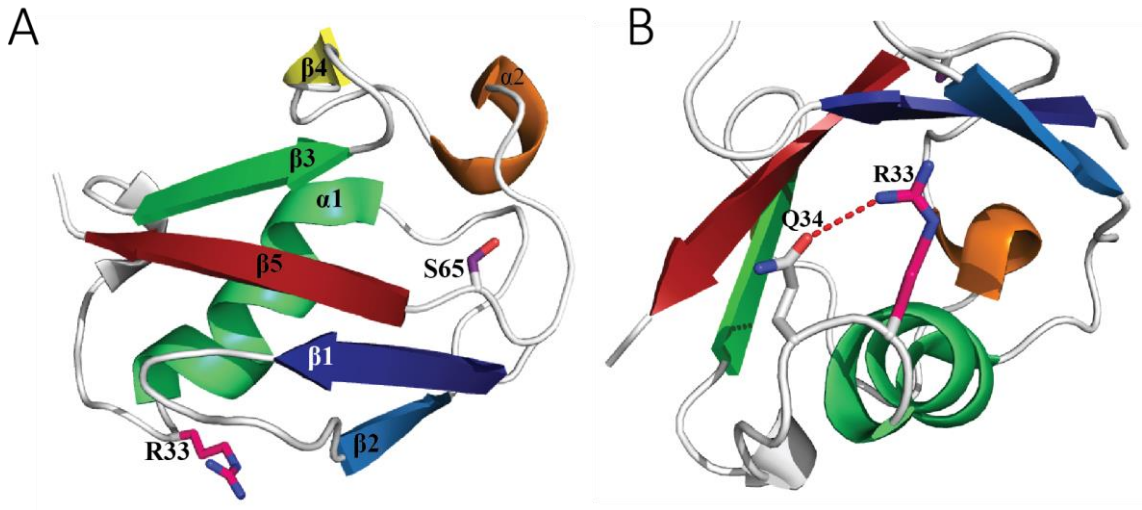

Figure 3.17 An overview of Parkin Ubl domain structure.

(A) Cartoon representation of Ubl domain with secondary structure elements labelled and coloured from blue through to red (N- to C-terminus) and the location of Ser^{65} (purple sticks) and Arg^{33} (pink sticks) shown (PDB code: 4K95). **(B)** Close up of interactions formed by residue Arg^{33}. Arg^{33} is shown as pink sticks and the adjacent interacting residue Gln^{34} is shown as white sticks. The stabilizing hydrogen bond between the residues is shown in red (PDB code: 4K95).

Previous reports on the effect of the G328E mutation on E3 ligase activity have also been controversial, with several groups reporting no change in E3 ligase activity (Hampe et al., 2006, Matsuda et al., 2006, Sriram et al., 2005) and one report suggesting a decreased autoubiquitylation activity (Trempe et al., 2013). The G328E mutation stimulated Miro1 ubiquitylation without any effect on the formation of free ubiquitin chains. Similar to R33Q, change in ubiquitylation activity was not associated with any significant change in E2 discharge of ubiquitin (Figure 3.16). A possible explanation for the lack of effect the G328E mutation has on the free chain formation relies on the positioning of this residue - Gly^{328} is located in the RING1:IBR interface and therefore may directly interact with the substrate, Miro1, rendering G328E mutation stabilising and leading to enhanced Miro1 ubiquitylation.

Biochemical and structural studies of the other RBR E3 ligases HOIP and HHARI have provided strong evidence that these RBR ligases form an intermediate ubiquitin-thioester

bond with the catalytic cysteine (Duda et al., 2013, Stieglitz et al., 2013, Stieglitz et al., 2012b, Wenzel et al., 2011). An intermediate oxyester of Parkin has been demonstrated in mammalian cells after two groups successfully trapped ubiquitin on a Cys431Ser mutant of Parkin after stimulation with the mitochondrial uncoupler CCCP (Lazarou et al., 2013, Zheng and Hunter, 2013). In contrast, direct experimental observation of a thioester intermediate state for full-length human Parkin has been elusive (Spratt et al., 2013, Wenzel et al., 2011). The strongest evidence for its existence to date comes from a study that utilised the isolated *Drosophila* Parkin IBR-RING2 domain. The homologous residue, Cys^{449}, was demonstrated to form a thioester, and this was prevented by the introduction of a Cys449Ala mutation (Spratt et al., 2013). I have not observed an intermediate ubiquitin-thioester state for activated full length wild-type Parkin (Figure 3.16), in accordance with other groups who have studied full-length Parkin (Spratt et al., 2013, Wenzel et al., 2011). However, Parkin R33Q displayed the ability to form a ubiquitin-thioester bond (Figure 3.16) representing the first experimental demonstration of the existence of a thioester-intermediate state for recombinant full-length Parkin (Figure 3.16).

3.5.5 Conclusions

Overall this work shed light into regulation of Parkin activity by PINK1 and firmly placed the two enzymes in a direct pathway. Phosphorylation of Ser^{65} in the Ubl domain was shown to play a critical part in Parkin activation although the mechanism underlying this effect remain unknown. This work utilized a novel substrate-based assay of untagged full-length Parkin that has provided further evidence that Miro1 is a bona fide target of Parkin.

4 Chapter 4: PINK1 phosphorylation of ubiquitin at Ser65 activates Parkin

4.1 Introduction

Post-translational modifications (PTMs) represent a master regulatory mechanism that exists in organisms spanning from bacteria, fungi, and unicellular eukaryotes to complex mammalian systems, as well as all life in between. According to Prabakaran and colleagues, PTMs represent 'nature's escape from genetic imprisonment' (Prabakaran et al., 2012). Protein ubiquitylation and phosphorylation represent two major components of this system, and in recent years have been found to work together, for example in the epidermal growth factor (EGF) receptor and NF-κB signalling pathways (Karin and Ben-Neriah, 2000, Nguyen et al., 2013). It is therefore not surprising that mutations in enzymes regulating such events lie at the heart of many human diseases, including cancer and Parkinson's Disease (Bras et al., 2015, Richardson et al., 2009).

In previously reported cases, protein phosphorylation has been shown to regulate ubiquitylation by modulating E3 ligase activity, either indirectly by creating or blocking a docking site for the E3 ligase, or directly, by inducing phosphorylation-dependent conformational change in the E3 (Lin et al., 2002, Gallagher et al., 2006, Dou et al., 2012). The discovery that PINK1 directly phosphorylates and activates Parkin at Ser^{65} (Kondapalli et al., 2012) (Chapter 3) represents another example of the close interplay between phosphorylation and ubiquitylation. In parallel with my analysis, additional lines of evidence have emerged linking these two enzymes, including the observation that PINK1 is required for Parkin translocation to the mitochondria upon mitochondrial outer membrane depolarisation in mammalian cell lines (Matsuda et al., 2010, Narendra et al., 2010, Vives-Bauza et al., 2010, Geisler et al., 2010). Moreover, it was reported that a Ser65Ala mutant of Parkin only showed partially disrupted recruitment to the mitochondria, suggesting that PINK1 may target additional, as yet undetermined substrates to mediate Parkin recruitment

(Shiba-Fukushima et al., 2012). Whilst studying the effects of PINK1-mediated Parkin phosphorylation, I made an unexpected finding - ΔUbl Parkin, lacking the Ser^{65} PINK1 phosphorylation site, nonetheless displayed enhanced activity upon incubation with TcPINK1. In a series of follow-up experiments I validated this finding, ultimately leading to the discovery that ubiquitin itself is a novel PINK1 substrate, and subsequently that PINK1-phosphorylated ubiquitin regulates Parkin activity.

Ubiquitin phosphorylation has previously been detected in global mass spectrometry screens at various sites including: Thr7 and Thr12 (Lee et al., 2009); Ser20 (Manes et al., 2011); Ser57 (Malik et al., 2009, Bennetzen et al., 2010); Tyr59 (Gu et al., 2011); and Ser65 (Zhou et al., 2013). However, its functional significance had been largely overlooked; no in-depth analysis has been undertaken and the identity of the upstream kinases responsible for phosphorylation of these sites remained unknown. In this chapter, I present my data, which unequivocally identifies ubiquitin phosphorylation at Ser^{65} as a second regulatory mechanism for Parkin activity.

4.2 The unexpected result

4.2.1 PINK1-dependent phosphorylation of ubiquitin activates ΔUbl Parkin E3 ligase activity

In the previous chapter (Chapter 3) I provided robust evidence of PINK1-mediated stimulation of Parkin activity via direct phosphorylation at Ser^{65} (Kondapalli et al., 2012, Kazlauskaite et al., 2014a). In order to better characterise the mechanism of activation and gain further insights into the importance of phosphorylation of the Parkin Ubl domain, E2 ubiquitin discharge assays were set up using a constitutively active fragment of Parkin lacking the N-terminal Ubl domain (ΔUbl Parkin; residues 80-465) (Burchell et al., 2012, Chaugule et al., 2011, Kazlauskaite et al., 2014a). I had previously found that ubiquitin discharge from UbcH7 could be catalysed by full-length Parkin only upon TcPINK1 phosphorylation of Ser^{65} (Figure 3.7, Chapter 3). Therefore, as a control experiment, I tested whether TcPINK1 had

any effect on ubiquitin discharge from UbcH7 mediated by ΔUbl Parkin. E2 discharge reactions were established using ΔUbl Parkin both alone and in the presence of wild-type or kinase-inactive TcPINK1, as described before (Figure 4.1). As expected, ΔUbl Parkin alone caused mild ubiquitin discharge from UbcH7, consistent with its previously reported moderate constitutive activity (Figure 4.1, lanes 3-4). Surprisingly, upon addition of wild-type but not kinase-inactive TcPINK1, I observed a striking increase in ubiquitin discharge from UbcH7 (Figure 4.1, lanes 5-6). Since ΔUbl Parkin lacks Ser^{65}, I therefore chose to determine if another site on Parkin within the C-terminal region was becoming phosphorylated by PINK1. To address this, I repeated the E2-discharge assay using 0.1 mM [γ-^{32}P]-ATP and monitored phosphorylation events using autoradiography. Although I did not observe any Parkin phosphorylation, the experiment clearly revealed strong ubiquitin phosphorylation in a manner dependent on TcPINK1 kinase activity, in addition to low levels of TcPINK1 autophosphorylation (Figure 4.1, lower panel).

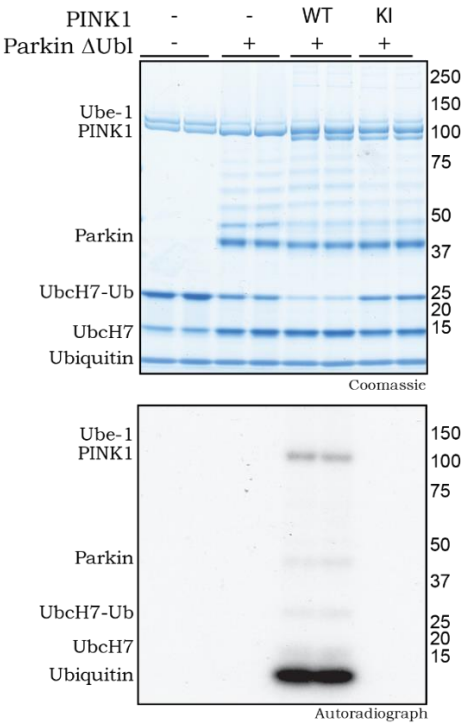

Figure 4.1 TcPINK1 enhances ΔUbl-Parkin mediated ubiquitin discharge from ubiquitin loaded UBcH7

ΔUbl Parkin activity was assessed in an E2 discharge assay. ΔUbl Parkin was tested alone as well as in the presence of wild-type (WT) or kinase-inactive (KI) TcPINK1 with ubiquitin loaded UbcH7 (UbcH7-ub). [γ-^{32}P]-ATP was used to detect phosphorylation activity. Reactions were allowed to continue for 15 min and stopped using LDS loading buffer in absence of reducing agent. Samples were analysed as before by SDS-PAGE. Protein phosphorylation was monitored by autoradiography (lower panel).

4.2.2 PINK1 phosphorylates ubiquitin at Ser^{65} *in vitro*

To determine the site of ubiquitin phosphorylation, I carried out a radioactive kinase assay with wild-type TcPINK1 that was subsequently analysed by SDS-PAGE and Coomassie staining. The phosphorylated ubiquitin band was cut out and a tryptic digest was performed, as described in Section 2.2.27.4. Together with Robert Gourlay, ^{32}P-labelled ubiquitin was analysed by chromatography on a C18 column, and one major ^{32}P-labelled phosphopeptide was observed whilst no peaks were identified following incubation with kinase-inactive TcPINK1 (not shown) (Figure 4.2 A). A combination of solid-phase Edman sequencing and

mass spectrometry revealed a peptide in which Ser^{65} was phosphorylated (Figure 4.2 B). A multiple sequence alignment of this region revealed a high degree of conservation of Ser^{65} across all aligned species (Figure 4.4). Furthermore, this peptide bears strong homology to the Parkin Ser^{65} peptide, with a hydrophobic residue at the -4 position and a His and Val at the +3 and +5 positions respectively (Figure 4.4).

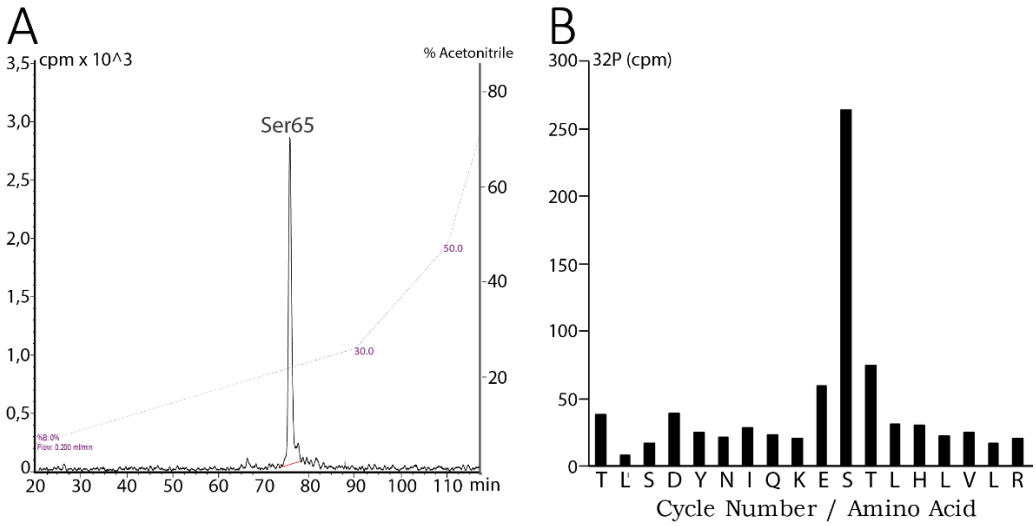

Figure 4.2 Mapping of phosphopeptides in ubiquitin after phosphorylation by TcPINK1 *in vitro*.

(A) Ubiquitin (10 µg) was incubated with 10 µg of either wild-type TcPINK1 or kinase-inactive TcPINK1 (D359A) in the presence of Mg^{2+}[γ-^{32}P]-ATP for 80 mins. Assays were terminated by addition of LDS loading buffer and separated by SDS-PAGE. Proteins were detected by Colloidal Coomassie blue staining and phosphorylated ubiquitin was digested with trypsin. Peptides were chromatographed on a reverse phase HPLC Vydac C18 column (Cat no. 218TP5215, Separations Group, Hesperia, CA) equilibrated in 0.1% (v/v) trifluoroacetic acid and the column developed with a linear acetonitrile gradient at a flow rate of 0.2 ml/min. Fractions (0.1 ml each) were collected and analysed for ^{32}P radioactivity by Cerenkov counting **(B)** The Phosphopeptide identified in (A) was analysed by solid-phase Edman sequencing and mass spectrometry. The amino-acid sequence deduced from the single phosphopeptide seen in the LC-MS/MS analysis is shown using the amino acid single-letter code.

4.2.3 Time course of ubiquitin phosphorylation

To further validate ubiquitin phosphorylation by TcPINK1, a time course analysis was undertaken. To confirm the site mapping data showing that PINK1 targets Ser^{65}, a Ser65Ala mutant of ubiquitin was included as a negative control. Kinase assays were set up using wild-type or kinase-inactive PINK1 as described in Section 2.2.28.1 and the reactions were allowed to continue for times indicated at the top of the Figure 4.3. The stoichiometry of phosphorylation was also determined at each time point (Figure 4.3).

A robust time-dependent phosphorylation of ubiquitin was observed only when wild-type TcPINK1 was used, and was absent with kinase-inactive TcPINK1 (Figure 4.3 A). The maximal stoichiometry of ubiquitin phosphorylation by TcPINK1 under these conditions was ~0.11 moles of phosphate per mole of ubiquitin (Figure 4.3 A). Notably, mutation of Ser^{65} to alanine (Ser65Ala) abolished ubiquitin phosphorylation by wild-type TcPINK1, confirming this residue as the major site of PINK1 phosphorylation (Figure 4.3 B).

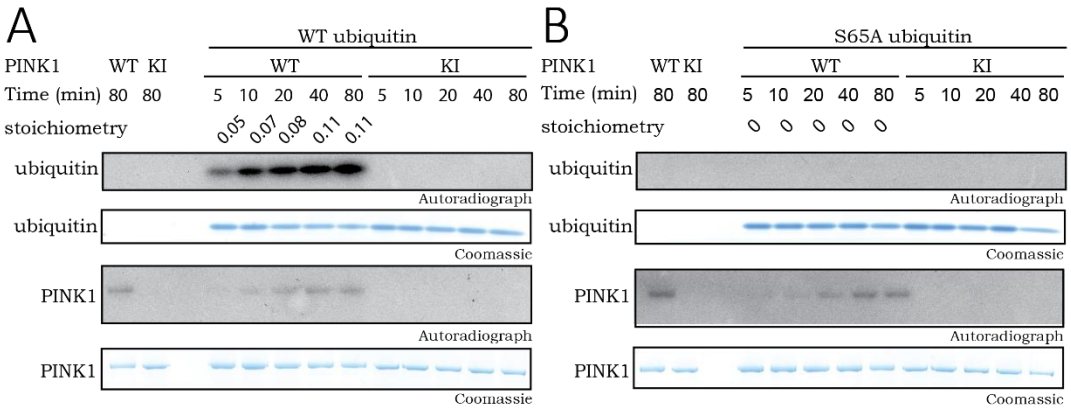

Figure 4.3 Mutation of Ser65Ala (S65A) abolishes ubiquitin phosphorylation by TcPINK1.

Wild-type (WT) or Ser65Ala (S65A) ubiquitin (1 μg) was incubated in the presence of wild-type or kinase inactive TcPINK1 (1 μg) and Mg^{2+}[γ-^{32}P]-ATP for the indicated times; assays were terminated by addition of SDS loading buffer. Samples were subjected to SDS-PAGE, proteins were detected by Colloidal Coomassie blue staining (lower panels) and incorporation of [γ-^{32}P]-ATP was detected by autoradiography (upper panels). Cerenkov counting was used to calculate the stoichiometry of ubiquitin phosphorylation indicated above autoradiographs as moles of [γ-^{32}P]-ATP incorporated per mole of ubiquitin.

4.3 Specificity of ubiquitin phosphorylation by PINK1

4.3.1 PINK1 displays selectivity in phosphorylating ubiquitin-like domains and proteins

The PINK1-dependent phosphorylation sites in ubiquitin and Parkin Ubl domain are two homologous Ser^{65} residues, with a degree of sequence conservation surrounding the site of phosphorylation (Figure 4.4). I therefore speculated that PINK1 might be a master regulatory kinase of all (or a subset of) proteins containing a Ubl domain, and possibly other ubiquitin-like modifiers in which a homologous Ser residue was present. In order to address this, a multiple sequence alignment aiming to identify other proteins carrying a homologous Ser residue was carried out by Professor Kay Hofmann. Multiple hits were identified (Figure 4.5) including the ubiquitin-like modifiers, Nedd8 and ISG15 (both domains), as well as Ubl

domain containing proteins including Midnolin (MIDN), UBL4A, UBL7, USP48, USP9X, and USP9Y (Figure 4.5).

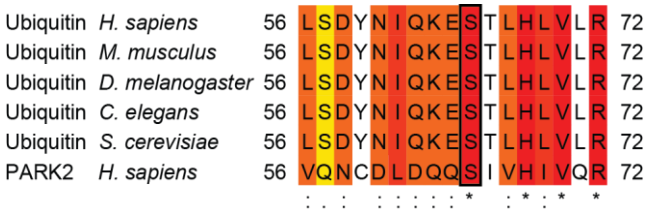

Figure 4.4 Ubiquitin Ser^{65} residue is highly conserved

Sequence alignment of residues around Ser^{65} in human Parkin and Ubiquitin in a variety of organisms showing high degree of conservation.

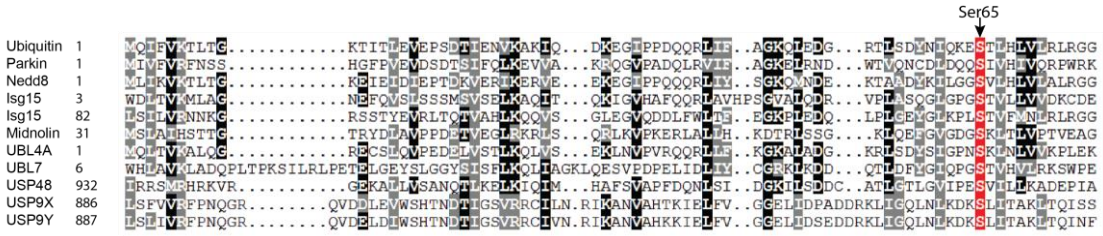

Figure 4.5 Multiple sequence alignment analysis of Parkin and ubiquitin Ser^{65}

Sequence alignment of residues around Ser^{65} in human ubiquitin and a range of ubiquitin-like-modifiers and UBL-domain containing human proteins.

To test whether the identified hits could be phosphorylated by PINK1, a subset of the identified proteins, including the ubiquitin-like modifiers ubiquitin, ISG15, and Nedd8, and the Ubl domain containing proteins Parkin and the Parkin Ubl domain were expressed in *E. coli*. In addition, other proteins lacking the homologous Ser^{65} phosphorylation site (OTU1, HOIL, Ubiquilin2, SUMO1) were included as a negative control. I then performed kinase assays using the aforementioned proteins as substrates with catalytically active recombinant wild-type or kinase-inactive TcPINK1 (D359A) in the presence of 0.1 mM [γ-^{32}P]-ATP (Figure 4.6). Phosphorylation of the putative substrates was monitored by autoradiography.

The phosphorylation levels of ubiquitin and the isolated Parkin Ubl domain (residues 1-76) were comparable and greater than full-length Parkin (Figure 4.6) in agreement with previous findings from the lab (Kondapalli et al., 2012). The only other protein that exhibited TcPINK1-dependent phosphorylation in this assay was NEDD8, a ubiquitin-like modifier, however the levels of ATP incorporation into NEDD8 were significantly lower than that of ubiquitin or the Ubl domain, suggesting that the phosphorylation might be non-specific, or alternatively that other co-factors are necessary for efficient catalysis. The low level of phosphorylation precluded mapping of the phosphorylation site(s) in NEDD8. All phosphorylation events observed in the assays were dependent on TcPINK1 kinase activity, since no signal was observed when the kinase-inactive mutant was used (Figure 4.6).

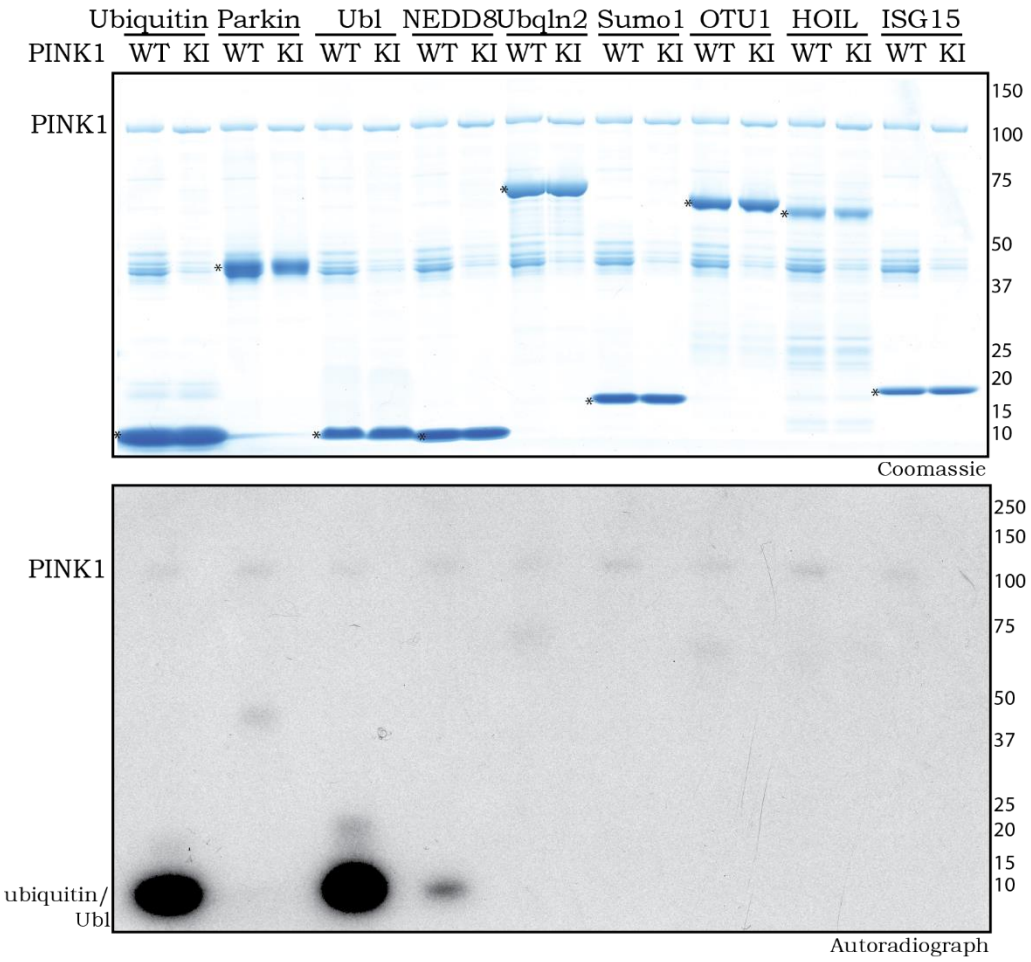

Figure 4.6 Ubiquitin and Parkin are specific substrates of TcPINK1.

The indicated ubiquitin-like modifiers and UBL-domain containing proteins (1 µg) were incubated with wild-type (WT) or kinase-inactive (KI) TcPINK1 and Mg^{2+}[γ-^{32}P]-ATP for 60 min. Assays were terminated by addition of SDS loading buffer and analysed by SDS-PAGE. Proteins were detected by Colloidal Coomassie blue staining (upper panel) and incorporation of [γ-^{32}P]-ATP was detected by autoradiography (lower panel). All substrates were human proteins expressed in *E. coli*. Tags on the substrates used for this experiment were as follows: glutathione S-transferase (GST)-OTU1; untagged-Nedd8; untagged-ISG15; His-SUMO1 (1-97); Ubiquilin2 (His-SUMO tag cleaved off); His-HOIL1; and His-USP4. Asterisks denote the correct substrate band.

4.3.2 PINK1 is a specific ubiquitin kinase

Multiple ubiquitin phosphorylation sites have been identified and reported over the last few years in global phosphoproteomic screens (http://www.phosphosite.org/), however the upstream kinases have not been determined or studied. To investigate if ubiquitin phosphorylation by PINK1 was a PINK1-specific event or a common phenomenon among protein kinases, I determined the ability of 8 other randomly selected protein kinases representative of the human kinome (MLK, CDK2, IKK epsilon, IKK beta, Aurora kinase A, NUAK1, GSK3 beta and PLK1) to phosphorylate ubiquitin, using equimolar quantities of ubiquitin and 0.1 mM [γ-^{32}P]-ATP, as described in Section 2.2.28.1. Since kinase-inactive versions of the majority of these kinases were unavailable, a control with no substrate was included for each enzyme tested. A robust phosphorylation of ubiquitin by TcPINK1 but no other kinase was observed, indicating that ubiquitin phosphorylation is a property that is specific to PINK1 (Figure 4.7).

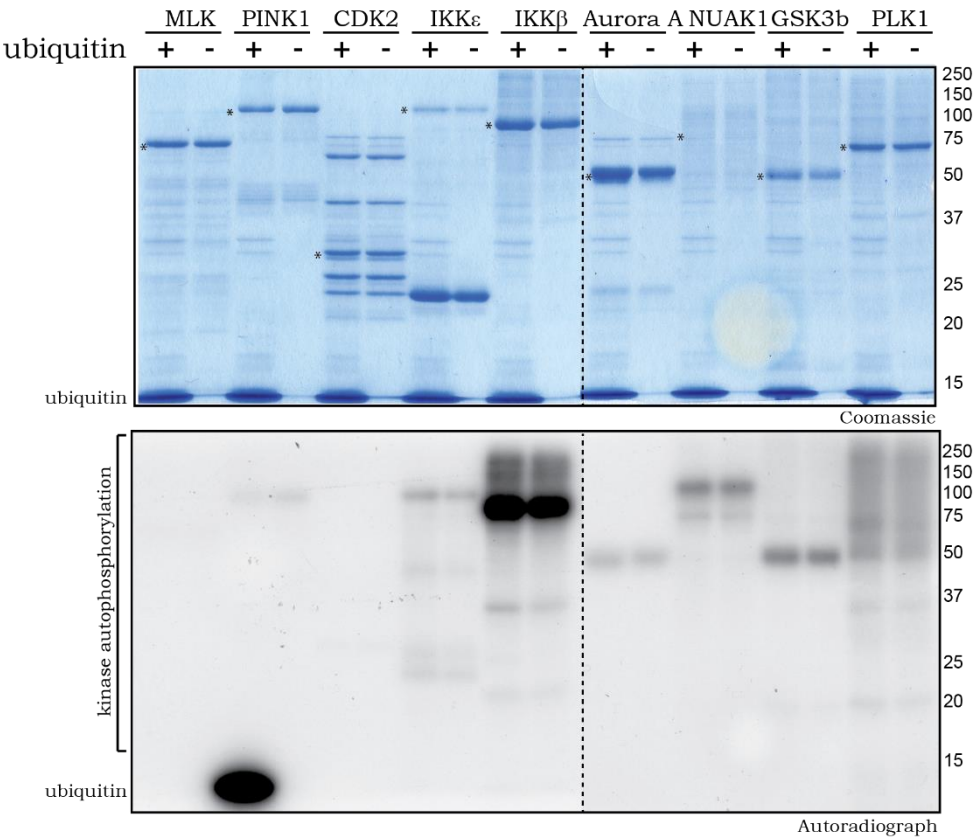

Figure 4.7 TcPINK1 is a specific upstream kinase of ubiquitin.

The indicated kinases (1 μg) were incubated with ubiquitin and Mg^{2+}[γ-^{32}P]-ATP for 60 min. Assays were terminated by addition of SDS loading buffer and analysed by SDS-PAGE. Proteins were detected by Colloidal Coomassie blue staining (upper panel) and incorporation of [γ-^{32}P]-ATP was detected by autoradiography (lower panel).

4.4 Evidence of Ubiquitin Ser^{65} phosphorylation in cells

4.4.1 Mitochondrial depolarisation in HEK293 cells stably overexpressing PINK1 leads to ubiquitin phosphorylation at Ser^{65}

In healthy cells, PINK1 is imported to mitochondria, where it undergoes sequential cleavage by the mitochondrial processing peptidase and the PARL protease, followed by rapid degradation via the N-end rule pathway (Greene et al., 2012, Yamano and Youle, 2013, Meissner et al., 2011) (Figure 1.7). Upon mitochondrial depolarisation, PINK1 is stabilised

and autophosphorylates at residue Thr257 (Thr^{257}) (Kondapalli et al., 2012). In parallel studies in our lab, Dr. Chandana Kondapalli had undertaken a SILAC-based quantitative phospho-proteomic screen in order to identify novel PINK1 substrates phosphorylated in response to mitochondrial depolarisation. FlpIn TRex HEK293 cells stably expressing either FLAG empty, wild-type or kinase-inactive human PINK1-FLAG were grown in light, heavy or medium media, respectively, and cells were subsequently stimulated with 10 μM CCCP for 3 hours to activate PINK1. Mitochondria-containing membrane-enriched fractions were made and solubilised in 1 % Rapigest, and lysates were mixed from each condition in a 1:1:1 ratio before being subjected to tryptic digestion. Digested peptides were subjected to phospho-peptide enrichment and analysis by mass spectrometry. Strikingly, a Ubiquitin phosphopeptide (TLSDYNIQKE<u>pS</u>TLHLVLR; pS corresponding to Ser^{65}) was found to be enriched 14-fold in stimulated mitochondrial extracts of wild-type PINK1 when compared to kinase-inactive PINK1 across all 4 biological replicates, providing compelling evidence that PINK1-mediated phosphorylation of ubiquitin is not only observable *in vitro*, but also occurs in cells (Figure 4.8, Figure 4.9; manuscript in preparation).

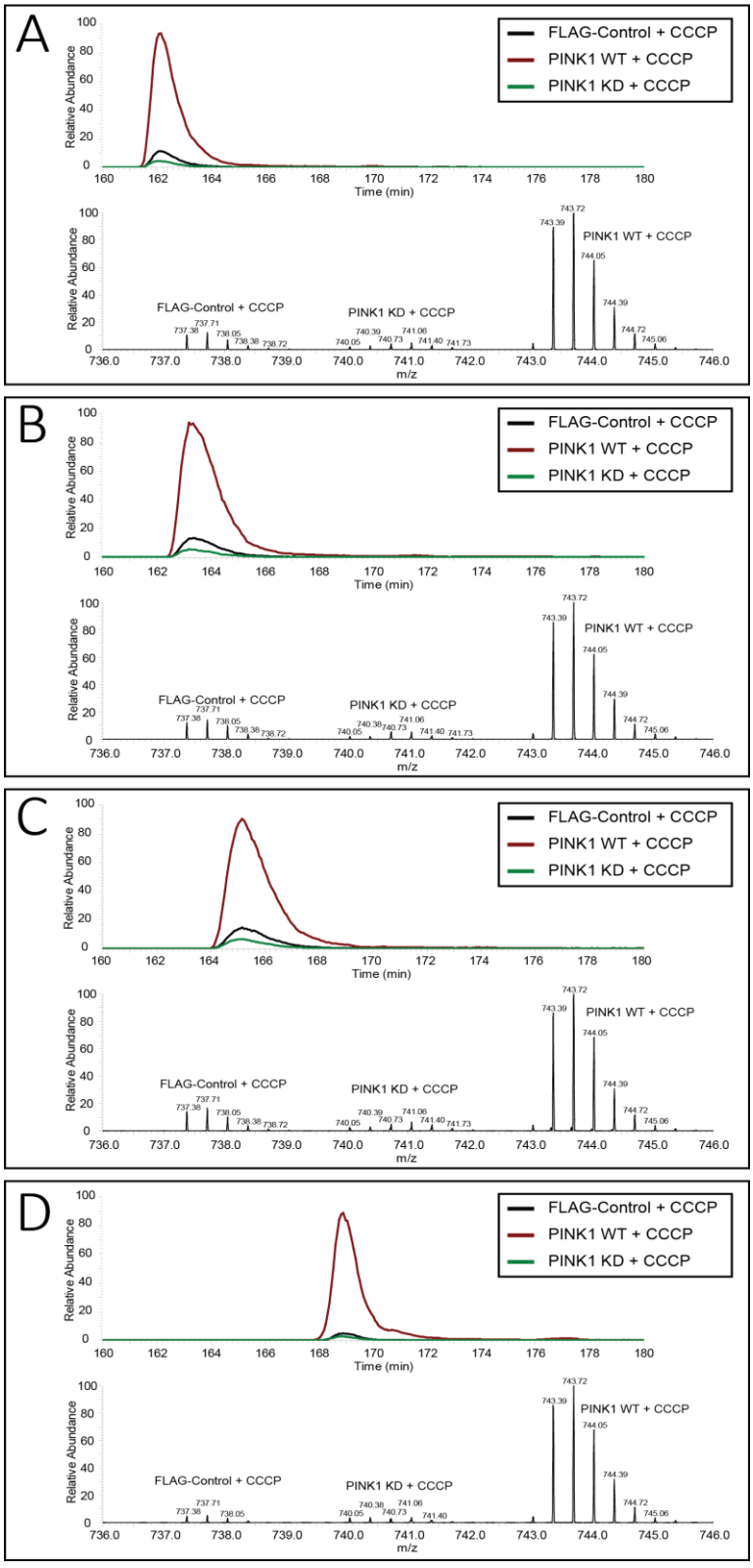
A
B
C
D
FLAG-Control + CCCP
PINK1 WT + CCCP
PINK1 KD + CCCP
Relative Abundance
Time (min)
m/z
743.72
743.39
744.05
744.39
744.72
745.06
737.71
737.38
738.05
738.38
738.72
740.39
740.73
741.06
741.40
741.73
740.05
740.38

Figure 4.8 Ubiquitin phospho Serine 65 peptide is upregulated in cells after PINK1 activation by CCCP.

FlpIn TRex HEK293 cells stably expressing FLAG empty, wild-type PINK1-FLAG or kinase-inactive PINK1-FLAG were grown in light, heavy, and medium SILAC media respectively. Cells in each condition were stimulated with 10 μM CCCP for 3 hours. Subsequently, membrane fractions were enriched by ultracentrifugation and solubilized in 1% Rapigest. Lysates from each of the three conditions were mixed in a 1:1:1 ratio and digested with trypsin prior to phosphopeptide enrichment by HILIC and TiO_2 and analysis by mass spectrometry. Data analysis was performed using MaxQuant. **(A-D)** Extracted ion chromatograms (XIC) representing the ubiquitin Serine 65 (Ser^{65}) phosphopeptide TLSDYNIQKEpSTLHLVLR in the three SILAC labelled conditions over all four biological replicates.

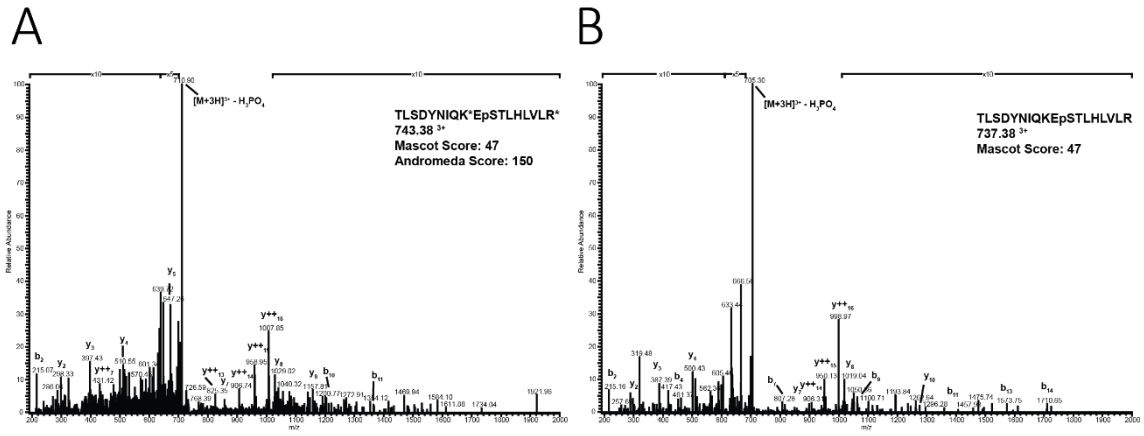

Figure 4.9 Tandem mass spectrometry fragmentation spectra of the Ser65 phosphorylated ubiquitin peptide TLSDYNIQKEpSTLHLVLR.

(A) Tandem mass spectrometry (MS/MS) spectrum of the heavy (R10K8)-labelled peptide TLSDYNIQKEpSTLHLVLR identified in wild-type PINK1-FLAG transfected cells. **(B)** Virtually identical MS/MS spectrum of TLSDYNIQKEpSTLHLVLR from a digest of ubiquitin *in vitro* phosphorylated by TcPINK1. Please note, the doubly-charged ion $[1105.5650]^{2+}$ of the same peptide was also positively identified in both experiments with Andromeda and Mascot Score of 202 and 54, respectively.

4.5 Elaboration of phospho ubiquitin effects on Parkin activity

4.5.1 PINK1-mediated activation of ΔUbl Parkin

Since I had previously observed that wild-type PINK1 enhanced the ability of ΔUbl Parkin to discharge ubiquitin from UbcH7, I next chose to determine whether PINK 1 also exerted a direct effect on ΔUbl Parkin-mediated ubiquitylation activity. I therefore performed a ubiquitylation assay with ΔUbl Parkin, in parallel with full-length Parkin, as described in Section 2.2.28.2. In agreement with previous data (Figure 3.5 & Figure 3.6), a marked activation of full-length Parkin E3 ligase activity was observed when incubated with wild-type but not kinase-inactive PINK1, as judged by the formation of free polyubiquitin chains and Miro1 multi-monoubiquitylation (Figure 4.10, lanes 1-2). Consistent with previous work (Burchell et al., 2012, Chaugule et al., 2011, Kazlauskaite et al., 2014a), ΔUbl Parkin appeared constitutively active and displayed detectable basal polyubiquitylation activity in the absence of PINK1 (Figure 4.10, lanes 9-10). However, in agreement with the UbcH7 discharge data (Figure 4.1), upon incubation with wild-type but not kinase-inactive TcPINK1, I observed a substantial further activation of ΔUbl Parkin, as judged by high molecular weight polyubiquitin chain formation and autoubiquitylation of Parkin (Figure 4.10 lanes 5-6,). Consistent with previous data (Figure 3.8), ΔUbl Parkin was unable to efficiently catalyse Miro1 multi-monoubiquitylation under any condition tested (Figure 4.10), suggesting that an intact Ubl domain might be necessary for substrate ubiquitylation.

In order to confirm that ΔUbl Parkin activation was mediated by ubiquitin phosphorylated at Ser^{65}, the ΔUbl Parkin ubiquitylation assays described above were repeated with wild-type and S65A mutant ubiquitin. Whilst normal activity levels in the presence of TcPINK1 were detected when wild-type ubiquitin was used (Figure 4.11, lanes 1-2), a dramatic reduction in ΔUbl Parkin activity in the presence of wild-type PINK1 was observed when using S65A

ubiquitin (Figure 4.11, lanes 3-4), suggesting that PINK1-mediated activation of ΔUbl Parkin is dependent on ubiquitin Ser^{65} phosphorylation.

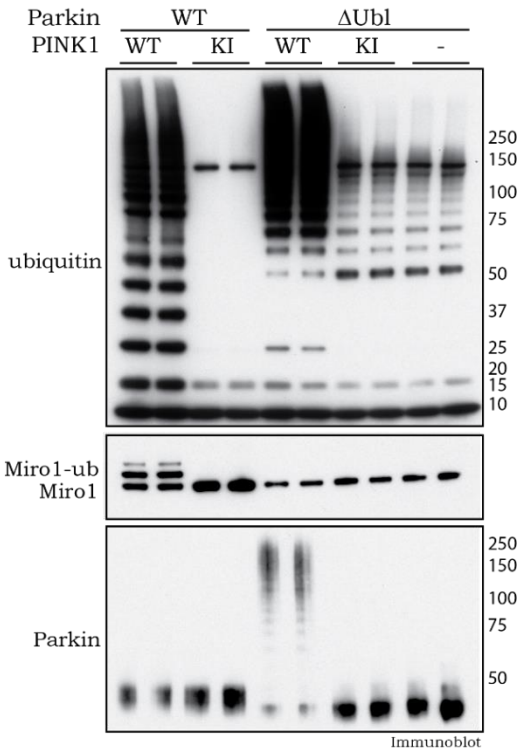

Figure 4.10 ΔUbl Parkin ubiquitylation activity is increased by WT TcPINK1.

2 μg of full-length (WT) or ΔUbl-Parkin were incubated with 1 μg of wild-type (WT), kinase-inactive (KI) or no TcPINK1 in a kinase reaction for 60 min. Ubiquitylation reactions were then initiated by addition of ubiquitylation assay components (E1, UbcH7 and Flag-ubiquitin) and 2 μg of His-Sumo-Miro1. Reactions were terminated after 60 min by addition of LDS loading buffer and analysed by SDS-PAGE. Miro1, ubiquitin and Parkin were detected using anti-SUMO, anti-FLAG and anti-Parkin antibodies, respectively.

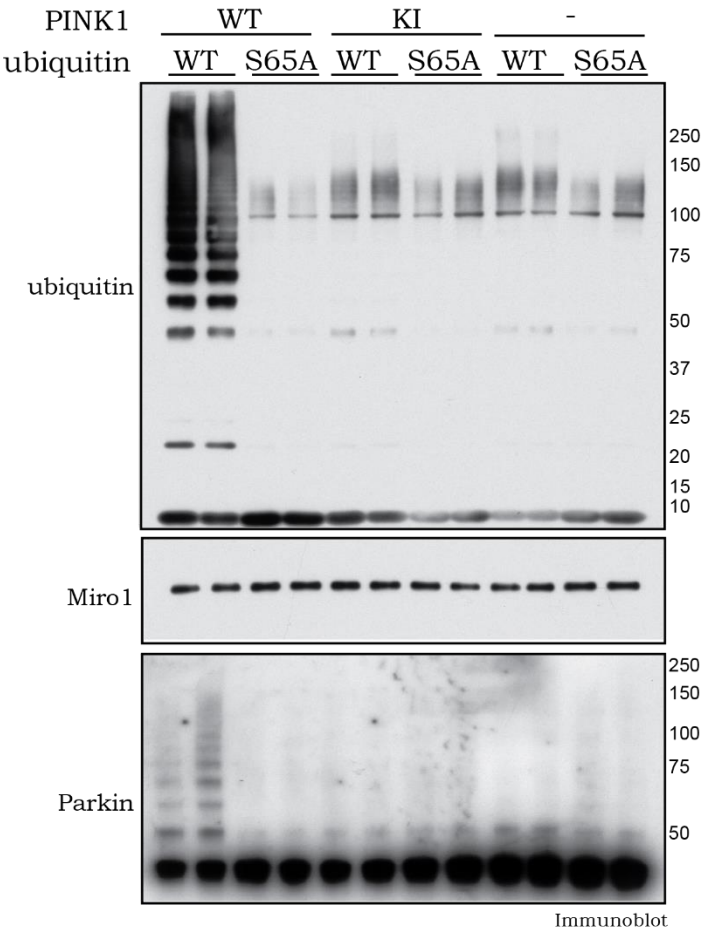

Figure 4.11 Enhanced activation of ΔUbl-Parkin by Tc-PINK1 is abrogated by Ser65Ala ubiquitin.

ΔUbl-Parkin was incubated in presence or absence of wild-type (WT) or kinase-inactive (KI) PINK1 in a kinase reaction. Ubiquitylation reactions were then initiated by addition of ubiquitylation assay components. Reactions were terminated after 60 min by addition of LDS loading buffer and analysed by SDS-PAGE. Miro1, ubiquitin and Parkin were detected using anti-SUMO, anti-FLAG and anti-Parkin antibodies, respectively.

4.5.2 Dual requirement of PINK1-dependent phosphorylation of Parkin and ubiquitin at Ser^{65} in mediating optimal activation of full-length Parkin

I next chose to investigate the role of PINK1-dependent phosphorylation of ubiquitin at Ser^{65} in the activation of full-length Parkin. I had previously found that the E3 ligase activity of full-length Parkin is dependent on PINK1 kinase activity, and that PINK1 phosphorylates

Parkin directly at residue Ser^{65} in the Ubl domain (Sections 3.2 & 3.3). Consolidating this finding, I showed that the Parkin S65A mutant largely abolished E3 ligase activity even in the presence of PINK1 (Sections 3.2.4 & 3.2.5), suggesting that phosphorylation of Parkin at Ser^{65} is a major driver of Parkin E3 ligase activity.

To further validate these results, as well as to test the effects of phosphorylated ubiquitin on full-length Parkin activity, I assessed whether full-length, S65A Parkin, which cannot be phosphorylated directly by TcPINK1, can be further activated by TcPINK1 in a manner dependent on ubiquitin phosphorylation. Wild-type and S65A Parkin was incubated with wild-type or kinase-inactive TcPINK1. After the initial kinase assay, a ubiquitylation reaction was performed with either wild-type or S65A ubiquitin.

The combination of full-length Parkin with wild-type TcPINK1 and wild-type ubiquitin resulted in maximal Parkin ubiquitylation activity, as judged by the generation of free polyubiquitin chains and multi-monoubiquitylation of Miro1 (Figure 4.12, lanes 1-2). The absolute dependence of Parkin on wild-type PINK1 for activation was confirmed by the absence of activity when kinase-inactive PINK1 was used (Figure 4.12, lanes 5-6). In the presence of S65A ubiquitin, a substantial decrease in Parkin E3 ligase activity was observed, however, activity was not completely abolished as Miro1 ubiquitylation was still detectable (Figure 4.12, lanes 3-4). In agreement with previous data, the Parkin S65A mutation led to a near complete loss of Parkin activity; Miro1 substrate ubiquitylation was completely lost, although low levels of high molecular weight polyubiquitylation could still be observed (Figure 4.12, lanes 9-10), indicating residual E3 ligase activity. As a whole, I found that a S65A mutation in either ubiquitin or Parkin alone can substantially reduce but not completely abolish Parkin E3 ligase activity, suggesting that *both* PINK1-dependent phosphorylation events are required for mediating maximal activation of Parkin. Conversely, a complete loss of Parkin activity was only observed upon incubation of both Ser65Ala ubiquitin with Ser65Ala Parkin with wild-type TcPINK1 (Figure 4.12, lanes 11-12).

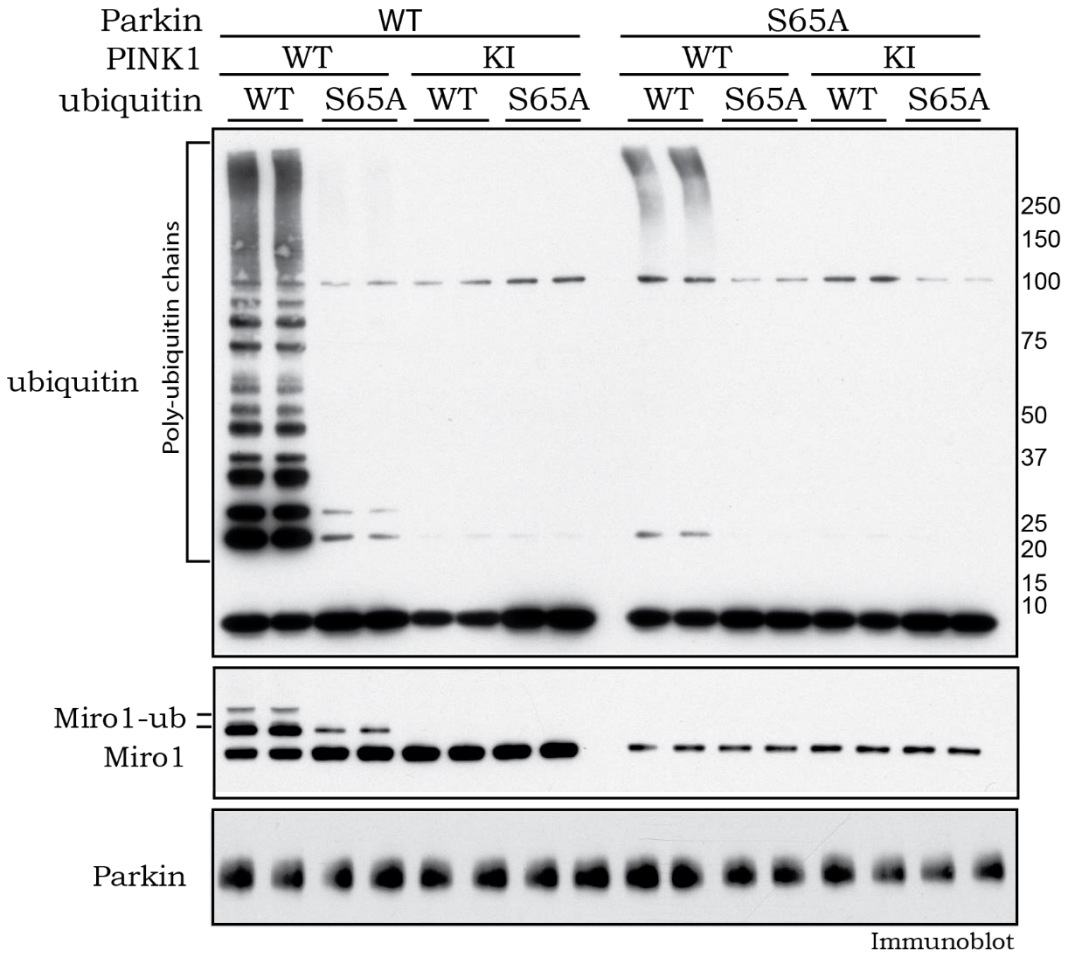

Figure 4.12 Phosphorylation of Parkin and ubiquitin at Serine65 are necessary for complete activation by PINK1.

Full-length (WT) and Ser65Ala (S65A) Parkin was incubated in presence or absence of wild-type (WT) or kinase-inactive (KI) PINK1 in a kinase reaction. Ubiquitylation reactions were then initiated by addition of ubiquitylation assay components, including 0.04 mM of wild-type (WT) or Ser65Ala (S65A) His-Flag-ubiquitin. Reactions were analysed by immunoblotting. Miro1, ubiquitin and Parkin were detected using anti-SUMO, anti-FLAG and anti-Parkin antibodies, respectively. Miro1-Ub indicates ubiquitylated Miro1.

4.6 Purification of Ser^{65}–phosphorylated ubiquitin and Ser^{65}–phosphorylated Ubl domain

In order to uncouple the separate roles played by ubiquitin and Parkin phosphorylation in mediating Parkin activation, it was necessary to conduct ubiquitylation assays utilising stoichiometrically phosphorylated and highly pure Ser^{65}-phosphorylated ubiquitin (ubiquitin$^{\text{Phospho-Ser65}}$), and additionally to compare the effect of the Ser^{65}-phosphorylated Ubl domain of Parkin (residues 1-76) (Ubl$^{\text{Phospho-Ser65}}$) to that of ubiquitin$^{\text{Phospho-Ser65}}$ on the activation of Parkin. In order to achieve this, both ubiquitin$^{\text{Phospho-Ser65}}$ and Ubl$^{\text{Phospho-Ser65}}$ were generated by TcPINK1 phosphorylation and subsequent purification (performed by Dr. Axel Knebel). Milligram amounts of ubiquitin and the Ubl domain of Parkin (residues 1-76) were phosphorylated by wild-type TcPINK1. TcPINK1 was then removed using a centricon centrifugal high molecular weight filter and the reaction mixture subjected to ion-exchange chromatography. Ubiquitin$^{\text{Phospho-Ser65}}$ was purified to homogeneity, yielding a highly pure protein with 100% stoichiometry of phosphorylation, as judged by SDS-PAGE and MALDI mass spectrometry (performed by Dr. Maria Ritorto) (Figure 4.13 A). Ubl$^{\text{Phospho-Ser65}}$ was incompletely separated from the nonphosphorylated form, resulting in a phospho-protein of around 60 % purity (Figure 4.13 B). Both preparations were free from contaminating TcPINK1.

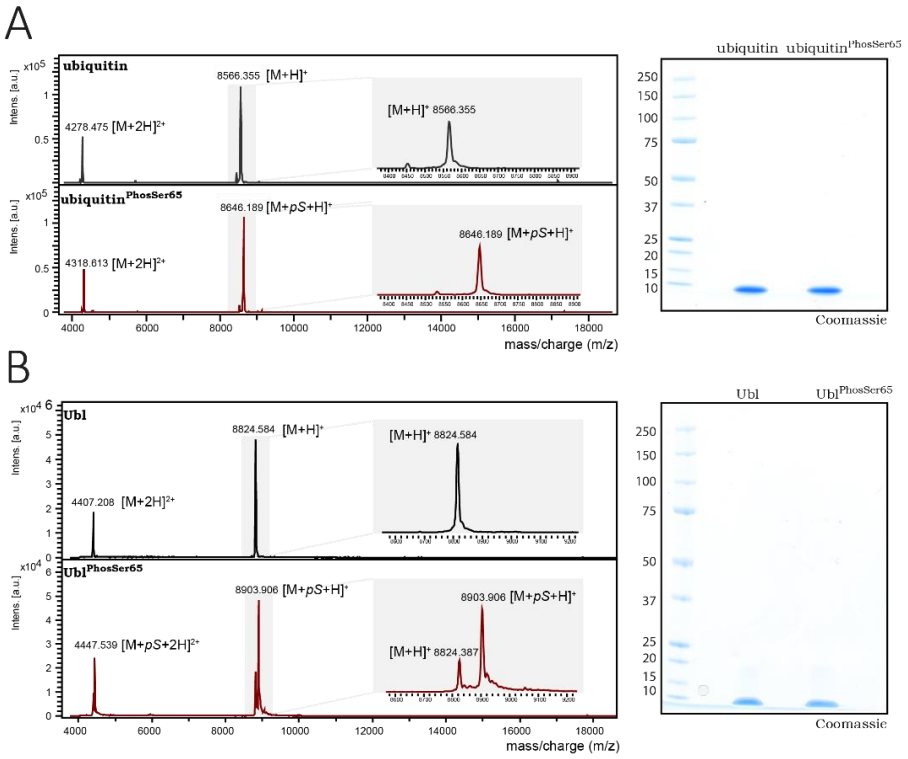

Figure 4.13 Quality control of Ser^{65}-phosphorylated Ubl (Parkin 1-76) and Ser^{65}-phosphorylated ubiquitin.

(A) MALDI-TOF spectra of non-phospho-ubiquitin (top panel) and ubiquitin$^{\text{Phospho-Ser65}}$ (bottom panel) after incubation with MBP-PINK1 and separation by Mono Q column. **(B)** MALDI-TOF spectra of non-phosphorylated Ubl (Parkin 1-76) (top panel) and mixed Ubl species (~60% phosphorylated and ~40% non-phosphorylated) (bottom panel). **(A,B)** Two micrograms of the non-phospho-ubiquitin and ubiquitin$^{\text{Phospho-Ser65}}$ **(A)** or non-phospho-Ubl and Ubl$^{\text{Phospho-Ser65}}$ **(B)** were resolved by SDS-PAGE, followed by staining with Colloidal Coomassie blue for quality control.

4.7 Ubiquitin$^{\text{Phospho-Ser65}}$ mediated effects on Parkin activity

4.7.1 Ubiquitin$^{\text{Phospho-Ser65}}$ and Ubl$^{\text{Phospho-Ser65}}$ can directly and differentially stimulate Parkin activity

My previous data has suggested that Parkin activity is regulated by a dual PINK1-dependent phosphorylation mechanism. However, the individual details of how each separate phosphorylation event affects Parkin remained unclear. To address, this I deployed purified

Ubiquitin$^{Phospho\text{-}Ser65}$ and Ubl$^{Phospho\text{-}Ser65}$ in Parkin activation assays, initially monitoring Miro1 ubiquitylation. In contrast to previous assays described in this thesis so far, TcPINK1 was omitted from the reactions and instead the activity of full-length or ΔUbl Parkin (~0.8 μM) was analysed upon addition of increasing amounts (0.04, 0.2, 1 and 5 μg) of ubiquitin$^{Phospho\text{-}Ser65}$ or non-phosphorylated ubiquitin to a normal ubiquitylation assay mixture containing 0.05mM FLAG-ubiquitin as well as other components. Full-length Parkin remained inactive in the absence of ubiquitin$^{Phospho\text{-}Ser65}$ (Figure 4.14, lanes 1 and 6), whilst a moderate level of constitutive basal activity of ΔUbl-Parkin (Figure 4.14, lanes 11 and 16) could be observed as, previously described (Section 3.3). Upon addition of increasing amounts of ubiquitin$^{Phospho\text{-}Ser65}$, a striking activation of both full-length Parkin (Figure 4.14, lanes 7-10) and ΔUbl-Parkin (Figure 4.14, lanes 17-20) was detected, as evaluated by the formation of polyubiquitin chains, increased autoubiquitylation and increased Miro1 ubiquitylation. Importantly, no activation of full-length Parkin (Figure 4.14, lanes 2-5) or ΔUbl-Parkin (Figure 4.14, lanes 12-15) could be detected following the addition of an equivalent amount of non-phosphorylated ubiquitin.

A striking difference in the sensitivity of full-length Parkin and ΔUbl Parkin to ubiquitin$^{Phospho\text{-}Ser65}$ was determined. Addition of 0.04 μg (~0.1 μM) of ubiquitin$^{Phospho\text{-}Ser65}$ led to activation of ΔUbl Parkin (Figure 4.14, lane 17) but at this concentration, no significant effect on full-length Parkin activation was observed (Figure 4.14, lane 7). Furthermore, a dose-dependent ubiquitylation profile catalysed by ΔUbl Parkin was revealed upon addition of increasing quantities of ubiquitin$^{Phospho\text{-}Ser65}$: intermediate-sized autoubiquitylation chains were formed upon addition 0.04 μg or 0.2 μg of ubiquitin$^{Phospho\text{-}Ser65}$ (Figure 4.14, lanes 17 and 18); and high molecular weight chains were formed on addition of 1 μg (~2.5 μM) or 5 μg (~12 μM) of ubiquitin$^{Phospho\text{-}Ser65}$ (Figure 4.14, lanes 19 and 20). Surprisingly, the addition of molar excess amounts of ubiquitin$^{Phospho\text{-}Ser65}$ enabled ΔUbl Parkin to catalyse monoubiquitylation of Miro1 (Figure 4.14, lanes 19 and 20), which is in contrast not observed upon the addition of TcPINK1 to ΔUbl Parkin (Section 3.3).

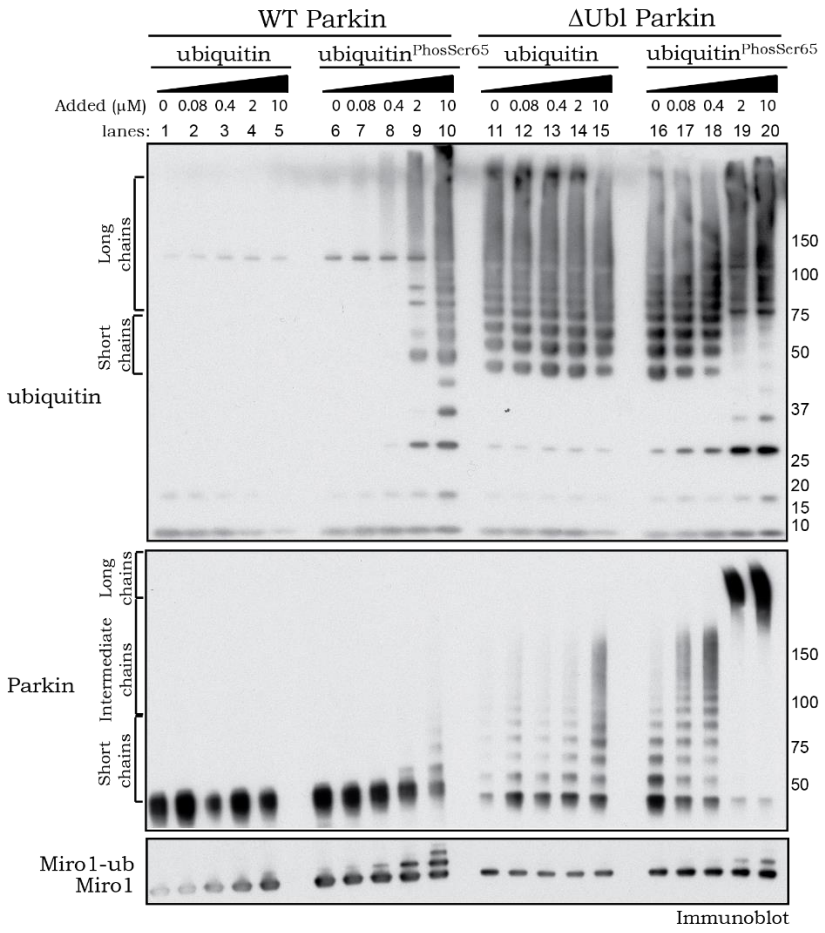

Figure 4.14 Full-length wild-type and ΔUbl Parkin are activated by ubiquitin$^{Phospho\text{-}Ser65}$.

2 μg of full-length (WT), and ΔUbl-Parkin were incubated with the ubiquitylation assay components (E1, UbcH7) in the presence of 0.05 mM FLAG-ubiquitin. Assays were spiked with indicated amounts of phospho (ubiquitin$^{Phospho\text{-}Ser65}$) or non-phospho ubiquitin as indicated. Reactions were terminated after 60 min by addition of SDS-PAGE loading buffer and analysed by SDS-PAGE. Miro1, ubiquitin and Parkin were detected using anti-SUMO, anti-FLAG and anti-Parkin antibodies, respectively. Formation of short, intermediate and long poly-ubiquitylated species is indicated by brackets.

I next determined the role of Ubl$^{Phospho\text{-}Ser65}$ in the activation of Parkin. In contrast to phosphorylated ubiquitin species, addition of increasing amounts of Ubl$^{Phospho\text{-}Ser65}$ (0.04, 0.2, 1 and 5 μg) had no significant effect on the activation of full length Parkin (Figure 4.15, 7-10). However, a striking increase in the activity of ΔUbl Parkin was observed upon addition

of Ubl$^{Phospho\text{-}Ser65}$, as judged by the formation of polyubiquitin chains, increased autoubiquitylation and the presence of Miro1 monoubiquitylation (Figure 4.15, lanes 17-20), similar to the effects induced by ubiquitin$^{Phospho\text{-}Ser65}$.

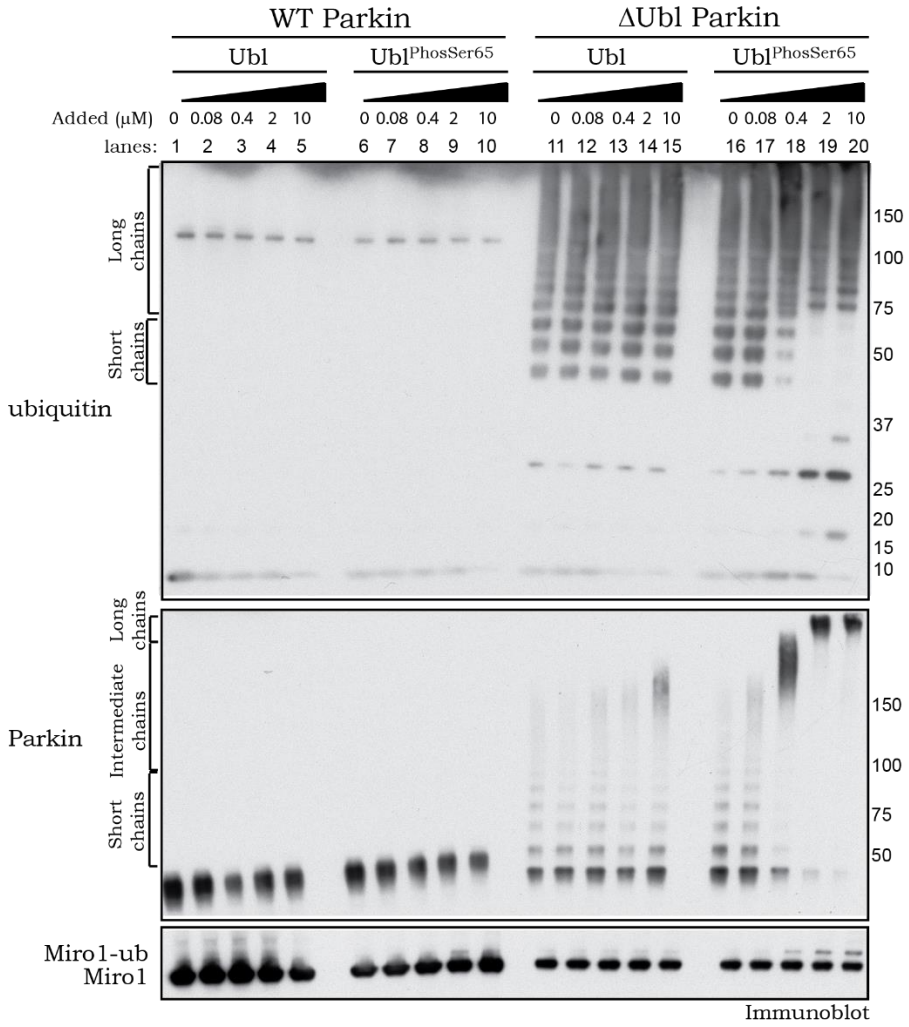

Figure 4.15 Ubl$^{Phospho\text{-}Ser65}$ activates ΔUbl, but not full-length Parkin.

2 μg of full-length (WT), and ΔUbl-Parkin were incubated with the ubiquitylation assay components (E1, UbcH7) in the presence of 0.05 mM FLAG-ubiquitin. Assays were spiked with indicated amounts of phospho (Ubl$^{Phospho\text{-}Ser65}$) or non-phospho Ubl as indicated. Reactions were terminated after 60 min by addition of SDS-PAGE loading buffer and analysed by SDS-PAGE. Miro1, ubiquitin and Parkin were detected using anti-SUMO, anti-FLAG and anti-Parkin antibodies, respectively. Formation of short, intermediate and long poly-ubiquitylated species is indicated by brackets.

4.7.2 Ubiquitin$^{Phospho\text{-}Ser65}$ and Ubl$^{Phospho\text{-}Ser65}$ can directly and differentially stimulate Parkin to discharge ubiquitin from UbcH7-loaded E2 ligase

To further probe the effect of Ubiquitin$^{Phospho\text{-}Ser65}$- and Ubl$^{Phospho\text{-}Ser65}$-mediated Parkin activation, I next assessed their ability to induce Parkin-dependent ubiquitin discharge from UbcH7-loaded E2 ligase. A fixed amount of ubiquitin$^{Phospho\text{-}Ser65}$ or non-phosphorylated ubiquitin (1 μg) was added to full-length wild-type or S65A Parkin, as well as to ΔUbl Parkin. UbcH7 loaded with ubiquitin was then added to the reaction mixture. The discharge was measured using LICOR and quantified by calculating the ratio of UbcH7-ub:UbcH7 (Figure 4.16, top panel). Consistent with previous results, full-length Parkin alone could not promote E2-ubiquitin discharge (Figure 4.16, lanes 2 and 3). However, the addition of ubiquitin$^{Phospho\text{-}Ser65}$ led to maximal observed ubiquitin discharge from UbcH7 (Figure 4.16, lanes 4 and 5) that was absent following addition of non-phosphorylated ubiquitin (Figure 4.16, lanes 6 and 7). ΔUbl Parkin alone caused slight ubiquitin discharge from UbcH7 (Figure 4.16, lanes 8 and 9), but addition of ubiquitin$^{Phospho\text{-}Ser65}$ enhanced the reaction, leading to higher levels of free ubiquitin being generated (Figure 4.16, lanes 10 and 11), which was not observed upon addition of non-phosphorylated ubiquitin (Figure 4.16, lanes 12 and 13).

S65A Parkin behaved like the wild-type enzyme; I observed maximal ubiquitin discharge from UbcH7 by S65A Parkin on addition of ubiquitin$^{Phospho\text{-}Ser65}$ (Figure 4.16, lanes 16-17) but not non-phosphorylated ubiquitin (Figure 4.16, lanes 18-19), indicating that under the assay conditions used, ubiquitin$^{Phospho\text{-}Ser65}$ alone is sufficient to activate Parkin-mediated ubiquitin discharge from UbcH7.

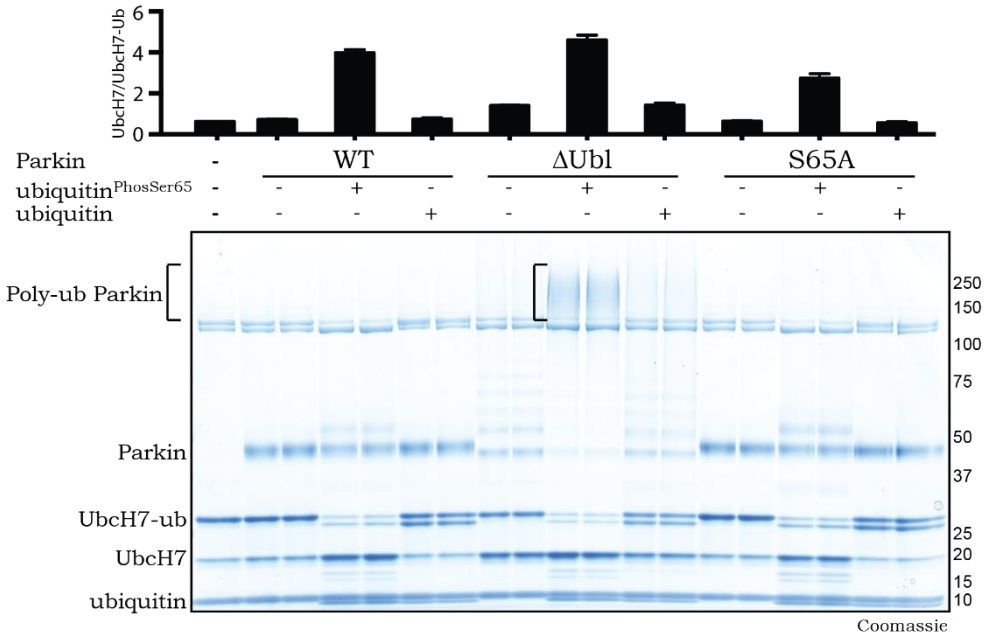

Figure 4.16 Ubiquitin$^{Phospho\text{-}Ser65}$ leads to increased ubiquitin discharge by full-length wild-type, Ser65A and ΔUbl-Parkin.

E2 discharge assay was established by incubation of full-length (WT), S65A or ΔUbl-Parkin in presence or absence of phospho (ubiquitin$^{Phospho\text{-}Ser65}$) or non-phospho ubiquitin (1 μg) as indicated with 2 μg of loaded UbcH7 loaded with FLAG-ubiquitin. Reactions were allowed to continue for 15 min and stopped using LDS loading buffer in absence of reducing agent. Reactions were resolved using SDS-PAGE and proteins were visualised by Colloidal Coomassie blue staining.

Subsequently, I tested the ability of Ubl$^{Phospho\text{-}Ser65}$ to stimulate Parkin-mediated ubiquitin discharge from UbcH7. Consistent with my ubiquitylation assay analysis (Figure 4.15), Ubl$^{Phospho\text{-}Ser65}$ (~5 μM) failed to stimulate full-length Parkin-mediated ubiquitin discharge (Figure 4.17, lanes 4-5). In contrast, ΔUbl Parkin-mediated E2-ubiquitin discharge was markedly stimulated by Ubl$^{Phospho\text{-}Ser65}$ (Figure 4.17, lanes 10-11) when compared to ΔUbl-Parkin alone (Figure 4.17, lanes 8-9) or ΔUbl Parkin in combination with non-phosphorylated Ubl (Figure 4.17, lanes 12-13). Similar to the result observed with full length wild-type Parkin, Ubl$^{Phospho\text{-}Ser65}$ could not stimulate S65A Parkin to discharge ubiquitin from UbcH7 (Figure 4.17, lanes 16-17).

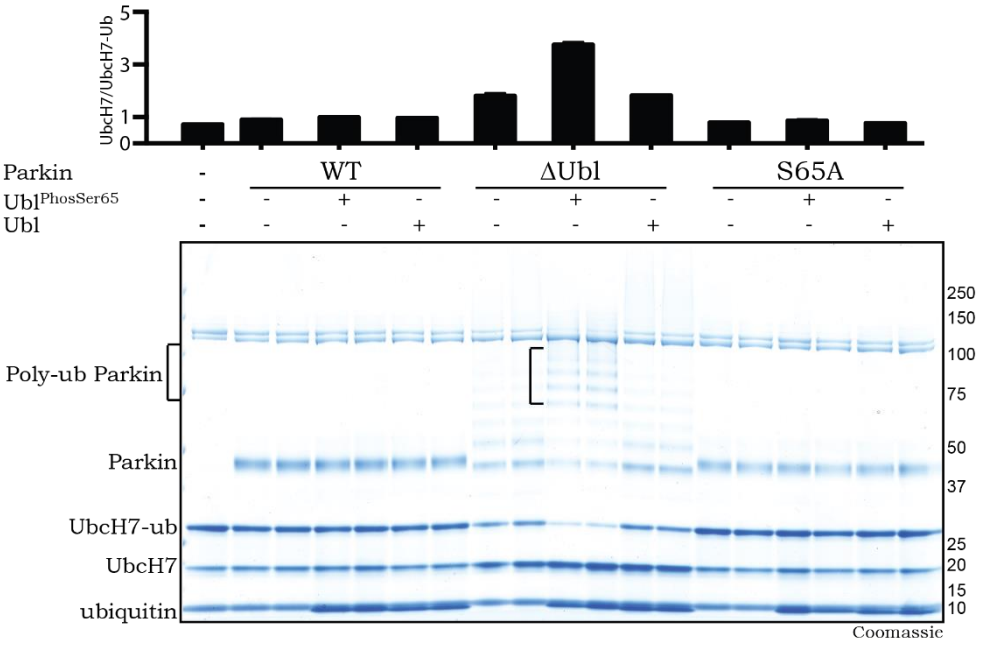

Figure 4.17 Ubl$^{Phospho\text{-}Ser65}$ leads to activation and increased ubiquitin discharge by ΔUbl-Parkin, but does not affect the full-length wild-type and Ser65A Parkin.

E2 discharge assay was established by incubation of full-length (WT), S65A or ΔUbl-Parkin in presence or absence of phospho (Ubl$^{Phospho\text{-}Ser65}$) or non-phospho Ubl (1 μg) as indicated with 2 μg of loaded UbcH7 loaded with FLAG-ubiquitin. Reactions were allowed to continue for 15 min and stopped using LDS loading buffer in absence of reducing agent. Reactions were resolved using SDS-PAGE and proteins were visualised by Colloidal Coomassie blue staining.

4.8 Discussion

The first reports of the post-translational modifications phosphorylation and ubiquitylation date back to the 1950s and 1980s respectively. Whilst cross-talk of these PTMs has been extensively demonstrated (Clark et al., 2013, Swaminathan and Tsygankov, 2006), the work discussed in this chapter unveils this interplay in its most stark form; ubiquitin itself becoming phosphorylated. The significance of this finding is by turns small yet fundamental. It sheds light only on a small aspect of the complex mechanisms underlying the regulation of Parkin E3 ligase activity, however, it also reveals a previously undiscovered class of interaction; that between modified ubiquitin and an E3 ligase, which raises many unanswered questions. Is

interaction with phosphorylated ubiquitin a widespread E3 ligase regulatory mechanism, or is it specific to Parkin? What is the identity of the other ubiquitin kinases? Can phosphorylated ubiquitin be assembled into ubiquitin chains in a similar fashion to non-phosphorylated ubiquitin, and if so, does the presence of phospho-ubiquitin in the different ubiquitin chain types affect recognition by the proteasome and deubiquitylases? Ser^{65} lies close to lysine 63 (K63), which is involved in the formation of one of the most common ubiquitin linkages. It is therefore possible to postulate that K63-specific deubiquitinases such as AMSH-like protease (Bedford et al., 2011) might exhibit altered sensitivity to K63 chains composed fully or partially of $ubiquitin^{Phospho\text{-}Ser65}$.

4.8.1 Dual activation of Parkin E3 ligase

In pursuit of understanding of the molecular basis underlying cellular dysfunction in PD, a number of PD-linked genetic mutations, including those in PINK1 and Parkin, have been identified (Bras et al., 2015). In order to uncover how these mutations lead to the development of the disease, an in-depth knowledge of the signalling pathways affected by these mutations is required. One of the outstanding questions in the field is the nature and mechanism of the molecular triggers leading to Parkin activation. In Chapter 3, I demonstrated that PINK1-dependent phosphorylation of Parkin Ser^{65}, which lies within the Ubl domain (Kondapalli et al., 2012), stimulates Parkin E3 ligase activity. The data presented in this chapter describe the discovery that PINK1-dependent phosphorylation of ubiquitin at Ser^{65} also plays a critical role in mediating Parkin activation. This discovery potentially explains why previously published high-resolution crystal structures of N-terminally truncated Parkin and one lower-resolution structure of the full-length protein were unable to fully explain how Parkin could be activated on the basis of Ubl Ser^{65} phosphorylation alone (Riley et al., 2013, Trempe et al., 2013, Wauer and Komander, 2013). The validity of my findings has been underpinned by results published by four other groups who have reached similar conclusions (Koyano et al., 2014, Kane et al., 2014, Ordureau et al., 2014, Wauer et al., 2015b).

These data indicate that ubiquitin$^{Phospho\text{-}Ser65}$ is a direct and potent activator of Parkin (Figure 4.14 & Figure 4.16). The results also demonstrate differential sensitivity of full-length and ΔUbl Parkin to ubiquitin$^{Phospho\text{-}Ser65}$-mediated activation, with the latter requiring smaller quantities of ubiquitin$^{Phospho\text{-}Ser65}$ for activation to occur (Figure 4.14). Whilst the exact mechanistic details of Parkin activation by ubiquitin$^{Phospho\text{-}Ser65}$ remain to be uncovered, these discoveries are consistent with a two-step activation mechanism of Parkin; either phosphorylation of Parkin at Ser^{65} by PINK1 leads to conformational changes that facilitate further activation by ubiquitin$^{Phospho\text{-}Ser65}$, or alternatively the opposite may be true and binding of ubiquitin$^{Phospho\text{-}Ser65}$ to Parkin facilitates Ubl phosphorylation by PINK1.

My results demonstrate that Ubl$^{Phospho\text{-}Ser65}$ is able to activate Parkin; more specifically, in contrast to ubiquitin$^{Phospho\text{-}Ser65}$, Ubl$^{Phospho\text{-}Ser65}$ enhanced the activity of ΔUbl Parkin but failed to influence the activity of full-length Parkin (Figure 4.15 & Figure 4.17). It is possible that this can be explained by the fact that the Ubl$^{Phospho\text{-}Ser65}$ protein utilised in these experiments was only 60% phosphorylated, whereas the ubiquitin$^{Phospho\text{-}Ser65}$ used was stoichiometrically phosphorylated (Figure 4.13). However, this is unlikely, since the activation of ΔUbl Parkin by ubiquitin$^{Phospho\text{-}Ser65}$ and Ubl$^{Phospho\text{-}Ser65}$was comparable. An alternative explanation may be that the binding site on Parkin for Ubl$^{Phospho\text{-}Ser65}$ overlaps with (but is still distinct from) that of ubiquitin$^{Phospho\text{-}}$Ser65. In full-length Parkin, this site would not be accessible due to steric hindrance imposed by the non-phosphorylated Ubl domain, whereas the binding pocket for ubiquitin$^{Phospho\text{-}Ser65}$ might still be partially accessible in the full-length conformation. In addition, it is plausible that the interaction between the Ubl domain and the C-terminal region of Parkin is of higher affinity when the Ubl domain is not phosphorylated, hence the inability of Ubl$^{Phospho\text{-}Ser65}$ to mediate activation of full-length E3 ligase in *trans*.

It is therefore possible to hypothesise that phosphorylation of the intrinsic full-length Parkin Ser^{65} is necessary, and could lead to release of Ubl-mediated autoinhibition and/or expose a binding site for Ubl$^{Phospho\text{-}Ser65}$, supported by the observation that PINK1-induced phosphorylation of Parkin can still activate E3 ligase activity in the presence of S65A

ubiquitin, as evidenced by Miro1 ubiquitylation (Figure 4.12). It would be illuminating to map and compare the region of interaction between Ubl$^{\text{Phospho-Ser65}}$ and Parkin with that of the interaction between Parkin and ubiquitin$^{\text{Phospho-Ser65}}$, as well as to determine the structural rearrangements in Parkin caused by their binding.

Overall, this chapter provides data identifying PINK1 as an upstream kinase of ubiquitin Ser^{65} and revealing a critical requirement of ubiquitin$^{\text{Phospho-Ser65}}$ for mediating the activation of Parkin E3 ligase activity. It provides further mechanistic detail on the regulation of Parkin and suggests a dual mechanism in which both the Ser^{65}-phosphorylated Ubl domain and ubiquitin$^{\text{Phospho-Ser65}}$ are required for optimal Parkin activation. More details of this regulation will be presented in the next chapter.

5 Chapter 5: Elaboration of molecular interaction of phosphorylated ubiquitin and Parkin

5.1 Introduction

Following the publication of my results, ubiquitin phosphorylation at Ser^{65} was additionally reported by two different groups (Koyano et al., 2014, Kane et al., 2014, Kazlauskaite et al., 2014c) (Chapter 4). Since then, PINK1-mediated ubiquitin phosphorylation at Ser^{65} has been shown to be required for optimal Parkin activation (Koyano et al., 2014, Kane et al., 2014, Kazlauskaite et al., 2014c) and has been demonstrated to facilitate Parkin recruitment to mitochondria (Okatsu et al., 2015, Shiba-Fukushima et al., 2014, Ordureau et al., 2014). In addition, phosphorylation on Ser^{65} was reported to induce secondary ubiquitin conformation as well as alter the rate of ubiquitin discharge from a range of E2 enzymes (Wauer et al., 2015b, Han et al., 2015). However, the mechanism of how $ubiquitin^{Phospho\text{-}Ser65}$ contributes to Parkin activation remained elusive.

Parkin exists in an autoinhibited conformation, mediated by multiple intramolecular interactions. The catalytic cysteine, Cys^{431}, is obscured by interaction between the UPD and RING2 domains (Riley et al., 2013, Spratt et al., 2013, Trempe et al., 2013, Wauer and Komander, 2013), and the predicted E2 binding site is blocked by an interaction between the Ubl domain, RING1 domain and the regulatory element of Parkin (REP) helix (Trempe et al., 2013). In addition, molecular modelling of a Parkin:UbcH5B complex revealed the E2 (UbcH5B) and Parkin active sites were 50 Å apart, with the UbcH5B active site pointing away from the Parkin active site (Wauer and Komander, 2013). Taken together, these data suggest that large structural rearrangements need to occur for Parkin to reach a catalytically active 'open' conformation.

Upon closer inspection of the truncated human Parkin crystal structure (Wauer and Komander, 2013), three positively charged regions on the surface of the protein that were bound to negatively charged sulphate ions were revealed, termed Pockets 1, 2 and 3 (Figure

5.1). The first Pocket, formed by Lys^{161}, Arg^{163} and Lys^{211}, was initially proposed to be responsible for Parkin recruitment to mitochondria via direct binding of PINK1 autophosphorylation sites (Wauer and Komander, 2013). Pocket 2, formed by Lys^{151}, His^{302}, Arg^{305} and Gln^{316}, resides in an interface between the UPD and RING1 domains, which makes it an attractive site for a regulatory binding event. Pocket 3 is unusual, since it is made up of only a single amino acid, Arg^{455}, and is therefore unlikely to have a significant regulatory binding role. Parkin has been convincingly demonstrated to be activated both by phosphorylation of the Ubl domain and by binding of ubiquitin$^{Phospho\text{-}Ser65}$ (Kondapalli et al., 2012, Ordureau et al., 2014). Both Ubl-phosphorylated Parkin and ubiquitin$^{Phospho\text{-}Ser65}$ carry a negatively charged phosphate group. It was therefore important to investigate whether any of the identified surface pockets on Parkin bound to these phosphorylated ligands, and if so, whether such a binding event influences Parkin activation.

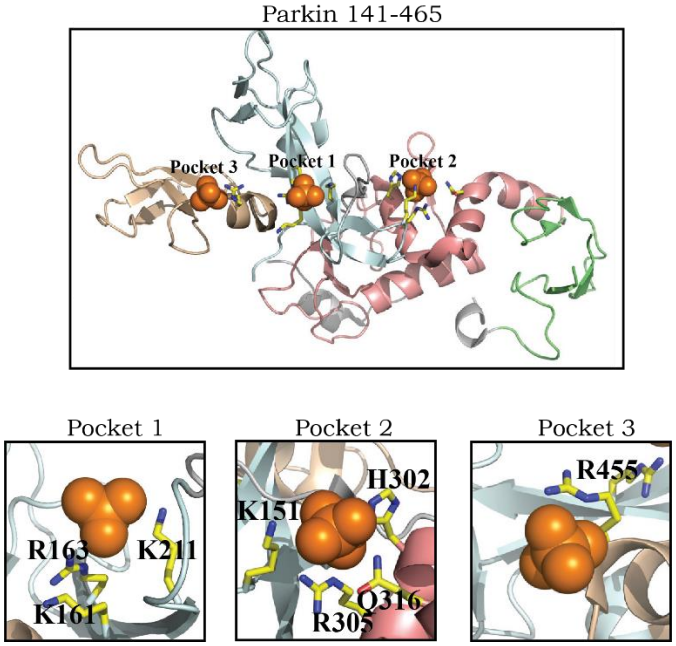

Figure 5.1 Parkin structure and putative phosphate-binding pockets.

Structure of human Parkin 141-465 displaying location of sulphate containing pockets surrounded by the following residues: Pocket 1 (K161/R163/K211); Pocket 2 (K151/H302/R305/Q316) and Pocket 3 (R455). PDB ID: 4bm9.

In this chapter, I report that ubiquitin$^{Phospho\text{-}Ser65}$ primes Parkin for efficient phosphorylation by PINK1 at Ser^{65} of its Ubl domain, which in turn leads to maximal activation of Parkin E3 ligase activity. The interaction between Parkin and ubiquitin$^{Phospho\text{-}Ser65}$ was investigated through biophysical and mutational analysis, and two residues forming Pocket 2, His^{302} and Lys^{151}, which play a critical role in ubiquitin$^{Phospho\text{-}Ser65}$ binding to Parkin and Ubl Ser^{65} phosphorylation by PINK1, were identified.

5.2 Ubiquitin$^{Phospho\text{-}Ser65}$ primes Parkin Ser^{65} for phosphorylation by PINK1

5.2.1 Ubiquitin$^{Phospho\text{-}Ser65}$-mediated enhancement of Parkin Ser^{65} phosphorylation by PINK1

My previous work demonstrated dual phosphorylation of the Parkin Ubl domain and ubiquitin by PINK1. To address whether these two phosphorylation events might influence each other, I performed a kinase assay involving a constant amount of wild-type or kinase-inactive TcPINK1, wild-type Parkin and increasing amounts of wild-type, Ser65Ala or phosphorylated ubiquitin. A marked increase in the rate as well as the stoichiometry of Parkin phosphorylation was observed upon addition of increasing amounts of ubiquitin$^{Phospho\text{-}Ser65}$, reaching a stoichiometry of ~0.9 in the presence of a 3-fold molar excess of ubiquitin$^{Phospho\text{-}Ser65}$ relative to Parkin, compared to ~0.2 without (Figure 5.2, left panel). In contrast, in the presence of a non-phosphorylatable S65A mutant of ubiquitin, no change in Parkin phosphorylation levels was detected (Figure 5.2, middle panel). Addition of increasing amounts of wild-type ubiquitin led to a moderate enhancement of Parkin phosphorylation due to PINK1-dependent generation of ubiquitin$^{Phospho\text{-}Ser65}$ species during the kinase reaction, as confirmed by autoradiography (Figure 5.2, right panel). No enhancement of phosphorylation of Parkin S65A nor ΔUbl Parkin (both of which lack the phosphorylatable residue Ser^{65}) by PINK1 in the presence of ubiquitin$^{Phospho\text{-}Ser65}$ was observed (Appendix Figure 1). This indicates that the ubiquitin$^{Phospho\text{-}Ser65}$-mediated enhancement of Parkin

phosphorylation by PINK1 is specific to the Ubl domain Ser^{65} and does not involve phosphorylation of any additional sites on Parkin (Appendix Figure 1).

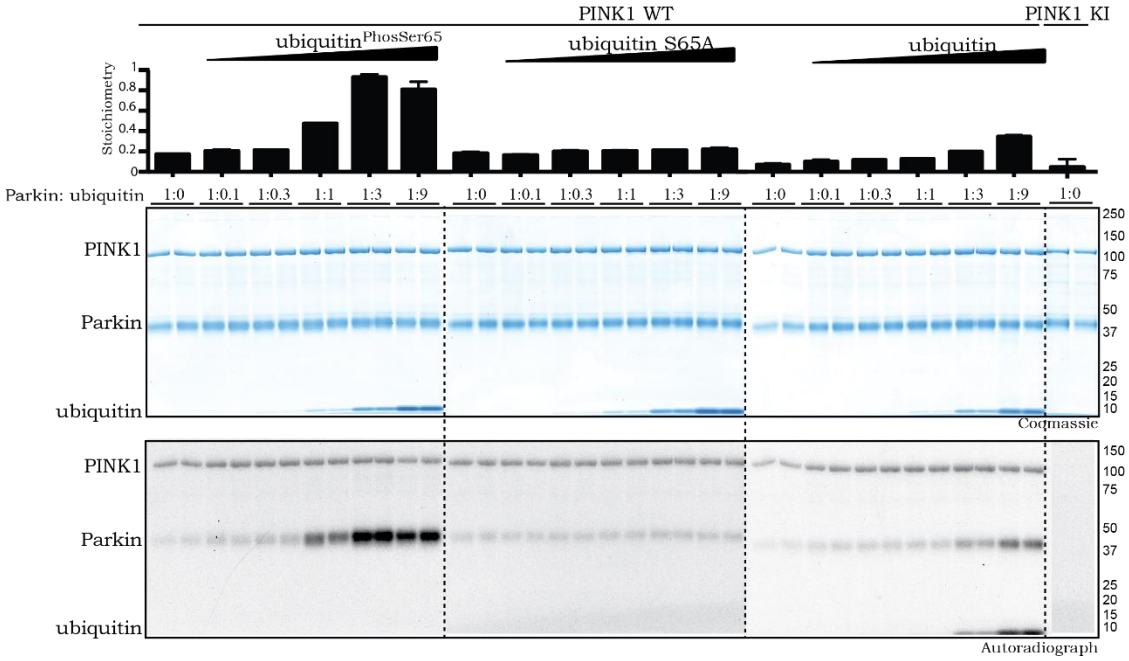

Figure 5.2 Ubiquitin^{PhosphoSer65} primes Parkin for phosphorylation by PINK1.

The effects of ubiquitin$^{Phospho\text{-}Ser65}$ (left), wild type (WT) (right) and Ser65Ala (S65A) (middle) ubiquitin on Parkin phosphorylation were investigated in a kinase assay. The indicated ubiquitin species were incubated with wild-type (WT) or kinase-inactive (KI) TcPINK1, Parkin and Mg2+ [γ-^{32}P] ATP for 60 min. Parkin concentration was kept constant, while ubiquitin concentration was varied, reaching the molar ratios indicated above the gel. Assays were terminated by the addition of LDS loading buffer and products were analysed by SDS/PAGE. Proteins were detected by Colloidal Coomassie Blue staining (top panel) and incorporation of [γ-^{32}P] ATP was detected by autoradiography (bottom panel). Data show mean of two trials +/- standard deviation (s.d.), n=2 for each condition.

5.2.2 Specificity of Ubiquitin$^{Phospho\text{-}Ser65}$-mediated effects

To test whether ubiquitin$^{Phospho\text{-}Ser65}$-dependent enhancement of Parkin phosphorylation by PINK1 was a specific event, I compared three different substrates of PINK1 (Parkin, the isolated Ubl domain of Parkin and GST-HAX1) in a kinase assay in the presence or absence of ubiquitin$^{Phospho\text{-}Ser65}$ (Figure 5.3 A). HAX1 is a mitochondrial intermembrane protein, which

our lab has recently identified as a robust *in vitro* substrate of PINK1, although the physiological relevance of this phosphorylation has not yet been explored (Appendix Figure 2, performed by Dr. Miratul Muqit). Ubiquitin$^{\text{Phospho-Ser65}}$ was found to only enhance the phosphorylation of full-length Parkin, and had no effect on the other two proteins tested, suggesting that ubiquitin$^{\text{Phospho-Ser65}}$ does not affect PINK1 activity *per se*, but mediates a specific effect likely via direct interaction with full-length Parkin (Figure 5.3 A).

The isolated Parkin Ubl domain phosphorylated at Ser65 (Ubl$^{\text{Phospho-Ser65}}$) was also tested in a kinase assay with full-length Parkin (Figure 5.3 B). In contrast to ubiquitin$^{\text{Phospho-Ser65}}$, addition of Ubl$^{\text{Phospho-Ser65}}$ did not affect Parkin phosphorylation, indicating that this effect is phospho-ubiquitin-specific (Figure 1C).

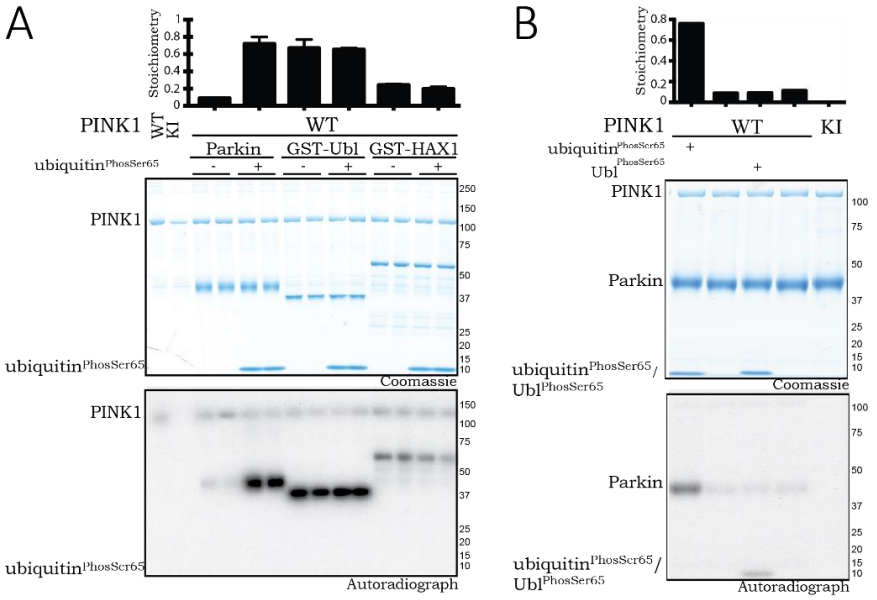

Figure 5.3 Selectivity of ubiquitin^{PhosphoSer65} enhanced Parkin phosphorylation.

(A) Full-length Parkin is a specific target of ubiquitin$^{Phospho\text{-}Ser65}$-mediated phosphorylation enhancement. Under similar conditions to Figure 5.2, the effects of ubiquitin$^{Phospho\text{-}Ser65}$ on phosphorylation of various PINK1 substrates were assessed. The kinase assays were set up with equimolar amounts of Parkin, GST-Ubl and GST-HAX1 (all expressed in *E. coli*) in the presence or absence of ubiquitin$^{Phospho\text{-}Ser65}$ and wild-type (WT) TcPINK1. The incorporation of radioactive [γ-^{32}P] ATP into substrate proteins was calculated and is displayed above the panels. Proteins were detected by Colloidal Coomassie Blue staining (top panel) and incorporation of [γ-^{32}P] ATP was detected by autoradiography (bottom panel). Dashed lines indicate separate gels; asterisks denote the kinase band. Data show mean of two trials +/- s.d., n=2 for each condition. **(C)** Ubiquitin$^{Phospho\text{-}Ser65}$, but not Ubl$^{Phospho\text{-}Ser65}$ enhances full-length Parkin phosphorylation by PINK1. Kinase assays in the presence or absence of ubiquitin$^{Phospho\text{-}Ser65}$ or Ubl$^{Phospho\text{-}Ser65}$ were carried out as in (A). Data representative of 2 independent experiments.

5.2.3 The enhancement of ubiquitin^{PhosphoSer65}-mediated phosphorylation of Ubl Ser^{65} is independent of ubiquitin chain topology and is achieved by mono-ubiquitylated substrates

Recent studies have demonstrated that in addition to phosphorylating monomeric ubiquitin PINK1 can phosphorylate polyubiquitin chains of different linkage types and lengths

(Ordureau et al., 2014, Wauer et al., 2015b, Okatsu et al., 2015). It was therefore important to investigate whether phosphorylated ubiquitin chains would have a similar effect as monomeric ubiquitin^{PhosphoSer65} in promoting Parkin phosphorylation by TcPINK1 (Figure 5.4 A). I therefore set up kinase assays with ubiquitin dimers of each linkage type (Met^{1}, Lys^{6}, Lys^{11}, Lys^{27}, Lys^{29}, Lys^{33}, Lys^{48} and Lys^{63}) or ubiquitin tetramers with Met^{1}, Lys^{6}, Lys^{11}, Lys^{29}, Lys^{33}, Lys^{48} and Lys^{63} linkages (Kristariyanto et al., 2015b, Kristariyanto et al., 2015a) and equimolar amounts of wild-type Parkin and wild-type TcPINK1 (Figure 5.4 A). All linkage types were found to be phosphorylated, as judged by autoradiography, and led to a similar enhancement of Parkin phosphorylation by TcPINK1 as that observed following addition of monomeric ubiquitin (Figure 5.4 A).

None of the reports describing ubiquitin phosphorylation by PINK1 at Ser^{65} have addressed whether PINK1 can efficiently phosphorylate monoubiquitin attached to substrate proteins; I therefore tested a model monoubiquitylated substrate in which ubiquitin has been C-terminally fused to a Dac tag (a ~28.5 kDa fragment of *E. coli* penicillin binding protein 5 comprising residues 37-297 that can be captured and released by binding to ampicillin-Sepharose) (Lee et al., 2012a). To achieve this, I performed a kinase assay with TcPINK1 and Parkin in the presence of monoubiquitin, Dac-ubiquitin or Dac tag alone (to control for any unspecific phosphorylation of the tag itself). This revealed that Dac-ubiquitin was readily phosphorylated by TcPINK1, and furthermore led to enhanced Parkin phosphorylation by PINK1 in a manner similar to monomeric ubiquitin (Figure 5.4 B). No phosphorylation activity was detected when the Dac tag alone was used, suggesting that the enhancement of Parkin phosphorylation was specific to ubiquitin phosphorylation by TcPINK1 (Figure 5.4 B).

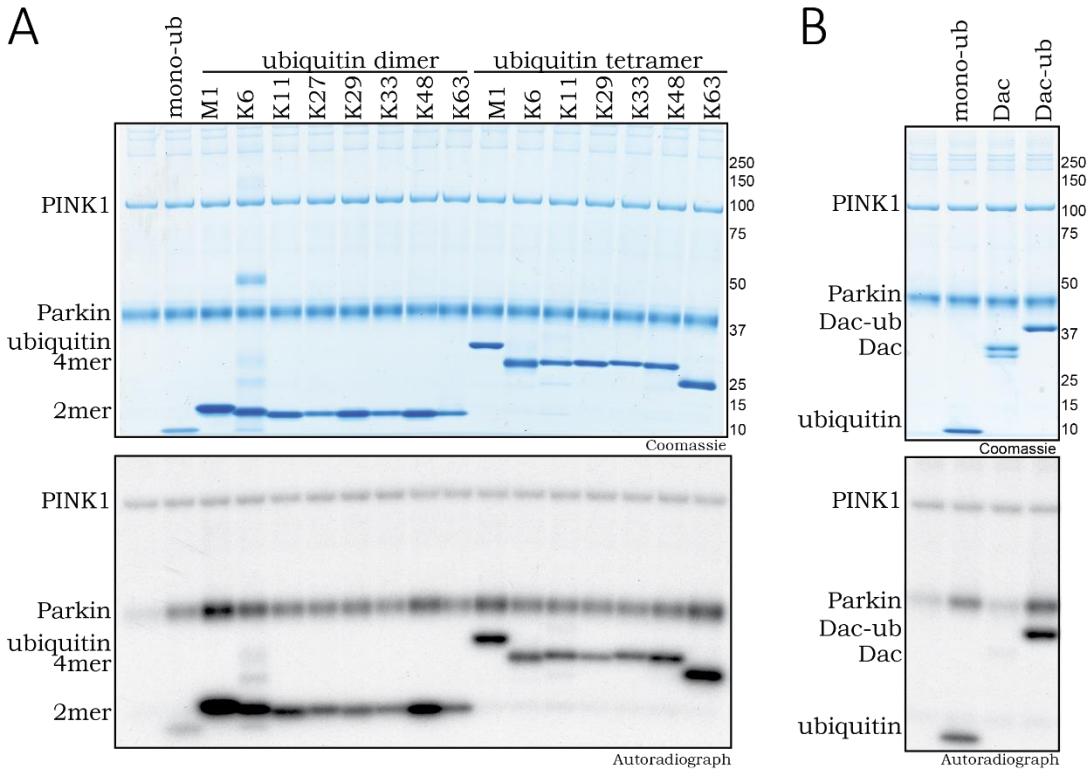

Figure 5.4 Ubiquitin dimers, tetramers and a mono-ubiquitylated substrate are capable of priming Parkin phosphorylation by PINK1.

(A) The effects of ubiquitin dimers of each linkage type (Met1 (M1), Lys6 (K6), Lys11 (K11), Lys27 (K27), Lys 29 (K29), Lys33 (K33), Lys48 (K48) and Lys63 (K63), ubiquitin tetramers with M1, K6, K11, K29, K33, K48 and K63 linkages and (**B**) the model mono-ubiquitylated substrate, Dac-ubiquitin (Dac-ub) were assessed in a TcPINK1 kinase assay. The indicated ubiquitin species were incubated with wild-type (WT) or kinase-inactive (KI) TcPINK1, Parkin and Mg2+ [γ-^{32}P] ATP for 60 min. Assays were terminated by the addition of LDS loading buffer and products were analysed by SDS/PAGE. Proteins were detected by Colloidal Coomassie Blue staining (top panel) and incorporation of [γ-^{32}P] ATP was detected by autoradiography (bottom panel).

5.3 Identification of Parkin histidine 302 and lysine 151 as key residues required for binding and maximal activation of Parkin by ubiquitin$^{\text{Phospho-Ser65}}$

5.3.1 Analysis of Parkin pocket mutants

To better understand the mechanism of how ubiquitin$^{\text{Phospho-Ser65}}$ promotes Parkin phosphorylation by PINK1, I next determined the ubiquitin$^{\text{Phospho-Ser65}}$ binding site on Parkin. As mentioned in Section 5.1, inspection of the published truncated human Parkin structure (Wauer and Komander, 2013) revealed three putative phosphate-binding pockets (Figure 5.1). Pocket 1 in UPD domain had been previously highlighted as a putative phosphate-binding pocket (Wauer and Komander, 2013), but it was later demonstrated not to be required for Parkin binding to ubiquitin$^{\text{Phospho-Ser65}}$ (Ordureau et al., 2014). To explore the potential contribution of residues forming these three pockets to ubiquitin$^{\text{Phospho-Ser65}}$-mediated activation of Parkin, Parkin containing a single point mutant of each residue was expressed in *E. coli* and subsequently purified. I then tested these point mutants in a PINK1 kinase assay in the presence of ubiquitin$^{\text{Phospho-Ser65}}$ (Figure 5.5). All of the Pocket 1 mutants (Lys161Ala, Arg163Ala and Lys211Asn), as well as the Pocket 3 mutant (Arg455Ala), behaved like the wild-type Parkin (Figure 5.5). By contrast, the Pocket 2 mutant - His302Ala (H302A) mutation almost completely prevented the enhancement of Parkin Ser^{65} phosphorylation by PINK1 (Figure 5.5). Furthermore, the Lys151Ala (K151A) mutation also disrupted the ability of ubiquitin$^{\text{Phospho-Ser65}}$ to modify the PINK1-dependent phosphorylation of Parkin, albeit to a lesser extent (Figure 5.5). The remaining Pocket 2 mutants, Arg305Ala and Gln316Ala), displayed respectively either a modest effect or no effect on ubiquitin$^{\text{Phospho-Ser65}}$ mediated phosphorylation of Parkin Ser^{65} (Figure 5.5).

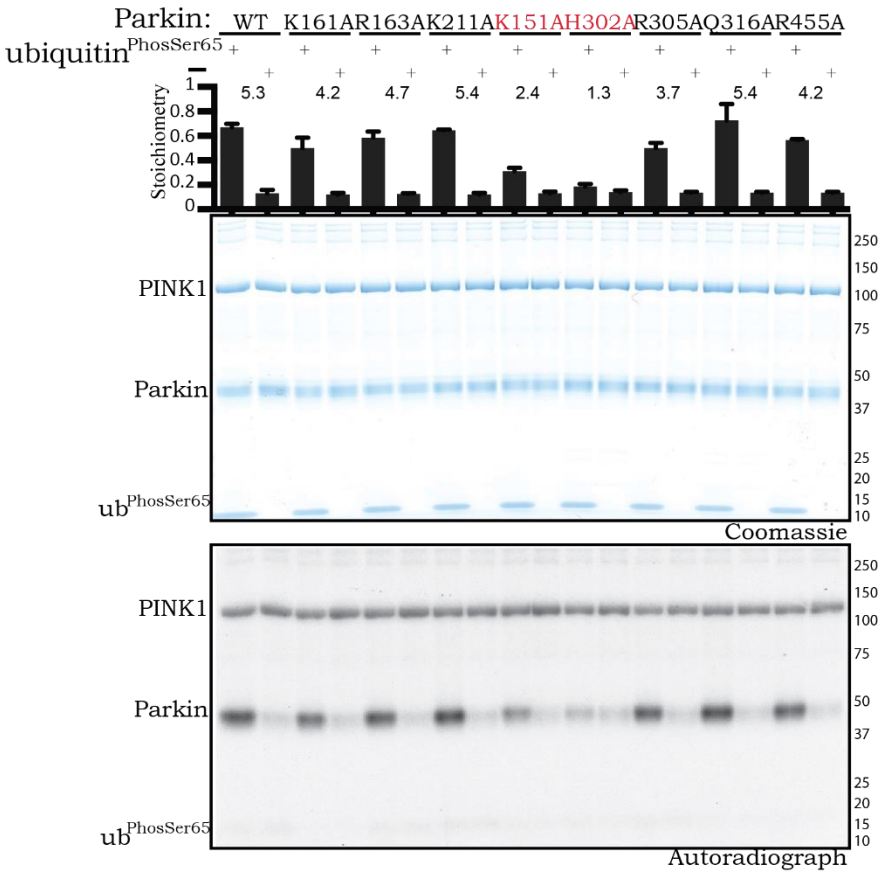

Figure 5.5 His302 and Lys151 are critical for mediating ubiquitin$^{Phospho\text{-}Ser65}$ enhanced phosphorylation of Parkin by TcPINK1.

Wild-type (WT) full length Parkin or the indicated alanine mutant was incubated with wild-type (WT) TcPINK1, Parkin and Mg2+ [γ-^{32}P] ATP in the presence or absence of ubiquitin^{PhosphoSer65}. Proteins were detected by Colloidal Coomassie Blue staining (top panel) and Parkin phosphorylation levels assessed by incorporation of [γ-^{32}P] ATP detected by autoradiography (bottom panel) and displayed above the panel. Data show mean of two trials +/- s.d., n=2 for each condition.

5.3.2 Stability of His302Ala and Lys151Ala mutants

To ensure that H302A and K151A mutations do not disrupt the Parkin:ubiquitin$^{Phospho\text{-}Ser65}$ interaction due to structural instability and/or unfolding caused by the mutations themselves, a thermal shift analysis was undertaken (performed by Dr. R. Julio Martinez-Torres). This demonstrated that the Parkin H302A and K151A mutants were as stable as the wild-type

protein, with no measurable change in thermal stability thus indicating no significant perturbation of fold or structural integrity (Figure 5.6).

The analysis conducted utilised full-length Parkin, however, the high-resolution crystal structures of Parkin have been obtained using N-terminally deleted fragments of Parkin comprising the UPD-RBR domains (Riley et al., 2013, Spratt et al., 2013, Trempe et al., 2013, Wauer and Komander, 2013). I am therefore unable to rule out the possibility that the topology of the ubiquitin$^{\text{Phospho-Ser65}}$ pocket may be different in the structure of the full-length protein and might involve additional amino acids not evident from the UPD-RBR structures. Nevertheless, my analysis strongly suggests a key role for His302 and Lys151 in ubiquitin$^{\text{Phospho-Ser65}}$ mediated effects on Parkin.

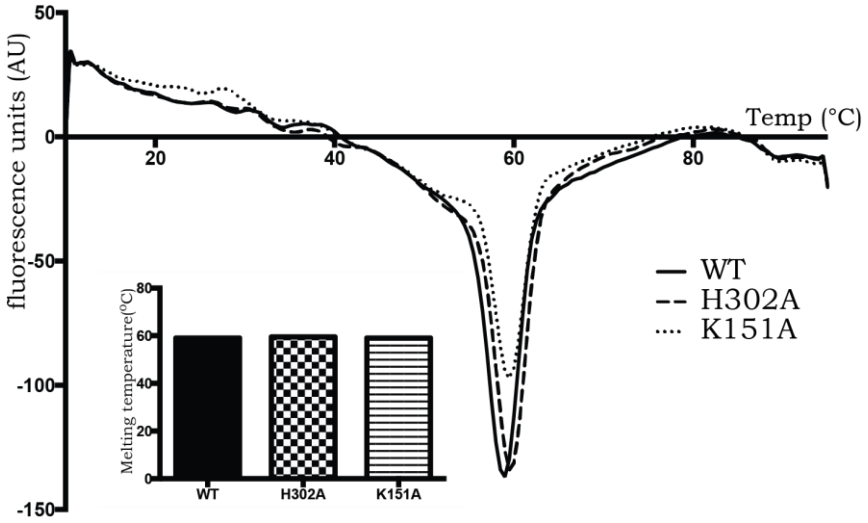

Figure 5.6 Analysis of stability and Ubiquitin$^{\text{PhosphoSer65}}$ independent E3 ligase activity of Pocket 2 mutants of Parkin.

Thermal denaturation curves obtained by differential scanning fluorimetry of wild-type (WT), His302Ala (H302A) and Lys151Ala (K151A) mutant Parkin. Results are displayed as the differential of the fluorescence in units divided by the differential of the temperature, plotted against temperature. Inset: Summary of melting points (Tm), indicated by the minimum of each curve, of each protein as follows: WT (59^{o}C); H302A (59.5^{o}C) and K151A (59.5^{o}C).

5.3.3 The role of Pocket 2 residues in ubiquitin$^{Phospho\text{-}Ser65}$ induced Parkin activation

It was next important to test the effect of the H302A and K151A mutations on the ubiquitin$^{Phospho\text{-}Ser65}$-mediated activation of Parkin. I addressed this by employing Parkin E3 ligase assays as described in Section 2.2.28.2. Wild-type Parkin as well as the Pocket 2 point mutants (K151A, H302A, R305A and Q316A) were tested in ubiquitylation assays in the presence or absence of ubiquitin$^{Phospho\text{-}Ser65}$. Parkin activity was assessed by monitoring the formation of free polyubiquitin chains, Miro1 multi-monoubiquitylation and Parkin auto-ubiquitylation.

Wild-type Parkin displayed activity only when ubiquitin$^{Phospho\text{-}Ser65}$ was present, in agreement with previous data (Figure 5.7 A, lanes 1-2). Consistent with the phosphorylation assay analysis, a large reduction in Parkin activation by ubiquitin$^{Phospho\text{-}Ser65}$ was detected following mutation of His^{302} to alanine, as judged by a complete loss of Miro1 ubiquitylation and substantial decrement in free poly-ubiquitin chain formation and Parkin autoubiquitylation (Figure 5.7 A, lanes 5-6). In addition, the K151A mutant exhibited a partial reduction in Parkin activity, as judged by Parkin autoubiquitylation and free poly-ubiquitin chain formation (Figure 5.7 A, lanes 3-4), the R305A mutant exhibited only modest negative effects on Parkin activation upon addition of ubiquitin$^{Phospho\text{-}Ser65}$ (Figure 5.7 A, lanes 7-8), and finally Q316A behaved like the wild-type protein.

In contrast, when the E3 ligase activity assay was performed in conjunction with phosphorylation by TcPINK1 (as described previously) under which conditions activation is imparted by TcPINK1-directed Parkin Ubl Ser^{65} phosphorylation, the activity of the H302A mutant was similar to that of the wild-type protein (Appendix Figure 3). These data suggest that H302A mutation is not causing large perturbations in the conformation of Parkin and instead is likely selectively affecting the ubiquitin$^{Phospho\text{-}Ser65}$ interaction (Appendix Figure 3). The non-phosphorylatable S65A ubiquitin mutant was included in this experiment in order to discriminate the effects mediated by Ubl$^{Phospho\text{-}Ser65}$ from those induced by ubiquitin$^{Phospho\text{-}Ser65}$ (Appendix Figure 3).

I also assessed Pocket 2 mutations for their impact on ubiquitin$^{\text{Phospho-Ser65}}$-dependent ubiquitin discharge from the loaded E2 enzyme UbcH7. The reactions were assembled as described in Section 2.2.28.3. Equimolar amounts of each of the Parkin mutants as well as the wild-type protein were tested with ubiquitin or ubiquitin$^{\text{Phospho-Ser65}}$. Whilst addition of ubiquitin$^{\text{Phospho-Ser65}}$ but not ubiquitin led to maximal E2-ubiquitin discharge by wild-type Parkin (Figure 5.7 B, lanes 4 and 5), this was completely disrupted by the H302A mutation (Figure 5.7 B, lanes 8 and 9) and partially by mutation of K151A (Figure 5.7 B, lanes 6 and 7) and Arg305Ala (Figure 5.7 B, lanes 10 and 11). The Gln316Ala mutant was largely unaffected (Figure 5.7 B, lanes 12, 13). Consistent with their critical regulatory role, the His302 and Lys151 residues are highly conserved in multiple species of Parkin (Figure 5.7 C).

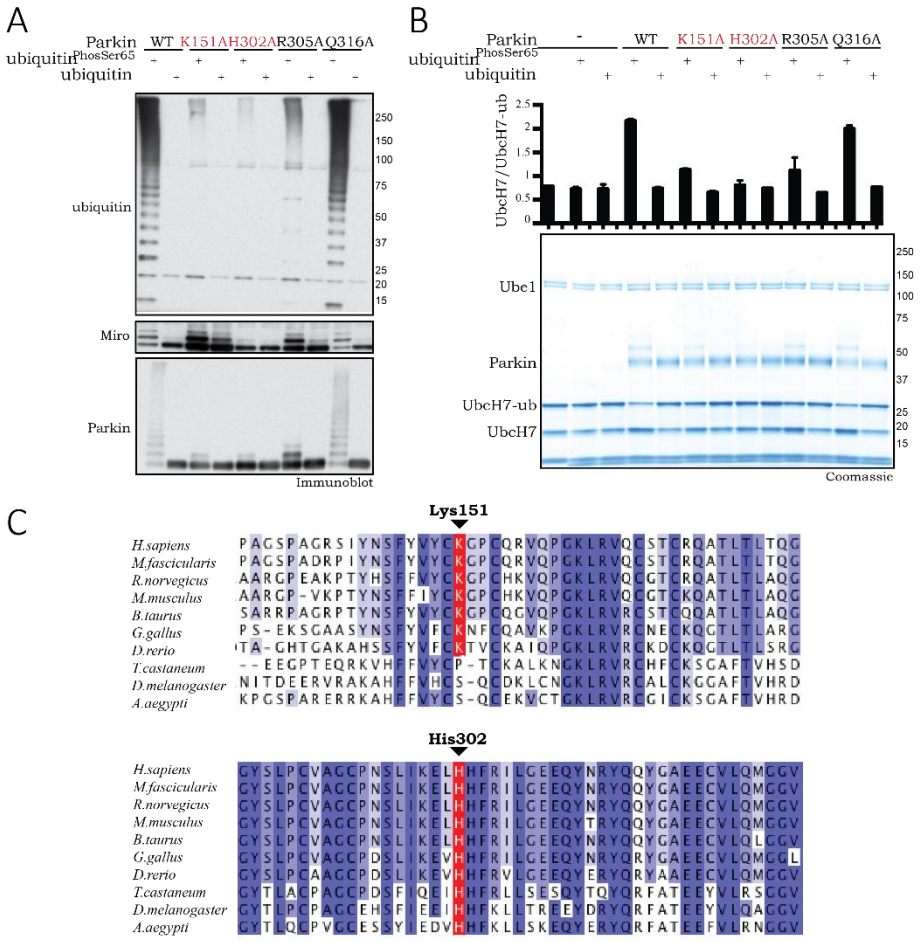

Figure 5.7 Parkin H302A and K151A mutants disrupt ubiquitin$^{Phospho\text{-}Ser65}$ mediated Parkin activation

(A) The activity of wild-type (WT) Parkin and putative Pocket 2 mutants (K151A, H302A, R305A, Q316A) were assessed using ubiquitylation assays. Each reaction contained 0.05 mM ubiquitin comprising 25 µg of FLAG-ubiquitin mixed with 5 µg of ubiquitin$^{Phospho\text{-}Ser65}$ or wild-type ubiquitin. E3 ligase activity was evaluated by immunoblotting. Data representative of 5 independent experiments. **(B)** H302A and K151A mutations hinder Parkin's ability to interact with ubiquitin$^{Phospho\text{-}Ser65}$ and discharge ubiquitin from a loaded E2. Wild-type (WT) Parkin and pocket 2 mutants were assessed for their ability to discharge ubiquitin from a loaded UbcH7 (UbcH7-ub) enzyme with or without ubiquitin$^{Phospho\text{-}Ser65}$ or non-phospho-ubiquitin. The activity was assessed by change in UbcH7 (E2):UbcH7-Ub (E2-Ub) ratio. The quantification of Coomassie bands was performed by LICOR and is presented above the panel. Data show mean of three trials +/- s.d., n=1 for each condition. **(C)** Parkin His302 and Lys151 are highly conserved across multiple species. Sequence alignment of residues around Lys151 and His302 in human Parkin and a variety of lower organisms showing high degree of conservation.

5.3.4 Analysis of Parkin disease mutants

Whilst His^{302} and Lys^{151} have not been identified as mutated in human patients with Parkinson's disease, a number of disease mutations lie in close structural proximity to these residues, including the RING1 mutant R275W, which was previously shown to be inactive (Section 3.4). I therefore investigated a panel of disease mutants, as described in Section 3.4, including R275W for their ability to interact with ubiquitin$^{Phospho\text{-}Ser65}$ and analysed their levels of PINK1-mediated Ser^{65} phosphorylation. I conducted a kinase assay with each of the mutants, as well as wild-type Parkin and TcPINK1, in the presence or absence ubiquitin$^{Phospho\text{-}Ser65}$ (Figure 5.8). This resulted in the identification of three disease mutants that prevented ubiquitin$^{Phospho\text{-}Ser65}$-enhanced Parkin Ser^{65} phosphorylation: K27N and A46P, which lie within the Ubl domain; and G430D, which lies within the RING2 domain, (Figure 5.8). However, the basal phosphorylation of these mutants in the absence of ubiquitin$^{Phospho\text{-}Ser65}$ was substantially lower than that of wild-type Parkin; it is therefore possible to speculate that these mutations trap Parkin in a conformation that leads to a decrease in Ubl domain accessibility and a subsequent reduction in phosphorylation. Conversely, the R33Q mutant, which I found previously to be better phosphorylated than wild-type Parkin (Section 3.4), potentially due to disruption of Ubl-mediated autoinhibition, showed only a moderate change in phosphorylation by PINK1 upon addition of ubiquitin$^{Phospho\text{-}Ser65}$ when compared to wild-type (Figure 5.8).

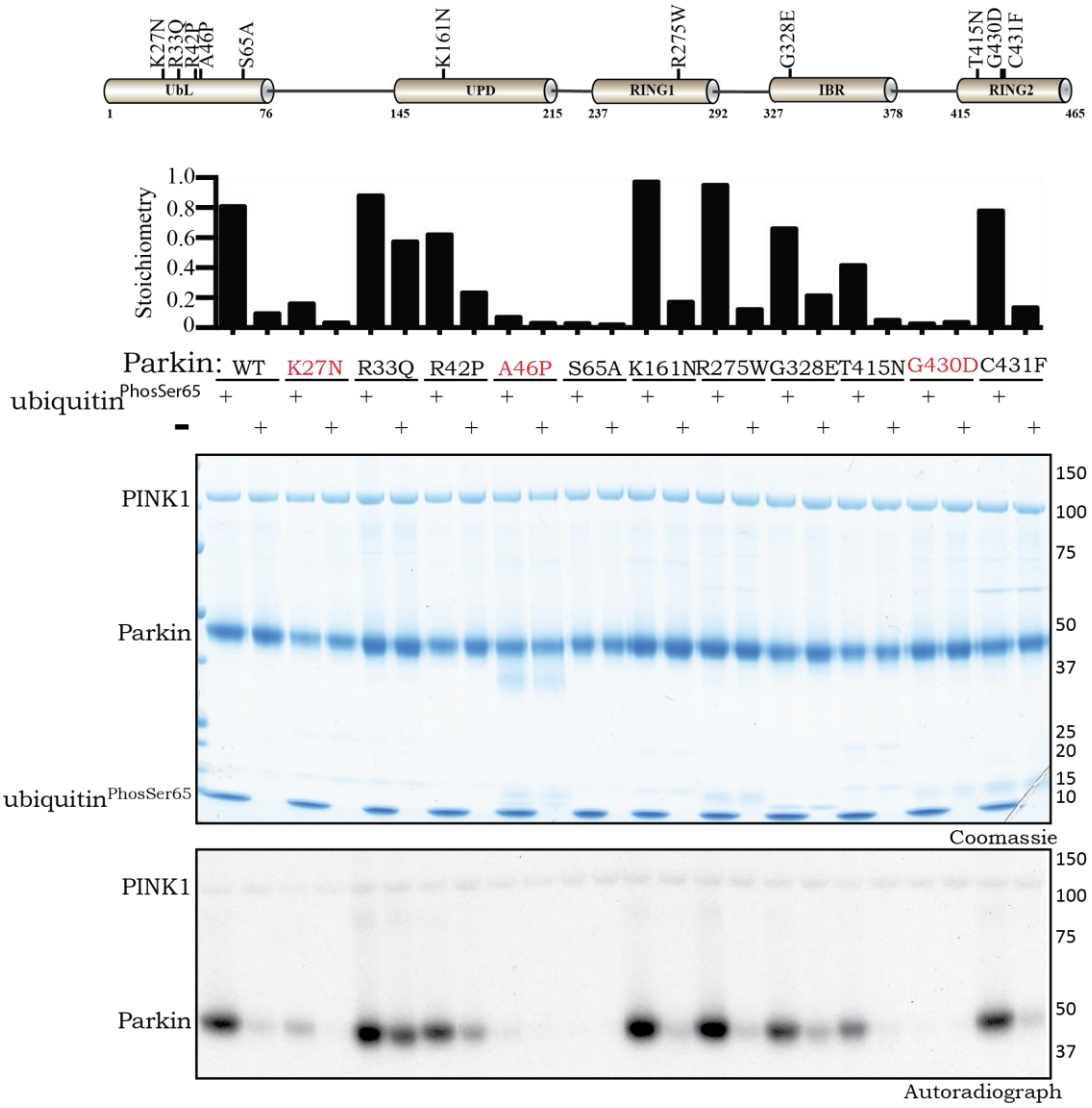

Figure 5.8 Identification of Parkinson's disease associated mutants that disrupt ubiquitin$^{\text{Phospho-Ser65}}$ enhanced phosphorylation of Parkin by TcPINK1.

Schematic of Parkin domain and location of disease-associated Parkin mutants (Upper panel). Wild-type (WT) full-length Parkin or the indicated disease point mutant was incubated with wild-type MBP-TcPINK1 and Mg2+ [γ-^{32}P] ATP in the presence or absence of ubiquitin$^{\text{PhosphoSer65}}$. Proteins were detected by Colloidal Coomassie Blue staining (top panel) and Parkin phosphorylation levels assessed by incorporation of [γ-^{32}P] ATP detected by autoradiography (bottom panel) and displayed above the panel (Lower Panel).

5.4 Parkin His302 and Lys151 are necessary for efficient binding to ubiquitin$^{Phospho\text{-}Ser65}$

5.4.1 Isothermal titration calorimetry analysis of Parkin binding to ubiquitin$^{Phospho\text{-}Ser65}$

To demonstrate direct involvement of the identified Pocket 2 residues in the binding of ubiquitin$^{Phospho\text{-}Ser65}$, isothermal titration calorimetry (ITC) analysis of ubiquitin$^{Phospho\text{-}Ser65}$ binding to full-length wild-type Parkin and the two most deleterious point mutants, H302A and K151A, was conducted by Dr. R. Julio Martinez-Torres (Figure 5.9). Similar to the findings of a recent study (Ordureau et al., 2014), wild-type Parkin bound to ubiquitin$^{Phospho\text{-}Ser65}$ with a K_d of 156 nM (Figure 5.9 A & B, left panel). In contrast, the K151A mutant was found to bind ubiquitin$^{Phospho\text{-}Ser65}$ with 45-fold lower affinity (K_d of ˜7μM) than wild-type Parkin (Figure 5.9 A & B, middle panel), and the H302A mutant exerted an even more dramatic effect, with a 265-fold reduction in the affinity of binding to ubiquitin$^{Phospho\text{-}Ser65}$ (Kd of ˜42μM) when compared to wild-type (Figure 5.9 A & B, right panel). Overall, these data indicate that residues H302 and K151 are required for optimal binding of ubiquitin$^{Phospho\text{-}Ser65}$ to Parkin.

A

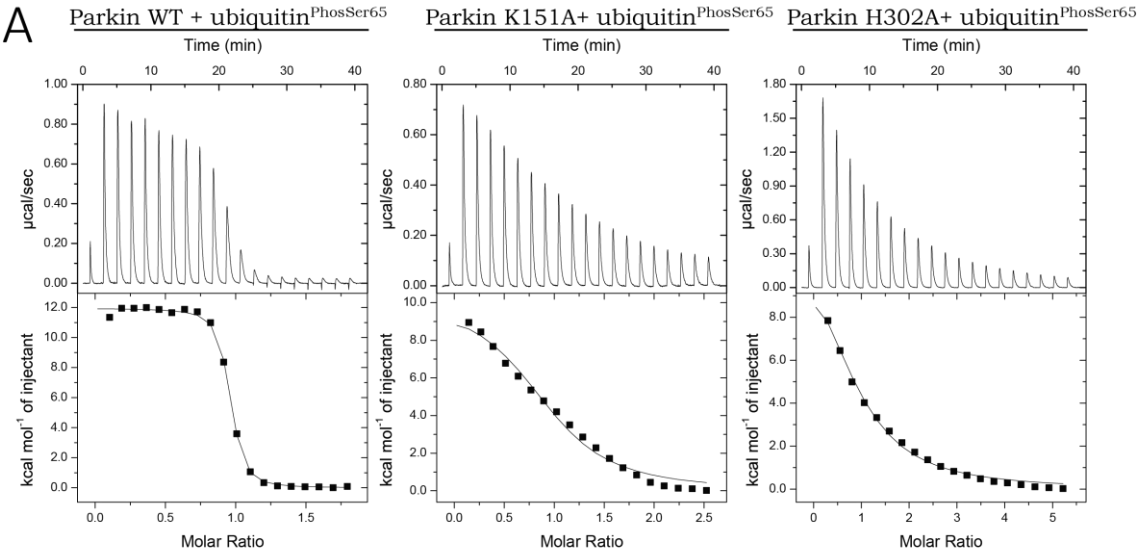

B

Parkin	Kd (µM)	DH (Kcal mol^{-1})	DS (Kcal mol^{-1}deg)	-TΔS (Kcal mol^{-1})
WT	0.156 ± 0.017	11.94	0.07	-0.86
K151A	7.143 ± 1.367	13.48	0.07	-0.89
H302A	41.494 ± 5.320	10.15	0.06	-0.59

Figure 5.9 Parkin His302 and Lys151 are required for optimal binding with Ubiquitin$^{Phospho\text{-}Ser65}$.

(A) Isothermal Calorimetry analysis of Parkin WT (left), K151A mutant (middle) and H302A mutant (right) with Ubiquitin$^{Phospho\text{-}Ser65}$. **(B)** Table showing the K_d values (in µM), ΔH values (in Kcal mol^{-1}), ΔS values (in Kcal mol^{-1} deg) and −TΔS (in Kcal mol^{-1}) derived from the graphs. Data representative of 2 independent experiments.

5.4.2 Gel filtration analysis of Parkin interaction with phosphorylated ubiquitin species

A complementary gel filtration analysis was undertaken to assess heterodimeric complex formation of wild-type Parkin with ubiquitin$^{Phospho\text{-}Ser65}$ (performed by Dr. Axel Knebel). N-terminal Dac-tagged ubiquitin (described in Section 5.2) was used, since it retains monomeric properties and is of a greater molecular weight than untagged ubiquitin, therefore it will produce a discernible increase in elution time upon binding to Parkin , which is necessary to determine if complex formation has occurred (Lee et al., 2012b). Dac-ubiquitin$^{Phospho\text{-}Ser65}$ was produced in manner similar to that described in Section 4.6. Dac-ubiquitin was first

phosphorylated by *Pediculus humanus corporis* PINK1 (PhcPINK1) and then the phosphorylated and non-phosphorylated forms were separated by ion-exchange chromatography. 100 μg of Dac-Ubiquitin or Dac-Ubiquitin$^{phospho\text{-}Ser65}$ were incubated with or without 100 μg of wild-type (WT), H302A or S65A Parkin for 30 min and subjected to size exclusion chromatography using a Superdex 200 Increase (10/300 GL) column. 250 μl of purified protein at a concentration of 0.8 mg/ml was injected on to the column (Figure 5.10). Dac-ubiquitin, Dac-Ubiquitin$^{phospho\text{-}Ser65}$, wild-type as well as H302A and S65A Parkin were also run alone to determine their individual elution profiles (Figure 5.10 A, B, C, D & I respectively). When wild-type Parkin was incubated with Dac-ubiquitin, no strong interaction could be seen between the two proteins, as two distinct peaks corresponding to those of the monomeric proteins were observed (Figure 5.10 E). In contrast, the binding of Dac-ubiquitin$^{Phos\text{-}Ser65}$ to wild-type Parkin resulted in a decrease in the elution time and an increase in the area of the Parkin peak, indicating heterodimer formation (Figure 5.10 F). The non-phosphorylatable S65A Parkin mutant behaved in a similar way to wild-type Parkin; two separate peaks were observed following incubation with Dac-ubiquitin (Figure 5.10 J), however heterodimer formation was seen upon incubation with Dac-ubiquitin$^{Phos\text{-}Ser65}$ (Figure 5.10 K). No evidence was found for binding between Parkin H302A mutant and Dac-ubiquitin$^{Phos\text{-}Ser65}$ or Dac-ubiquitin, as judged by the presence of 2 separate protein elution peaks corresponding to the monomeric proteins in both cases (Figure 5.10 G & H respectively).

Overall, these binding studies indicate a critical involvement of His302 and Lys151 in ubiquitin$^{Phospho\text{-}Ser65}$ binding, and suggest that these residues may lie within the ubiquitin$^{Phospho\text{-}Ser65}$ binding pocket of Parkin.

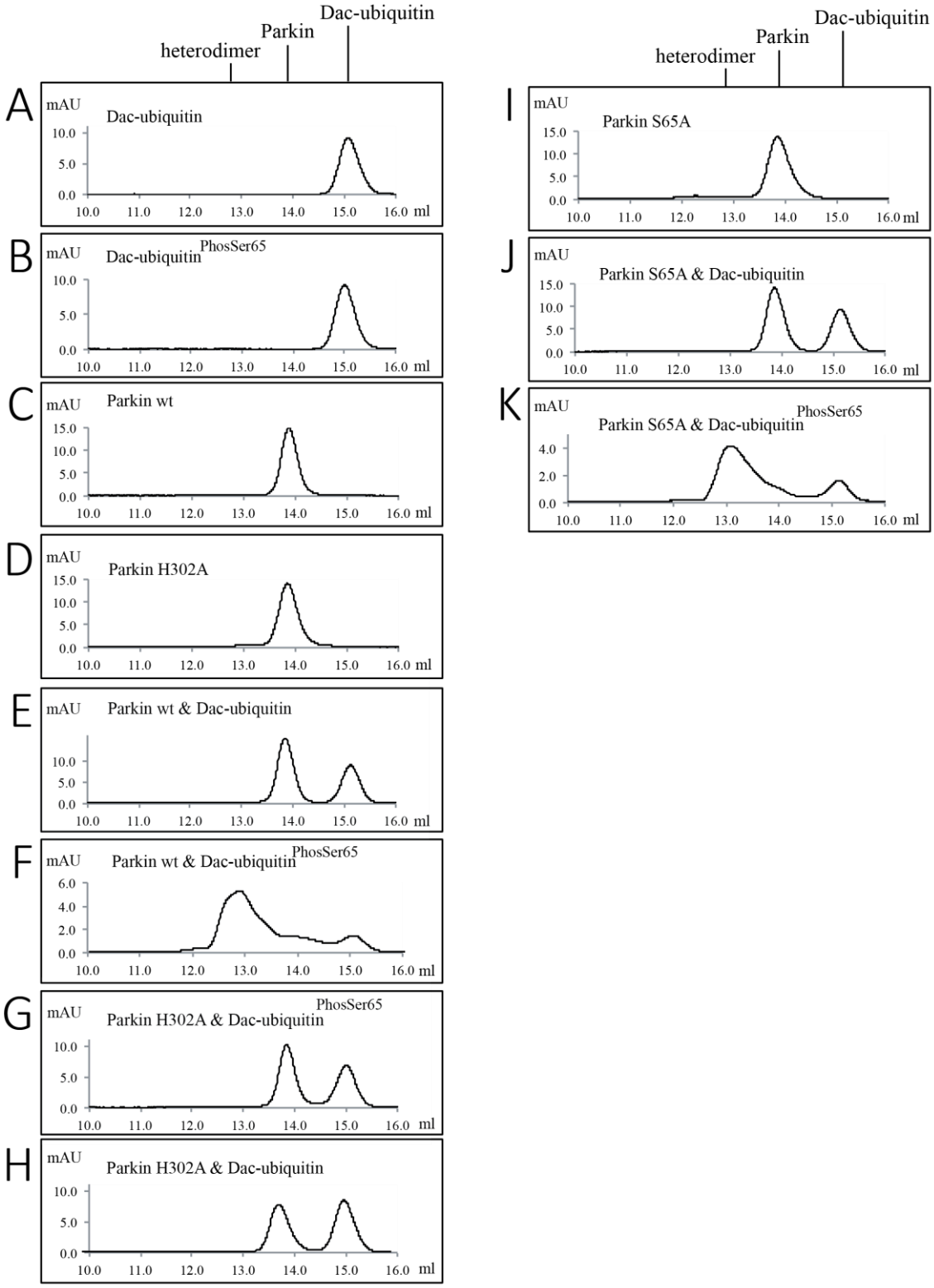
heterodimer
Parkin
Dac-ubiquitin
A
mAU
Dac-ubiquitin
B
Dac-ubiquitin PhosSer65
C
Parkin wt
D
Parkin H302A
E
Parkin wt & Dac-ubiquitin
F
Parkin wt & Dac-ubiquitin PhosSer65
G
Parkin H302A & Dac-ubiquitin PhosSer65
H
Parkin H302A & Dac-ubiquitin
I
Parkin S65A
J
Parkin S65A & Dac-ubiquitin
K
Parkin S65A & Dac-ubiquitin PhosSer65
ml

Figure 5.10 Analysis of heterodimer formation between Ser^{65}-phosphorylated Dac-ubiquitin and Parkin using gel filtration chromatography.

100 µg of Dac-Ubiquitin or Dac-Ubiquitin^{phosphoSer65} (both ~38.3 kDa) were incubated with or without 100 µg of wild-type Parkin (WT) or Parkin His302Ala (H302A) (both ~51.6kDa) for 30 min and subjected to chromatography on a Superdex 200 Increase column (Ge-Healthcare Life Sciences). Parkin eluted at 13.8 ml and Dac-Ubiquitin at 15.1 ml. The dimer eluted at 12.9 ml. The x-axis is ml elution volume and the Y-axis is arbitrary milli absorption Units. **(A)** Profile of Dac-ubiquitin. **(B)** Profile of Dac-Ubiquitin^{phosphoSer65}. **(C)** Profile of WT Parkin. **(D)** Profile of Parkin H302A mutant. **(E)** Profile of WT Parkin and Dac-ubiquitin. **(F)** Profile of WT Parkin and Dac-Ubiquitin ^{phosphoSer65}. **(G)** Profile of H302A Parkin and Dac-Ubiquitin^{phosphoSer65}. **(H)** Profile of H302A Parkin and Dac-ubiquitin. **(I)** Profile of S65A Parkin. **(J)** Profile of S65A Parkin and Dac-Ubiquitin. **(K)** Profile of S65A Parkin and Dac-Ubiquitin$^{phospho\ Ser65}$.

5.5 Evidence that Ubiquitin$^{Phospho\text{-}Ser65}$ influences Parkin Ser^{65} phosphorylation in cells

5.5.1 His302Ala mutation causes a reduction in cellular Parkin$^{Phospho\text{-}Ser65}$ levels

I next explored whether the H302A mutation had any effect on Parkin phosphorylation in cells. To address this, I transiently overexpressed wild-type, S65A and H302A Parkin in wild-type HeLa as well as PINK1 knock-out HeLa cells (Narendra et al., 2013a). I included an untransfected control to ensure the specificity of the antibodies utilised. 24 hours after transfection, cells were treated with 10 µM CCCP or DMSO for 6 hours. CCCP was used to depolarise the mitochondria and stabilise and activate PINK1. After treatment, the cells were lysed and extracts analysed by immunoblotting with a phospho-specific antibody raised against a previously characterised Parkin Ser^{65} epitope (Section 3.2). Consistent with the *in vitro* analysis (Figure 5.5), the level of Parkin phosphorylation was substantially diminished in cells expressing H302A Parkin (Figure 5.11, lanes 7-9) compared to wild-type Parkin (Figure 5.11, lanes 1-3). Antibody specificity was confirmed by the absence of Parkin Ser^{65} phosphorylation signal in cells expressing the S65A Parkin mutant (Figure 5.11, lanes 4-6) as well as in untransfected cells (Figure 5.11, lanes 10-12). The strict dependence of the Parkin Ser^{65} site on active PINK1 was also demonstrated by the lack of Parkin phosphorylation at Ser^{65} in PINK1 knock-out cells (Figure 5.11, bottom).

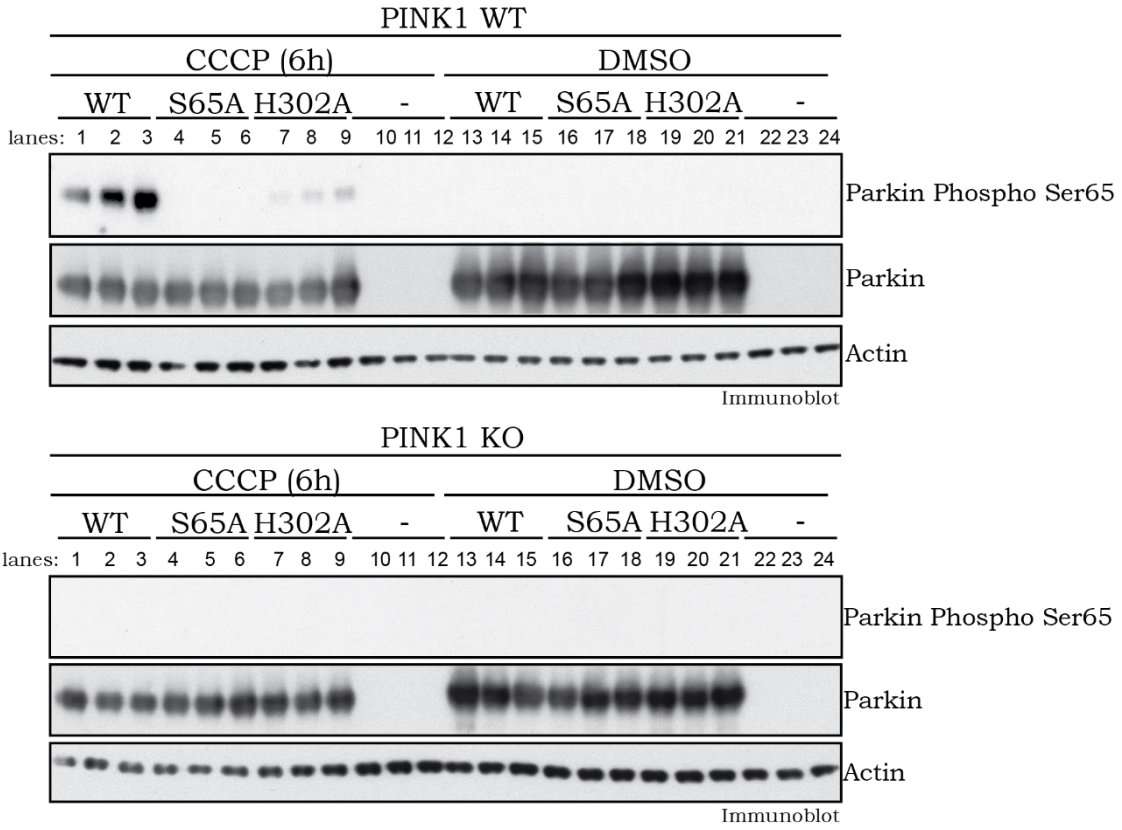

Figure 5.11 Parkin H302A mutant displays a marked decrease in Parkin Ser^{65} phosphorylation upon PINK1 activation.

Wild-type HeLa (upper panel) or PINK1 knock-out HeLa cells (lower panel) were transfected with untagged wild-type (WT), Ser65Ala (S65A) or H302A mutant Parkin and stimulated with 10 μM of CCCP or DMSO for 6 h in triplicates. The lysates were subjected to immunoblotting as follows: Parkin Ser65 phosphorylation (anti-phospho-Ser65 antibody, 1:1000), Parkin (anti-Parkin antibody SantaCruz, 1:1000), Actin (anti-actin antibody Sigma, 1:5000) and PINK1 (anti-PINK1 antibody, 1:1000). Data representative of 3 independent experiments.

5.5.2 His302Ala mutation diminishes Parkin activity in cells

Under similar conditions, I investigated the requirement of His302 for optimal Parkin E3 ligase activity in wild-type HeLa cells stimulated with either CCCP or DMSO. Previous mass spectrometric analysis has identified numerous mitochondrial proteins as Parkin substrates, including the Fe-S cluster-containing protein CISD1 (Sarraf et al., 2013). I chose to monitor the ubiquitylation of this protein as a marker of Parkin E3 ligase activity in cells. The cells

were transfected as described above, and a Cys431Phe disease mutant of Parkin was also included. As mentioned previously, Cys431 is the catalytic cysteine, and I have previously shown that mutating it to phenylalanine causes a complete loss of Parkin activity *in vitro* (Figure 3.15, Chapter 3). It therefore serves as a good negative control in this cell-based experiment. Cells were stimulated for 6 hours with CCCP or DMSO, followed by harvesting in PBS supplemented with 200 mM chloroacetamide. A membrane fraction, enriched in mitochondria, was prepared, as described in Section 2.2.11. Ubiquitylated proteins were then selectively pulled down from 1 mg of lysate using tandem ubiquitin binding entity (TUBE) technology (Hjerpe et al., 2009), in which the ubiquitin associated (UBA) domain of ubiquilin1 was expressed in 4 tandem repeats with an N-terminal Halo tag. This was coupled to Halo beads followed by pulldowns from the membrane fractions. The resulting proteins were analysed by immunoblotting (Figure 5.12).

Upon stimulation with CCCP, a clear poly-ubiquitylation signal of CISD1 was observed in mitochondrial extracts of cells expressing wild-type but not the catalytically inactive C431F RING2 mutant of Parkin (Figure 5.12). A dramatic reduction in CISD1 poly-ubiquitylation was detected in cells expressing the H302A mutant (Figure 5.12, lane 3), confirming that binding involving His302 is essential for optimal Parkin activation in cells, consistent with the *in vitro* analysis of the H302A mutant (Figure 5.5). A significant reduction in CISD1 poly-ubiquitylation levels was also detected in cells expressing the Parkin S65A mutant (Figure 5.12, lane 2) providing further evidence for the critical role of Ubl Ser^{65} phosphorylation in the activation of Parkin E3 ligase activity in cells. CISD1 ubiquitylation was absent in cells stimulated with DMSO.

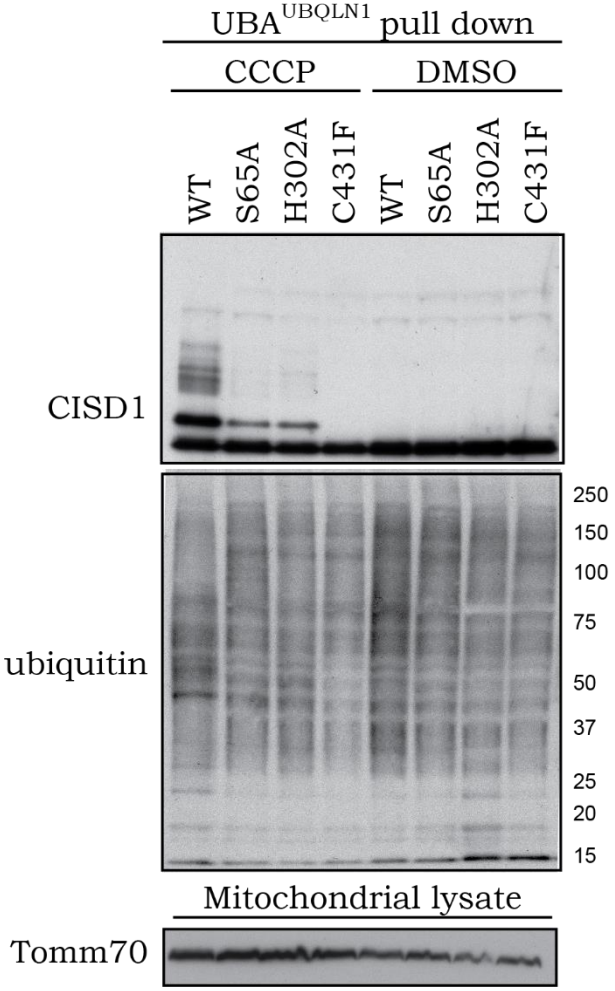

Figure 5.12 Parkin His302 is required for optimal activation of Parkin ubiquitin E3 ligase activity at mitochondria in response to PINK1 activation by CCCP.

Wild-type HeLa cells were transfected with untagged wild-type (WT), Ser65Ala (S65A), His302Ala (H302A) or Cys431Phe (C431F) mutant Parkin and stimulated with 10 μM of CCCP or DMSO for 6 h. Mitochondrial enriched extracts were incubated with a ubiquitin binding resin derived from His-Halo-Ubiquilin1 UBA-domain tetramer (UBA^{UBQLN1}). Captured ubiquitylated proteins were subjected to immunoblotting with CISD1 (1:1000) and ubiquitin (1:1000) antibodies. In parallel mitochondrial input extracts were immunoblotted with Tomm70 antibody (1:1000).

5.5.3 Parkin^{PhosphoSer65} is tethered to mitochondria in cells after stimulation with CCCP

Multiple groups have reported PINK1-dependent phosphorylation of ubiquitin on mitochondrial membranes, leading to the hypothesis that ubiquitin$^{Phospho\text{-}Ser65}$ acts as a Parkin acceptor/receptor on the mitochondria and drives Parkin mitochondrial recruitment (Okatsu et al., 2015, Ordureau et al., 2014). To address how a decrease in ubiquitin$^{Phospho\text{-}Ser65}$ binding would affect Parkin phosphorylation at the mitochondria, I established an immunofluorescence assay using a recently generated highly sensitive monoclonal anti-phospho-Parkin Ser^{65} antibody. I initially generated inducible FlpIn TRex HeLa cells stably overexpressing wild-type Parkin and the S65A, H302A and C431F Parkin point mutants. Cells were plated on glass coverslips, protein expression was induced using doxycycline and PINK1 activation was stimulated using CCCP, with DMSO as a negative control. Total Parkin, Parkin phospho Ser^{65} and mitochondrial distribution was monitored using immunofluorescent probes, as described in Section 2.2.22. Upon stimulation of cells expressing wild-type Parkin with 10 μM CCCP, a striking accumulation of Parkin Ser^{65} phosphorylation on the mitochondria, as judged by staining with the mitochondrial dye Mito-ID red, was observed (Figure 5.13, top row). Furthermore, the mitochondria appeared to be clustered around the nucleus in a peri-nuclear distribution (Figure 5.13, top row). The high specificity of the phospho-antibody was confirmed by an absence of Parkin Ser^{65} phosphorylation signal in S65A Parkin-expressing cells (Figure 5.13, third row). Consistent with the western blot analysis (Figure 5.11) a large reduction of Parkin Ser^{65} phosphorylation in cells expressing H302A Parkin was detected. In addition, the Ser^{65}-phosphorylated H302A Parkin signal was diffuse within the cytosol, in agreement with requirement of ubiquitin$^{Phospho\text{-}Ser65}$ binding ability for mitochondrial translocation (Figure 5.13, fourth row). Finally, there was a substantial reduction in total Parkin translocation in cells expressing the C431F mutant, however, Parkin still became phosphorylated and the Parkin$^{Phospho\text{-}Ser65}$ signal was mainly confined to mitochondria, albeit at levels significantly lower than wild-type Parkin (Figure 5.13, fifth row).

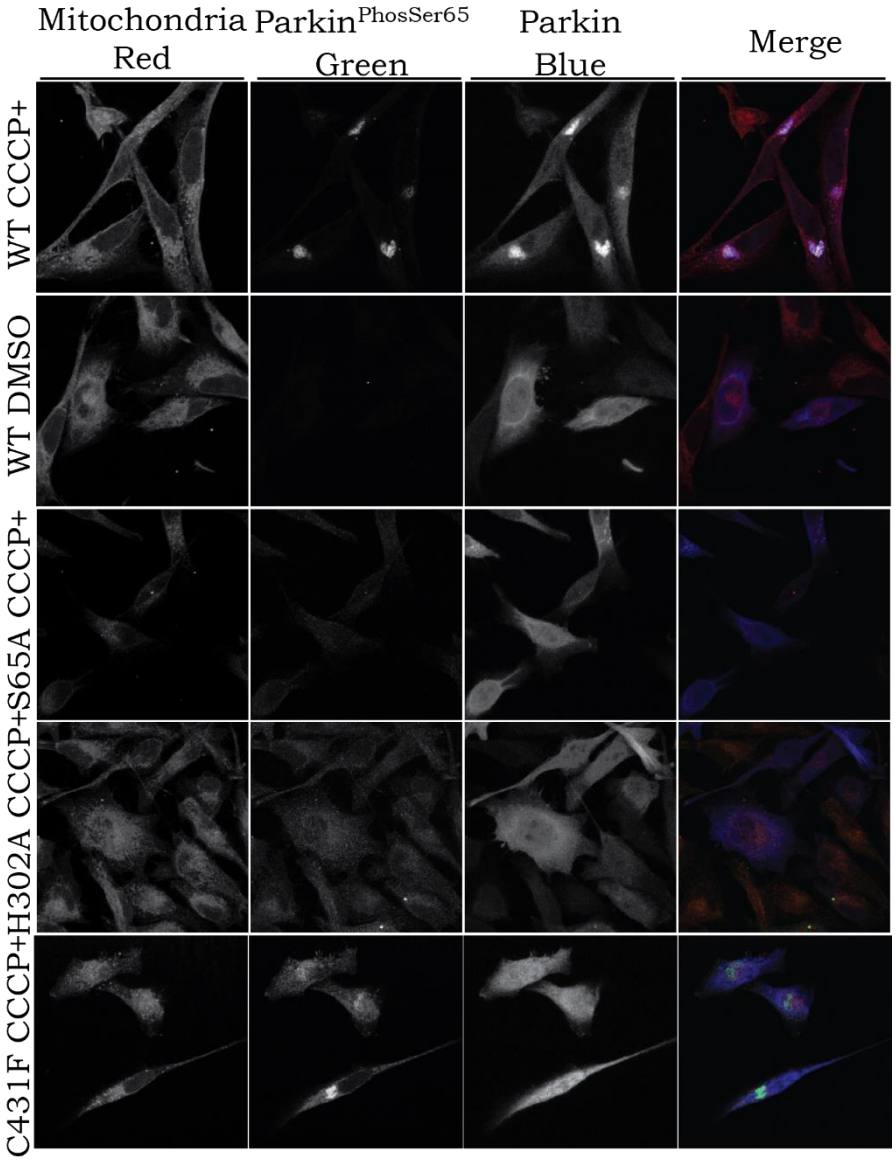

Figure 5.13 Parkin H302A mutant disrupts mitochondrial accumulation of Parkin Ser^{65} phosphorylation.

Wild-type HeLa cells stably expressing untagged wild-type (WT) (top row and second row), Ser65Ala (S65A) (third row) or His302Ala (H302A) (fourth row) mutant Parkin were stimulated with 10 μM of CCCP for 6 h. HeLa cells expressing WT Parkin were also treated with DMSO for 6h (second row). Cells were stained for Parkin Ser65 phosphorylation (anti-phospho-Ser65 antibody) or total Parkin (anti-Parkin antibody); mitochondria were labelled using MITO-ID® Red. Data representative of 4 independent experiments.

5.6 Analysis of Ubl domain interaction with ΔUbl Parkin: regulation by Ubiquitin$^{Phospho\text{-}Ser65}$

5.6.1 Ubiquitin$^{Phospho\text{-}Ser65}$ disrupts Ubl binding to Parkin

To probe the mechanism by which ubiquitin$^{Phospho\text{-}Ser65}$ enhances Parkin Ser^{65} phosphorylation, the crystal and NMR structures of the Ubl domain and full-length Parkin were examined (Sakata et al., 2003, Tashiro et al., 2003, Tomoo et al., 2008, Riley et al., 2013, Spratt et al., 2013, Trempe et al., 2013, Wauer and Komander, 2013). Structural analysis of the Ubl domain revealed that Ser^{65} resides in a loop adjacent to the fifth β-strand that exhibits conformational flexibility (Sakata et al., 2003, Tashiro et al., 2003, Tomoo et al., 2008) and may only be partially surface accessible in the full-length structure. The Ubl domain itself binds to the RING1 domain (Trempe et al., 2013) and can interact with ΔUbl Parkin *in trans* (Chaugule et al., 2011). It is therefore plausible that ubiquitin$^{Phospho\text{-}Ser65}$ binding might alter the interaction between the Ubl domain and the C-terminal domain in a way that renders Ser^{65} of the Ubl domain more accessible for phosphorylation by PINK1.

In order to address this possibility, an Alphascreen® *in vitro* binding assay was developed by Dr. Jinwei Zhang, in collaboration with members of the Drug Discovery Unit (University of Dundee). This robustly quantified the interaction between the Ubl domain (GST-Ubl, residues 1-76) and a C-terminal fragment of Parkin that contains the RING1 domain (Parkin 80-465-biotin). The proteins were first expressed in *E. coli* (Appendix Figure 4) followed by binding to streptavidin coated donor beads (GST-Ubl) and glutathione coated acceptor beads (Parkin-80-465-biotin). Binding was established by monitoring the proximity-based luminescent signal and the optimal assay conditions were determined by titrating GST-Ubl at concentrations from 0-300 nM against Parkin-biotin at concentrations from 0-300nM. Cross titration analysis revealed the strongest binding signal was detectable at concentrations of 10 nM Parkin (80-465)-biotin and 10 nM GST-Ubl.

These optimised conditions were then used to determine whether ubiquitin$^{Phospho\text{-}Ser65}$ may influence the interaction between the Ubl domain and the rest of Parkin (Figure 5.14, performed by Dr. Scott Wilkie). The addition of increasing amounts of ubiquitin$^{Phospho\text{-}Ser65,}$ but not non-phosphorylated ubiquitin, led to dose-dependent disruption of GST-Ubl (1-76) binding to Parkin (80-465)-biotin with an IC_{50} of ~0.2 μM (Figure 5.14 A & E). This strongly suggested that upon binding to Parkin, ubiquitin$^{Phospho\text{-}Ser65}$ disrupts the interaction of the Ubl domain with the Parkin C-terminal domain.

The role of residue His302 in the ubiquitin$^{Phospho\text{-}Ser65}$-mediated disruption of Ubl binding was next addressed. The binding of GST-Ubl to the Parkin H302A mutant was insensitive to increasing amounts of ubiquitin$^{Phospho\text{-}Ser65}$ (Figure 5.14 B & E), in agreement with residue His302 playing an essential role in the binding of ubiquitin$^{Phospho\text{-}Ser65}$ and promotion of PINK1-mediated Parkin phosphorylation and the subsequent activation of Parkin. The activity of BAP tagged Parkin (80-465) wild-type and the H302A mutant was tested in parallel to that of ΔUbl Parkin to ensure that their activity is intact and any effects detected in the Alphascreen assay are not due to protein instability (Appendix Figure 3). Both BAP-tagged versions of Parkin displayed a similar activity to that of wild-type ΔUbl Parkin (Appendix Figure 3).

To assess any interplay between ubiquitin$^{Phospho\text{-}Ser65}$ and Ser^{65}-phosphorylated Ubl domain (Ubl$^{Phospho\text{-}Ser65}$) in the activation of Parkin, Ubl$^{Phospho\text{-}Ser65}$ was generated, as described in Section 2.2.30.1 to a stoichiometry of phosphorylation of ~90%, and Alphascreen assays were undertaken using this protein in addition to wild-type and H302A Parkin. The ability of Ubl$^{Phospho\text{-}Ser65}$ to disrupt the GST-Ubl:Parkin (80-465) biotin interaction was tested, and under similar assay conditions, the ability of Ubl$^{Phospho\text{-}Ser65}$ to disrupt the GST-Ubl:Parkin WT interaction was greatly reduced compared to that of the untagged Ubl domain or ubiquitin$^{Phospho\text{-}Ser65.}$ The mild disruptive effect observed is likely to be due to the presence of unphosphorylated Ubl (<10%) present in the Ubl$^{Phospho\text{-}Ser65}$ sample (Figure 5.14 C & E) and is consistent with the lack of effect of Ubl$^{Phospho\text{-}Ser65}$ in promoting PINK1-dependent

phosphorylation of Parkin (Figure 5.3). Similarly, Ubl$^{\text{Phospho-Ser65}}$ was only able to weakly disrupt the GST-Ubl to Parkin H302A interaction (Figure 5.14 D & E), which is again likely to be due to unphosphorylated Ubl in the Ubl$^{\text{Phospho-Ser65}}$ sample.

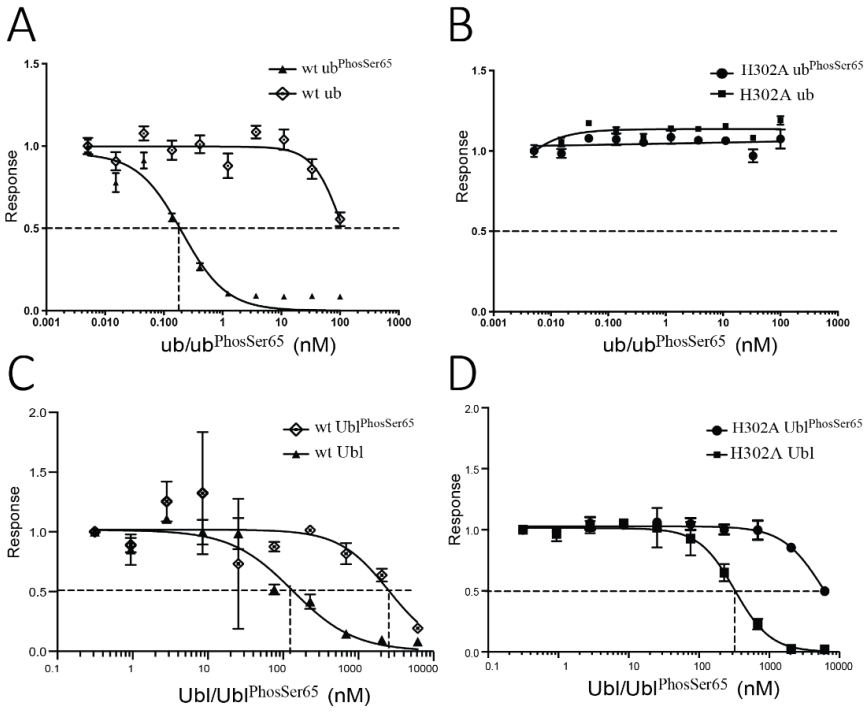

E

	IC_{50} (nM)	
Parkin	WT	H302A
Ubl	133.5	323
Ubl$^{\text{PhosSer65}}$	>2530	ND
ub	ND	ND
ub$^{\text{PhosSer65}}$	0.2	ND

Figure 5.14 Ubiquitin$^{\text{Phospho-Ser65}}$-mediated disruption of binding between the Ubl domain and ΔUbl Parkin is dependent on residue His302.

An AlphaScreen™ binding assay of Parkin Ubl domain and C-terminus of Parkin was established. GST-Ubl (residues 1-76) and wild-type C-terminal Parkin-Biotin (residues 80-465) were incubated with streptavidin-coated donor beads and Glutathione acceptor beads for 60 min. **(A, B)** Phosphorylated (ub$^{\text{PhosSer65}}$) and wild-type (ub) ubiquitin was tested with wild-type (wt) (A), or H302A Parkin (B). **(C, D)** Phosphorylated (Ubl$^{\text{PhosSer65}}$) or wild-type Ubl domain was tested with wild-type (C) or H302A Parkin (D). **(E)** Table showing the IC_{50} values (in nM) derived from graphs. ND indicates incomplete inhibition of the interaction. Data show mean of one trial +/- s.d., n=3 for each condition (A-D).

5.7 Purified Ser^{65}–phosphorylated Parkin exhibits constitutive activity that is no longer sensitive to Ubiquitin$^{Phospho\text{-}Ser65}$

All the data presented so far indicate that binding of ubiquitin$^{Phospho\text{-}Ser65}$ to Parkin may represent a critical first step in the Parkin activation cascade. This suggests that the ensuing Parkin Ubl Ser^{65} phosphorylation by PINK1 is likely to represent the critical effector step leading to activation of Parkin E3 ligase activity. To obtain further experimental evidence for this model, I investigated whether near-maximally phosphorylated purified Ser^{65}–phosphorylated Parkin (Parkin$^{Phospho\text{-}Ser65}$) could be further activated by addition of ubiquitin$^{Phospho\text{-}Ser65}$. His-SUMO tagged full-length Parkin was purified from *E. coli*, captured on Ni-NTA-agarose and phosphorylated by MBP-TcPINK1 before the His-SUMO-tag was removed and Parkin was purified via nickel affinity and size exclusion chromatography (performed by Dr Axel Knebel). Under super-saturating phosphorylation conditions, a heterogeneous mixture containing approximately 60% phosphorylated Parkin was obtained, as confirmed directly by Aquapeptide analysis (performed by Dr. Julien Peltier, Figure 5.15).

	Parkin WT	p-Parkin WT	p-Parkin H302A
non-phosphorylated (%)	91	40	6
phosphorylated (%)	background	60	94

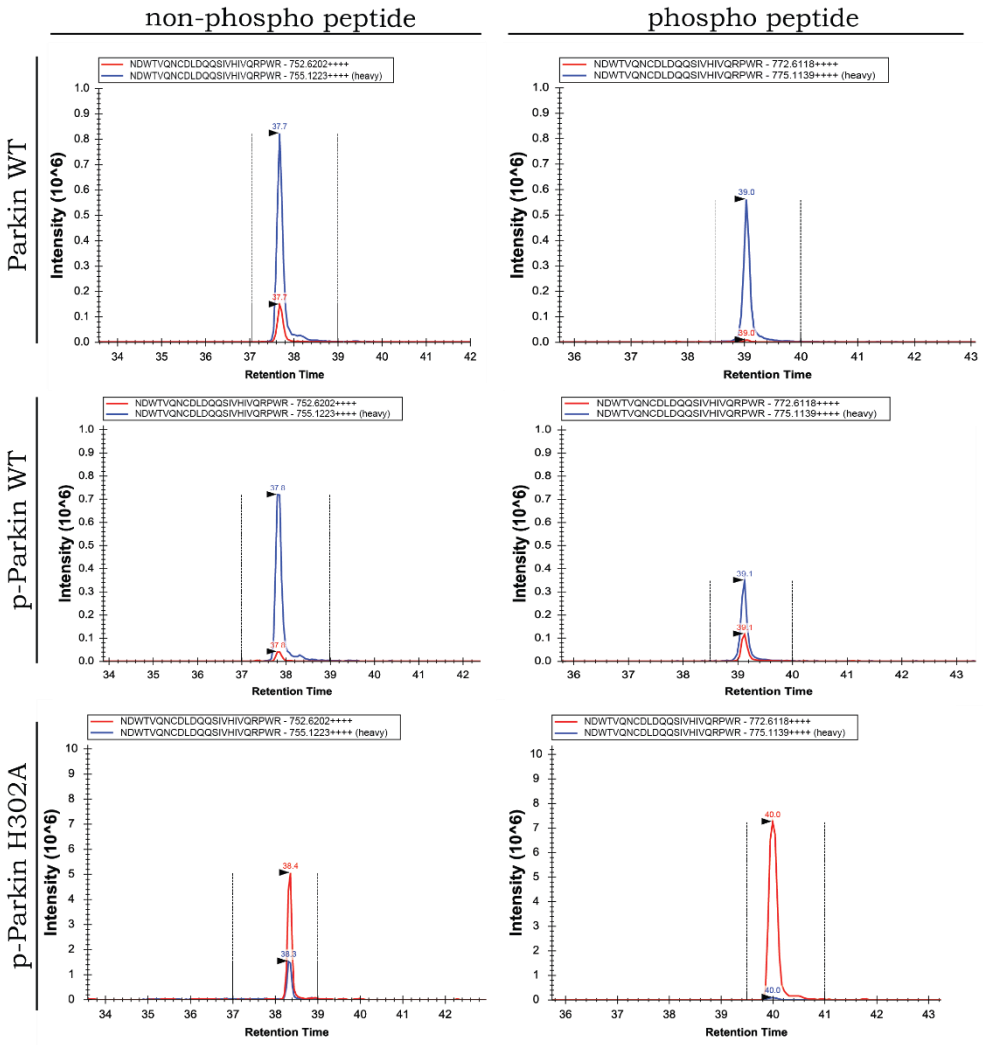

Figure 5.15 Quantitative analysis of phosphorylation of full length Parkin at Ser^{65} using Aquapeptides for p-Ser^{65}.

Table summarising the peptides in wild-type Parkin (WT) (left), WT Parkin$^{\text{Phospho-Ser65}}$ (P-Parkin WT) samples (middle), and H302A Parkin$^{\text{Phospho-Ser65}}$ (P-Parkin H302A) samples (right). LC-MS/MS spectra (left panel) of non-phospho peptides of WT Parkin (top), P-Parkin WT (middle) and P-Parkin H302A (bottom). LC-MS/MS spectra (right panel) of phospho peptides of WT Parkin (top), P-Parkin WT (middle) and P-Parkin H302A (bottom).

5.7.1 Purified Ser^{65}–phosphorylated Parkin is no longer sensitive to Ubiquitin$^{Phospho\text{-}Ser65}$

Next, I compared the activity of Parkin$^{Phospho\text{-}Ser65}$ and wild-type Parkin in the presence or absence of increasing amounts of non-phosphorylated ubiquitin or ubiquitin$^{Phospho\text{-}Ser65}$. I assembled the ubiquitylation assays as described in Section 2.2.28.2: 0.05 mM Flag-ubiquitin was used in conjunction with the indicated amounts of untagged phospho or non-phospho ubiquitin. As previously described (Section 4.7), wild-type Parkin was inactive upon titration of ubiquitin, however, a dose-dependent increase in activity was observed when ubiquitin$^{Phospho\text{-}Ser65}$ was added, as judged by the formation of free ubiquitin chains, Miro1 ubiquitylation and Parkin autoubiquitylation (Figure 5.16). Strikingly, the purified Parkin$^{Phospho\text{-}Ser65}$ was insensitive to both ubiquitin and ubiquitin$^{Phospho\text{-}Ser65}$; it exhibited marked basal E3 ligase activity evidenced by free polyubiquitin chain formation, Miro1 multi-monoubiquitylation and Parkin autoubiquitylation (Figure 5.16). The basal activity of Parkin$^{Phospho\text{-}Ser65}$ was substantially greater than that of wild-type Parkin, based on levels of Miro1 ubiquitylation.

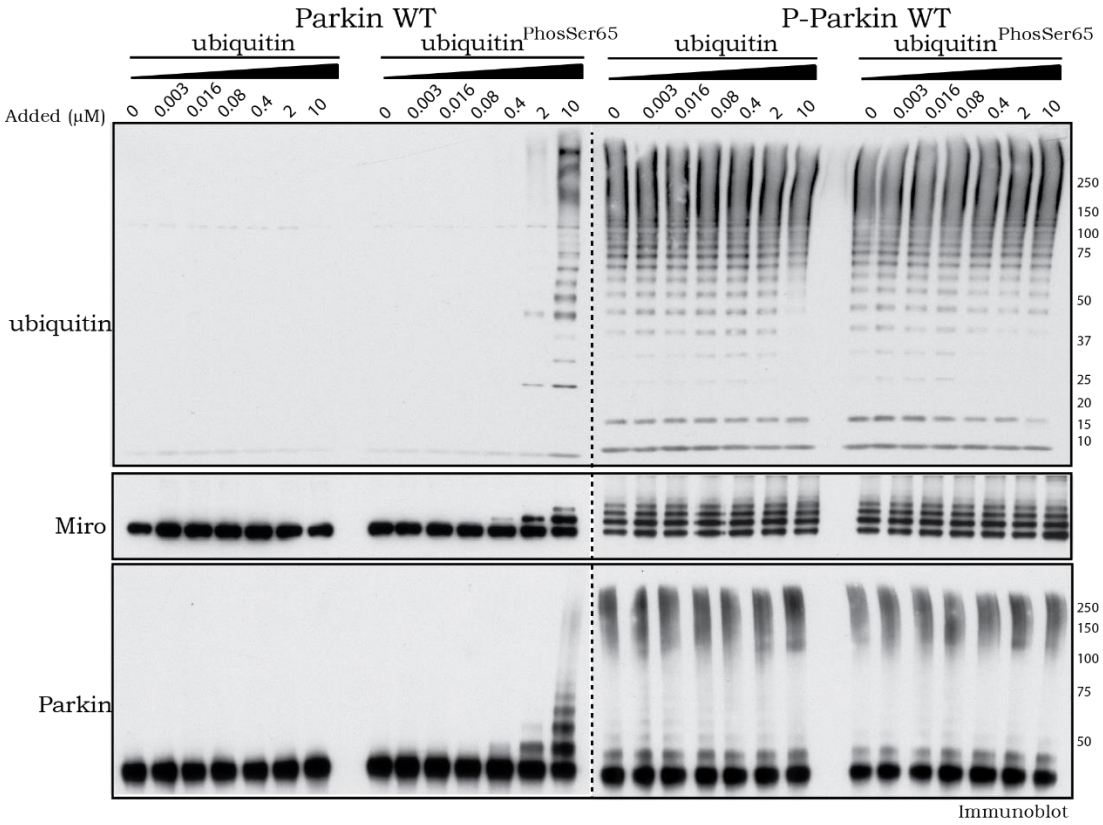

Figure 5.16 Phosphorylated Parkin at Ser[65] exhibits significant constitutive activity.

2 μg of full-length wild-type (Parkin WT) or phosphorylated at Ser65 (P-Parkin WT) Parkin were analysed using E3 ligase assay with increasing amounts of non-phospho-ubiquitin or ubiquitin^{PhosphoSer65} as indicated. Parkin activity was evaluated by immunoblotting as follows: ubiquitin (anti-FLAG-HRP), Parkin (anti-Parkin antibody) and Miro-1 (anti-SUMO1 antibody). Data representative of 3 independent experiments.

To test if the insensitivity to ubiquitin$^{Phospho\text{-}Ser65}$ was a result of Parkin$^{Phospho\text{-}Ser65}$ activity having reached a plateau, I set up a ubiquitylation assay using 10-fold less wild-type or phosphorylated Parkin in conjunction with increasing ubiquitin$^{Phospho\text{-}Ser65}$ levels, as before (Figure 5.17). No change in Parkin$^{Phospho\text{-}Ser65}$ activity was observed when ubiquitin$^{Phospho\text{-}Ser65}$ was added, whilst wild-type Parkin displayed a similar activity pattern to that seen at the higher concentration (Figure 5.17), suggesting that insensitivity may be an intrinsic trait of Parkin$^{Phospho\text{-}Ser65}$.

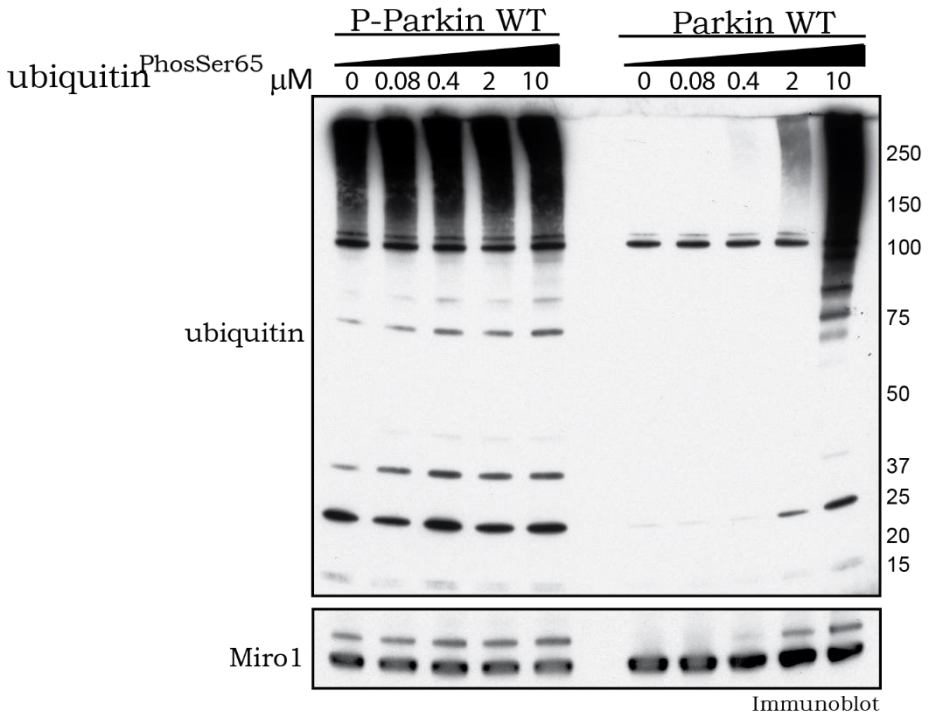

Figure 5.17 A lower titre of Ser[65]-phosphorylated Parkin activity remains insensitive to ubiquitin[Phospho-Ser65].

0.22 μg of wild-type (Parkin WT) or Parkin phosphorylated at Ser65 (P-Parkin WT) were incubated in an E3 ligase assay supplemented with non-phospho-ubiquitin or ubiquitin$^{Phospho\text{-}Ser65}$ as indicated. Parkin activity was evaluated by immunoblotting as follows: ubiquitin (anti-FLAG-HRP antibody; 1:10000) and Miro-1 (anti-SUMO1 antibody; 1:2000).

5.7.2 Time course analysis of ParkinPhospho-Ser65 activity

Subsequently, I tested if ubiquitin$^{Phospho\text{-}Ser65}$ sensitivity could be observed in a time-dependent fashion and has not been previously detected due to inadequacies in the dynamic range of the assay detection method or the reaction reaching a non-linear phase. To achieve this, I undertook a time course analysis of Parkin E3 ligase activity, wherein wild-type or phosphorylated Parkin protein was incubated with a fixed amount of FLAG-ubiquitin and 5 μg of untagged wild-type or phosphorylated ubiquitin. The reactions were allowed to continue for the times indicated (Figure 5.18). In agreement with the previous analysis, no enhancement of Parkin$^{Phospho\text{-}Ser65}$ activity by ubiquitin$^{Phospho\text{-}Ser65}$ could be observed at any of

the time points tested (Figure 5.18) as judged by free polyubiquitin chain formation and Parkin autoubiquitylation.

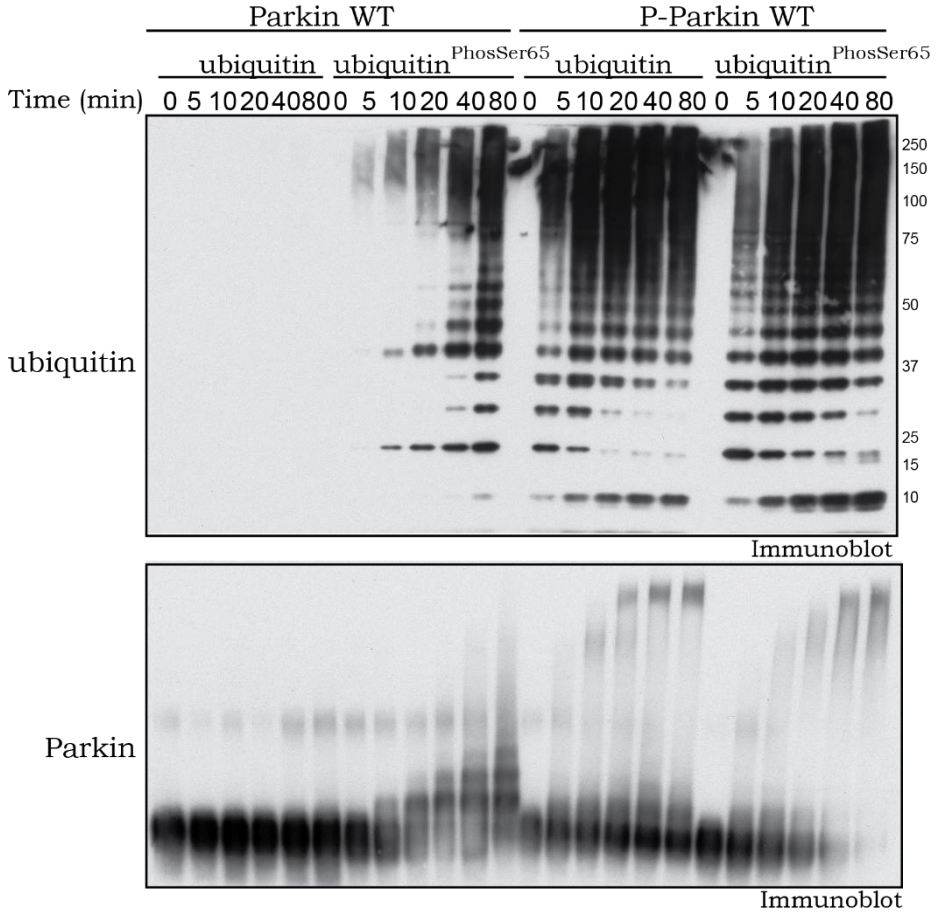

Figure 5.18 Timecourse analysis of Ser^{65}-phosphorylated Parkin activity in the presence or absence of ubiquitin$^{Phospho\text{-}Ser65}$.

2 µg of wild-type (Parkin WT) or Parkin phosphorylated at Ser65 (P-Parkin WT) were subjected to E3 ligase assays in the presence of non-phospho-ubiquitin or ubiquitin$^{Phospho\text{-}Ser65}$ as indicated. Reactions were terminated at the indicated timepoints by the addition of LDS loading buffer. Parkin activity was evaluated by immunoblotting as follows: ubiquitin (anti-FLAG-HRP antibody), and Parkin (anti-Parkin antibody).

5.7.3 Parkin$^{Phospho\text{-}Ser65}$ His302Ala mutant is constitutively active

A ~90% phosphorylated H302A mutant Parkin was also generated by Dr. Axel Knebel (Figure 5.15) and tested in the ubiquitylation assays. I assembled the E3 ligase assays in parallel with

wild-type as well as Parkin$^{Phospho\text{-}Ser65}$ with or without ubiquitin$^{Phospho\text{-}Ser65}$, as described in Section 2.2.28.2 (Figure 5.19). Both Parkin$^{Phospho\text{-}Ser65}$ and the Parkin$^{Phospho\text{-}Ser65}$ H302A mutant displayed similar levels of activity independent of ubiquitin$^{Phospho\text{-}Ser65}$, providing further evidence that the H302A mutation is not significantly perturbing the structural fold and integrity of Parkin.

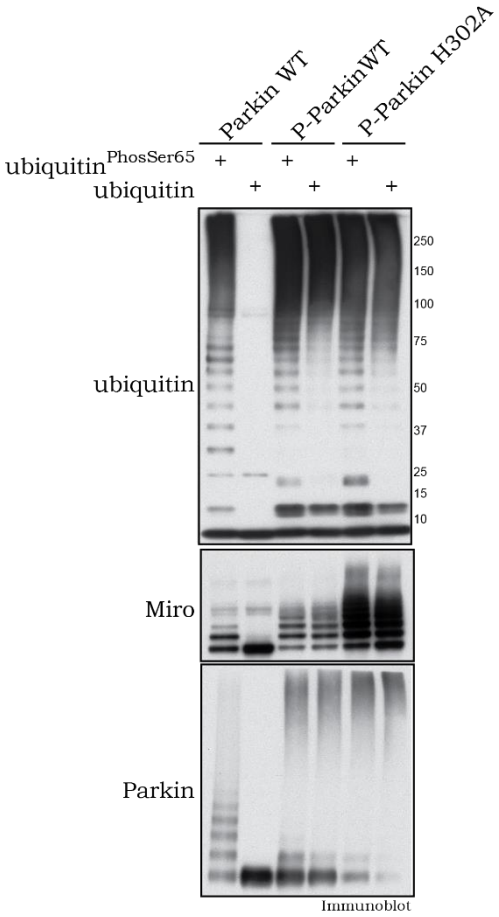

Figure 5.19 Purified Ser^{65}-phosphorylated Parkin H302A exhibits constitutive E3 ligase activity that is insensitive to ubiquitin$^{Phospho\text{-}Ser65}$.

2 µg of full-length wild-type (P-Parkin WT) or H302A (P-Parkin H302A) Parkin phosphorylated at Ser65 were subjected to E3 ligase assays supplemented with non-phospho-ubiquitin or ubiquitin$^{Phospho\text{-}Ser65}$ as indicated. Parkin activity was evaluated by immunoblotting as follows: ubiquitin (anti-FLAG-HRP antibody), Parkin (anti-Parkin antibody) and Miro-1 (anti-SUMO1 antibody).

5.7.4 Parkin$^{Phospho\text{-}Ser65}$ loses activity upon dephosphorylation by calf alkaline phosphatase

To confirm that the constitutive activity of Parkin$^{Phospho\text{-}Ser65}$ was caused by phosphorylation rather than structural instability caused by the phosphorylation and subsequent repurification conditions, I treated Parkin$^{Phospho\text{-}Ser65}$ with increasing amounts of calf alkaline phosphatase, and a subsequent dose-dependent reduction in its activity was observed, as indicated by diminishing free polyubiquitin chain formation and Parkin autoubiquitylation, which correlated with the decreased phosphorylation at Parkin Ser^{65} (Figure 5.20).

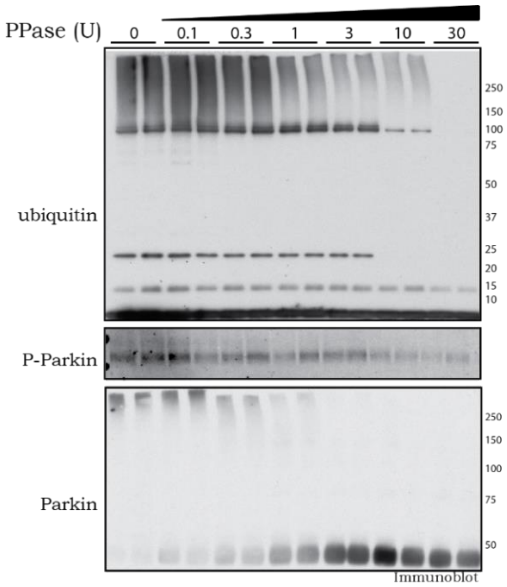

Figure 5.20 Dephosphorylation of Parkin at Ser^{65} leads to reversal of Parkin E3 ligase constitutive activity.

1 μg of full-length Parkin phosphorylated at Ser65 was subjected to increasing amounts of alkaline phosphatase as indicated. Reactions were then incubated with ubiquitylation assay components (E1 and UbcH7) in the presence of 0.05 mM FLAG-ubiquitin. Reactions were terminated after 60 min by the addition of LDS loading buffer. The effects on Parkin E3 ligase activity were evaluated by ubiquitin chain formation ubiquitylation and Parkin autoubiquitylation evaluated by immunoblotting as follows: ubiquitin (anti-FLAG-HRP antibody), Parkin (anti-Parkin antibody). The degree of Parkin Ser^{65} dephosphorylation was monitored using anti-pSer^{65} Parkin antibody. Data representative of 4 independent experiments.

5.8 Discussion and Summary

Parkin was historically reported to be a constitutively active RING E3 ligase, later found to interact with another PD-linked protein PINK1. During the last 4 years, the field of PINK1 and Parkin study has undergone a 'violent intellectual revolution' (Kuhn, 1962) that has not only refuted the initial conclusions, demonstrating Parkin to be a tightly-regulated autoinhibited E3 ligase (Okatsu et al., 2015, Shiba-Fukushima et al., 2014, Ordureau et al., 2014, Chaugule et al., 2011), but also uncovered a multi-dimensional regulatory mechanism underpinning this previously enigmatic relationship. This chapter presents recent insights into the cogs of the complicated machinery, uncovering the regulation of Parkin in the context of mitochondrial health.

It was previously known that upon mitochondrial damage, PINK1 becomes stabilized on the mitochondrial membrane via association with the TOM complex (Lazarou et al., 2012), followed by its activation, Parkin recruitment (Geisler et al., 2010, Narendra et al., 2010, Vives-Bauza et al., 2010) and activation (Matsuda et al., 2010) as well as substrate ubiquitylation. More specifically, following PINK1 activation, Parkin and ubiquitin were found to be phosphorylated at Ser^{65} (Kondapalli et al., 2012, Shiba-Fukushima et al., 2012, Koyano et al., 2014, Kane et al., 2014, Kazlauskaite et al., 2014c) and $ubiquitin^{Phospho\text{-}Ser65}$ was shown to subsequently enhance Parkin activity (Figure 5.21 A). Several recent studies have revealed that $ubiquitin^{Phospho\text{-}Ser65}$ acts as Parkin receptor on the mitochondria (Shiba-Fukushima et al., 2014, Okatsu et al., 2015) and contributes to a feed-forward cascade, wherein autoinhibited Parkin continuously samples the mitochondrial membrane and upon membrane depolarisation becomes activated via phosphorylation at Ser^{65} by PINK1 (Figure 5.21 B). Activated Parkin is then able to ubiquitylate outer mitochondrial membrane proteins, which can then be phosphorylated by PINK1, further enhancing recruitment of Parkin (Ordureau et al., 2014) (Figure 5.21 B). My discoveries presented in this chapter, together with a recent structural paper (Wauer et al., 2015a), add missing details into the picture.

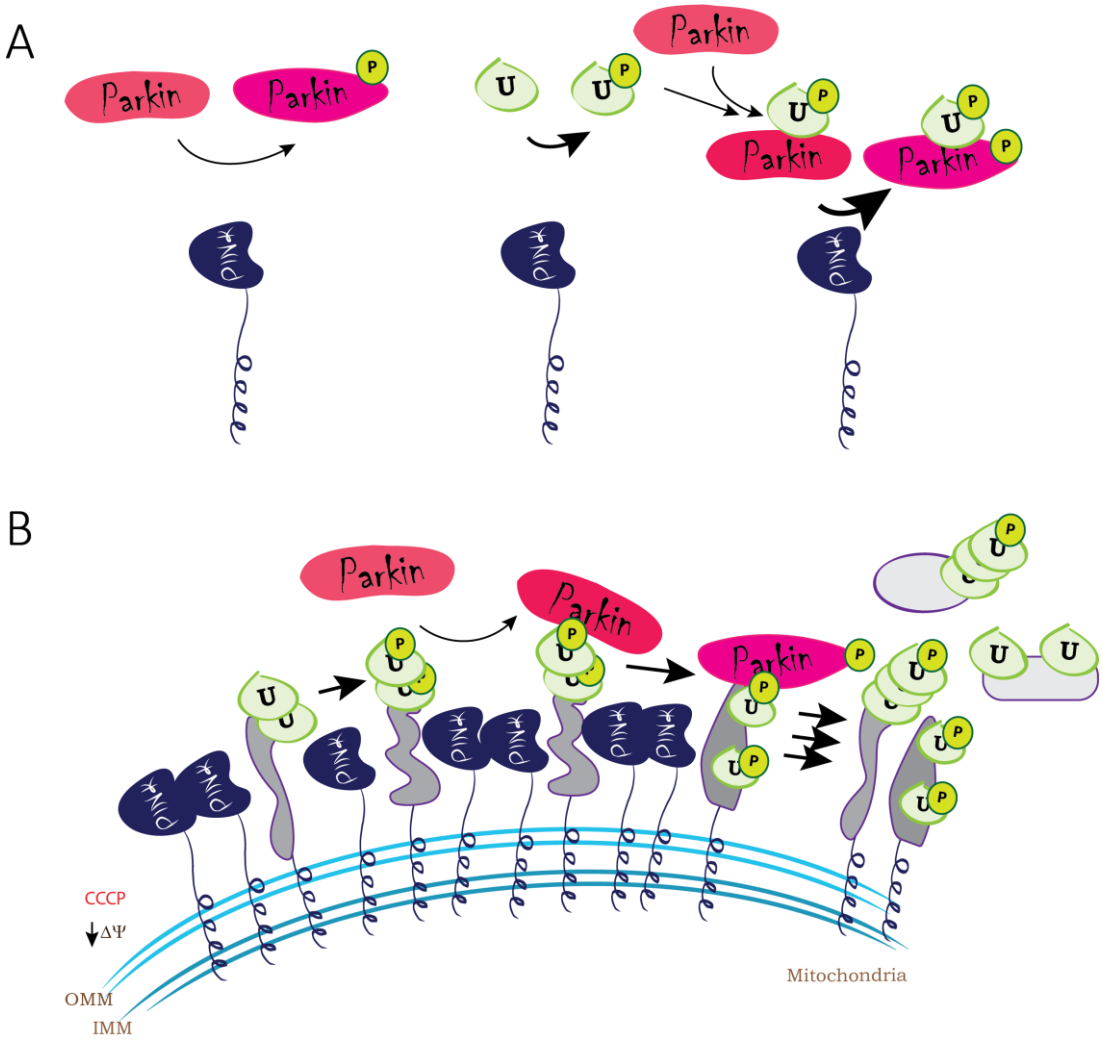

Figure 5.21 Regulation of Parkin E3 ligase activity by PINK1-mediated phosphorylation

A PINK1 mediates phosphorylation of Parkin and ubiquitin at Ser^{65}, phosphorylation of ubiquitin$^{Phospho\text{-}Ser65}$ bound Parkin is largely enhanced. **B** Upon mitochondrial membrane depolarization, PINK1 gets stabilized on the OMM, where it phosphorylates ubiquitin at Ser^{65} on the ubiquitylated OMM proteins. Cytoplasmic Parkin samples the mitochondrion and gets recruited by binding to ubiquitin$^{Phospho\text{-}Ser65}$ when it itself gets phosphorylated at Ser^{65} and fully activated. This leads to further ubiquitylation of OMM and cytoplasmic proteins and subsequent recruitment of mitophagy machinery.

Firstly, upon binding to full-length Parkin, ubiquitin$^{\text{Phospho-Ser65}}$ enhances Ubl Ser^{65} phosphorylation by PINK1 in a highly specific manner (Figure 5.2 & Figure 5.3). Notably, all species of dimeric and tetrameric ubiquitin tested, as well as a model mono-ubiquitylated substrate (Figure 5.4) could be phosphorylated by PINK1 to a similar, if not equivalent, extent and led to increased Parkin phosphorylation, suggesting that this is a wide-spread effect. This is particularly interesting since Parkin has been demonstrated by myself and others to form multiple ubiquitin chain linkages (Chapter 3) (Ordureau et al., 2014). It will be necessary in future to understand how uniform the phosphorylation of each of the linkages is *in vivo* as well as to determine the biological outcomes of these phosphorylation events. Given that ubiquitin phosphorylation is not as yet a well understood phenomenon, it will be important to search for phospho-ubiquitin specific adaptor proteins and to learn if ubiquitin chain topology-driven cellular events are similarly controlled and effected once one or more phospho moieties are present. It would also be insightful to assess whether (multi)-monoubiquitylated and polyubiquitylated substrates of Parkin such as Miro1/2 or Mitofusin1/2 (Sarraf et al., 2013, Kazlauskaite et al., 2014b) become phosphorylated at ubiquitin Ser^{65}, and if so whether this plays a role in aiding Parkin activation. Finally, it will be critical to define the interactions and timeline of PINK1 phosphorylation of free and substrate-bound mono- and poly- ubiquitin and how the PINK1-modified ubiquitome lead to altered cellular function and mitochondrial quality control.

In addition, His^{302} and Lys^{151} in Parkin were defined as critical residues for ubiquitin$^{\text{Phospho-Ser65}}$ binding. The results presented in this chapter clearly show the direct involvement of both residues in direct binding between Parkin and phospho-ubiquitin (Figure 5.9), as well as the functional impairment upon mutation of these residues to alanine (Figure 5.5 & Figure 5.7). The importance of His302 was also confirmed in cell studies, where a loss of Parkin phosphorylation as well as activity were observed when the Parkin H302A mutant was analysed (Figure 5.11 & Figure 5.12). Whilst my study did not define the entire phospho-ubiquitin binding site, several recent papers have provided structural insights into ubiquitin$^{\text{Phospho-Ser65}}$ binding to Parkin (Wauer et al., 2015a, Kumar et al., 2015, Sauve et al., 2015). It was revealed that in addition to RING1 domain, Ubl interacts with IBR and REP

(Sauve et al., 2015, Kumar et al., 2015). It was demonstrated that besides Lys151 and His302, Arg305, Ala320 and Gly284 are important for ubiquitin$^{\text{Phospho-Ser65}}$-mediated Parkin activation (Wauer et al., 2015a, Sauve et al., 2015). In addition, it was shown that binding of phosphorylated ubiquitin destabilizes the Ubl interaction with the RING1-IBR-RING2 catalytic core of Parkin, leading to displacement of the Ubl domain and it being rendered more accessible for PINK1 phosphorylation (Wauer et al., 2015a, Sauve et al., 2015). These results agree well with the Alphascreen data presented in this chapter (Figure 5.14), which display a loss of interaction between the Ubl domain and ΔUbl Parkin *in trans* upon binding of ubiquitin$^{\text{Phospho-Ser65}}$. The Alphascreen technology could therefore be exploited as a tool for high-throughput screening of Parkin activators; candidate molecules could be screened for their ability to disrupt the *in trans* interaction between the Ubl domain and ΔUbl Parkin, thereby mimicking the effects of phosphorylated ubiquitin.

Immunocytochemistry has been an invaluable tool in studying PINK1-Parkin mitochondrial dynamics in the past as well as in the present. Results displayed in Figure 5.13 confirm the essential role of ubiquitin phosphorylation in Parkin recruitment to the mitochondrial membrane. However, this data also illuminates several other important points: Parkin phosphorylation by PINK1 is highly specific, as no signal could be detected when cells were treated with DMSO and only extremely low levels of signal were observed after CCCP treatment when a Parkin S65A mutant was used. In addition, once the H302A mutant was analysed, I observed that it was still becoming phosphorylated although no retention on the mitochondrial membrane could be detected. This might reflect the decreased binding efficiency between H302A Parkin and ubiquitin$^{\text{Phospho-Ser65}}$ (›250 times lower than wild-type Parkin, Figure 5.9) and therefore a much more transient state of interaction. Alternatively, this could be a result of dynamic Parkin sampling of the mitochondrial surface after PINK1 activation and the lack of the key element required for binding to phosphorylated ubiquitin. Lastly, a very important observation comes from the C431F mutant. Most of the studies analysing Parkin recruitment to the mitochondrial membranes look at the shift in the global cytosolic Parkin levels to a membrane-retained form. However, analysis of the C431F mutant

suggests that this approach is insufficient. While no change in global Parkin distribution of the C431F mutant could be observed when the total Parkin antibody was used (similar to previously published studies (Ordureau et al., 2014, Kane et al., 2014, Koyano et al., 2014, Fiesel et al., 2015)), Parkin$^{Phospho\text{-}Ser65}$ staining reveals a clear cluster of Parkin C431F tethered to the mitochondria. This data raises questions regarding the sequence of events in the Parkin recruitment cascade – while Ordeau and colleagues claim that Parkin activity is a prerequisite for mitochondrial translocation (Ordureau et al., 2014), their interpretation is based on inspection of total Parkin levels. The data presented in Figure 5.13 throw these results into question, since the signal from the catalytically dead phosphorylated Parkin C431F is located exclusively on the mitochondria. It will therefore be extremely important to develop tools that enable the scientific community to look at this signalling cascade in much greater and finer detail – a detailed study on ubiquitin phosphorylation combined with Parkin phosphorylation will need to be conducted in a way that examines these events as they occur in both time and space, which would make it possible to more firmly determine the sequence of events. This finding also raises the question of other E3 ligases present on the mitochondria and their contribution to the signalling cascade. In addition, Okatsu and colleagues have revealed that free ubiquitin can be phosphorylated and diffuse throughout the cell (Okatsu et al., 2015); it will therefore be important to test whether Parkin perhaps gets activated to differing levels in different subcellular locations, and if so, whether this also contributes to the maintenance of cell health in the same way as mitophagy.

Finally, a question as to the distinct function of the two phosphorylation events remains only partially answered. The results presented in the last part of this chapter strongly argue in favour of Parkin phosphorylation being the main E3 ligase activating event (Figure 5.16, Figure 5.17, Figure 5.18, Figure 5.19 & Figure 5.20), in agreement with other reports (Ordureau et al., 2014, Shiba-Fukushima et al., 2014). However, multiple studies have displayed *in vitro* ubiquitin$^{Phospho\text{-}Ser65}$-driven Parkin activation (Kane et al., 2014, Koyano et al., 2014, Kazlauskaite et al., 2014c). The structure of ubiquitin$^{Phospho\text{-}Ser65}$ bound to *Pediculus humanus* Parkin has revealed that while several autoinhibitory surfaces have been dismantled,

the catalytic cysteine remains obscured (Wauer et al., 2015a). It will therefore be important to reconcile these data and reach an in-depth understanding of each contributing factor in this signalling cascade.

6 Appendix

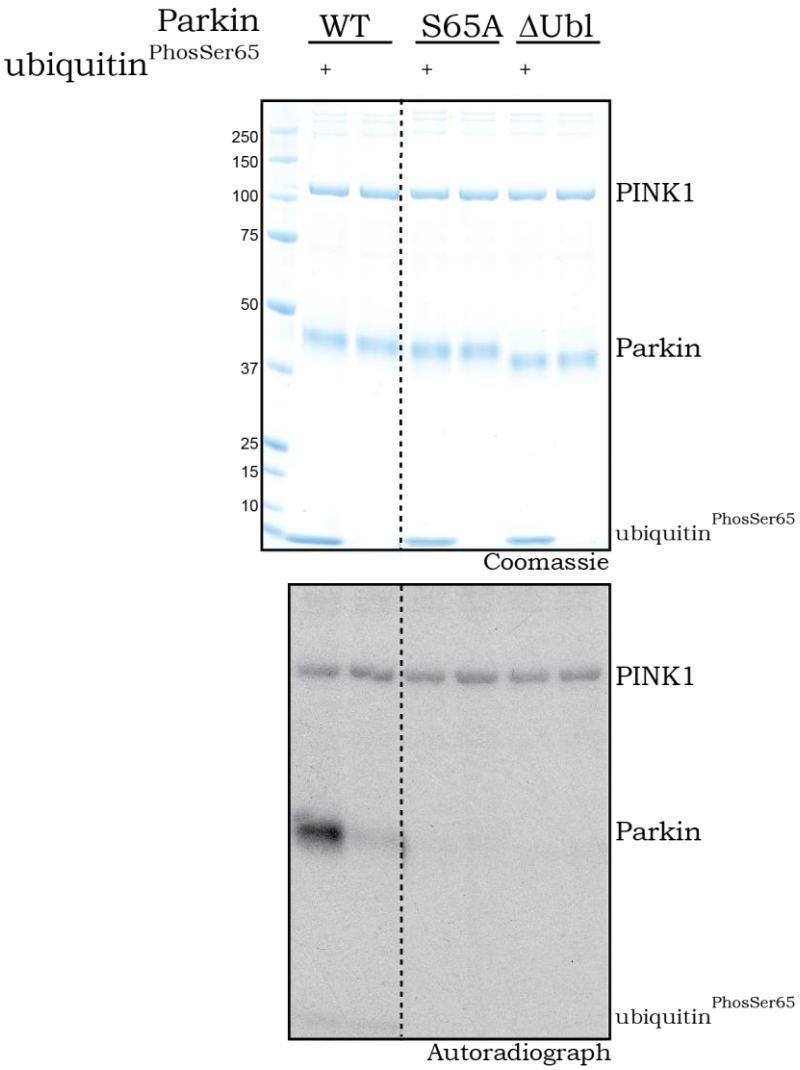

Figure 6.1 Ubiquitin^{PhosphoSer65} specifically promotes Parkin Ser^{65} phosphorylation by PINK1.

The effect of ubiquitin^{PhosphoSer65} on the ability of TcPINK1 to phosphorylate wild-type (WT), S65A, and Ubl-deleted (ΔUbl; residues 80-465) Parkin was investigated in a kinase assay. The indicated Parkin species was incubated with or without ubiquitin^{PhosphoSer65}in a kinase assay analysed by SDS/PAGE. Proteins were detected by Colloidal Coomassie Blue staining (top panel) and incorporation of [γ-^{32}P] ATP was detected by autoradiography (bottom panel).

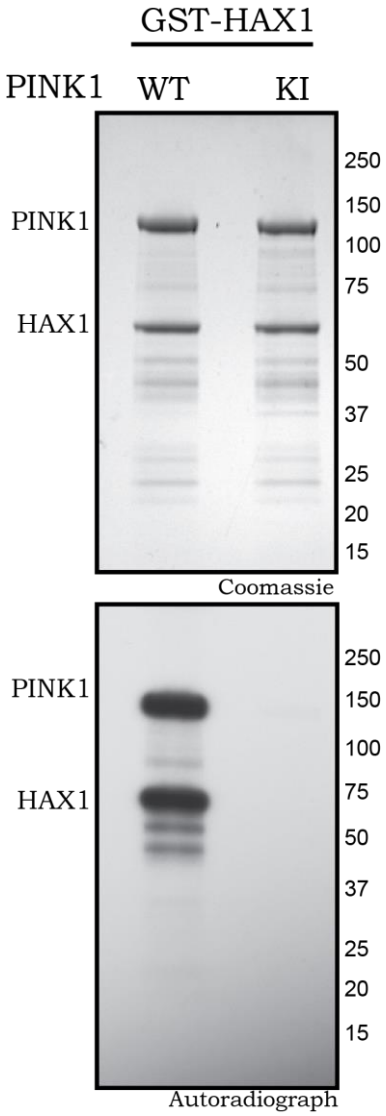

Figure 6.2 The mitochondrial protein HAX1 is phosphorylated by TcPINK1 *in vitro*.

GST-HAX1 (full length) (2 μM) was incubated in the presence of full-length wild-type TcPINK1 (1–570) and kinase inactive TcPINK1 (D359A) and Mg2+ [γ-^{32}P] ATP. Assays were terminated by addition of LDS loading buffer and separated by SDS-PAGE. Proteins were detected by Colloidal Coomassie Blue staining (upper panel) and incorporation of [γ-^{32}P] ATP was detected by autoradiography (lower panel).

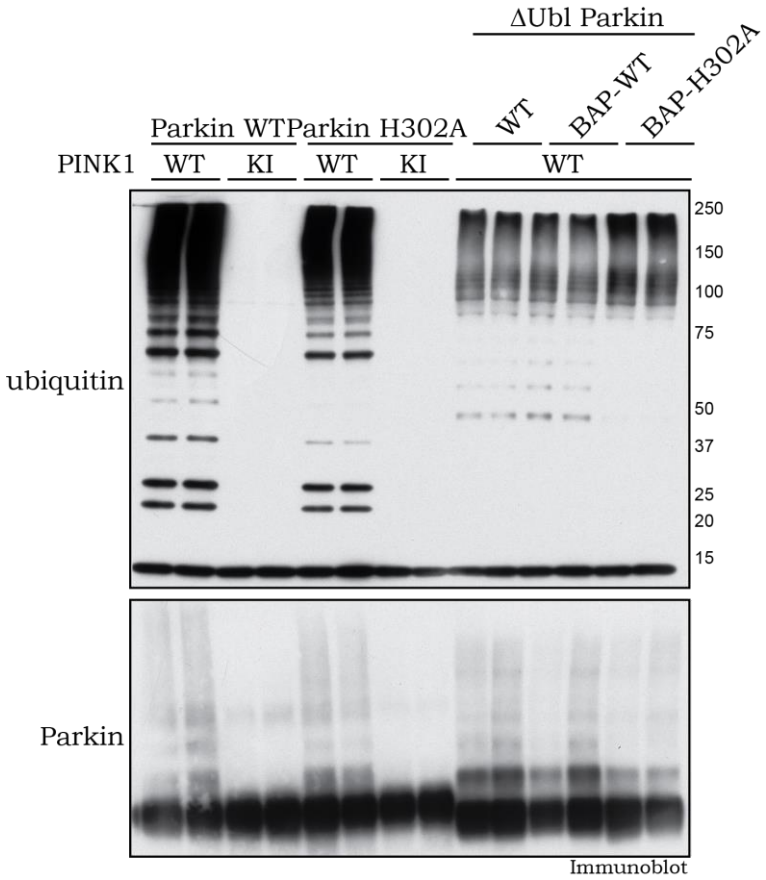

Figure 6.3 Parkin H302A does not disrupt E3 ligase activity

Full-length wild-type (WT), H302A or ΔUbl WT, BAP-tagged WT (BAP-WT) or BAP-tagged H302A (BAP-H302A) Parkin was incubated in presence or absence of wild-type (WT) or kinase-inactive (KI) PINK1 in a kinase reaction as indicated. Ubiquitylation reactions were then initiated by addition of ubiquitylation assay components, including 0.05 mM Flag-ubiquitin. Reactions were analysed by immunoblotting. Ubiquitin and Parkin were detected using anti-FLAG and anti-Parkin antibodies, respectively.

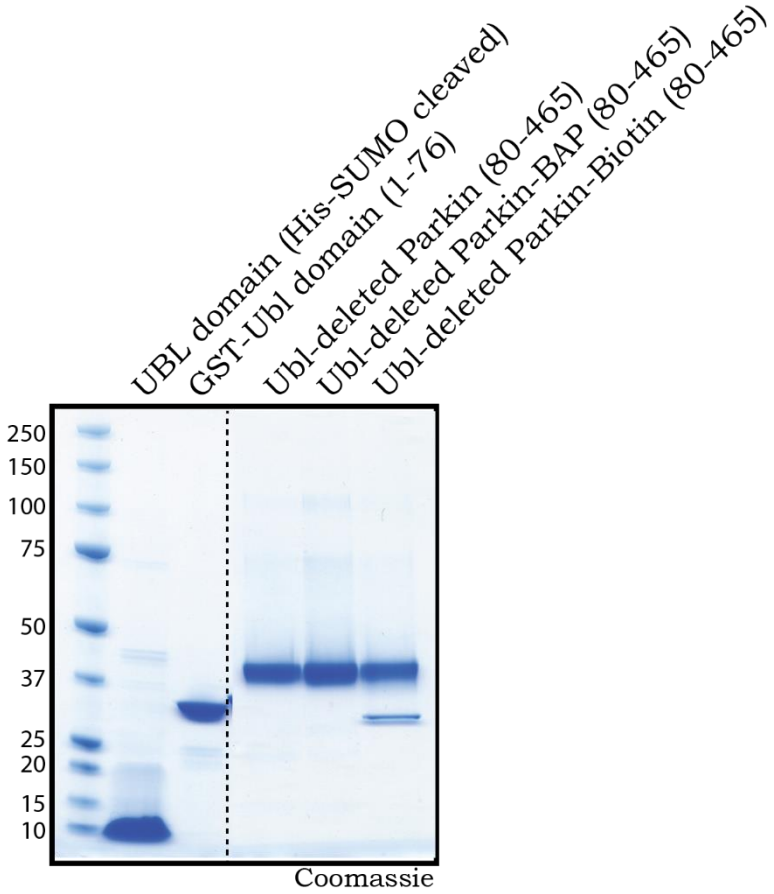

Figure 6.4 Expression of proteins utilised in Alphascreen binding assay.

2µg of the following proteins were analysed by SDS/PAGE and proteins were detected by Colloidal Coomassie Blue. Parkin Ubl (residues 1-76), GST-Parkin Ubl, Parkin (80-465), Parkin (80-465)-biotin affinity peptide (BAP), Parkin (80-465)-biotin.

7 BIBLIOGRAPHY

ABBAS, N., LUCKING, C. B., RICARD, S., DURR, A., BONIFATI, V., DE MICHELE, G., BOULEY, S., VAUGHAN, J. R., GASSER, T., MARCONI, R., BROUSSOLLE, E., BREFEL-COURBON, C., HARHANGI, B. S., OOSTRA, B. A., FABRIZIO, E., BOHME, G. A., PRADIER, L., WOOD, N. W., FILLA, A., MECO, G., DENEFLE, P., AGID, Y. & BRICE, A. 1999. A wide variety of mutations in the parkin gene are responsible for autosomal recessive parkinsonism in Europe. French Parkinson's Disease Genetics Study Group and the European Consortium on Genetic Susceptibility in Parkinson's Disease. *Human molecular genetics,* 8**,** 567-74.

ALLEN, G. F., TOTH, R., JAMES, J. & GANLEY, I. G. 2013. Loss of iron triggers PINK1/Parkin-independent mitophagy. *EMBO reports,* 14**,** 1127-35.

ANDERSON, P. C. & DAGGETT, V. 2008. Molecular basis for the structural instability of human DJ-1 induced by the L166P mutation associated with Parkinson's disease. *Biochemistry,* 47**,** 9380-93.

BEDFORD, L., LOWE, J., DICK, L. R., MAYER, R. J. & BROWNELL, J. E. 2011. Ubiquitin-like protein conjugation and the ubiquitin-proteasome system as drug targets. *Nature reviews. Drug discovery,* 10**,** 29-46.

BEITZ, J. M. 2014. Parkinson's disease: a review. *Front Biosci (Schol Ed),* 6**,** 65-74.

BENNETZEN, M. V., LARSEN, D. H., BUNKENBORG, J., BARTEK, J., LUKAS, J. & ANDERSEN, J. S. 2010. Site-specific phosphorylation dynamics of the nuclear proteome during the DNA damage response. *Molecular & cellular proteomics : MCP,* 9**,** 1314-23.

BERGER, A. K., CORTESE, G. P., AMODEO, K. D., WEIHOFEN, A., LETAI, A. & LAVOIE, M. J. 2009. Parkin selectively alters the intrinsic threshold for mitochondrial cytochrome c release. *Hum Mol Genet,* 18**,** 4317-28.

BERGINK, S. & JENTSCH, S. 2009. Principles of ubiquitin and SUMO modifications in DNA repair. *Nature,* 458**,** 461-7.

BERNDSEN, C. E. & WOLBERGER, C. 2014. New insights into ubiquitin E3 ligase mechanism. *Nat Struct Mol Biol,* 21**,** 301-7.

BERTLER, A. & ROSENGREN, E. 1959. Occurrence and distribution of dopamine in brain and other tissues. *Experientia,* 15**,** 10-1.

BERTONCINI, C. W., JUNG, Y. S., FERNANDEZ, C. O., HOYER, W., GRIESINGER, C., JOVIN, T. M. & ZWECKSTETTER, M. 2005. Release of long-range tertiary interactions potentiates aggregation of natively unstructured alpha-synuclein. *Proc Natl Acad Sci U S A,* 102**,** 1430-5.

BIRKMAYER, W. & HORNYKIEWICZ, O. 1961. [The L-3,4-dioxyphenylalanine (DOPA)-effect in Parkinson-akinesia]. *Wien Klin Wochenschr,* 73**,** 787-8.

BIRSA, N., NORKETT, R., WAUER, T., MEVISSEN, T. E., WU, H. C., FOLTYNIE, T., BHATIA, K., HIRST, W. D., KOMANDER, D., PLUN-FAVREAU, H. & KITTLER, J. T. 2014. Lysine 27 ubiquitination of the mitochondrial transport protein Miro is dependent on serine 65 of the Parkin ubiquitin ligase. *J Biol Chem,* 289**,** 14569-82.

BLASCHKO, H. 1957. Metabolism and storage of biogenic amines. *Experientia,* 13**,** 9-12.

BONIFATI, V., RIZZU, P., VAN BAREN, M. J., SCHAAP, O., BREEDVELD, G. J., KRIEGER, E., DEKKER, M. C., SQUITIERI, F., IBANEZ, P., JOOSSE, M., VAN DONGEN, J. W., VANACORE, N., VAN SWIETEN, J. C., BRICE, A., MECO, G., VAN DUIJN, C. M., OOSTRA, B. A. & HEUTINK, P. 2003. Mutations in the DJ-1 gene associated with autosomal recessive early-onset parkinsonism. *Science,* 299**,** 256-9.

BOWER, J. H., MARAGANORE, D. M., MCDONNELL, S. K. & ROCCA, W. A. 1999. Incidence and distribution of parkinsonism in Olmsted County, Minnesota, 1976-1990. *Neurology,* 52**,** 1214-20.

BRADFORD, M. M. 1976. A rapid and sensitive method for the quantitation of microgram quantities of protein utilizing the principle of protein-dye binding. *Anal Biochem,* 72**,** 248-54.

BRADY, S., SIEGEL, G., ALBERS, R. W. & PRICE, D. 2005. *Basic neurochemistry: molecular, cellular and medical aspects*, Academic Press.

BRANIGAN, E., PLECHANOVOVA, A., JAFFRAY, E. G., NAISMITH, J. H. & HAY, R. T. 2015. Structural basis for the RING-catalyzed synthesis of K63-linked ubiquitin chains. *Nat Struct Mol Biol,* 22**,** 597-602.

BRAS, J., GUERREIRO, R. & HARDY, J. 2015. SnapShot: Genetics of Parkinson's disease. *Cell,* 160**,** 570-570 e1.

BRISSAUD, É. 1895. *Leçons sur les maladies nerveuses*, Masson.

BURCHELL, L., CHAUGULE, V. K. & WALDEN, H. 2012. Small, N-terminal tags activate parkin e3 ubiquitin ligase activity by disrupting its autoinhibited conformation. *PloS one,* 7**,** e34748.

BURNETT, G. & KENNEDY, E. P. 1954. The enzymatic phosphorylation of proteins. *J Biol Chem,* 211**,** 969-80.

CAMPBELL, D. G. & MORRICE, N. A. 2002. Identification of protein phosphorylation sites by a combination of mass spectrometry and solid phase Edman sequencing. *Journal of biomolecular techniques : JBT,* 13**,** 119-30.

CAPDEVILLE, R., SILBERMAN, S. & DIMITRIJEVIC, S. 2002. Imatinib: the first 3 years. *Eur J Cancer,* 38 Suppl 5**,** S77-82.

CARDONA, F., SANCHEZ-MUT, J. V., DOPAZO, H. & PEREZ-TUR, J. 2011. Phylogenetic and in silico structural analysis of the Parkinson disease-related kinase PINK1. *Hum Mutat,* 32**,** 369-78.

CESARI, R., MARTIN, E. S., CALIN, G. A., PENTIMALLI, F., BICHI, R., MCADAMS, H., TRAPASSO, F., DRUSCO, A., SHIMIZU, M., MASCIULLO, V., D'ANDRILLI, G., SCAMBIA, G., PICCHIO, M. C., ALDER, H., GODWIN, A. K. & CROCE, C. M. 2003. Parkin, a gene implicated in autosomal recessive juvenile parkinsonism, is a candidate tumor suppressor gene on chromosome 6q25-q27. *Proc Natl Acad Sci U S A,* 100**,** 5956-61.

CHAUGULE, V. K., BURCHELL, L., BARBER, K. R., SIDHU, A., LESLIE, S. J., SHAW, G. S. & WALDEN, H. 2011. Autoregulation of Parkin activity through its ubiquitin-like domain. *The EMBO journal,* 30**,** 2853-67.

CHEW, K. C., MATSUDA, N., SAISHO, K., LIM, G. G., CHAI, C., TAN, H. M., TANAKA, K. & LIM, K. L. 2011. Parkin mediates apparent E2-independent monoubiquitination in

vitro and contains an intrinsic activity that catalyzes polyubiquitination. *PLoS One,* 6, e19720.

CIEHANOVER, A., HOD, Y. & HERSHKO, A. 1978. A heat-stable polypeptide component of an ATP-dependent proteolytic system from reticulocytes. *Biochem Biophys Res Commun,* 81, 1100-5.

CLARK, I. E., DODSON, M. W., JIANG, C., CAO, J. H., HUH, J. R., SEOL, J. H., YOO, S. J., HAY, B. A. & GUO, M. 2006. Drosophila pink1 is required for mitochondrial function and interacts genetically with parkin. *Nature,* 441, 1162-6.

CLARK, K., NANDA, S. & COHEN, P. 2013. Molecular control of the NEMO family of ubiquitin-binding proteins. *Nature reviews. Molecular cell biology,* 14, 673-85.

COHEN, P. & ALESSI, D. R. 2013. Kinase drug discovery--what's next in the field? *ACS Chem Biol,* 8, 96-104.

COHEN, P. T. 2011. Phosphatase families dephosphorylating serine and threonine residues in proteins. *Transduction Mechanisms in Cellular Signaling*, 105-122.

COOKSON, M. R. 2015. LRRK2 Pathways Leading to Neurodegeneration. *Curr Neurol Neurosci Rep,* 15, 42.

DAWSON, T. M. & DAWSON, V. L. 2010. The role of parkin in familial and sporadic Parkinson's disease. *Movement disorders : official journal of the Movement Disorder Society,* 25 Suppl 1, S32-9.

DEAS, E., PLUN-FAVREAU, H., GANDHI, S., DESMOND, H., KJAER, S., LOH, S. H., RENTON, A. E., HARVEY, R. J., WHITWORTH, A. J., MARTINS, L. M., ABRAMOV, A. Y. & WOOD, N. W. 2011. PINK1 cleavage at position A103 by the mitochondrial protease PARL. *Human molecular genetics,* 20, 867-79.

DESHAIES, R. J. & JOAZEIRO, C. A. 2009. RING domain E3 ubiquitin ligases. *Annual review of biochemistry,* 78, 399-434.

DORSEY, E. R., CONSTANTINESCU, R., THOMPSON, J. P., BIGLAN, K. M., HOLLOWAY, R. G., KIEBURTZ, K., MARSHALL, F. J., RAVINA, B. M., SCHIFITTO, G., SIDEROWF, A. & TANNER, C. M. 2007. Projected number of people with Parkinson disease in the most populous nations, 2005 through 2030. *Neurology,* 68, 384-6.

DOU, H., BUETOW, L., HOCK, A., SIBBET, G. J., VOUSDEN, K. H. & HUANG, D. T. 2012. Structural basis for autoinhibition and phosphorylation-dependent activation of c-Cbl. *Nat Struct Mol Biol,* 19, 184-92.

DUDA, D. M., OLSZEWSKI, J. L., SCHUERMANN, J. P., KURINOV, I., MILLER, D. J., NOURSE, A., ALPI, A. F. & SCHULMAN, B. A. 2013. Structure of HHARI, a RING-IBR-RING Ubiquitin Ligase: Autoinhibition of an Ariadne-Family E3 and Insights into Ligation Mechanism. *Structure,* 21, 1030-41.

EHRINGER, H. & HORNYKIEWICZ, O. 1960. Verteilung Von Noradrenalin Und Dopamin (3-Hydroxytyramin) Im Gehirn Des Menschen Und Ihr Verhalten Bei Erkrankungen Des Extrapyramidalen Systems. *Klinische Wochenschrift,* 38, 1236-1239.

EXNER, N., LUTZ, A. K., HAASS, C. & WINKLHOFER, K. F. 2012. Mitochondrial dysfunction in Parkinson's disease: molecular mechanisms and pathophysiological consequences. *EMBO J,* 31, 3038-62.

FARRER, M., CHAN, P., CHEN, R., TAN, L., LINCOLN, S., HERNANDEZ, D., FORNO, L., GWINN-HARDY, K., PETRUCELLI, L., HUSSEY, J., SINGLETON, A., TANNER, C., HARDY, J. & LANGSTON, J. W. 2001. Lewy bodies and parkinsonism in families with parkin mutations. *Annals of neurology,* 50**,** 293-300.

FARRIOL-MATHIS, N., GARAVELLI, J. S., BOECKMANN, B., DUVAUD, S., GASTEIGER, E., GATEAU, A., VEUTHEY, A. L. & BAIROCH, A. 2004. Annotation of post-translational modifications in the Swiss-Prot knowledge base. *Proteomics,* 4**,** 1537-50.

FIESEL, F. C., CAULFIELD, T. R., MOUSSAUD-LAMODIERE, E. L., OGAKI, K., DOURADO, D. F., FLORES, S. C., ROSS, O. A. & SPRINGER, W. 2015. Structural and Functional Impact of Parkinson Disease-Associated Mutations in the E3 Ubiquitin Ligase Parkin. *Hum Mutat,* 36**,** 774-86.

FINLEY, D., CIECHANOVER, A. & VARSHAVSKY, A. 2004. Ubiquitin as a central cellular regulator. *Cell,* 116**,** S29-32, 2 p following S32.

FORNO, L. S. 1996. Neuropathology of Parkinson's disease. *Journal of neuropathology and experimental neurology,* 55**,** 259-72.

FORTIER, C., DE CRESCENZO, G. & DUROCHER, Y. 2013. A versatile coiled-coil tethering system for the oriented display of ligands on nanocarriers for targeted gene delivery. *Biomaterials,* 34**,** 1344-53.

FROYEN, G., CORBETT, M., VANDEWALLE, J., JARVELA, I., LAWRENCE, O., MELDRUM, C., BAUTERS, M., GOVAERTS, K., VANDELEUR, L., VAN ESCH, H., CHELLY, J., SANLAVILLE, D., VAN BOKHOVEN, H., ROPERS, H. H., LAUMONNIER, F., RANIERI, E., SCHWARTZ, C. E., ABIDI, F., TARPEY, P. S., FUTREAL, P. A., WHIBLEY, A., RAYMOND, F. L., STRATTON, M. R., FRYNS, J. P., SCOTT, R., PEIPPO, M., SIPPONEN, M., PARTINGTON, M., MOWAT, D., FIELD, M., HACKETT, A., MARYNEN, P., TURNER, G. & GECZ, J. 2008. Submicroscopic duplications of the hydroxysteroid dehydrogenase HSD17B10 and the E3 ubiquitin ligase HUWE1 are associated with mental retardation. *Am J Hum Genet,* 82**,** 432-43.

FUCHS, J., NILSSON, C., KACHERGUS, J., MUNZ, M., LARSSON, E. M., SCHULE, B., LANGSTON, J. W., MIDDLETON, F. A., ROSS, O. A., HULIHAN, M., GASSER, T. & FARRER, M. J. 2007. Phenotypic variation in a large Swedish pedigree due to SNCA duplication and triplication. *Neurology,* 68**,** 916-22.

FUTREAL, P. A., LIU, Q., SHATTUCK-EIDENS, D., COCHRAN, C., HARSHMAN, K., TAVTIGIAN, S., BENNETT, L. M., HAUGEN-STRANO, A., SWENSEN, J., MIKI, Y. & ET AL. 1994. BRCA1 mutations in primary breast and ovarian carcinomas. *Science,* 266**,** 120-2.

GALLAGHER, E., GAO, M., LIU, Y. C. & KARIN, M. 2006. Activation of the E3 ubiquitin ligase Itch through a phosphorylation-induced conformational change. *Proc Natl Acad Sci U S A,* 103**,** 1717-22.

GEISLER, S., HOLMSTROM, K. M., SKUJAT, D., FIESEL, F. C., ROTHFUSS, O. C., KAHLE, P. J. & SPRINGER, W. 2010. PINK1/Parkin-mediated mitophagy is dependent on VDAC1 and p62/SQSTM1. *Nature cell biology,* 12**,** 119-31.

GOLDKNOPF, I. L. & BUSCH, H. 1977. Isopeptide linkage between nonhistone and histone 2A polypeptides of chromosomal conjugate-protein A24. *Proc Natl Acad Sci U S A,* 74**,** 864-8.

GOLDSTEIN, G., SCHEID, M., HAMMERLING, U., SCHLESINGER, D. H., NIALL, H. D. & BOYSE, E. A. 1975. Isolation of a polypeptide that has lymphocyte-differentiating

properties and is probably represented universally in living cells. *Proc Natl Acad Sci U S A,* 72**,** 11-5.

GREENE, A. W., GRENIER, K., AGUILETA, M. A., MUISE, S., FARAZIFARD, R., HAQUE, M. E., MCBRIDE, H. M., PARK, D. S. & FON, E. A. 2012. Mitochondrial processing peptidase regulates PINK1 processing, import and Parkin recruitment. *EMBO Rep,* 13**,** 378-85.

GREENE, J. C., WHITWORTH, A. J., KUO, I., ANDREWS, L. A., FEANY, M. B. & PALLANCK, L. J. 2003. Mitochondrial pathology and apoptotic muscle degeneration in Drosophila parkin mutants. *Proc Natl Acad Sci U S A,* 100**,** 4078-83.

GU, T. L., DENG, X., HUANG, F., TUCKER, M., CROSBY, K., RIMKUNAS, V., WANG, Y., DENG, G., ZHU, L., TAN, Z., HU, Y., WU, C., NARDONE, J., MACNEILL, J., REN, J., REEVES, C., INNOCENTI, G., NORRIS, B., YUAN, J., YU, J., HAACK, H., SHEN, B., PENG, C., LI, H., ZHOU, X., LIU, X., RUSH, J. & COMB, M. J. 2011. Survey of tyrosine kinase signaling reveals ROS kinase fusions in human cholangiocarcinoma. *PloS one,* 6**,** e15640.

GU, W. J., CORTI, O., ARAUJO, F., HAMPE, C., JACQUIER, S., LUCKING, C. B., ABBAS, N., DUYCKAERTS, C., ROONEY, T., PRADIER, L., RUBERG, M. & BRICE, A. 2003. The C289G and C418R missense mutations cause rapid sequestration of human Parkin into insoluble aggregates. *Neurobiology of disease,* 14**,** 357-64.

HAAS, A. L., WARMS, J. V., HERSHKO, A. & ROSE, I. A. 1982. Ubiquitin-activating enzyme. Mechanism and role in protein-ubiquitin conjugation. *J Biol Chem,* 257**,** 2543-8.

HALL, J. M., LEE, M. K., NEWMAN, B., MORROW, J. E., ANDERSON, L. A., HUEY, B. & KING, M. C. 1990. Linkage of early-onset familial breast cancer to chromosome 17q21. *Science,* 250**,** 1684-9.

HAMACHER-BRADY, A. & BRADY, N. R. 2015. Mitophagy programs: mechanisms and physiological implications of mitochondrial targeting by autophagy. *Cell Mol Life Sci*.

HAMPE, C., ARDILA-OSORIO, H., FOURNIER, M., BRICE, A. & CORTI, O. 2006. Biochemical analysis of Parkinson's disease-causing variants of Parkin, an E3 ubiquitin-protein ligase with monoubiquitylation capacity. *Human molecular genetics,* 15**,** 2059-75.

HAN, C., PAO, K. C., KAZLAUSKAITE, A., MUQIT, M. M. & VIRDEE, S. 2015. A Versatile Strategy for the Semisynthetic Production of Ser65 Phosphorylated Ubiquitin and Its Biochemical and Structural Characterisation. *Chembiochem*.

HARDY, J., CAI, H., COOKSON, M. R., GWINN-HARDY, K. & SINGLETON, A. 2006. Genetics of Parkinson's disease and parkinsonism. *Ann Neurol,* 60**,** 389-98.

HASHIZUME, R., FUKUDA, M., MAEDA, I., NISHIKAWA, H., OYAKE, D., YABUKI, Y., OGATA, H. & OHTA, T. 2001. The RING heterodimer BRCA1-BARD1 is a ubiquitin ligase inactivated by a breast cancer-derived mutation. *J Biol Chem,* 276**,** 14537-40.

HEDRICH, K., ESKELSON, C., WILMOT, B., MARDER, K., HARRIS, J., GARRELS, J., MEIJA-SANTANA, H., VIEREGGE, P., JACOBS, H., BRESSMAN, S. B., LANG, A. E., KANN, M., ABBRUZZESE, G., MARTINELLI, P., SCHWINGER, E., OZELIUS, L. J., PRAMSTALLER, P. P., KLEIN, C. & KRAMER, P. 2004. Distribution, type, and origin of Parkin mutations: review and case studies. *Movement disorders : official journal of the Movement Disorder Society,* 19**,** 1146-57.

HENN, I. H., GOSTNER, J. M., LACKNER, P., TATZELT, J. & WINKLHOFER, K. F. 2005. Pathogenic mutations inactivate parkin by distinct mechanisms. *Journal of neurochemistry,* 92**,** 114-22.

HEO, J. M., ORDUREAU, A., PAULO, J. A., RINEHART, J. & HARPER, J. W. 2015. The PINK1-PARKIN Mitochondrial Ubiquitylation Pathway Drives a Program of OPTN/NDP52 Recruitment and TBK1 Activation to Promote Mitophagy. *Mol Cell*.

HICKE, L. 2001. Protein regulation by monoubiquitin. *Nature reviews. Molecular cell biology,* 2**,** 195-201.

HICKE, L., SCHUBERT, H. L. & HILL, C. P. 2005. Ubiquitin-binding domains. *Nat Rev Mol Cell Biol,* 6**,** 610-21.

HJERPE, R., AILLET, F., LOPITZ-OTSOA, F., LANG, V., ENGLAND, P. & RODRIGUEZ, M. S. 2009. Efficient protection and isolation of ubiquitylated proteins using tandem ubiquitin-binding entities. *EMBO Rep,* 10**,** 1250-8.

HOCHSTRASSER, M. 2009. Origin and function of ubiquitin-like proteins. *Nature,* 458**,** 422-9.

HUSNJAK, K. & DIKIC, I. 2012. Ubiquitin-binding proteins: decoders of ubiquitin-mediated cellular functions. *Annual review of biochemistry,* 81**,** 291-322.

IBANEZ, P., BONNET, A. M., DEBARGES, B., LOHMANN, E., TISON, F., POLLAK, P., AGID, Y., DURR, A. & BRICE, A. 2004. Causal relation between alpha-synuclein gene duplication and familial Parkinson's disease. *Lancet,* 364**,** 1169-71.

IGUCHI, M., KUJURO, Y., OKATSU, K., KOYANO, F., KOSAKO, H., KIMURA, M., SUZUKI, N., UCHIYAMA, S., TANAKA, K. & MATSUDA, N. 2013. Parkin catalyzed ubiquitin-ester transfer is triggered by PINK1-dependent phosphorylation. *The Journal of biological chemistry*.

IMAI, Y., SODA, M., HATAKEYAMA, S., AKAGI, T., HASHIKAWA, T., NAKAYAMA, K. I. & TAKAHASHI, R. 2002. CHIP is associated with Parkin, a gene responsible for familial Parkinson's disease, and enhances its ubiquitin ligase activity. *Molecular cell,* 10**,** 55-67.

INOUE, H., NOJIMA, H. & OKAYAMA, H. 1990. High efficiency transformation of Escherichia coli with plasmids. *Gene,* 96**,** 23-8.

JALEEL, M., NICHOLS, R. J., DEAK, M., CAMPBELL, D. G., GILLARDON, F., KNEBEL, A. & ALESSI, D. R. 2007. LRRK2 phosphorylates moesin at threonine-558: characterization of how Parkinson's disease mutants affect kinase activity. *Biochem J,* 405**,** 307-17.

JIN, J., LI, X., GYGI, S. P. & HARPER, J. W. 2007. Dual E1 activation systems for ubiquitin differentially regulate E2 enzyme charging. *Nature,* 447**,** 1135-8.

JIN, S. M., LAZAROU, M., WANG, C., KANE, L. A., NARENDRA, D. P. & YOULE, R. J. 2010. Mitochondrial membrane potential regulates PINK1 import and proteolytic destabilization by PARL. *The Journal of cell biology,* 191**,** 933-42.

JOHNSON, L. N. & LEWIS, R. J. 2001. Structural basis for control by phosphorylation. *Chem Rev,* 101**,** 2209-42.

KAMADURAI, H. B., QIU, Y., DENG, A., HARRISON, J. S., MACDONALD, C., ACTIS, M., RODRIGUES, P., MILLER, D. J., SOUPHRON, J., LEWIS, S. M., KURINOV, I., FUJII, N., HAMMEL, M., PIPER, R., KUHLMAN, B. & SCHULMAN, B. A. 2013. Mechanism of ubiquitin ligation and lysine prioritization by a HECT E3. *Elife,* 2**,** e00828.

KANE, L. A., LAZAROU, M., FOGEL, A. I., LI, Y., YAMANO, K., SARRAF, S. A., BANERJEE, S. & YOULE, R. J. 2014. PINK1 phosphorylates ubiquitin to activate Parkin E3 ubiquitin ligase activity. *The Journal of cell biology,* 205**,** 143-53.

KARIN, M. & BEN-NERIAH, Y. 2000. Phosphorylation meets ubiquitination: the control of NF-[kappa]B activity. *Annu Rev Immunol,* 18**,** 621-63.

KAZLAUSKAITE, A., KELLY, V., JOHNSON, C., BAILLIE, C., HASTIE, C. J., PEGGIE, M., MACARTNEY, T., WOODROOF, H. I., ALESSI, D. R., PEDRIOLI, P. G. & MUQIT, M. M. 2014a. Phosphorylation of Parkin at Serine65 is essential for activation: elaboration of a Miro1 substrate-based assay of Parkin E3 ligase activity. *Open Biol,* 4**,** 130213.

KAZLAUSKAITE, A., KELLY, V., JOHNSON, C., BAILLIE, C., HASTIE, C. J., PEGGIE, M., MACARTNEY, T., WOODROOF, H. I., ALESSI, D. R., PEDRIOLI, P. G. & MUQIT, M. M. 2014b. Phosphorylation of Parkin at Serine65 is essential for activation: elaboration of a Miro1 substrate-based assay of Parkin E3 ligase activity. *Open biology,* 4**,** 130213.

KAZLAUSKAITE, A., KONDAPALLI, C., GOURLAY, R., CAMPBELL, D. G., RITORTO, M. S., HOFMANN, K., ALESSI, D. R., KNEBEL, A., TROST, M. & MUQIT, M. M. 2014c. Parkin is activated by PINK1-dependent phosphorylation of ubiquitin at Ser65. *Biochem J,* 460**,** 127-39.

KEENEY, P. M., XIE, J., CAPALDI, R. A. & BENNETT, J. P., JR. 2006. Parkinson's disease brain mitochondrial complex I has oxidatively damaged subunits and is functionally impaired and misassembled. *J Neurosci,* 26**,** 5256-64.

KENTSIS, A., GORDON, R. E. & BORDEN, K. L. 2002. Control of biochemical reactions through supramolecular RING domain self-assembly. *Proc Natl Acad Sci U S A,* 99**,** 15404-9.

KHAN, N. L., VALENTE, E. M., BENTIVOGLIO, A. R., WOOD, N. W., ALBANESE, A., BROOKS, D. J. & PICCINI, P. 2002. Clinical and subclinical dopaminergic dysfunction in PARK6-linked parkinsonism: an 18F-dopa PET study. *Annals of neurology,* 52**,** 849-53.

KHOURY, G. A., BALIBAN, R. C. & FLOUDAS, C. A. 2011. Proteome-wide post-translational modification statistics: frequency analysis and curation of the swiss-prot database. *Sci Rep,* 1.

KIM, H. T., KIM, K. P., LLEDIAS, F., KISSELEV, A. F., SCAGLIONE, K. M., SKOWYRA, D., GYGI, S. P. & GOLDBERG, A. L. 2007. Certain pairs of ubiquitin-conjugating enzymes (E2s) and ubiquitin-protein ligases (E3s) synthesize nondegradable forked ubiquitin chains containing all possible isopeptide linkages. *J Biol Chem,* 282**,** 17375-86.

KIMURA, Y. & TANAKA, K. 2010. Regulatory mechanisms involved in the control of ubiquitin homeostasis. *J Biochem,* 147**,** 793-8.

KISHINO, T., LALANDE, M. & WAGSTAFF, J. 1997. UBE3A/E6-AP mutations cause Angelman syndrome. *Nat Genet,* 15**,** 70-3.

KITADA, T., ASAKAWA, S., HATTORI, N., MATSUMINE, H., YAMAMURA, Y., MINOSHIMA, S., YOKOCHI, M., MIZUNO, Y. & SHIMIZU, N. 1998. Mutations in the parkin gene cause autosomal recessive juvenile parkinsonism. *Nature,* 392**,** 605-8.

KLEIN, C. & WESTENBERGER, A. 2012. Genetics of Parkinson's disease. *Cold Spring Harb Perspect Med,* 2**,** a008888.

KLOSOWIAK, J. L., FOCIA, P. J., CHAKRAVARTHY, S., LANDAHL, E. C., FREYMANN, D. M. & RICE, S. E. 2013. Structural coupling of the EF hand and C-terminal GTPase domains in the mitochondrial protein Miro. *EMBO Rep,* 14**,** 968-74.

KOMANDER, D. & RAPE, M. 2012. The ubiquitin code. *Annu Rev Biochem,* 81**,** 203-29.

KONDAPALLI, C., KAZLAUSKAITE, A., ZHANG, N., WOODROOF, H. I., CAMPBELL, D. G., GOURLAY, R., BURCHELL, L., WALDEN, H., MACARTNEY, T. J., DEAK, M., KNEBEL, A., ALESSI, D. R. & MUQIT, M. M. 2012. PINK1 is activated by mitochondrial membrane potential depolarization and stimulates Parkin E3 ligase activity by phosphorylating Serine 65. *Open Biol,* 2**,** 120080.

KOYANO, F., OKATSU, K., ISHIGAKI, S., FUJIOKA, Y., KIMURA, M., SOBUE, G., TANAKA, K. & MATSUDA, N. 2013. The principal PINK1 and Parkin cellular events triggered in response to dissipation of mitochondrial membrane potential occur in primary neurons. *Genes to cells : devoted to molecular & cellular mechanisms*.

KOYANO, F., OKATSU, K., KOSAKO, H., TAMURA, Y., GO, E., KIMURA, M., KIMURA, Y., TSUCHIYA, H., YOSHIHARA, H., HIROKAWA, T., ENDO, T., FON, E. A., TREMPE, J. F., SAEKI, Y., TANAKA, K. & MATSUDA, N. 2014. Ubiquitin is phosphorylated by PINK1 to activate parkin. *Nature,* 510**,** 162-6.

KREEGIPUU, A., BLOM, N. & BRUNAK, S. 1999. PhosphoBase, a database of phosphorylation sites: release 2.0. *Nucleic Acids Res,* 27**,** 237-9.

KRISTARIYANTO, Y. A., ABDUL REHMAN, S. A., CAMPBELL, D. G., MORRICE, N. A., JOHNSON, C., TOTH, R. & KULATHU, Y. 2015a. K29-selective ubiquitin binding domain reveals structural basis of specificity and heterotypic nature of k29 polyubiquitin. *Mol Cell,* 58**,** 83-94.

KRISTARIYANTO, Y. A., CHOI, S. Y., REHMAN, S. A., RITORTO, M. S., CAMPBELL, D. G., MORRICE, N. A., TOTH, R. & KULATHU, Y. 2015b. Assembly and structure of Lys33-linked polyubiquitin reveals distinct conformations. *Biochem J,* 467**,** 345-52.

KUHN, T. S. 1962. The structure of scientific revolutions.

KULATHU, Y. & KOMANDER, D. 2012. Atypical ubiquitylation - the unexplored world of polyubiquitin beyond Lys48 and Lys63 linkages. *Nat Rev Mol Cell Biol,* 13**,** 508-23.

KUMAR, A., AGUIRRE, J. D., CONDOS, T. E., MARTINEZ-TORRES, R. J., CHAUGULE, V. K., TOTH, R., SUNDARAMOORTHY, R., MERCIER, P., KNEBEL, A., SPRATT, D. E., BARBER, K. R., SHAW, G. S. & WALDEN, H. 2015. Disruption of the autoinhibited state primes the E3 ligase parkin for activation and catalysis. *EMBO J.*

LAHIRY, P., TORKAMANI, A., SCHORK, N. J. & HEGELE, R. A. 2010. Kinase mutations in human disease: interpreting genotype–phenotype relationships. *Nature Reviews Genetics,* 11**,** 60-74.

LANGSTON, J. W., BALLARD, P., TETRUD, J. W. & IRWIN, I. 1983. Chronic Parkinsonism in humans due to a product of meperidine-analog synthesis. *Science,* 219**,** 979-80.

LAZAROU, M., JIN, S. M., KANE, L. A. & YOULE, R. J. 2012. Role of PINK1 binding to the TOM complex and alternate intracellular membranes in recruitment and activation of the E3 ligase Parkin. *Developmental cell,* 22**,** 320-33.

LAZAROU, M., NARENDRA, D. P., JIN, S. M., TEKLE, E., BANERJEE, S. & YOULE, R. J. 2013. PINK1 drives Parkin self-association and HECT-like E3 activity upstream of mitochondrial binding. *The Journal of cell biology,* 200**,** 163-72.

LAZAROU, M., SLITER, D. A., KANE, L. A., SARRAF, S. A., WANG, C., BURMAN, J. L., SIDERIS, D. P., FOGEL, A. I. & YOULE, R. J. 2015. The ubiquitin kinase PINK1 recruits autophagy receptors to induce mitophagy. *Nature,* 524**,** 309-14.

LEE, D. W., PEGGIE, M., DEAK, M., TOTH, R., GAGE, Z. O., WOOD, N., SCHILDE, C., KURZ, T. & KNEBEL, A. 2012a. The Dac-tag, an affinity tag based on penicillin-binding protein 5. *Anal Biochem,* 428**,** 64-72.

LEE, D. W., PEGGIE, M., DEAK, M., TOTH, R., GAGE, Z. O., WOOD, N., SCHILDE, C., KURZ, T. & KNEBEL, A. 2012b. The Dac-tag, an affinity tag based on penicillin-binding protein 5. *Analytical biochemistry,* 428**,** 64-72.

LEE, H. J., NA, K., KWON, M. S., KIM, H., KIM, K. S. & PAIK, Y. K. 2009. Quantitative analysis of phosphopeptides in search of the disease biomarker from the hepatocellular carcinoma specimen. *Proteomics,* 9**,** 3395-408.

LESAGE, S., ANHEIM, M., LETOURNEL, F., BOUSSET, L., HONORE, A., ROZAS, N., PIERI, L., MADIONA, K., DURR, A., MELKI, R., VERNY, C., BRICE, A. & FRENCH PARKINSON'S DISEASE GENETICS STUDY, G. 2013. G51D alpha-synuclein mutation causes a novel parkinsonian-pyramidal syndrome. *Ann Neurol,* 73**,** 459-71.

LEWY, F. 1912. Handbuch der Neurologie. *Handbuch Der Neurologie,* 3.

LI, W., BENGTSON, M. H., ULBRICH, A., MATSUDA, A., REDDY, V. A., ORTH, A., CHANDA, S. K., BATALOV, S. & JOAZEIRO, C. A. 2008. Genome-wide and functional annotation of human E3 ubiquitin ligases identifies MULAN, a mitochondrial E3 that regulates the organelle's dynamics and signaling. *PLoS One,* 3**,** e1487.

LIM, K. L., CHEW, K. C., TAN, J. M., WANG, C., CHUNG, K. K., ZHANG, Y., TANAKA, Y., SMITH, W., ENGELENDER, S., ROSS, C. A., DAWSON, V. L. & DAWSON, T. M. 2005. Parkin mediates nonclassical, proteasomal-independent ubiquitination of synphilin-1: implications for Lewy body formation. *J Neurosci,* 25**,** 2002-9.

LIN, H. K., WANG, L., HU, Y. C., ALTUWAIJRI, S. & CHANG, C. 2002. Phosphorylation-dependent ubiquitylation and degradation of androgen receptor by Akt require Mdm2 E3 ligase. *EMBO J,* 21**,** 4037-48.

LIN, W. & KANG, U. J. 2008. Characterization of PINK1 processing, stability, and subcellular localization. *Journal of neurochemistry,* 106**,** 464-74.

LIU, S., SAWADA, T., LEE, S., YU, W., SILVERIO, G., ALAPATT, P., MILLAN, I., SHEN, A., SAXTON, W., KANAO, T., TAKAHASHI, R., HATTORI, N., IMAI, Y. & LU, B. 2012. Parkinson's disease-associated kinase PINK1 regulates Miro protein level and axonal transport of mitochondria. *PLoS genetics,* 8**,** e1002537.

LUCKING, C. B., DURR, A., BONIFATI, V., VAUGHAN, J., DE MICHELE, G., GASSER, T., HARHANGI, B. S., MECO, G., DENEFLE, P., WOOD, N. W., AGID, Y. & BRICE, A. 2000. Association between early-onset Parkinson's disease and mutations in the parkin gene. *The New England journal of medicine,* 342**,** 1560-7.

MACASKILL, A. F., RINHOLM, J. E., TWELVETREES, A. E., ARANCIBIA-CARCAMO, I. L., MUIR, J., FRANSSON, A., ASPENSTROM, P., ATTWELL, D. & KITTLER, J. T. 2009. Miro1 is a calcium sensor for glutamate receptor-dependent localization of mitochondria at synapses. *Neuron,* 61**,** 541-55.

MACE, P. D., LINKE, K., FELTHAM, R., SCHUMACHER, F. R., SMITH, C. A., VAUX, D. L., SILKE, J. & DAY, C. L. 2008. Structures of the cIAP2 RING domain reveal conformational changes associated with ubiquitin-conjugating enzyme (E2) recruitment. *J Biol Chem,* 283**,** 31633-40.

MACLEAN, B., TOMAZELA, D. M., SHULMAN, N., CHAMBERS, M., FINNEY, G. L., FREWEN, B., KERN, R., TABB, D. L., LIEBLER, D. C. & MACCOSS, M. J. 2010.

Skyline: an open source document editor for creating and analyzing targeted proteomics experiments. *Bioinformatics,* 26**,** 966-8.

MALIK, R., LENOBEL, R., SANTAMARIA, A., RIES, A., NIGG, E. A. & KORNER, R. 2009. Quantitative analysis of the human spindle phosphoproteome at distinct mitotic stages. *Journal of proteome research,* 8**,** 4553-63.

MANES, N. P., DONG, L., ZHOU, W., DU, X., REGHU, N., KOOL, A. C., CHOI, D., BAILEY, C. L., PETRICOIN, E. F., 3RD, LIOTTA, L. A. & POPOV, S. G. 2011. Discovery of mouse spleen signaling responses to anthrax using label-free quantitative phosphoproteomics via mass spectrometry. *Mol Cell Proteomics,* 10**,** M110 000927.

MANNING, G., WHYTE, D. B., MARTINEZ, R., HUNTER, T. & SUDARSANAM, S. 2002. The protein kinase complement of the human genome. *Science,* 298**,** 1912-34.

MATSUDA, N., KITAMI, T., SUZUKI, T., MIZUNO, Y., HATTORI, N. & TANAKA, K. 2006. Diverse effects of pathogenic mutations of Parkin that catalyze multiple monoubiquitylation in vitro. *The Journal of biological chemistry,* 281**,** 3204-9.

MATSUDA, N., SATO, S., SHIBA, K., OKATSU, K., SAISHO, K., GAUTIER, C. A., SOU, Y. S., SAIKI, S., KAWAJIRI, S., SATO, F., KIMURA, M., KOMATSU, M., HATTORI, N. & TANAKA, K. 2010. PINK1 stabilized by mitochondrial depolarization recruits Parkin to damaged mitochondria and activates latent Parkin for mitophagy. *The Journal of cell biology,* 189**,** 211-21.

MEISSNER, C., LORENZ, H., WEIHOFEN, A., SELKOE, D. J. & LEMBERG, M. K. 2011. The mitochondrial intramembrane protease PARL cleaves human Pink1 to regulate Pink1 trafficking. *Journal of neurochemistry,* 117**,** 856-67.

METZGER, M. B., PRUNEDA, J. N., KLEVIT, R. E. & WEISSMAN, A. M. 2013. RING-type E3 ligases: Master manipulators of E2 ubiquitin-conjugating enzymes and ubiquitination. *Biochimica et biophysica acta*.

MODEL, K., PRINZ, T., RUIZ, T., RADERMACHER, M., KRIMMER, T., KUHLBRANDT, W., PFANNER, N. & MEISINGER, C. 2002. Protein translocase of the outer mitochondrial membrane: role of import receptors in the structural organization of the TOM complex. *J Mol Biol,* 316**,** 657-66.

MOORE, D. J. 2006. Parkin: a multifaceted ubiquitin ligase. *Biochem Soc Trans,* 34**,** 749-53.

NARENDRA, D., TANAKA, A., SUEN, D. F. & YOULE, R. J. 2008. Parkin is recruited selectively to impaired mitochondria and promotes their autophagy. *The Journal of cell biology,* 183**,** 795-803.

NARENDRA, D. P., JIN, S. M., TANAKA, A., SUEN, D. F., GAUTIER, C. A., SHEN, J., COOKSON, M. R. & YOULE, R. J. 2010. PINK1 is selectively stabilized on impaired mitochondria to activate Parkin. *PLoS biology,* 8**,** e1000298.

NARENDRA, D. P., WANG, C., YOULE, R. J. & WALKER, J. E. 2013a. PINK1 rendered temperature sensitive by disease-associated and engineered mutations. *Human molecular genetics,* 22**,** 2572-89.

NARENDRA, D. P., WANG, C., YOULE, R. J. & WALKER, J. E. 2013b. PINK1 rendered temperature sensitive by disease-associated and engineered mutations. *Hum Mol Genet,* 22**,** 2572-89.

NARHI, L., WOOD, S. J., STEAVENSON, S., JIANG, Y., WU, G. M., ANAFI, D., KAUFMAN, S. A., MARTIN, F., SITNEY, K., DENIS, P., LOUIS, J. C., WYPYCH, J., BIERE, A.

L. & CITRON, M. 1999. Both familial Parkinson's disease mutations accelerate alpha-synuclein aggregation. *J Biol Chem,* 274**,** 9843-6.

NASCIMENTO, R. M., OTTO, P. A., DE BROUWER, A. P. & VIANNA-MORGANTE, A. M. 2006. UBE2A, which encodes a ubiquitin-conjugating enzyme, is mutated in a novel X-linked mental retardation syndrome. *Am J Hum Genet,* 79**,** 549-55.

NGUYEN, L. K., KOLCH, W. & KHOLODENKO, B. N. 2013. When ubiquitination meets phosphorylation: a systems biology perspective of EGFR/MAPK signalling. *Cell Commun Signal,* 11**,** 52.

NICKLAS, W. J., VYAS, I. & HEIKKILA, R. E. 1985. Inhibition of NADH-linked oxidation in brain mitochondria by 1-methyl-4-phenyl-pyridine, a metabolite of the neurotoxin, 1-methyl-4-phenyl-1,2,5,6-tetrahydropyridine. *Life sciences,* 36**,** 2503-8.

OKATSU, K., KOYANO, F., KIMURA, M., KOSAKO, H., SAEKI, Y., TANAKA, K. & MATSUDA, N. 2015. Phosphorylated ubiquitin chain is the genuine Parkin receptor. *J Cell Biol,* 209**,** 111-28.

OKATSU, K., OKA, T., IGUCHI, M., IMAMURA, K., KOSAKO, H., TANI, N., KIMURA, M., GO, E., KOYANO, F., FUNAYAMA, M., SHIBA-FUKUSHIMA, K., SATO, S., SHIMIZU, H., FUKUNAGA, Y., TANIGUCHI, H., KOMATSU, M., HATTORI, N., MIHARA, K., TANAKA, K. & MATSUDA, N. 2012. PINK1 autophosphorylation upon membrane potential dissipation is essential for Parkin recruitment to damaged mitochondria. *Nature communications,* 3**,** 1016.

ORDUREAU, A., SARRAF, S. A., DUDA, D. M., HEO, J. M., JEDRYCHOWSKI, M. P., SVIDERSKIY, V. O., OLSZEWSKI, J. L., KOERBER, J. T., XIE, T., BEAUSOLEIL, S. A., WELLS, J. A., GYGI, S. P., SCHULMAN, B. A. & HARPER, J. W. 2014. Quantitative proteomics reveal a feedforward mechanism for mitochondrial PARKIN translocation and ubiquitin chain synthesis. *Mol Cell,* 56**,** 360-75.

PAISAN-RUIZ, C., JAIN, S., EVANS, E. W., GILKS, W. P., SIMON, J., VAN DER BRUG, M., LOPEZ DE MUNAIN, A., APARICIO, S., GIL, A. M., KHAN, N., JOHNSON, J., MARTINEZ, J. R., NICHOLL, D., CARRERA, I. M., PENA, A. S., DE SILVA, R., LEES, A., MARTI-MASSO, J. F., PEREZ-TUR, J., WOOD, N. W. & SINGLETON, A. B. 2004. Cloning of the gene containing mutations that cause PARK8-linked Parkinson's disease. *Neuron,* 44**,** 595-600.

PANKRATZ, N., PAUCIULO, M. W., ELSAESSER, V. E., MAREK, D. K., HALTER, C. A., WOJCIESZEK, J., RUDOLPH, A., SHULTS, C. W., FOROUD, T., NICHOLS, W. C. & PARKINSON STUDY GROUP, P. I. 2006. Mutations in DJ-1 are rare in familial Parkinson disease. *Neurosci Lett,* 408**,** 209-13.

PARK, J., LEE, S. B., LEE, S., KIM, Y., SONG, S., KIM, S., BAE, E., KIM, J., SHONG, M., KIM, J. M. & CHUNG, J. 2006. Mitochondrial dysfunction in Drosophila PINK1 mutants is complemented by parkin. *Nature,* 441**,** 1157-61.

PARKER, W. D., JR., PARKS, J. K. & SWERDLOW, R. H. 2008. Complex I deficiency in Parkinson's disease frontal cortex. *Brain Res,* 1189**,** 215-8.

PARKINSON, J. 1817. An Essay on the Shaking palsy London: Whittingham and Rowland for Sherwood, Neely and Jones.

.

PEARCE, J. M. 1989. Aspects of the history of Parkinson's disease. *J Neurol Neurosurg Psychiatry,* Suppl**,** 6-10.

PERIQUET, M., LATOUCHE, M., LOHMANN, E., RAWAL, N., DE MICHELE, G., RICARD, S., TEIVE, H., FRAIX, V., VIDAILHET, M., NICHOLL, D., BARONE, P., WOOD, N. W., RASKIN, S., DELEUZE, J. F., AGID, Y., DURR, A. & BRICE, A. 2003. Parkin mutations are frequent in patients with isolated early-onset parkinsonism. *Brain : a journal of neurology,* 126**,** 1271-8.

PETROSKI, M. D. 2008. The ubiquitin system, disease, and drug discovery. *BMC Biochem,* 9 Suppl 1**,** S7.

PICKRELL, A. M. & YOULE, R. J. 2015. The roles of PINK1, parkin, and mitochondrial fidelity in Parkinson's disease. *Neuron,* 85**,** 257-73.

PLECHANOVOVA, A., JAFFRAY, E. G., TATHAM, M. H., NAISMITH, J. H. & HAY, R. T. 2012. Structure of a RING E3 ligase and ubiquitin-loaded E2 primed for catalysis. *Nature,* 489**,** 115-20.

POLYMEROPOULOS, M. H., LAVEDAN, C., LEROY, E., IDE, S. E., DEHEJIA, A., DUTRA, A., PIKE, B., ROOT, H., RUBENSTEIN, J., BOYER, R., STENROOS, E. S., CHANDRASEKHARAPPA, S., ATHANASSIADOU, A., PAPAPETROPOULOS, T., JOHNSON, W. G., LAZZARINI, A. M., DUVOISIN, R. C., DI IORIO, G., GOLBE, L. I. & NUSSBAUM, R. L. 1997. Mutation in the alpha-synuclein gene identified in families with Parkinson's disease. *Science,* 276**,** 2045-7.

POOLE, A. C., THOMAS, R. E., YU, S., VINCOW, E. S. & PALLANCK, L. 2010. The mitochondrial fusion-promoting factor mitofusin is a substrate of the PINK1/parkin pathway. *PLoS One,* 5**,** e10054.

PRABAKARAN, S., LIPPENS, G., STEEN, H. & GUNAWARDENA, J. 2012. Post-translational modification: nature's escape from genetic imprisonment and the basis for dynamic information encoding. *Wiley Interdiscip Rev Syst Biol Med,* 4**,** 565-83.

PROUKAKIS, C., DUDZIK, C. G., BRIER, T., MACKAY, D. S., COOPER, J. M., MILLHAUSER, G. L., HOULDEN, H. & SCHAPIRA, A. H. 2013. A novel alpha-synuclein missense mutation in Parkinson disease. *Neurology,* 80**,** 1062-4.

RAMSER, J., AHEARN, M. E., LENSKI, C., YARIZ, K. O., HELLEBRAND, H., VON RHEIN, M., CLARK, R. D., SCHMUTZLER, R. K., LICHTNER, P., HOFFMAN, E. P., MEINDL, A. & BAUMBACH-REARDON, L. 2008. Rare missense and synonymous variants in UBE1 are associated with X-linked infantile spinal muscular atrophy. *Am J Hum Genet,* 82**,** 188-93.

REN, Y., ZHAO, J. & FENG, J. 2003. Parkin binds to alpha/beta tubulin and increases their ubiquitination and degradation. *The Journal of neuroscience : the official journal of the Society for Neuroscience,* 23**,** 3316-24.

RICHARDSON, C. J., GAO, Q., MITSOPOULOUS, C., ZVELEBIL, M., PEARL, L. H. & PEARL, F. M. 2009. MoKCa database--mutations of kinases in cancer. *Nucleic Acids Res,* 37**,** D824-31.

RIEDERER, P., REICHMANN, H., YOUDIM, M. B. H. & GERLACH, M. 2006. *Parkinson's Disease and Related Disorders*, Springer Vienna.

RIEDERER, P. & WUKETICH, S. 1976. Time course of nigrostriatal degeneration in parkinson's disease. A detailed study of influential factors in human brain amine analysis. *J Neural Transm,* 38**,** 277-301.

RILEY, B. E., LOUGHEED, J. C., CALLAWAY, K., VELASQUEZ, M., BRECHT, E., NGUYEN, L., SHALER, T., WALKER, D., YANG, Y., REGNSTROM, K., DIEP, L., ZHANG, Z., CHIOU, S., BOVA, M., ARTIS, D. R., YAO, N., BAKER, J., YEDNOCK,

T. & JOHNSTON, J. A. 2013. Structure and function of Parkin E3 ubiquitin ligase reveals aspects of RING and HECT ligases. *Nature communications,* 4, 1982.

RODRIGO-BRENNI, M. C. & MORGAN, D. O. 2007. Sequential E2s drive polyubiquitin chain assembly on APC targets. *Cell,* 130, 127-39.

SADOWSKI, M., SURYADINATA, R., TAN, A. R., ROESLEY, S. N. & SARCEVIC, B. 2012. Protein monoubiquitination and polyubiquitination generate structural diversity to control distinct biological processes. *IUBMB life,* 64, 136-42.

SAKATA, E., YAMAGUCHI, Y., KURIMOTO, E., KIKUCHI, J., YOKOYAMA, S., YAMADA, S., KAWAHARA, H., YOKOSAWA, H., HATTORI, N., MIZUNO, Y., TANAKA, K. & KATO, K. 2003. Parkin binds the Rpn10 subunit of 26S proteasomes through its ubiquitin-like domain. *EMBO reports,* 4, 301-6.

SANO, I., GAMO, T., KAKIMOTO, Y., TANIGUCHI, K., TAKESADA, M. & NISHINUMA, K. 1959. Distribution of catechol compounds in human brain. *Biochim Biophys Acta,* 32, 586-7.

SARRAF, S. A., RAMAN, M., GUARANI-PEREIRA, V., SOWA, M. E., HUTTLIN, E. L., GYGI, S. P. & HARPER, J. W. 2013. Landscape of the PARKIN-dependent ubiquitylome in response to mitochondrial depolarization. *Nature,* 496, 372-6.

SAUVE, V., LILOV, A., SEIRAFI, M., VRANAS, M., RASOOL, S., KOZLOV, G., SPRULES, T., WANG, J., TREMPE, J. F. & GEHRING, K. 2015. A Ubl/ubiquitin switch in the activation of Parkin. *EMBO J.*

SCHAPIRA, A. H., COOPER, J. M., DEXTER, D., JENNER, P., CLARK, J. B. & MARSDEN, C. D. 1989. Mitochondrial complex I deficiency in Parkinson's disease. *Lancet,* 1, 1269.

SCHEFFNER, M. & KUMAR, S. 2014. Mammalian HECT ubiquitin-protein ligases: biological and pathophysiological aspects. *Biochim Biophys Acta,* 1843, 61-74.

SCHLESINGER, D. H. & GOLDSTEIN, G. 1975. Molecular conservation of 74 amino acid sequence of ubiquitin between cattle and man. *Nature,* 255, 423-4.

SCHULMAN, B. A. & HARPER, J. W. 2009. Ubiquitin-like protein activation by E1 enzymes: the apex for downstream signalling pathways. *Nat Rev Mol Cell Biol,* 10, 319-31.

SCHWARZ, S. E., ROSA, J. L. & SCHEFFNER, M. 1998. Characterization of human hect domain family members and their interaction with UbcH5 and UbcH7. *J Biol Chem,* 273, 12148-54.

SHI, Y. 2009. Serine/threonine phosphatases: mechanism through structure. *Cell,* 139, 468-84.

SHIBA-FUKUSHIMA, K., ARANO, T., MATSUMOTO, G., INOSHITA, T., YOSHIDA, S., ISHIHAMA, Y., RYU, K. Y., NUKINA, N., HATTORI, N. & IMAI, Y. 2014. Phosphorylation of mitochondrial polyubiquitin by PINK1 promotes Parkin mitochondrial tethering. *PLoS Genet,* 10, e1004861.

SHIBA-FUKUSHIMA, K., IMAI, Y., YOSHIDA, S., ISHIHAMA, Y., KANAO, T., SATO, S. & HATTORI, N. 2012. PINK1-mediated phosphorylation of the Parkin ubiquitin-like domain primes mitochondrial translocation of Parkin and regulates mitophagy. *Scientific reports,* 2, 1002.

SHIMURA, H., HATTORI, N., KUBO, S., MIZUNO, Y., ASAKAWA, S., MINOSHIMA, S., SHIMIZU, N., IWAI, K., CHIBA, T., TANAKA, K. & SUZUKI, T. 2000. Familial

Parkinson disease gene product, parkin, is a ubiquitin-protein ligase. *Nature genetics,* 25**,** 302-5.

SHIMURA, H., SCHLOSSMACHER, M. G., HATTORI, N., FROSCH, M. P., TROCKENBACHER, A., SCHNEIDER, R., MIZUNO, Y., KOSIK, K. S. & SELKOE, D. J. 2001. Ubiquitination of a new form of alpha-synuclein by parkin from human brain: implications for Parkinson's disease. *Science,* 293**,** 263-9.

SHOJAEE, S., SINA, F., BANIHOSSEINI, S. S., KAZEMI, M. H., KALHOR, R., SHAHIDI, G. A., FAKHRAI-RAD, H., RONAGHI, M. & ELAHI, E. 2008. Genome-wide linkage analysis of a Parkinsonian-pyramidal syndrome pedigree by 500 K SNP arrays. *Am J Hum Genet,* 82**,** 1375-84.

SINGLETON, A. B., FARRER, M., JOHNSON, J., SINGLETON, A., HAGUE, S., KACHERGUS, J., HULIHAN, M., PEURALINNA, T., DUTRA, A., NUSSBAUM, R., LINCOLN, S., CRAWLEY, A., HANSON, M., MARAGANORE, D., ADLER, C., COOKSON, M. R., MUENTER, M., BAPTISTA, M., MILLER, D., BLANCATO, J., HARDY, J. & GWINN-HARDY, K. 2003. alpha-Synuclein locus triplication causes Parkinson's disease. *Science,* 302**,** 841.

SMIT, J. J., MONTEFERRARIO, D., NOORDERMEER, S. M., VAN DIJK, W. J., VAN DER REIJDEN, B. A. & SIXMA, T. K. 2012. The E3 ligase HOIP specifies linear ubiquitin chain assembly through its RING-IBR-RING domain and the unique LDD extension. *EMBO J,* 31**,** 3833-44.

SMIT, J. J. & SIXMA, T. K. 2014. RBR E3-ligases at work. *EMBO Rep,* 15**,** 142-54.

SPILLANTINI, M. G., CROWTHER, R. A., JAKES, R., CAIRNS, N. J., LANTOS, P. L. & GOEDERT, M. 1998. Filamentous alpha-synuclein inclusions link multiple system atrophy with Parkinson's disease and dementia with Lewy bodies. *Neuroscience letters,* 251**,** 205-8.

SPRATT, D. E., JULIO MARTINEZ-TORRES, R., NOH, Y. J., MERCIER, P., MANCZYK, N., BARBER, K. R., AGUIRRE, J. D., BURCHELL, L., PURKISS, A., WALDEN, H. & SHAW, G. S. 2013. A molecular explanation for the recessive nature of parkin-linked Parkinson's disease. *Nature communications,* 4**,** 1983.

SPRATT, D. E., WALDEN, H. & SHAW, G. S. 2014. RBR E3 ubiquitin ligases: new structures, new insights, new questions. *The Biochemical journal,* 458**,** 421-37.

SRIRAM, S. R., LI, X., KO, H. S., CHUNG, K. K., WONG, E., LIM, K. L., DAWSON, V. L. & DAWSON, T. M. 2005. Familial-associated mutations differentially disrupt the solubility, localization, binding and ubiquitination properties of parkin. *Human molecular genetics,* 14**,** 2571-86.

STIEGLITZ, B., MORRIS-DAVIES, A. C., KOLIOPOULOS, M. G., CHRISTODOULOU, E. & RITTINGER, K. 2012a. LUBAC synthesizes linear ubiquitin chains via a thioester intermediate. *EMBO Rep,* 13**,** 840-6.

STIEGLITZ, B., MORRIS-DAVIES, A. C., KOLIOPOULOS, M. G., CHRISTODOULOU, E. & RITTINGER, K. 2012b. LUBAC synthesizes linear ubiquitin chains via a thioester intermediate. *EMBO reports,* 13**,** 840-6.

STIEGLITZ, B., RANA, R. R., KOLIOPOULOS, M. G., MORRIS-DAVIES, A. C., SCHAEFFER, V., CHRISTODOULOU, E., HOWELL, S., BROWN, N. R., DIKIC, I. & RITTINGER, K. 2013. Structural basis for ligase-specific conjugation of linear ubiquitin chains by HOIP. *Nature*.

SULIMAN, H. B. & PIANTADOSI, C. A. 2016. Mitochondrial Quality Control as a Therapeutic Target. *Pharmacol Rev,* 68**,** 20-48.

SURINOVA, S., HUTTENHAIN, R., CHANG, C. Y., ESPONA, L., VITEK, O. & AEBERSOLD, R. 2013. Automated selected reaction monitoring data analysis workflow for large-scale targeted proteomic studies. *Nature protocols,* 8**,** 1602-19.

SWAMINATHAN, G. & TSYGANKOV, A. Y. 2006. The Cbl family proteins: ring leaders in regulation of cell signaling. *Journal of cellular physiology,* 209**,** 21-43.

TANAKA, A., CLELAND, M. M., XU, S., NARENDRA, D. P., SUEN, D. F., KARBOWSKI, M. & YOULE, R. J. 2010. Proteasome and p97 mediate mitophagy and degradation of mitofusins induced by Parkin. *J Cell Biol,* 191**,** 1367-80.

TANAKA, K., SUZUKI, T., CHIBA, T., SHIMURA, H., HATTORI, N. & MIZUNO, Y. 2001. Parkin is linked to the ubiquitin pathway. *J Mol Med (Berl),* 79**,** 482-94.

TASHIRO, M., OKUBO, S., SHIMOTAKAHARA, S., HATANAKA, H., YASUDA, H., KAINOSHO, M., YOKOYAMA, S. & SHINDO, H. 2003. NMR structure of ubiquitin-like domain in PARKIN: gene product of familial Parkinson's disease. *Journal of biomolecular NMR,* 25**,** 153-6.

TOMOO, K., MUKAI, Y., IN, Y., MIYAGAWA, H., KITAMURA, K., YAMANO, A., SHINDO, H. & ISHIDA, T. 2008. Crystal structure and molecular dynamics simulation of ubiquitin-like domain of murine parkin. *Biochimica et biophysica acta,* 1784**,** 1059-67.

TONKS, N. K. 2006. Protein tyrosine phosphatases: from genes, to function, to disease. *Nat Rev Mol Cell Biol,* 7**,** 833-46.

TREMPE, J. F., SAUVE, V., GRENIER, K., SEIRAFI, M., TANG, M. Y., MENADE, M., AL-ABDUL-WAHID, S., KRETT, J., WONG, K., KOZLOV, G., NAGAR, B., FON, E. A. & GEHRING, K. 2013. Structure of parkin reveals mechanisms for ubiquitin ligase activation. *Science,* 340**,** 1451-5.

TRÉTIAKOFF, C. 1919. *Contribution à l'étude de l'anatomie pathologique du locus niger de Soemmering avec quelques déductions relatives à la pathogénie des troubles du tonus musculaire et de la maladie de Parkinson.*

TROUSSEAU, A. Lecture XV: Senile trembling and Paralysis Agitans. Lectures on Clinical Medicine delivered at the Hotel-Dieu, Paris. , 1868.

UNOKI, M. & NAKAMURA, Y. 2001. Growth-suppressive effects of BPOZ and EGR2, two genes involved in the PTEN signaling pathway. *Oncogene,* 20**,** 4457-65.

VALENTE, E. M., ABOU-SLEIMAN, P. M., CAPUTO, V., MUQIT, M. M., HARVEY, K., GISPERT, S., ALI, Z., DEL TURCO, D., BENTIVOGLIO, A. R., HEALY, D. G., ALBANESE, A., NUSSBAUM, R., GONZALEZ-MALDONADO, R., DELLER, T., SALVI, S., CORTELLI, P., GILKS, W. P., LATCHMAN, D. S., HARVEY, R. J., DALLAPICCOLA, B., AUBURGER, G. & WOOD, N. W. 2004. Hereditary early-onset Parkinson's disease caused by mutations in PINK1. *Science,* 304**,** 1158-60.

VALENTE, E. M., BENTIVOGLIO, A. R., DIXON, P. H., FERRARIS, A., IALONGO, T., FRONTALI, M., ALBANESE, A. & WOOD, N. W. 2001. Localization of a novel locus for autosomal recessive early-onset parkinsonism, PARK6, on human chromosome 1p35-p36. *Am J Hum Genet,* 68**,** 895-900.

VILARINO-GUELL, C., WIDER, C., ROSS, O. A., DACHSEL, J. C., KACHERGUS, J. M., LINCOLN, S. J., SOTO-ORTOLAZA, A. I., COBB, S. A., WILHOITE, G. J., BACON, J. A., BEHROUZ, B., MELROSE, H. L., HENTATI, E., PUSCHMANN, A., EVANS, D. M., CONIBEAR, E., WASSERMAN, W. W., AASLY, J. O., BURKHARD, P. R., DJALDETTI, R., GHIKA, J., HENTATI, F., KRYGOWSKA-WAJS, A., LYNCH, T., MELAMED, E., RAJPUT, A., RAJPUT, A. H., SOLIDA, A., WU, R. M., UITTI, R. J., WSZOLEK, Z. K., VINGERHOETS, F. & FARRER, M. J. 2011. VPS35 mutations in Parkinson disease. *Am J Hum Genet,* 89**,** 162-7.

VIVES-BAUZA, C., ZHOU, C., HUANG, Y., CUI, M., DE VRIES, R. L., KIM, J., MAY, J., TOCILESCU, M. A., LIU, W., KO, H. S., MAGRANE, J., MOORE, D. J., DAWSON, V. L., GRAILHE, R., DAWSON, T. M., LI, C., TIEU, K. & PRZEDBORSKI, S. 2010. PINK1-dependent recruitment of Parkin to mitochondria in mitophagy. *Proceedings of the National Academy of Sciences of the United States of America,* 107**,** 378-83.

WALDEN, H. & MARTINEZ-TORRES, R. J. 2012. Regulation of Parkin E3 ubiquitin ligase activity. *Cellular and molecular life sciences : CMLS*.

WALLACE, D. C., FAN, W. & PROCACCIO, V. 2010. Mitochondrial energetics and therapeutics. *Annu Rev Pathol,* 5**,** 297-348.

WANG, X., WINTER, D., ASHRAFI, G., SCHLEHE, J., WONG, Y. L., SELKOE, D., RICE, S., STEEN, J., LAVOIE, M. J. & SCHWARZ, T. L. 2011. PINK1 and Parkin target Miro for phosphorylation and degradation to arrest mitochondrial motility. *Cell,* 147**,** 893-906.

WAUER, T. & KOMANDER, D. 2013. Structure of the human Parkin ligase domain in an autoinhibited state. *The EMBO journal*.

WAUER, T., SIMICEK, M., SCHUBERT, A. & KOMANDER, D. 2015a. Mechanism of phospho-ubiquitin-induced PARKIN activation. *Nature*.

WAUER, T., SWATEK, K. N., WAGSTAFF, J. L., GLADKOVA, C., PRUNEDA, J. N., MICHEL, M. A., GERSCH, M., JOHNSON, C. M., FREUND, S. M. & KOMANDER, D. 2015b. Ubiquitin Ser65 phosphorylation affects ubiquitin structure, chain assembly and hydrolysis. *EMBO J,* 34**,** 307-25.

WENZEL, D. M. & KLEVIT, R. E. 2012. Following Ariadne's thread: a new perspective on RBR ubiquitin ligases. *BMC biology,* 10**,** 24.

WENZEL, D. M., LISSOUNOV, A., BRZOVIC, P. S. & KLEVIT, R. E. 2011. UBCH7 reactivity profile reveals parkin and HHARI to be RING/HECT hybrids. *Nature,* 474**,** 105-8.

WEST, A. B., MOORE, D. J., BISKUP, S., BUGAYENKO, A., SMITH, W. W., ROSS, C. A., DAWSON, V. L. & DAWSON, T. M. 2005. Parkinson's disease-associated mutations in leucine-rich repeat kinase 2 augment kinase activity. *Proc Natl Acad Sci U S A,* 102**,** 16842-7.

WHITWORTH, A. J., LEE, J. R., HO, V. M., FLICK, R., CHOWDHURY, R. & MCQUIBBAN, G. A. 2008. Rhomboid-7 and HtrA2/Omi act in a common pathway with the Parkinson's disease factors Pink1 and Parkin. *Disease models & mechanisms,* 1**,** 168-74; discussion 173.

WINNER, B., REGENSBURGER, M., SCHREGLMANN, S., BOYER, L., PROTS, I., ROCKENSTEIN, E., MANTE, M., ZHAO, C., WINKLER, J., MASLIAH, E. & GAGE, F. H. 2012. Role of alpha-synuclein in adult neurogenesis and neuronal maturation in the dentate gyrus. *J Neurosci,* 32**,** 16906-16.

WINTERMEYER, P., KRUGER, R., KUHN, W., MULLER, T., WOITALLA, D., BERG, D., BECKER, G., LEROY, E., POLYMEROPOULOS, M., BERGER, K., PRZUNTEK, H.,

SCHOLS, L., EPPLEN, J. T. & RIESS, O. 2000. Mutation analysis and association studies of the UCHL1 gene in German Parkinson's disease patients. *Neuroreport,* 11, 2079-82.

WOODROOF, H. I., POGSON, J. H., BEGLEY, M., CANTLEY, L. C., DEAK, M., CAMPBELL, D. G., VAN AALTEN, D. M. F., WHITWORTH, A. J., ALESSI, D. R. & MUQIT, M. M. K. 2011. Discovery of catalytically active orthologues of the Parkinson's disease kinase PINK1: analysis of substrate specificity and impact of mutations. *Open Biology,* 1.

WU, P., NIELSEN, T. E. & CLAUSEN, M. H. 2015. FDA-approved small-molecule kinase inhibitors. *Trends in Pharmacological Sciences,* 36, 422-439.

YAMANO, K. & YOULE, R. J. 2013. PINK1 is degraded through the N-end rule pathway. *Autophagy,* 9, 1758-69.

YAMAUCHI, T., SAKURAI, M., ABE, K., MATSUMIYA, G. & SAWA, Y. 2008. Ubiquitin-mediated stress response in the spinal cord after transient ischemia. *Stroke,* 39, 1883-9.

YANG, Y., GEHRKE, S., IMAI, Y., HUANG, Z., OUYANG, Y., WANG, J. W., YANG, L., BEAL, M. F., VOGEL, H. & LU, B. 2006. Mitochondrial pathology and muscle and dopaminergic neuron degeneration caused by inactivation of Drosophila Pink1 is rescued by Parkin. *Proceedings of the National Academy of Sciences of the United States of America,* 103, 10793-8.

YE, Y. & RAPE, M. 2009. Building ubiquitin chains: E2 enzymes at work. *Nat Rev Mol Cell Biol,* 10, 755-64.

ZARRANZ, J. J., ALEGRE, J., GOMEZ-ESTEBAN, J. C., LEZCANO, E., ROS, R., AMPUERO, I., VIDAL, L., HOENICKA, J., RODRIGUEZ, O., ATARES, B., LLORENS, V., GOMEZ TORTOSA, E., DEL SER, T., MUNOZ, D. G. & DE YEBENES, J. G. 2004. The new mutation, E46K, of alpha-synuclein causes Parkinson and Lewy body dementia. *Ann Neurol,* 55, 164-73.

ZHANG, Y., GAO, J., CHUNG, K. K., HUANG, H., DAWSON, V. L. & DAWSON, T. M. 2000. Parkin functions as an E2-dependent ubiquitin- protein ligase and promotes the degradation of the synaptic vesicle-associated protein, CDCrel-1. *Proceedings of the National Academy of Sciences of the United States of America,* 97, 13354-9.

ZHENG, X. & HUNTER, T. 2013. Parkin mitochondrial translocation is achieved through a novel catalytic activity coupled mechanism. *Cell research,* 23, 886-97.

ZHOU, C., HUANG, Y., SHAO, Y., MAY, J., PROU, D., PERIER, C., DAUER, W., SCHON, E. A. & PRZEDBORSKI, S. 2008. The kinase domain of mitochondrial PINK1 faces the cytoplasm. *Proc Natl Acad Sci U S A,* 105, 12022-7.

ZHOU, H., DI PALMA, S., PREISINGER, C., PENG, M., POLAT, A. N., HECK, A. J. & MOHAMMED, S. 2013. Toward a comprehensive characterization of a human cancer cell phosphoproteome. *J Proteome Res,* 12, 260-71.

ZIMPRICH, A., BISKUP, S., LEITNER, P., LICHTNER, P., FARRER, M., LINCOLN, S., KACHERGUS, J., HULIHAN, M., UITTI, R. J., CALNE, D. B., STOESSL, A. J., PFEIFFER, R. F., PATENGE, N., CARBAJAL, I. C., VIEREGGE, P., ASMUS, F., MULLER-MYHSOK, B., DICKSON, D. W., MEITINGER, T., STROM, T. M., WSZOLEK, Z. K. & GASSER, T. 2004. Mutations in LRRK2 cause autosomal-dominant parkinsonism with pleomorphic pathology. *Neuron,* 44, 601-7.